Vascularised Scaffolds for Cutaneous Wound Reconstruction

Using Stem/Progenitor Cells

Mr Daniel Markeson, MBBS, BSc (Hons) MRCS

Restore Research Fellow

University College London

Supervisor: Professor Alexander Seifalian

Co-supervisor: Professor Suzanne Watt

Thesis submitted for the degree: Doctor of Medicine (MD) Res

Declaration

I, Daniel Markeson, confirm that the work presented in this thesis is my own. Where information has been derived from other sources, I confirm that this has been indicated in the thesis.

Abstract

The synthetic replacement of full thickness skin is suboptimal both aesthetically and functionally. One approach to improve existing dermal substitutes is to pre-vascularise them to facilitate incorporation. In so doing, the aim is to improve the trajectory of wound healing. More expeditious maturation has been suggested to improve outcomes.

Endothelial colony forming cells (ECFCs), specialised progenitor cells required for vasculogenesis, were isolated from cord (CBECFC) and peripheral (PBECFC) blood. Mesenchymal stromal cells were separated from adipose tissue (AdMSCs). Using a proprietary device (*μ-chemotaxis 3D*), human umbilical vein endothelial cells, and CBECFC- and PBECFC-derived cells were compared for chemokinetic and chemotactic movement within collagen I gels, with or without fibronectin. PBECFC-derived cells migrated further than CBECFC-derived cells and HUVECs towards the chemoattractant.

These data informed the fabrication of collagen I gels containing co-cultures of ECFC-derived cells with MSCs. An attempt was made to compress these gels to facilitate handling, but vascular tubule formation was not amenable to compression. HUVECs seeded as a monoculture within compressed gels also had a 100% mortality rate, although 62.5% AdMSCs and 66.4% human dermal fibroblasts survived the compression process.

Since pre-formed tubules did not survive the compression process, various concentrations of ECFC-derived cells and MSCs were seeded within uncompressed collagen I gels in order to obtain an optimised vascular network. AdMSCs were compared to BMMSCs. PBECFC-derived cells were compared to CBECFC-derived cells and HUVECs. Optimised gels containing tubules formed by adult derived PBECFC-derived cells and AdMSCs were then scaled up and implanted into an *in vivo* immunodeficient mouse model. Host incorporation of the construct within this pre-vascularised gel was significantly improved compared to an empty gel control ($p=0.04$).

In summary, it was possible to fabricate a pre-vascularised collagen I scaffold, using adult-derived stem/progenitor cells, increasing the rate of host incorporation in an *in vivo* murine model.

Publications and conferences

Publications

- Watt SM, Gullo F, van der Garde M, Markeson D, Camicia R, Khoo CP, Zwaginga JJ. The angiogenic properties of mesenchymal stem/stromal cells and their therapeutic potential. Br Med Bull. 2013;108:25-53.
- Markeson D, Pleat JM, Sharpe JR, Harris AL, Seifalian AM, Watt SM. Scarring, stem cells, scaffolds and skin repair; J Tissue Eng Regen Med. Oct 2013; epub ahead of print.
- Watt SM, Leeson P, Cai S, Markeson D, Khoo CP, Newton L, Zhang YY, Sourri S, Channon K. Cord and cord blood derived endothelial cells; In: Umbilical Cord Blood Stem Cells and Regenerative Medicine. Chapter 5. Stavropoulos C, Navarette C, Charron D. Eds. Elsevier Press, Amsterdam. The Netherlands. 2014 (in press)

Presentations

- Markeson D, Seifalian A, Watt SM. Adipose mesenchymal stem/stromal cells (AdMSCs) and peripheral blood endothelial colony forming cells (ECFCs) for tissue engineering; European Society for Plastic Reconstructive and Aesthetic Surgery, Jul 2014. Edinburgh, Scotland.
- Markeson D, Seifalian A, Watt SM. Tissue engineering for wound healing – endothelial colony forming cell (ecfc) migration, 3d tubule formation and expansion; Society of Academic and Research Surgery, Patey Prize session, Jan 2014. Cambridge, UK.
- Markeson D, Sweeney D, Khoo CP, Watt SM. The role of endothelial colony forming cells for tissue engineering – chemotaxis, 3D tubule formation and enhanced expansion using bioreactors; NHS Blood and Transplant Annual Meeting, Oct 2013. Oxford, UK

Acknowledgements

First of all I would like to acknowledge the stem cell research group in Oxford as a whole. The atmosphere within the lab made it very easy for me to make the transition from the clinical environment of a hospital to the laboratory bench.

Certain individuals must also be singled out for their particular contributions to my MD.

Professors Alexander Seifalian and Suzanne Watt as my supervisor and co-supervisor, guided me and advised me throughout on how to best approach my project and ensured that I stayed on track throughout. For their guidance and encouragement I am very grateful. In addition, Jon Pleat, Michael Tyler and all the team at Restore for not only sponsoring me and providing me with my adipose tissue but for also constantly giving me ideas and keeping me on the right path in my first foray into post-graduate research.

My neighbours Laura Newton/David Cook and in particular Dominic Sweeney – thank you for putting up with me! I'll be the first to admit that I have the concentration span of a goldfish (it is a wonder I finished this MD!) and I appreciated the chats about everything from football to cricket (and even rarely science). Even if you were just humouring me with my constant distracting chats, thank you.

Sandy Britt and Jan Walton, thank you for supplying me with more cord blood than I knew what to do with and for the banter around the lab and in the coffee room.

Dom – in addition to keeping me sane chatting about football thank you for teaching me to (almost) be a scientist. Without your help in getting started I would never have learnt how to isolate and expand stem cells and both you and Enca have helped me a great deal with reagents, the lentiviral vector and with general advice throughout my MD! Cheen, Anna, Sarah and Emma – you have also helped massively with the scientific side of things and I have enjoyed spending time with you over tea, coffee and cakes!

Brenda – it has been good chatting with you about all things American as well as your busy social life!

Fra, Mark, Youyi, Pat, Hua-Jun, Christine and Tao – it has been great getting to know you all and I hope we stay in touch.

Rosalba – grazie mille per tutto che mi hai insegnato - Io non lo dimentichero mai. Spero ci incontreremo ancora in futura. Tvb a

Fadi, I only used your expertise briefly at the end of my thesis but nevertheless you were invaluable in helping me to complete the *in vivo* work and were good to have around to deflect attention at the (rather frequent) Restore meetings!

Last but not least I want to thank my wife Laura and two gorgeous kids Seth and Alice for putting up with my erratic timetable, stressing about my write-up and endless job applications, and having to come in at random times to 'look after my cells!?'. I could not have achieved this MD without your help and encouragement.

List of abbreviations

FTSG: Full thickness skin graft

STSG: Split thickness skin graft

BM: Bone marrow

HFSC: Hair follicle stem cells

SGSC: Sweat gland stem cells

PDGF: Platelet-derived growth factor

TGF-β: Transforming growth factor beta

ECM: Extracellular matrix

DCD: Decellularised cadaveric dermis

VAC: Vacuum assisted closure

ECFC: Endothelial colony forming cell

EC: Endothelial cell

CFU-EC: Colony forming unit-endothelial cell

BOEC: Blood outgrowth endothelial cell

FN: Fibronectin

FBS/FCS: Fetal bovine/calf serum

vWF: vonWillebrand Factor

MNC: Mononuclear cell

pHPL: Pooled human platelet lysate

CB: Cord blood

PB: Peripheral blood

MSC: Mesenchymal stem cell

BMMSC: Bone marrow derived MSC

HUVEC: Human umbilical vein endothelial cell

VEGF: Vascular endothelial growth factor

bFGF: Basic fibroblast growth factor

HIF-1α: Hypoxia inducible factor-1α

SVSMC: Saphenous vein smooth muscle cell

HDMEC: Human dermal microvasular endothelial cell

hDF: Human dermal fibroblast

hPASMC: Human pulmonary artery smooth muscle cell

GMP: Good medical practice

FACS: Flow activated cell sorting

EBM-2/EGM-2: Endothelial basal/growth medium-2

hEGF: Human epidermal growth factor

EDTA: Ethylenediaminetetraacetic acid

D-PBS: Dulbecco's phosphate buffered saline

DMSO: Dimethyl sulfoxide

MEM: Modified Eagle Medium

LV: Lentivirus

eGFP: Enhanced green fluorescent protein

MOI: Multiplicity of infection

VT: Viral titre

LN: Liquid nitrogen

RT: Room temperature

PFA: Paraformaldehyde

AdMSC: Adipose derived MSC

WJ: Whartons Jelly

MSC-GM: MSC growth medium

FMI: Forward migration index

SDF-1α: Stromal-cell derived factor 1α

IL-3: Interleukin 3

SCF: Stem cell factor

RBC: Red blood cell

PLGA: Poly(lactide-co-glycolide

TLS: Tubule-like structure

Table of Contents

Abstract **3**

1 Background **12**

1.1 Introduction 12

1.2 The structure of human skin 13

1.3 The stem cell niche and its role in skin renewal 17

1.4 Mammalian wound healing – regeneration versus scarring 19

1.5 The tissue engineering challenge for full thickness wound repair 21

1.6 Clinically available dermal scaffolds that mimic the niche 22

1.7 Revascularisation of engineered grafts 27

1.8 Endothelial progenitor cells and vessel formation 28

1.9 Isolation and culturing of endothelial colony forming cells 30

1.10 Developing the next generation vascularised scaffolds and smart biomaterials 34

1.11 Perspectives 41

1.12 Aims and objectives of this thesis 43

2 Methods **45**

2.1 Reagents 45

2.2 Cells

2.2.1 Pooled human umblicial vein endothelial cells (pHUVECs) 48

2.2.2 Bone marrow mesenchymal stem/stromal cells (BMMSCs)/human dermal fibroblasts (hDFs) 49

2.2.3 Mononuclear cells from umbilical cord blood (MNCs) 52

2.2.4 Endothelial cells from umbilical cord blood (CBECs) 53

2.2.5 Peripheral blood endothelial cells (PBECs) 58

2.2.6 Adipose derived mesenchymal stem cells (Ad MSCs) 63

2.2.7 Differentiation of Ad MSCs 67

2.2.7.1 Adipogenesis culture protocol 67

2.2.7.2 Chondrogenesis culture protocol 69

2.2.7.3 Osteogenesis culture protocol 70

2.2.8 Cell passage, counting and freezing procedures 71

2.3 Fluorescence-activated cell sorter (FACS) analysis 72

2.4 μ-chemotaxis 3D assay 76

2.5 Lentiviral transduction of cells

2.5.1 Human embryonic kidney (HEK) 293 FT cells 79

2.5.2 Titration of lentiviral vector stocks 79
2.5.3 eGFP lentiviral transduction 81
2.6 Compressed collagen gels
2.6.1 Optimisation of compressed collagen gels 82
2.6.2 Compressed collagen I gels with ECs 84
2.6.3 Compressed collagen I gels with hDFs, BMMSCs or AdMSCs 85
2.6.4 LIVE/DEAD® stain protocol 85
2.7 Uncompressed collagen gels
……86
2.7.1 Upscaling to a 12 and 24 well plate 89
2.8 Fixing of gels
2.8.1 Making 4% paraformaldehyde (PFA) 91
2.9 In vivo: uncompressed PBECFC/AdMSC gel in a humanized mouse model……91
2.11
Statistics……92
3 Fabrication of a pre-vascularised scaffold 94
3.1 Migration of endothelial cells: μ-Chemotaxis 3D 94
3.1.1 Aims and objectives for the μ-chemotaxis 3D assay 97
3.1.2 Results: μ-chemotaxis assay 91
3.1.3 μ-chemotaxis findings 107
3.2 Compressed collagen gels
3.2.1 Rationale and aims for use of compressed collagen gels 108
3.2.2 Prevascularising uncompressed gels prior to compression 110
3.2.3 Results for compressed gels 111
3.2.4 Compressed gels – summary 115
3.3 Uncompressed collagen gels
3.3.1 Aims for use of uncompressed collagen I gels 116
3.3.2 Results for uncompressed gels – Pilot experiments using HUVECs and BMMSCs 116
3.3.3 Will TLSs form with 3 different batches of PB ECFCs/CB ECFCs/HUVECs 119
3.3.4 Will TLSs form with 3 different batches of AdMSCs/BMMSCs 129
3.4 Discussion 138
4 Scaling up of pre-vascularised collagen I gels and their in vivo application 142
4.1 Introduction 142
4.2 Results

4.2.1 Scaling up pre-vascularised collagen I gels 143
4.2.2 Implantation of gels in immunodeficient murine model 143
4.3 Discussion 151
5 Discussion and future perspectives 153
5.1 Introduction 153
5.2 Scarring 153
5.3 Stem/progenitor cells and vasculogenesis 154
5.4 From bench to bedside 156
5.4.1 Can a suitable scaffold be produced on a large enough scale to be clinically viable? 157
5.4.2 What are the safety barriers to producing such a product? 158
5.4.3 Can this pre-vascularised scaffold be used in humans? 158

APPENDICES 160
REFERENCES 164

Chapter 1

Background

1.1 Introduction

Geoffrey Chaucer famously stated ‘as tyme hem hurt, a tyme doth hem cure’ (‘time heals all wounds’) (1). However, those with visible scars, whether small and seemingly insignificant to a neutral observer, or considerably more extensive, may disagree with this statement. An unsightly appearance can stigmatise and marginalise an individual from society, preventing social interaction and engendering psychological illness and low self-esteem (2). Over £1 billion is spent in the United Kingdom every year on the management of chronic wounds and scarring (3), with much larger amounts spent annually in the United States of America and worldwide. From the personal to the societal viewpoint, it is vital that scientists and clinicians continue to work towards methods to reduce the physical and psychological consequences of scarring.

Burns are the main causative factor for substantial body surface area scars. Despite improvements to health and safety standards in the United Kingdom, the most recent published data suggest that over 250,000 people are burnt every year with 13,000 admitted to hospital and 300 deaths recorded (4). In 2004, nearly 11 million people worldwide were burned severely enough to require medical attention and although no recent studies have identified current incidence rates, it is likely that at least this many are still being affected. The average cost of treating an individual adult burn in 2012 was estimated to be as high as US $73,552 (5).

Skin autografts are the current gold standard for burns and other full thickness defects including trauma, abnormal development of skin in utero and infection. The obvious advantages for an autograft include immunological acceptance, and colour and texture match. However, they may provide a less than satisfactory outcome if the wound is too large to use a full thickness skin graft (FTSG) or because of the many recognised complications associated with split thickness skin grafting (STSG) where the epidermis and only part of the dermis are harvested. These include donor and recipient site scarring and a lack of full sensation and thermoregulation in grafted skin. In addition, contracture and reduced pliability are common side-effects, particularly in meshed

STSGs where fenestrations are made to reduce haematoma formation and to allow the graft to expand over a wider area. These interstices of the mesh may take several weeks to re-epithelialise, thereby increasing the risk of developing a hypertrophic scar (6). An additional problem arises when treating full thickness burns of 40% total body surface area or more. In these patients, there may be insufficient donor skin to cover the patients' wounds. Even if sufficient donor skin exists, in harvesting the unburned donor site the size of the wound may be increased to almost 100% of the body surface area. This has profound and dangerous consequences including massive fluid shifts and an increase in the risk of developing bacterial sepsis. Additionally, in extensive full thickness burns, regenerative elements from the wound edge or deeper dermal adnexal structures are destroyed, thereby retarding repair. Such cases may necessitate the use of temporary cadaveric or xenograft skin coverage, bioengineered skin in the form of cultured keratinocytes (epidermal autografts) or a first generation artificial dermal substitute. Each of these options has limitations including an inability to use epidermal grafts alone in full thickness defects, high cost, pigmentation mismatch, lack of reliable engraftment with dermal substitutes, lack of thermoregulation, the temporary nature of xeno- and allo-grafts and failure to restore relevant adnexal skin structures (pigment, sweat glands, hair) and hence fully functional skin (7).

1.2 The structure of human skin

The structure of skin, the largest human organ, varies in different locations, but is essentially composed of three basic layers ranging from superficial to deep - the 'epidermis', the 'dermis' and the subcutaneous fatty layer or 'hypodermis' (8). The components and function of normal skin are outlined in Table 1.1 and Figure 1.1.

The epidermis is the outermost layer and ranges in thickness from 0.04 mm (eyelids) to 1.6 mm (soles of the feet and palms of the hands). It is thin, avascular and consists of multiple epithelial layers, the interfollicular epidermis, adnexal structures and a limited number of non-epithelial cell types, e.g. Merkel cells. The specialised epithelial cells of the epidermis, the keratinocytes, gradually differentiate and mature by moving from the lowest layer, the *stratum basale,* through stereotypically organised layers which include the *stratum spinosum* and the *stratum granulosum* to the uppermost layer, the *stratum*

corneum. Keratinocytes are continually shed from the skin surface. In thick epidermis, the *stratum lucidum* is a structurally discrete layer between the stratum granulosum and the stratum corneum.

The dermis, lying below the epidermis, is thicker (ranging from 1-4mm in depth) and rich in connective tissue elements collagen (70% of the dermis), elastin and proteoglycans such as hyaluronic acid. It contains several cellular structures including nerves, blood vessels, lymphatics, muscle fibres and, depending on the location, hair follicles and sweat glands. It is self-evident that species diversity exists in skin structures. For example, although used as a basis for human studies, genetically distinct mice display diversity in the distribution of hair follicles throughout the skin, while, in the human, hair follicles are located mainly on the scalp for terminal hair growth and generate vellus hair on the face/trunk.

The dermis is partitioned into an upper *papillary dermis* that interdigitates with the overlying epidermis and a thicker, denser *reticular dermis* that extends to subcutaneous fat and contains irregular elastin fibres interspersed with large collagen fibres (9). In-between the dermis and the epidermis lies a basement membrane, an integral part of skin containing several laminins as well as type IV collagen, perlecan, heparan sulphate proteoglycans, fibronectin (FN) and nidogens 1 and 2 (10). The basement membrane (BM) assists with water retention, adds thickness to the skin and anchors the epidermal appendages (hair follicles, sweat glands).

Table 1.1 The components and functions of skin and the fibrin clot

	Components	Functions
Normal skin Epidermis 0.04-1.6mm Avascular	95% Keratinocytes (cells in lowest layer [Stratum Basale] divide and rise through Stratum Spinosum, Granulosum, Lucidum and Corneum] regulated by TGFα/KGF	Metabolic (Vitamin D production) (11); rradiation (UV) and physical (pathogens) protection; thermoregulation and regulation of water loss (lipids arranged between cells of S.Corneum).
	Merkel cells (S.Basale)	Light touch sensation
	Langerhans cells (S.Spinosum)	Immunological surveillance
	Melanocytes (S.Basale)	Skin colour
Basement membrane	Fibronectin; Collagen (Type IV); Laminins (332, α5); Perlecan; Heparan sulphate proteoglycans; Nidogens 1 and 2 (10)	Water retention, anchoring of epidermal appendages and secures epidermis to dermis
Dermis 1-4mm Superficial and deep vascular plexus	Collagen (Type III papillary dermis; Type I reticular dermis)	Tensile strength
	Elastin	Elasticity/pliability, reduces wound contracture after injury
	Ground substance (glycosaminoglycans & acid mucopolysaccharides)	Fills space between collagen/elastin fibres. Diffusion of nutrients & waste
	Mast cells	Inflammation and allergic reactions (12)
	Adnexal structures (hair follicles, sebaceous/eccrine/apocrine glands)	House stem cell populations including hair follicular & interfollicular SCs
The fibrin clot Inflammatory phase	Tissue factor (released by damaged tissue)	Begins clotting cascade ending in formation of Fibrin clot
	Platelets (enter through leaky vessels)	Degranulate releasing PDGF and TGF-β
	Neutrophils and macrophages	Phagocytosis of debris and bacteria. Attraction of fibroblasts and ECs
	Keratinocytes	Migrate over clot re-epithelialising wound
Proliferative phase	Fibroblasts	Lay down ECM. Replace fibrin clot with type III Collagen then later type I.
	Endothelial cells	Neovascularisation
Remodelling phase	Myofibroblasts	Wound contraction

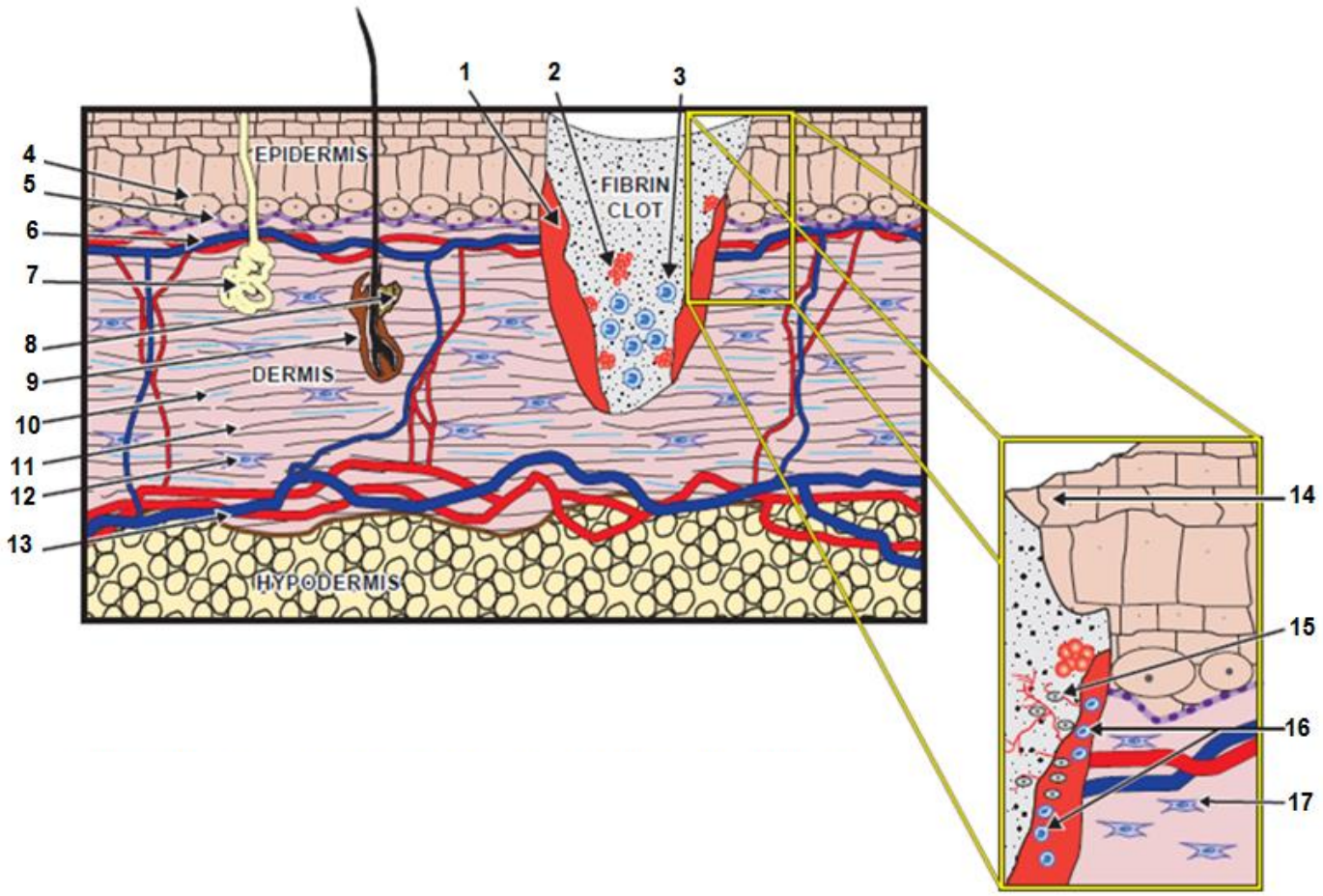

Figure 1.1 – The components and functions of skin and the fibrin clot: 1. Necrotic tissue; 2. Platelets; 3. Neutrophils; 4. Stratum basale; 5. Basement membrane; 6. Superficial dermal plexus; 7. Eccrine gland; 8. Sebaceous gland; 9. Hair follicle; 10. Elastic fibres; 11. Collagen fibres; 12. Fibroblasts; 13. Deep dermal plexus; 14. Keratinocytes migrating over fibrin clot; 15. Endothelial cells migrate to edge of clot and participate in neovascularisation; 16. Macrophages and neutrophils digest necrotic tissue; 17. Fibroblasts secrete ECM and myofibroblasts induce wound contraction.

1.3 The stem cell niche and its role in skin renewal

Cells which constantly renew, such as within blood and the skin, are sustained and repaired by a small population of resident stem cells. The ability of stem cells to self-renew is thought to be intrinsic to the regenerative capacity of the epidermis and adnexal structures throughout normal post-natal life (13–15). The basal layer of the murine epidermis houses two populations of self-renewing epidermal stem cells differing in their proliferative capacities and their ability to repair the epidermis after injury. One consists of slow cycling stem cells with high longevity and represents the stem cell reservoir that contributes to wound repair. These cells give rise to actively dividing committed progenitor cells, which undergo several cell divisions before eventually generating differentiated cells and may also give rise to transit amplifying cells (16). While the committed progenitors purportedly contribute to short term wound repair, the more quiescent epidermal stem cells persist throughout the animal's lifetime and contribute to repair and long-term regeneration of the epidermis (16). Whether these high and low turnover self-renewing populations occur in the human is unclear.

Stem cells that can generate epidermis are also found around hair follicles and sebaceous glands (13,14,17). In particular, the bulge region of the outer root sheath of the hair follicle houses hair follicular stem cells (HFSCs) that can produce epidermis, sebaceous glands and hair follicles (18,19) as demonstrated in murine genetic models and stem cell grafting into immunodeficient mice. Lineage tracing and clonal analysis studies suggest that the potentiality of these bulge resident stem cells differs during normal homeostasis and in wound repair or when grafting to alternative sites. Under normal homeostatic conditions, bulge stem cells become cyclically activated and can differentiate into all hair follicle lineages but not interfollicular epidermal cells. However, within the wound healing or grafting environment, the bulge resident stem cells can also give rise to interfollicular epidermal cells (20). Negative feedback loops allow lineage specific progeny to regulate the quiescence of the HFSCs by modulating their activation or cycling (15), while the dermal papilla can act as a temporary niche for HFSCs during distinct phases of the hair follicle cycle (13,14). Stem cells with different potencies are reported to exist within different regions of the bulge, with the $Lgr6^{+}$ isthmus stem cells

in mice generating sebaceous gland cells under normal homeostatic conditions, but also giving rise to interfollicular epidermal cells when provoked by wound healing (15,20,21).

Eccrine sweat glands are the most abundant glandular structures in the human body reaching densities of 200-700/cm^2. They assist in regulating body temperature in hot climates and secrete salt-enriched sweat fluids in response to emotional stimuli. The possible existence of sweat gland stem cells has recently been addressed by Lu et al. (22). This group characterised three adult progenitor cell types in the murine sweat gland and duct using elegant lineage tracing technologies. Each of these progenitors demonstrates a selective response when exposed to different injuries in the skin or on transplantation into different environments *in vivo*. It is of interest that, at least in the murine environment, these stem/progenitor cells appear to be unipotent in response to wound healing, but exhibit multipotency when grafted into different skin locations. The applicability of studies in the rodent to the location and potentiality of stem cell types found in the human skin however remains to be more fully defined.

In addition to this work examining the murine sweat gland, several groups have also noted the presence of epidermal stem cells within the human eccrine sweat gland. Biedermann et al. (23) directly compared human eccrine sweat gland cells to epidermal keratinocytes in terms of their ability to form multi-layered epithelia on collagen hydrogels *in vitro* and *in vivo* and showed that they could indeed provide an additional source of keratinocytes to generate a stratified epidermis. This raises the possibility that, rather than only epidermal and more specifically hair follicle stem cells being responsible for all homeostatic renewal of epidermis following injury as previously suspected, human skin may also be repaired and/or permanently renewed by eccrine sweat glands. Regardless of the site of harvest (scalp, axilla, abdomen and retro-auricular areas) (23,24), eccrine sweat gland stem cells (SGSC) acquire the properties of epidermal keratinocytes in engineered dermo-epidermal substitutes. In an alternative approach to placing scaffolds onto full thickness defects, Rittié et al (25) showed that in partial thickness human wounds, eccrine sweat glands and pilosebaceous units contributed more than hair follicles to re-epithelialisation by generating keratinocyte outgrowths that ultimately form new epidermis. Although the outgrowths expand at a similar rate, whether derived from sweat glands or pilosebaceous units, the former outnumber the

latter by around 3 to 1 indicating a major contribution of SGSCs to reepithelialisation of human wounds.

Two potential explanations for the transformation of sweat gland-derived epithelial cells exist. The first argues that a multipotent stem cell population proliferates and the new cells then differentiate in response to their epidermal environment. The other explanation states that sweat gland cells de-differentiate into a more naïve state after which they differentiate into a new phenotype, i.e., epidermal keratinocytes. As the newly created sweat gland-derived epidermis reaches a state of homeostasis *in vivo* (23), it is likely that both re-programmed sweat-gland derived cells and SGSCs are involved in forming and maintaining the epidermis.

Human SGSCs, in addition to helping to create and maintain epidermis have also been shown to adhere to polystyrene with a fibroblast-like morphology, proliferate rapidly (doubling time 4.3d) and when seeded on Matrigel, acquire an endothelial-like behaviour forming capillary-like structures and migrating across a scratch assay. Further, when implanted to rats, scaffolds seeded with SGSCs form widespread vascular networks compared to control (non-seeded) scaffolds outlining another function for these cells in addition to their role in homeostasis of the epidermis (24).

1.4 Mammalian wound healing – regeneration versus scarring

Wound healing involves a dynamic balance between the regeneration of the original tissue type versus the production of scar tissue, usually in response to a physical disruption of normal architecture. The equilibrium shifts depend on the specific tissue injured, the species involved and the stage of development of the organism. For example, post-natal bone and liver frequently heal by regeneration whilst central nervous system injury normally reverts to scar tissue. The enormous variability in species-specific healing is demonstrated by tail amputation in a newt (*Salamandridae*) with complete regeneration of structure as the rule. However in the mammalian limb, an amputation heals predominantly through scarring (26).

Normal mammalian wound healing involves three phases, which alter the intrinsic microenvironment (26). First, the *inflammatory* phase is characterised by a clearance of microbial contamination and removal of devitalised tissue. This is followed by a

proliferative phase where scar formation and tissue regeneration take place to varying degrees. Finally, a *remodelling* phase supervenes where the strength and structural integrity of the wound are optimised. After injury, platelets enter the wound through damaged blood vessels and initiate the inflammatory phase by degranulating to release, amongst other mediators, platelet-derived growth factor (PDGF) and transforming growth factor beta (TGF-β). Concurrently, the clotting cascade begins when tissue factor is released by damaged tissue and culminates in the formation of a fibrin clot which provides the scaffold for migrating cells to repair the wound (Figure 1.1). These cells include neutrophils, keratinocytes and macrophages that phagocytose debris and bacteria. With time, keratinocytes migrate over the fibrin gel to provide a new epidermal layer. Simultaneously, fibroblastic or mesenchymal cells proliferate to produce extracellular matrix (ECM) and endothelial cells (ECs) create new blood vessels, with both of these latter cells having been attracted by factors released by earlier cells such as macrophages. Over time, the fibrin matrix is gradually replaced with type III and, subsequently, type I collagen and covered by a layer of keratinocytes.

Changes in the skin microenvironment, during wound healing or where stem cells are transplanted to alternate locations, appear to alter their fate or differentiation along alternate lineage pathways. Superficial wounds heal by epithelialisation with keratinocyte growth and differentiation resulting in the resurfacing of the wound. The hair follicular, sweat gland and interfollicular stem cells are particularly important here as they enable reconstitution of the top layers of the skin without the need for grafting. Laminin α5 produced by pericytes has been demonstrated to regulate keratinocyte proliferation and migration and hence to promote epidermal regeneration and wound healing (27). If wounds cannot be re-approximated and are so deep as to have destroyed sweat glands and HFSCs, then re-epithelialisation can only occur from the wound margins, significantly delaying healing and leading to higher degrees of scarring and contracture (6).

The extent of the primary defect and time to healing are the predominant factors in determining the degree of scarring, although there are, additionally, clear genetic influences. Examples of the latter include a clear racial predisposition to certain forms of fibroproliferative scarring and the association of keloid scarring with specific gene signatures (28). When producing the optimal skin substitute, investigators need to be

aware of the wide spectrum of cells involved in wound healing in order to understand and replicate the wealth of functions imparted by such cells and their products.

1.5 The tissue engineering challenge for full thickness wound repair

Variability in skin thickness, and the type and density of adnexal structures determines the size of the reserve pool of stem cells and their progeny and this in turn allows skin in certain parts of the body to heal more readily than others. To enhance superficial wound healing, several keratinocyte preparations either in the form of a sheet (Myskin; Epicel) or a spray (Recell) have been developed (29,30), although they have limited use in full thickness defects lacking an *in situ* dermal component. There are also biological (31) and synthetic (32) proprietary materials that can be placed onto superficial/mixed depth wounds, that protect the wound bed and encourage healing, although these cannot be used for the treatment of full thickness wounds. These deeper wounds, where the epidermal and dermal layers, including the hair follicles and sweat glands, are destroyed, will attempt to heal from the peripheries. In the clinical setting, if, as a result of an extensive wound, healing is likely to take more than two weeks, skin grafting becomes advisable to minimise scarring (6). Whilst the depth and location of the insult determines whether or not skin grafting is required, the thickness of the applied skin graft is a key determinant of the final outcome. It has been suggested that collagen and ECM proteins in the dermis reduce wound contracture associated with myofibroblast infiltration (33). In contrast, healed skin with minimal dermal support is friable and susceptible to mechanical damage.

Despite significant advances in the treatment of full thickness wounds (in particular burns) to reduce their tendency to scar, improvements continue to be sought. One major target for tissue engineering is to create a composite layered skin substitute that replicates a standard FTSG, thereby negating the deleterious effect of creating a new wound at the donor site. A more practical alternative may be to produce a dermal substitute which, when co-applied with a standard STSG, significantly improves the final result comparable to a conventional FTSG. Significant limitations exist in the ability to recreate such a structure especially where this involves very large, acute full thickness wounds (29,34,35). Thus, in wounds where dermal preservation is not possible due to extensive full thickness skin loss that cannot be closed directly or because of a paucity

of donor sites for a FTSG, acellular skin substitutes have attempted to satisfy the need for a substantive dermal layer thereby aiming to limit any potential contraction and to improve the overall structural integrity of the healed wound (29). This approach is particularly important for burns and for the elderly and paediatric populations as thin STSGs are often used in the former because of a suboptimal recipient bed and in the latter because they have thin skin and a thick STSG would contribute to a significant delay in donor site healing.

1.6 Clinically available dermal scaffolds that mimic the niche

In developing the optimal skin substitute, Shevchenko *et al.* have highlighted the three most important requirements as patient safety, clinical effectiveness and convenience in application (29). Additionally, the ideal scaffold should also be both supportive and biodegradable.

The starting point for developing an artificial dermis should be the production of a 3-D scaffold that facilitates the migration and organised relationship of cellular constituents. Optimally, the composition of the scaffold should mirror that of normal skin. Collagen represents by far the most abundant structural protein within the connective tissue of the dermis (36). Collagen fibres are distributed either as a finely woven network in the papillary layer of the dermis or as thick bundles within the reticular dermis. The pilosebaceous units, eccrine glands and apocrine glands are also encircled by a thin meshwork of collagen fibres as are the blood vessels of the dermis (36). The papillary dermis and the surrounds of these structures are primarily composed of type III collagen in contrast to the thicker reticular dermis which is mainly type I collagen and the basement membrane (BM) in which type IV collagen is the predominant isoform. Smaller elastin fibres are also present throughout the dermis and start to appear after collagen at 22 weeks of gestation in the human (36). They are thickest in the lower dermis where, like collagen bundles, they lie parallel to the surface of the skin. Recently, it has been recognised that elastin may also play a significant role in production of the optimal dermal substitute particularly in relation to reducing wound contracture (37).

Ground substance describes the amorphous substance containing glycosaminoglycans and acid mucopolysaccharides filling the space between collagen and elastin fibres.

Mature dermal ground substance consists mainly of nonsulphated acid mucopolysaccharides such as hyaluronic acid, although healing wounds contain a greater proportion of sulphated acid mucopolysaccharides such as chondroitin sulphate (36).

The ECM supports the dermal microvasculature which is divided into two important strata. The superficial vascular plexus, between the papillary and reticular dermis, is in close proximity with the overlying epidermis and anastomoses with deeper arterioles and venules. The deep vascular plexus is found within and below the reticular dermis and contains larger calibre vessels that extend into underlying subcutaneous fat (Figure 1.1) (36).

The options for a dermal substitute are manifold. Given the constituents of normal skin and the histological features of a healing wound, it is not surprising that the most commonly used materials have previously been donor derived dermis or dermal substitutes based on such constituents as collagen, fibrin and hyaluronic acid. Many of these are, however, of animal origin. Burns and/or wounds have been treated with proprietary first generation decellularised human donor cadaveric dermis (DCD) such as Alloderm® or Epiflex®, decellularised porcine derived dermis such as Permacol™, synthetic acellular skin substitutes such as the bovine collagen type I based dermal equivalents Matriderm® and Integra®, and hyaluronic acid-based dermal equivalents such as Hyalomatrix PA and Hyalograft 3D. Tables 1.2a and 1.2b summarise these and other examples of dermal substitutes that have been used in the clinical setting.

DCD preparations require removal of allogeneic cells in the epidermis and dermis, while preserving extracellular matrix, elastin and collagen fibres and if possible the basement membrane. Meshing of the DCD, which is normally attached to the wound bed with a fibrin glue to limit shear forces and placed below a meshed autologous STSG or cultured epidermal cells, has been reported to be preferential to a solid DCD graft and to improve revascularisation of the autograft in acute burn injuries (33). Secreted factors from the STSG or an epidermal sheet are thought to enhance DCD revascularisation, with biopsied material approximating to normal skin histology where the burn area is relatively limited (29,33). Although the use of DCD for the management of full thickness or extensive acute burn injuries remains to be fully evaluated, these DCD-autologous STSGs have also

been used for the reconstruction of burn scar contractures and for keloid scar management (33,38).

For synthetic, acellular dermal substitutes, Integra® has been used widely to treat full thickness burns (39), but its architectural complexity results in delays of neovascularisation for 10-14 days. Matriderm®, although more expensive, has the benefit that it can be applied simultaneously with a STSG ensuring earlier wound coverage and negating further surgery for the patient. Matriderm® results in good graft take, improved elasticity and reduced wound contracture (40,41). Although a thinner form of Integra® has been developed recently in order to meet the demand for single-stage repair, there is only one published account of single-stage Integra® use (42). This has not been compared to a suitable control such as STSG alone and has only been used for the reconstruction of defects in the face which has a good vasculature. Therefore, evidence is lacking to demonstrate confidence in Integra® as a dermal substitute for single-stage wound repair.

Hyalomatrix PA is hyaluronic acid esterified with benzyl alcohol with a silicon layer that acts as an epidermal layer prior to grafting. Although there are no prospective or randomised studies for this dermal substitute, a retrospective series of patients treated with deep partial thickness burns produced encouraging results (43). Hyalograft 3D has a similar make-up but contains cultured autologous fibroblasts and has no silicon pseudo-epithelial layer. It has been reported to reduce wound contracture and to promote keratinocyte take and basement membrane formation *in vitro* (29), yet there are no significant prospective observational or randomised control studies reported and there is the necessity for a 2-stage reconstruction. The only publication on Hyalograft 3D is a small study in which a keratinocyte layer (Laserskin®) was compared with or without the autologous fibroblast-containing dermal substitute in high body surface area burns of 6 patients (3 for each subgroup). Although the results showed improved keratinocyte take when Hyalograft 3D was used, the power of this study is limited, particularly with regards to the small number of participants and the lack of a suitable control (44). Substitutes that are similar to Hyalograft 3D but use allogeneic rather than autologous fibroblasts (e.g. Dermagraft (45,46) and Apligraft (47,48)) have also been created with limited success.

Table 1.2a: Acellular scaffolds that have been used for partial/full-thickness wounds.

	Derivation	Technique/indications	Pros	Cons
AlloDerm® (33)	**De-cellularised cadaveric dermis** (DCD).	Meshed ultrathin STSG placed onto meshed AlloDerm in one-stage procedure	ECM composition closely mimics dermis Less contraction than graft alone Can use thin skin graft → donor heals quicker	Delayed revasc → immobilize 7-10d Questionable revascularisation (29) if 1 stage so STSG @ 4-7d advised
Epiflex® (49)	**DCD**	Directions for use not published – likely to require 2 stage procedure	2 year sterility (5 year shelf-life approval anticipated)	Limited human use. Only 1 human series in Peyronie's disease (50)
SureDerm®	**DCD**	Full thickness of deep partial thickness wounds and for scar reconstruction	2 year shelf life (refrigerated)	Necessity for 2-stage procedure.
dCell®(51)	**DCD**	Applied onto prepared wound bed with overlying vacuum assisted cl osure (VAC)® device	Healed chronic wound with no STSG Easy to handle and cheap (NHS produces from donor skin)	Only evidence was a chronic venous ulcer. Not yet tried for acute/large wounds.
Permacol®	Porcine **collagen**.	Mainly used in abdominal wall defect repair – sutured over defect. Revascularisation over months	Cheaper than human collagen matrices. Used in hernia repair (rapid bio-integration less essential).	Slow biointegration/ vascularisation so use for dermal reconstruction limited (52).
Matriderm®	Bovine **collagen**+**elastin**.	Single-stage procedure if healthy wound bed. If vascularisation suboptimal or 2 mm Matriderm®, 2 stage (STSG after 5-7d)	Can use as single stage to cover tendon, bone or joint (53) Long shelf life (5 years) Haemostatic (40)	High cost 2-stage repair for 2mm (or thicker) Matriderm®.
Integra® (29,39)	Bovine **collagen** and shark **chondroitin-6- sulphate**; **silicon** pseudo-epidermis.	Full thickness/deep partial thickness wounds/scar reconstruction. Coverage by thin meshed STSG 14-21d (54)	Long shelf life Low risk immune response/disease transmission Reduced contraction and scarring	10–14 days for vascularization 2-stage procedure High cost
Hyalomatrix PA®	**Hyaluronic acid** esterified with benzyl alcohol; **silicon** pseudo-epidermis.	Application to wound bed after debridement. 7-15d: silicon removed and STSG applied (55)	No animal/allogeneic/human-derived components. 4 year shelf life (room temperature) Good adult and paediatric safety profile	No prospective studies/RCTs. 2-stage procedure
EZDerm®	Porcine **collagen** cross-linked with aldehyde.	Applied to partial-thickness skin loss, donor sites or skin ulcers or as a temporary dressing for full-thickness skin loss	Minimises protein/water loss 18 month shelf life. Similar to allograft but cheaper Analgesic on application	Doesn't incorporate into wound Outcomes similar to petrolatum non-adherent gauze in partial-thickness burns (56).

Table 1.2b: Cellular scaffolds that have been used for partial/full-thickness wounds.

	Derivation	Technique/indications	Pros	Cons
Hyalograft 3D®	Esterified H**yaluronic acid** & autologous fibroblasts	Ulcers and deep/full thickness burns. Small skin biopsy → Fibroblasts cultured on Hyalograft 3D for 16d then grafted onto wound. Keratinocytes from biopsy also cultured and applied 7d later (Laserskin®)	All autologous. Reduced wound contracture and improved keratinocyte take and BM formation (*in vitro*) (29).	No prospective study/RCT 2-stage procedure.
Dermagraft®	**Polyglactin** mesh seeded with allogeneic neonatal **fibroblasts**	Predominant use chronic ulcers or burns (with STSG) Contra-indicated if exposed tendon /joint capsule/bone. Thawed, rinsed 3 times saline and placed into wound	Facilitates fibrovascular ingrowth and re-epithelialization. Faster wound closure in ulcers vs conventional therapy (45).	Stored at –60 to –80°C No difference vs meshed STSG alone (46) Similar outcome to allograft (38).
MySkin®	Subconfluent autologous **keratinocytes** on **silicone**	Ulcers, superficial burns and donor sites; full-thickness wounds with meshed skin grafts. 2x2cm shave biopsy → keratinocytes isolated and stored or grown on silicon layer → placed onto wound	Autologous cells.	3d shelf life. Often needs many applications. High cost.
ReCell (previously Cellspray)®	Autologous **keratinocyte** suspension & melanocytes, fibroblasts & langerhans cells	Chronic ulcers, donor sites & partial thickness wounds. Thin split thickness biopsy processed by surgical staff (20-30 minutes) → spray over area 80x that of biopsy	Autologous. On-site processing. Good cell viability. Better aesthetics + function (30).	Not suitable for full thickness wounds unless with dermal element.
Apligraf®	Allogeneic neonatal **fibroblasts** in bovine **collagen** I + allogeneic neonatal **keratinocytes** (29)	2x2cm shave biopsy. Cells frozen or grown on silicon-based scaffold for 2-14d then applied onto wound. Re-epithelialisation approx 4d. Can apply with STSG if full-thickness defect	Improved cosmetic and functional outcomes when with STSG vs. graft alone (47).	Requires STSG if full-thickness. 5d shelf life Only case reports (57) and comparison to placebo (48).
Epicel®	Autologous cultured **epidermal** autograft	Deep dermal or full thickness burns of total body surface area ≥ 30% (+ STSG or alone if not possible). Keratinocytes from 2 small (6cm) biopsies grown into approx. 50cm^2 sheets 2-8 cell layers	Reduced mortality compared to control in large burns (58).	Residual amounts murine cells (xenotransplantation product). Must be used within 24 hours once released by laboratory.

1.7 Revascularisation of engineered grafts

Although recent research has focused on defining the stem cell niche in the skin (particularly in rodents) and the circulating stem and progenitor cells involved in wound healing, one critical consideration for tissue engineering skin in the clinical setting is the issue of maintaining a sufficient blood supply to the graft. For dermal substitutes covered with STSGs, the process of *inosculation* is of major importance. This describes how established vessel networks within the dermal component of the STSG and recipient wound bed connect to one another across the interface of the dermal substitute (59,60). This has the vital role of nourishing the emerging epidermal layer.

Clinically, there are at least two suggested strategies to produce a vascularised dermal equivalent to improve wound healing. One uses the scaffold's physicochemical properties to mimic the optimal microenvironment to encourage rapid host cell ingress and maturation (61). The other involves the establishment of a pre-formed vascular network *in vitro* prior to grafting onto a host wound bed (62). Both techniques accelerate wound healing with improved neovascularisation and migration of host cells *in vivo* using immunodeficient mouse models (61,62) and both options take a similar total timeframe to achieve revascularisation with the host, approximately 2-3 weeks (62,63). Of the two strategies and in view of the similar timeframe for development of a neo-circulation, the more powerful approach, pragmatically would be the assured creation of a vascular network in a portable scaffold *ex vivo*. This would be preferable to expecting a scaffold with no intrinsic microcirculation to form one and link up to the wound-periphery or recipient bed, particularly in a patient with high total body surface area burns in whom a large acute wound bed is less receptive to neovascularisation and has a high risk of infection. An early systemic concern which might limit the success of immediate graft placement is the massive fluid shift in patients with large burns due to increased capillary permeability, the resulting systemic hypotension triggering intense peripheral vasoconstriction hindering the capability of a scaffold to integrate with a wound bed. Whilst early systemic compromise was being reversed, for example by fluid administration, production of an autologous, pre-vascularised, dermo-epidermal graft would ensure it did not interfere with other patient treatments. Practically, a time window of several weeks is frequently present in severe burns where limitations in donor site availability may necessitate temporising a wound with cadaveric skin until a

suitable alternative, such as re-epithelialised donor site or a newly created pre-vascularised scaffold, becomes available.

1.8 Endothelial progenitor cells and vessel formation

A detailed understanding of the process of revascularisation is essential for the development of vascularised grafts. Over recent years there has been significant debate surrounding the identification of endothelial progenitor cells, which give rise to the vasculature and the microenvironment in which the vasculature develops. The various different endothelial progenitor cell populations have recently been reviewed (64–66) and show endothelial colony forming cells (ECFCs) to be 'true' progenitors. This is in contrast to early endothelial progenitor cells (EPCs), also called colony forming unit-endothelial cells (CFU-ECs) or CFU-Hill (67) that are described as endothelial progenitors but are in fact haemopoietic in origin (although they may possess pro-angiogenic abilities). Such 'EPCs' are positive for the cell-surface markers CD31, CD45, CD14, CD105, CD146, VEGFR-2, CD144 and vonWillebrand Factor (vWF), have the ability to take up acetylated low-density lipoprotein, and do not form secondary/tertiary endothelial colonies on re-plating. Morphologically, they appear 'spindle like' and functionally they do not form vascular tubules (67–70). The presence of CD14 and CD45 on these cells indicates that they are haemopoietic/monocytic rather than endothelial in origin. In addition, markers such as CD31, CD144, VEGFR-2, vWF and endothelial nitric oxide synthase are not necessarily endothelial specific (64) and can be detected, for example, in monocytes cultured with endothelial growth factors (65). To investigate these subpopulations of ECs further, *Gulati et al.* (70) seperated $CD14^+$ and $CD14^-$ MNC fractions showing that CFU-ECs developed from the $CD14^+$ population of cells whilst cells with a more pronounced endothelial phenotype and intrinsic angiogenic potential developed from the $CD14^-$ fraction. The separation was repeated at d7 in culture with the same outcome confirming that the vast majority of cells reported to be EPCs express CD14, originate from $CD14^+$ MNCs, and, critically, do not serve as precursors for the endothelial lineage. Thus, CFU-Hill or early EPCs do not belong to the endothelial lineage.

The $CD14^-$ cells have been described in the literature as late EPCs, endothelial colony forming cells (ECFCs), blood outgrowth endothelial cells (BOECs) and endothelial

outgrowth cells (EOCs), and have been confirmed to belong to the endothelial lineage (64,70). The cells have 'cobblestone' morphology when cultured *in vitro* (65,69,71–77) and are found in cord blood (CB), peripheral blood (PB), bone marrow and in vessel walls, such as the umbilical vein (71–78). ECFCs have a hierarchy of proliferative abilities, comprising high proliferative potential (HPP)-ECFCs, low proliferative potential (LPP)-ECFCs and endothelial clusters. A higher percentage of ECFCs with relatively greater telomerase activity are found in cord blood (CB) than in adult peripheral blood (PB) (65,69,71–77).

There is no single marker to define ECFCs, and a combination of markers has been used to confirm their identity within a heterogeneous population. Positive markers include CD31, CD34, CD105, CD146, VEGFR-2, vWF and Tie-2, while ensuring these are $CD45^-$ and $CD14^-$. These cells form vascular tubule networks both *in vitro* and *in vivo* (69,70,72,78–83). The main phenotypic difference between these cells and CFU-Hill is that the latter also express CD45 (haemopoietic specific cell surface antigen) and CD14 (monocyte/macrophage cell surface antigen), whereas ECFCs do not.

The problem with creating a vascular network using an autologous population of ECFCs is their relative scarcity in adult PB. Furthermore, phlebotomy to isolate sufficient numbers of ECFCs from patients with significant burns would require such large volumes of blood that, even accounting for expansion in culture, there is a serious ethical issue of compromising an already unwell patient further by risking hypovolaemia. Other practical issues relating to the use of PB ECFCs is that their growth kinetics are slower than for umbilical cord or CB ECFCs, the time taken to grow ECFC-derived colonies from PB is 1-2 weeks more than from CB and PB colonies also often appear smaller (72,73,77,84). In addition, CB ECFCs can be expanded for more than 100 population doublings (PDs) without signs of senescence, whilst PB ECFCs can only be passaged for 20 to 30 PDs(72). Thus there are potential barriers to using autologous PB–ECFCs to rapidly create a pre-vascularised dermal substitute for clinical use (85,86).

A recently identified alternative source of ECFCs is adult adipose tissue (87). The harvest of such cells would not significantly compromise systemic physiology in patients already under anaesthesia for wound debridement of a major burn, but again absolute numbers may be limited in adult tissues. In addition, adipose tissue contains mesenchymal stem/stromal cells (MSCs) which are also required to stabilise newly formed vessels (88).

In semi-elective cases, such as scar revision, or resurfacing after skin malignancy or a chronic nonhealing ulcer, there may be a role for harvesting and growing ECFCs in order to produce a suitable pre-vascularised scaffold *in vitro* in preparation for a planned trip to theatre to cover the wound. Unlike the situation for acute burns, there is no time constraint prior to undergoing definitive surgery. As an example, in giant congenital melanocytic naevus, in view of the risk of malignant transformation (4-7% lifetime risk) (89) and the aesthetic improvement conferred by removal, surgical excision is common (90). Although the majority of such cases can be managed through serial excision or expansion followed by excision, there are cases where STSGs may still be used (91,92). In these cases, there may be a role for using easily isolated and propagated ECFCs (which in this particular case could be directly isolated from CB or umbilical cord) to produce a pre-vascularised dermal scaffold that would augment a STSG. Although autologous CB or umbilical cord ECFCs would work in this case and in other congenital skin disorders such as Aplasia Cutis Congenita, there would be issues using banked allogeneic umbilical cord or CB ECFCs in adult populations as ECFC survival may be compromised by CB cryopreservation (73) while allo-transplantation would induce graft rejection.

1.9 Isolation and culturing of endothelial colony forming cells

Table 1.3 summarises the various techniques for isolating and culturing ECFCs from different sources including purification steps and plating substrates/medium. The most commonly used plate coatings are gelatin, fibronectin (FN) or collagen I and the different techniques add either fetal bovine serum (FBS), human plasma or pooled human platelet lysate to medium to optimise ECFC expansion.

Standard adult blood samples of 300mls have been reported to contain as little as a single ECFC, but this varies amongst donors (73,82). Our own studies indicate that there are <1-2 ECFCs per 10^8 MNCS in adult PB and approximately 15 fold more in CB, with the number isolated from the latter correlating inversely with placental weight at birth (74,93). With certain donors, a single CB unit could produce at least 10^{12} to 10^{14} endothelial progeny over 1-2 months of culture. In comparison, a single PB donation can produce at least 10^7, and sometimes significantly more, ECs over 1-2 months of culture. Both CB and PB ECFCs can be used to produce tubular structures when co-cultured with fibroblasts or MSCs though CB ECFCs seem to do so more consistently and robustly

(73,94). In view of the limited number of ECFCs present in PB, one would intuitively expect to need prohibitively large quantities of peripheral blood to isolate sufficient ECFCs to use in tissue engineering yet this is not necessarily the case with one research group isolating more than $1x10^8$ ECFCs by day 30 from 5ml of fresh blood (95).

Isolation of ECFCs from adipose tissue is a recent development whereby minced adipose tissue or lipoaspirate can be processed to isolate the cells, and is accompanied by cell selection procedure(s) to purify the ECFCs. $CD44^-$ (87) and $CD31^+$ fractions (96) can produce characteristic colonies by day 4 or 7 respectively with the added benefit that the 'waste' product from the cell selection ($CD44^+/CD31^-$) can be used to generate a population of Adipose-derived MSCs. Other groups have sought to isolate ECFCs using alternative cell surface markers combined with either magnetic bead or polychromatic flow cytometry approaches. This has the advantage that the proliferative ability of the isolated cells is not compromised by prior culture. Tura *et al.* (78) for example enriched $CD133^-CD34^+CD146^+$ ECFCs from CB and PB. Case and colleagues (97,98) further demonstrated that CB ECFCs could be enriched after $CD34^+CD45^-$ selection and more closely defined the phenotype of ECFCs with a set of cell surface markers (99). Despite these advances, a single specific marker to purify ECFCs still remains elusive.

Table 1.3: Techniques for the isolation of ECFCs.

	Source	Purification	Plate coating	Culture conditions	Cell progeny	Other findings
Lin 2000 (79)	50-100ml PB	-	Type 1 collagen/ Fibronectin	• EGM-2 • Wash at 24h • Daily media change	• 10^{19} cells by 6 weeks	Most circulating ECs from vessel walls & limited growth capability. ECFCs mainly from transplanted BM
Hur 2003 (61)	50ml PB	-	2% gelatin	• EGM-2 + 5% FBS • Wash at d6 • Media change every 3d	• ECFCs after 2 weeks • 1 x10^{11} cells by 12 weeks	ECFCs incorporated with HUVECs better than CFU-ECs.
Gulati 2003 (70)	50-100ml PB	$CD14^-$	Fibronectin	• EGM-2 + 2% FBS • Daily medium change	• ECFCs seen after 2 weeks • >20 passages	ECFCs from $CD14^-$ fraction, CFU-ECs from $CD14^+$ fraction. Capillaries better in ECFCs than CFU-ECs
Ingram 2004 (72)	50ml PB; 20-70ml CB	-	Type 1 collagen	• EGM-2 + 10% FBS • Wash at 24h • Daily media change for 7d	• ECFCs d5(CB), d14(PB) • 10^{33} (CB) d200 • 10^{10} (PB) d100	15x ECFCs in CB vs. PB; CB & PB formed capillary-like structures in Matrigel (CB faster)
Melero-Martin 2007 (83)	50ml PB; 20-70ml CB	$CD31^+$	1% gelatin	• EGM-2 + 20% FBS • Wash at 48h (CB) or d4 (PB) • CD31+ ECFCs FN–coated plates	• CB ECFCs 1 week • 10^{14} CB ECFCs 40d (PB ECFCs 10^8)	CB ECFCs combined with SMCs (4:1 ratio) in Matrigel (47.5 microvessels/mm^2).
Hofmann 2009 (95)	5ml PB (use within 2 hours)	-	Uncoated	• EGM-2 + pHPL. • 24h wash and media change. • 30% medium change 2x/week	• ECFCs by d12.	4 ECFC-colonies per ml PB. > 1 x 10^8 cells in 30 days
Reinisch et al 2009 (132)	6-24ml PB		Uncoated	• Fresh blood diluted EGM/10% pHPL before seeding. Wash at 24h.	• 1st colonies d8.6 • 1.5x10^8 after 1 passage	4 colonies/1mL whole blood vs <1/ml after density gradient separation. *In vivo* PB/CB ECFC microvessels similar

Athanassop-oulos et al 2010 (73)	50ml PB; 60-120ml CB	-	Type 1 collagen	• EGM-2 + 10% FBS. • 24h wash • Medium change alternate days	• ECFCs d5(CB); d14 (PB) • d60: $2.2x10^{11}$ (PB); $1.8x10^{13}$ (CB) ECFCs.	27x CB ECFC colonies than PB. Youngest PB donor (33 y.o.) 295 fold expansion vs. average (1 month). CB ECFC > PB ECFC tubules.
Szöke et al 2012 (87)	300-600ml lipoaspirate	$CD44^-$ECFCs; $CD44^+$MSCs	1% gelatin	• Cells in MCDB 131 medium + 7.5% FBS + abx + growth factors. • d4-5 wash.	• ECFCs d5. PD time 2.3d. Log growth to p14-p19. d42-56 $>1x10^{11}$ cells	Fresh ECs - no capillary-like structures on Matrigel unlike cultured ECs. Tubule-like structures with AT-ECs alone (better +AT-MSCs)

1.10 Developing the next generation vascularised scaffolds and smart biomaterials

Table 1.4 summarises examples of research where a variety of scaffolds with or without ECs have been used in an attempt to promote and improve wound healing in *in vitro* and *in vivo* models (62,63,74,94,100–112). In such examples, human umbilical vein endothelial cells (HUVECs), CB ECFCs or human dermal microvascular endothelial cells (HDMECs) together with fibroblasts or various sources of MSCs, seeded within fibrin, collagen or matrigels, produced a well-formed capillary network *in vitro*. These constructs *in vivo*, in a subcutaneous pocket murine model (63) or a full thickness cutaneous wound in a rat (62), accelerated functional anastomoses with the host vasculature, fibroblasts, pericytes or MSCs stabilising vessels, encouraging lumen formation and promoting basement membrane assembly (60,113–116).

Seeding commercially available and compatible biosynthetic dermal scaffolds such as Integra™® or Matriderm® with ECFCs and human dermal fibroblasts (hDFs) or MSCs has enabled vascular networks to form to a depth of approximately 100µm *in vitro* 1-2 weeks (73). In other examples, ECFCs on a fibroblast sheet placed onto a murine full thickness wound (85), fibroblasts within and keratinocytes on top of a collagen gel in a lapine full thickness wound (112) and ECFCs together with MSCs within Matrigel® in a subcutaneous pocket of a mouse (105) have demonstrated significantly improved neovascularisation in comparison to gel alone.

The alternative to pre-forming microvascular networks is to create a perfectly ordered scaffold (cellular or acellular) that can initiate rapid host cell migration and integration. For example, the placement of a simple 1mm-thick dextran-based hydrogel without cellular components into an *in vivo* murine full thickness wound encouraged a rapid influx of host ECs and enabled more rapid neovascularisation than an identical thickness of Integra®, further illustrating the potential benefits of novel gels over current dermal replacement scaffolds (61). Gel fabrication with functional amine groups enhanced host biocompatibility while substitution of cross-linking groups promoted tissue infiltration, neovascularisation and hydrogel degradation ensuring almost complete digestion of the hydrogel by day 7. This all contributed to host repair of the area with significant skin maturation to normal thickness including hair follicles and sweat glands by 5 weeks (61).

Prior to neovascularisation, primary ischaemia limits the thickness and viability of any potential engineered construct. Therefore, authors have recently attempted to create *in vitro* perfusable blood vessels within cell sheets by placing them over resected tissue with a connectable artery and vein as a vascular bed. Media passed below the sheets via a bioreactor produce perfusable blood vessels within the sheets as long as endothelial cells are included within constructs (117). Thicker engineered tissues can subsequently be produced by overlaying several sheets *in vitro*. Alternatively, cell sheets can be placed over collagen-based microchannels, again with medium passed through the channels to stimulate the formation of new capillaries (118). Theoretically, such a template could be used to produce a pre-vascularised scaffold to mimic skin *in vitro* by placing the scaffold (collagen, fibrin or alternative gel) containning endothelial cells over a vascularised bed or a gel containing perfused microchannels.

Early inosculation as a result of implant pre-vascularisation would allow for a more rapid ingress of host cells and factors, increasing the trajectory of wound maturation and repair (6). Recent research into biomaterials has focussed on the potential to imprint blood vessel patterns with ordered geometry using computer controlled techniques into 3D flexible, elastic and biocompatible scaffolds. These approaches are being further refined by functionalising the inner walls of the synthetic tubules, for example with proteoglycans such as heparan sulphate and anchor peptides which will capture vascular cells and their products, thereby resulting in the generation of functional vessels extending more deeply within scaffolds while being capable of rapid inosculation with host vessels (119–121).

Some authors advocate combining fibronectin (FN), a high molecular weight component of the ECM, with a standard collagen I gel in order to amalgamate the structural properties of the latter with the cell-adhesive and survival enhancing properties of the former. FN also plays a significant role in growth, migration and wound healing (122). By seeding HUVECs into these constructs, particularly with MSCs, it was possible to create fully functional and longer lasting vessels *in vivo* (100,101). FN is widely expressed by multiple cell types and is critically important in vertebrate development. It is an abundant soluble constituent of plasma (300 μg/ml) and other body fluids and also part of the insoluble extracellular matrix. It is often subdivided based on its solubility into plasma FN (more soluble) and cellular FN (less soluble). Of note, the alternative splicing

of precursor mRNA from the single FN gene has the capacity to produce a large number of variants, generating FNs with different cell-adhesive, ligand-binding, and solubility properties thereby affecting the composition of the ECM in a tissue-specific manner. FN has a wide variety of functional activities besides binding to cell surfaces through integrins. It also binds to a number of biologically important molecules including heparin, collagen/gelatin and fibrin. The collagen-binding domain binds far more effectively to denatured collagen than to native collagen implying that FN may bind to unfolded regions of the collagen triple helix. The physiological function of the collagen binding domain may be more related to binding and clearance of denatured collagenous materials from blood and tissue than to mediating cell adhesion to collagen (122).

The concentration of collagen matrices also significantly influences ECFC induced vasculogenesis. Comparing collagen I gel (containing FN) at concentrations ranging from 0.5mg/ml to 3.5mg/ml, Critser *et al.* (123) demonstrated that increasing the collagen concentration significantly decreased ECFC derived vessels per area (density), but significantly increased vessel sizes (total cross sectional area). These examples provide some insight into how a variety of parameters determine the extent to which the scaffold is incorporated including its density and surface composition.

Recent research is more closely defining the molecular mechanisms which regulate vessel formation as exemplified in (124–128). The addition of pro-angiogenic proteins or molecules such as vascular endothelial growth factor (VEGF) and basic fibroblast growth factor (bFGF) to scaffolds is a further strategy that has been used in attempts to improve wound healing outcomes. As early as 2005, Stahl *et al.* confirmed that by adding VEGF or bFGF to HUVECs and early EPC–spheroids within a collagen matrix, it was possible to significantly improve vascular sprouting activity *in vitro* (104). More recently, human dermal fibroblast (hDF)-seeded dense-collagen depots were preconditioned under physiological cell-generated hypoxia to up-regulate key angiogenic factors such as hypoxia inducible factor-1α (HIF-1α) and VEGF. Angiogenic factor delivery from pre-conditioned, non-viable depots rapidly induced an angiogenic response within HUVEC-seeded constructs *in vitro*. Implanted acellular 3D collagen constructs incorporating such angiogenic depots in their core were infiltrated with perfused vessels by 1 week *in vivo*, at which stage non-angiogenic implants were minimally perfused (108). In another example of VEGF incorporation improving angiogenesis, VEGF encapsulated into

nanoparticles and then seeded into Matrigel or onto poly(lactic-co-glycolic acid) (PLGA) scaffolds showed consistently improved levels of angiogenesis when placed into murine intraperitoneal fat pads (106).

The next generation of therapies attempt to combine various cells and biologics with smart biomaterials with defined topography, porosity and well-ordered geometry in order to increase the speed of cell infiltration and to improve and direct oxygen and nutrient transport and vascular patterning (119–121,129).

Table 1.4: Acellular and cellularised gels and scaffolds for re-vascularisation

	Cell(s)	Scaffold/gel	Method	Outcome(s)
Schechner 2000 (100)	HUVECs	Collagen I [C](1.5mg/ml) and FN (90mg/ml)	• After 20h construct implanted into subcutaneous pouch in SCID mice.	• *In vitro* @18 h HUVECs organize into cords @24h cords developed lumena. @48h HUVECs dead. • *In vivo* @d31 thin-walled tubes containing erythrocytes.
Koike 2004 (101)	HUVECs; 10T1/2 murine MSCs	C (1.5mg/ml) and F (90mg/ml)	• $1x10^6$ HUVECs (HUVEC alone) or $8x10^5$ HUVECs and $2x10^5$ 10T1/2 MSCs (co-implantation group) in 12 well plates. • D1: 4mm disc implanted in SCID mouse.	• D4: lumena present in co-implantation group. • 4 months: engineered vessels stable and functional. • HUVEC alone group vessels disappeared by 60d.
Wu 2004 (102)	ECFCs; SVSMCs	PGA-PLLA (polyglycolic acid-poly-L-lactic acid)	• CD34pos CD133pos cell selection from CB. • Loss of CD133 expression in culture (i.e. ECFCs) • ECFCs $\pm$ SVSMCs onto scaffold *in vitro*.	• 76.5 microvessels/mm^2 in ECFC + SVSMC group. • None if ECFCs used alone.
Tonello 2005 (103)	hDFs; HDMECs; Keratinocytes	Esterified Hyaluronan (form of Hyaluronic acid)	• hDFs within scaffold – culture 1 week • Add HDMECs – further 10d culture • Add Keratinocytes – culture 1 week; air-liquid interface 3 weeks.	Well-developed dermal structure beneath stratified epidermis. Capillary like structures (CLS) by d21.
Stahl 2005 (104)	HUVECs/early EPCs + osteoblasts	C (1.5mg/ml)	• HUVECs/EPCs spheroids seeded into C gel with osteoblasts. • EGF and bFGF added.	• 36h: low baseline sprouting • +VEGF and bFGF: sprout number/length increased • +osteoblasts in matrix: HUVEC sprouting inhibited.
Melero-Martin 2008 (105)	PB/CB ECFCs and BM/CB MSCs	Matrigel	• $1.9x10^6$ cells (acellular control) in 200µl Matrigel® (ECFCs:MSCs 100:0, 80:20, 60:40, 40:60, 20:80, 0:100) • Implanted onto backs of athymic mice.	• CB ECFC:MSC: numerous vessels with erythrocytes. • Matrigel®:CB ECFCs alone: no vessels. • MSCs alone: murine capillaries; no human vessels.

Chen 2009 (63)	HUVECs; fibroblasts [1:5]	Fibrin (10mg/ml)	3 groups implanted in immunodeficient mice: • UVECs + fibroblasts 7d prior to insertion /HUVECs + fibroblasts 24hrs before insertion (+ve control) / HUVECs only	• 4: lumenised capillaries; d7: anastomosing capillaries. No fibroblasts → no capillaries • *In vivo*: Vessels d5 (control d14). HUVECs only →No perfusion
Montano 2010 (62)	HDMECs	Fibrin (7-15 mg/ml), C (2.5-3.5mg/ml) or mix	• $1x10^4$, $3x10^4$, $5x10^4$, $1x10^5$, $2x10^5$ HDMECs added • Gels cultured for 3 weeks → Placed onto 2.6mm full thickness wounds on immuno-incompetent rats.	• Optimal gel: 10 and 11mg/ml fibrin → 3D lumenized vascular structures; optimal cell number $3x10^4$ cells/ml. • D15 first lumenized segments.
Helary 2010 (107)	hDFs; acellular in vivo	C (0.66 [normal collagen hydrogel], 1, 3 and 5mg/ml [concentrated collagen hydrogels 1, 3 and 5])	• *in vitro*: hDF added to NCH and CCH 1, 3 and 5. *In vivo:* acellular NCH versus CCH3	• hDFs contract NCH 3% after 14d; CCH5 gels granulous & heterogenous; CCH3: no contraction 7d; <50% 14d. • 14d *in vivo*: NCH hydrolysed; CCH3 integrated & colonized by host cells with neovascularisation.
Des Rieux 2010 (106)	Acellular	Matrigel™ hydrogels and PLGA scaffolds	• VEGF encapsulated into nanoparticles → seeded into Matrigel™ → subcut. injection/ PLGA scaffolds in intraperitoneal fat pad	VEGF encapsulation improved angiogenesis *in vivo* with both type 3D matrices.
Hadjipanayi 2011 (108)	HUVECs; hDFs	C	• hDFs seeded within collagen • Pre-conditioned to up-regulate HIF1α and VEGF • nap-frozen, Pplaced into collagen gel with HUVECs.	• Angiogenic response in EC constructs in vitro. • Implanted acellular 3D constructs with angiogenic depots infiltrated with perfused vessels by 1 week *in vivo*.
Hegen 2011 (109)	HDMECs; hPASMCs	Poly-L Lactic Acid (PLLA) scaffolds filled with Matrigel®	• Scaffolds: $1×10^6$ cells in 36 µl 50:50 EGM-2/Matrigel. • Scaffolds seeded with $1×10^6$ HMVEC; $1×10^6$ hPASMC; 1:1 ($5x10^5$ HMVEC: $5x10^5$ hPASMC); 1:4 ($2x10^5$ HMVEC: $8x10^5$ hPASMC); acellular	• D7: Patent vessels in HDMECs & hPASMCs scaffolds. • No vessels in acellular or hPASMC only. • D14: Microvasc density in HMVEC-hPASMC (1:1 and 1:4) scaffolds enhanced 2.5- and 4-fold vs HMVEC alone.
Yee 2011 (110)	CB ECFCs	Hyaluronic acid (HA)	• $2x10^6$/ml ECFCs within 3 different concentrations of HA hydrogels.	• Stiff (0.22%) matrix ECFCs remained rounded and could not form CLS @96hrs. • CLS best @48hrs in lowest concentration gel (0.056%).

				• CLS not seen in non-supplemented media (no VEGF).
Sun 2011 (61)	Acellular	Dextran hydrogel versus Integra® versus no treatment	• Full thickness murine burn model (8mm burn). • Wound excised and covered with dextran/Integra® and Duoderm® dressing or dressing alone.	• D5 hydrogel: ECs & lumina. Integra/control: no ECs. • 3 weeks: Dermal regeneration with appendages. Degradation of hydrogel (scaffold undigested in control). • 5 weeks: new hair growth; appearance of normal skin.
Rao 2012 (111)	HUVECs and BM MSCs	Fibrin, C or mix	• C/Fibrin 2.5 mg/ml composite gels (ratios 100/0, 60/40, 50/50, 40/60, and 0/100. • HUVEC:MSC 5:1, 3:2, 1:1, 2:3 and 1:5 ($6x10^5$ cells).	• Vasculogenesis decreased in highest EC:MSC ratio. • Network formation increased with increasing F content • D7: ECs and MSCs co-localized as capillary like structures.
Ananta 2012 (112)	Keratinocytes and fibroblasts.	C I stabilised with PLGA (Vicryl) mesh then compressed	• LSE-M (living skin equivalent – monolayer) – Keratinocytes. • LSE-M to air liquid interface 11d → LSE-S (stratified). • 2x2cm skin defect to panniculus carnosus muscle. 4 variables (LSE-M, LSE-S, FTSG, no treatment).	• Good fibroblast viability within gel • More inflammation in LSE than acellular group (CD45+). • 4x lumina (CD31+) in LSE-S group than acellular group.

1.11 Perspectives

Investigators have identified the improvement of existing dermal substitutes as a fundamental objective in reducing scarring following full thickness skin loss. Comprehensive knowledge of the stem cell niche within skin, the normal and abnormal wound healing responses, vessel-forming endothelial progenitor and pro-angiogenic cells, ECM proteins, next generation scaffolds and the molecular mechanisms of vessel formation provides a clear foundation on which to improve existing dermal replacements. The ability to optimise scaffolds based on imprinted biomaterials, which can be enhanced with specific molecular and cellular constituents, should enable the creation of off-the-shelf products which, when used either in isolation or together with STSGs, closely mimic the structure and function of human skin.

Solving the problem of how to rapidly re-vascularise grafts/substitutes will expedite the wound healing process and thus limit scar formation. Currently, the ability to select ECFCs post-natally from PB and adipose tissue is possible, but the process still takes several weeks and the ECFC content is generally considered low. Although recent interest in tissue engineering for skin regeneration has centred on these cells and the overall strategy of enhancing vasculogenic potential of scaffolds, lack of autologous ECFC availability after injury may require an alternative approach. The adaptation of the healing skin microenvironment to the structure of potential matrices may be a more suitable and achievable future perspective in the first instance. For example, the production of a scaffold that closely replicates the microenvironment of a healing wound may potentially enable improved host progenitor cell migration and integration with consequent earlier wound healing and regeneration of normal tissue. Already, a plethora of acellular scaffolds has been made from collagen, hyaluronic acid and fibrin in an attempt to replicate the microenvironment of normal skin regeneration for larger wounds. Through further study of skin and vascular stem/progenitor cells, reprogramming mechanisms, signalling pathways, cell adhesion molecules and the cellular secretomes that affect endothelial proliferation, differentiation, migration, angiogenesis and vasculogenesis, it may be possible to create a product that further improves the speed of graft ‘take’ and therefore the quality of regenerated skin. Replication of skin microenvironments in novel pre-patterned functionalised scaffolds

with key biologics and/or cells can then be used as a springboard for further studies that promote vasculogenesis and angiogenesis to further improve outcomes in wound repair. Figure 1.2 summarises some of the many novel therapeutic possibilities that should enable increased options for skin resurfacing and improved therapeutic outcomes.

A key determinant for the development of future skin substitutes involves the manufacture of such products under good manufacturing practice (GMP) conditions. In addition to the cost implications of producing a scaffold containing autologous human cells or unique biologics under GMP, account needs to be taken of automation and increased regulatory requirements and costs. In the current climate of financial instability, some medical institutions may be loath to sanction expensive tissue-engineered products with only limited clinical benefits over existing therapies. The production of a novel scaffold containing autologous cells and/or biologics will need to show a significant clinical benefit to overcome these hurdles. Although the literature suggests that it is relatively straightforward to culture autologous cells and implant them within and onto scaffolds to enhance wound repair, the complexity of quality control testing is a significant obstacle to achieving this goal. In the case of autologous cells obtained via tissue biopsies, tissue collected in various clinical surroundings under differing conditions may result in variances in size, condition, and site of harvest. Because each patient presents a unique set of clinical circumstances, these and other variables tend to be outside of the control of the tissue engineering facility but can affect the growth and performance of the living cells. The costs of controlling the multiple in-process variables including cleaning, sterilization, personnel training and the maintenance/calibration of equipment cannot be underestimated. This is particularly the case for a product where adult derived autologous ECFCs are used as the timeframe for culture and neovascularisation within a novel scaffold is likely to be several weeks. Existing ‘user-friendly’ substitutes that do not require specialist expertise have multiple weaknesses and, were it possible to create an improved scaffold using autologous cells and biologics to reproduce the physical characteristics and appearance of skin, then providing this is financially viable it would be universally accepted.

A significant benefit of using autologous cells for a skin substitute is that infectious risks associated with allogeneic/xenogeneic tissues are negated. The full spectrum of

infectious agents that might be transmitted by xenotransplantation in particular is not known, and agents that produce only minimal symptoms in animals may have the capacity to cause severe disease in humans. The GMP manufacture of an autologous cell-containing skin substitute is therefore theoretically more straightforward, however, the process is still very labour intensive from the harvest of cells under aseptic conditions to the careful management of cell culture operations in terms of quality of materials, manufacturing controls, equipment validation and monitoring. Further, acceptance criteria must be established for all media and components, including serum additives and growth factors and relevant records kept of components used including culture media. Maintenance of cell viability and/or relevant biologic function(s) must also be demonstrated post processing and all materials being implanted into a patient with the cells or tissue must be tested and documented as biocompatible with other cells or tissues at the implant site.

1.12 Aims and objectives of this thesis

In this MD thesis, the main aim was to use existing knowledge of scaffolds and progenitor cells in order to **produce a novel dermal substitute containing vascular networks formed through the interactions of purely adult derived stem/progenitor cells**.

In order to do this it was necessary to:

- Establish a bank of and characterise ECFCs sourced from cord and peripheral blood and MSCs from adipose tissue for wound repair.
- Examine ECFC chemotaxis and chemokinesis within various collagen and fibrin gels.
- Examine vascular network formation within compressed and uncompressed collagen gels.
- Assess up scaled, pre-vascularised dermal scaffolds within immunodeficient mice.

Figure 1.2: Novel methods to generate tissue engineered skin/dermis that will improve the reconstruction of full thickness defects

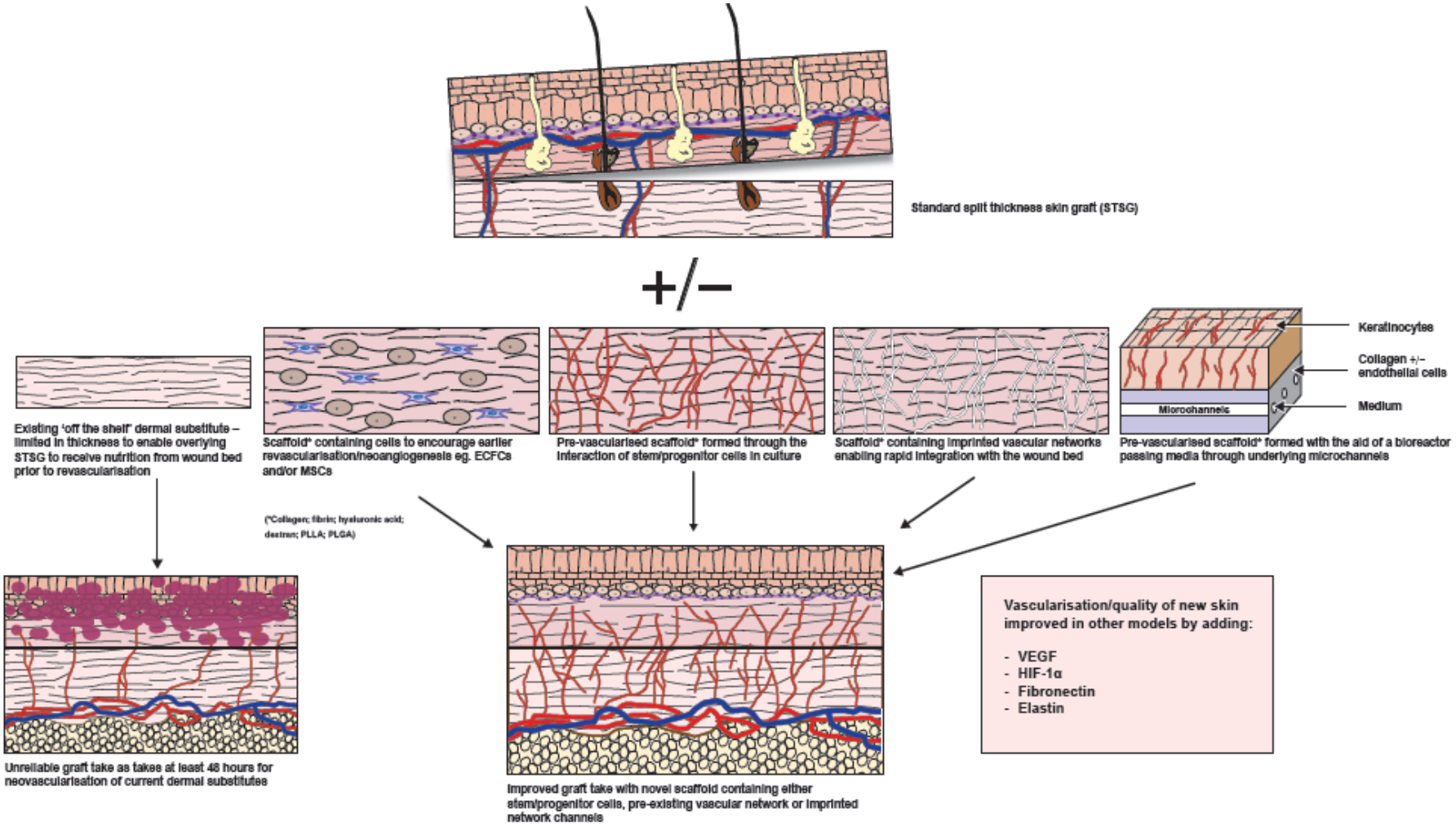

CHAPTER 2

Materials and Methods

2.1 Reagents

Reagents	Company
Accutase in PBS with 0.5mM Ethylenediaminetetraacetic acid (EDTA)	PAA Laboratories GmbH, Pasching, Austria
Adipogenic maintainance/induction medium	Lonza Biologics, Tewkesbury, UK
Alcian blue	Sigma-Aldrich Ltd., Gillingham, UK
Alizarin red S	Sigma-Aldrich Ltd., Gillingham, UK
Antibodies for staining umbilical cord:	
CD10 (56C6) CD45 (ab781) CD90 (ab225) R4A smoothelin (ab76549) (clone)	Abcam, Cambridge, UK
CD31 (M0823)	Dako UK Ltd, Cambridge, UK
Biotinylated secondary goal anti-mouse IgG Mouse IgG	Vector Laboratories Inc., Burlingame, CA, USA
Antibodies for FACS:	
IgG1 PE (MOPC-21), IgG1 FITC (MOPC-21), IgG2a PeCy7 (G155478), CD10 PE (555375), CD31 PE (WM59), CD14 PE-Cy7 (M5E2), CD73 PE (Ad2), CD90 FITC (5E10), IgG1-PerCP (550672) (clone)	BD Biosciences, Franklin Lakes, CA, USA
IgG2a APC (S43.10), IgG2b APC (130092217), CD133 PE (293C3), CD34 APC (AC136); CD45 PerCP (345809),	Miltenyi Biotec GmbH, Bergisch Gladbach, Germany
CD105 FITC (166707), CD144 PE (16B1)	R & D Systems, Abingdon, UK
CD146 FITC (P1H12)	Millipore, Abingdon, UK
Aquamount	Fisher scientific, Loughborough, UK
Bovine Serum albumin (BSA)	Sigma-Aldrich Ltd., Gillingham, UK
Citroclear	TCS Biosciences, Buckingham, UK
Cloning cylinders, polystyrene (4.7mm, 8mm)	Sigma-Aldrich Ltd., Gillingham, UK
Collagen I bovine gel	Invitrogen Ltd., Paisley, UK
Collagenase A	Roche, Watford, UK
Cryovials	Sigma-Aldrich Ltd., Gillingham, UK

DAPI (4',6-diamidino-2-phenylindole)	Invitrogen Ltd., Paisley, UK
DAB substrate kit	Vector Laboratories Inc., Burlingame, CA, USA
Dimethylsulphoxide (DMSO) Hybri-Max	Sigma-Aldrich Ltd., Gillingham, UK
Dulbecco's Phosphate Buffered Saline (D-PBS)	Lonza Biologics, Tewkesbury, UK
Dulbecco's Modified Eagle Medium (DMEM)	Lonza Biologics, Tewkesbury, UK
Ethylenediaminetetraacetic acid (EDTA)	Sigma-Aldrich Ltd., Gillingham, UK
Endothelial Cell Basal Medium-2 (EBM-2)	Lonza Biologics, Tewkesbury, UK
Endothelial Growth Medium-2 (EGM-2)	Lonza Biologics, Tewkesbury, UK
Ethanol	Sigma-Aldrich Ltd., Gillingham, UK
Falcon centrifuge tubes	BD Biosciences, Franklin Lakes, CA, USA
FcR Blocking Reagent	Miltenyi Biotec GmbH, Bergisch Gladbach, Germany
Fetal Calf Serum (FCS)	Hyclone, Salt Lake City, USA or PAA Laboratories GmbH, Pasching, Austria
Fibronectin from human plasma lyophilized powder	Sigma-Aldrich Ltd., Gillingham, UK
Fibrinogen Type 1	Sigma-Aldrich Ltd., Gillingham, UK
Fungizone Amphothericin B	Invitrogen Ltd., Paisley, UK
Hanks' Balanced Salt Solution (HBSS)	PAA Laboratories GmbH, Pasching, Austria or Lonza Biologics, Tewkesbury, UK
Haematoxylin solution, Gill no.3	Sigma-Aldrich Ltd., Gillingham, UK
Heraeus Biofuge pico	DJB Labcare, Newport Pagnell, UK
HettichRotina 46R centrifuge	DJB Labcare, Newport Pagnell, UK
Holo-transferrin	Sigma-Aldrich Ltd., Gillingham, UK
[1M] Hydrochloric acid	Sigma-Aldrich Ltd., Gillingham, UK
Leica RM2135 microtome	Leica Biosystems, Peterborough, UK
L-glutamine	PAA Laboratories GmbH, Pasching, Austria
LSM 1077 Lymphocyte Separation Medium (1.077g/ml)	PAA Laboratories GmbH, Pasching, Austria
MEM-α Non Essential Amino Acids (NEAA) medium	Invitrogen Ltd., Paisley, UK

Mesenchymal Stem Cell Growth Medium (MSC-GM)	Lonza Biologics, Tewkesbury, UK
Medium(M)-199 and 10x M-199	Sigma-Aldrich Ltd., Gillingham, UK
µ-Slide Chemotaxis^{3D} plates	Ibidi GmbH, Thisle Sciences Ltd, Glasgow, UK
Nalgene® Mr Frosty	Sigma-Aldrich Ltd., Gillingham, UK
Nuaire DH autoflow incubator	Nuaire, MN, USA
Oil red O	Sigma-Aldrich Ltd., Gillingham, UK
Oleic acid	Sigma-Aldrich Ltd., Gillingham, UK
Optimal cutting temperature (O.C.T.) compound	Tissue-Tek, Fisher Scientific, Loughborough, UK
Paraffin sectioning mounting bath	Barnstead International, Dubuque, IA, USA
Penicillin/Streptomycin	PAA Laboratories GmbH, Pasching, Austria
6 (collagen coated and uncoated), 12, 24 and 96 well plates	BD Biosciences, Franklin Lakes, CA, USA
Real architecture for 3D tissues (RAFT) 96 well plates	TAP Biosystems, Royston, UK
Sodium Bicarbonate	Invitrogen Ltd., Paisley, UK
Sodium Hydroxide	VWR International, Lutterworth, UK
Sodium Pyruvate	Invitrogen Ltd., Paisley, UK
Sodium Selenite	Sigma-Aldrich Ltd., Gillingham, UK
Sutures (6/0 Prolene and 5/0 Vicryl rapide)	Ethicon Europe, Norderstedt, Germany
Recombinant Human Basic-Fibroblast Growth Factor	R and D Systems, Minneapolis, MN, USA
Recombinant Human Insulin	Sigma-Aldrich Ltd., Gillingham, UK
Recombinant Human Interleukin-3	R and D Systems, Minneapolis, MN, USA
Recombinant Human Stromal Cell-Derived Factor (SDF)-1α	R and D Systems, Minneapolis, MN, USA
Recombinant Human Stem Cell Factor (SCF)	R and D Systems, Minneapolis, MN, USA
Saponin	Sigma-Aldrich Ltd., Gillingham, UK
Sodium Selenite	Sigma-Aldrich Ltd., Gillingham, UK
Syringe filter 22 (0.22µm)	Techno Plastic Products (TPP) AG, Trasadingen, Switzerland

Sysmex Haematology Analyser	Sysmex Corporation, Hyogo, Japan
Thrombin	Sigma-Aldrich Ltd., Gillingham, UK
Trisodium citrate	VWR International Ltd., Lutterworth, UK
Trypan Blue stain 0.4% (w/v)	Invitrogen Ltd., Paisley, UK
Trypsin-EDTA (1x) 0.5mg/ml-0.22mg/ml in PBS without Ca++ and Mg++	PAA Laboratories GmbH, Pasching, Austria
Rh-insulin	Sigma-Aldrich Ltd., Gillingham, UK
Vaseline®	Unilever, UK
VECTASTAIN ABC kit	Vector Laboratories Inc., Burlingame, CA, USA

2.2 Cells

2.2.1 Pooled human umbilical vein endothelial cells (pHUVECs)

pHUVECs were acquired from Lonza Biologics at passage 1 and were cultured in complete endothelial growth medium-2 (EGM-2) (made from endothelial cell basal medium-2 (EBM-2) (Lonza Biologics) supplemented with EGM-2 Single Quots (consisting of 10ml fetal calf serum (FCS), 0.2ml hydrocortisone, 2ml fibroblast growth factor-B (hFGF-B), 0.5ml vascular endothelial growth factor (VEGF), 0.5ml long R insulin-like growth factor-1 (R^3-IGF-1), 0.5ml ascorbic acid, 0.5ml epidermal growth factor (hEGF), 0.5ml gentamicin sulphate, amphotericin-B (GA-1000) and 0.5ml heparin per 500ml EBM-2, all from Lonza Biologics) (72). They were passaged as per section 2.2.8 and frozen in aliquots at passage 2 to 4, and used at a given passage as described in specific experiments (*vide infra*).

The typical cobblestone endothelial morphology of these cells and their phenotype are shown in Figures 2.1a and 2.1b respectively.

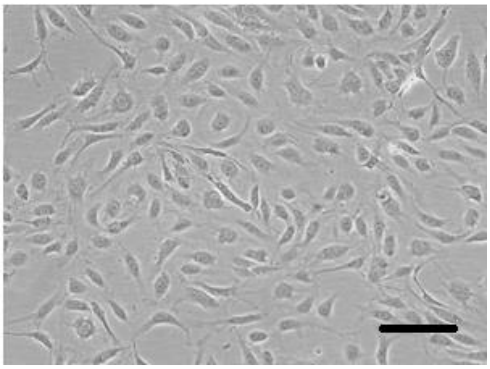

Figure 2.1a – Morphology of HUVECs: Morphology of HUVECs. Phase contrast image showing x10 magnification of pHUVECs at p3 (scale bar 200µm). Note the cobblestone morphology that is characteristic of endothelial cultures.

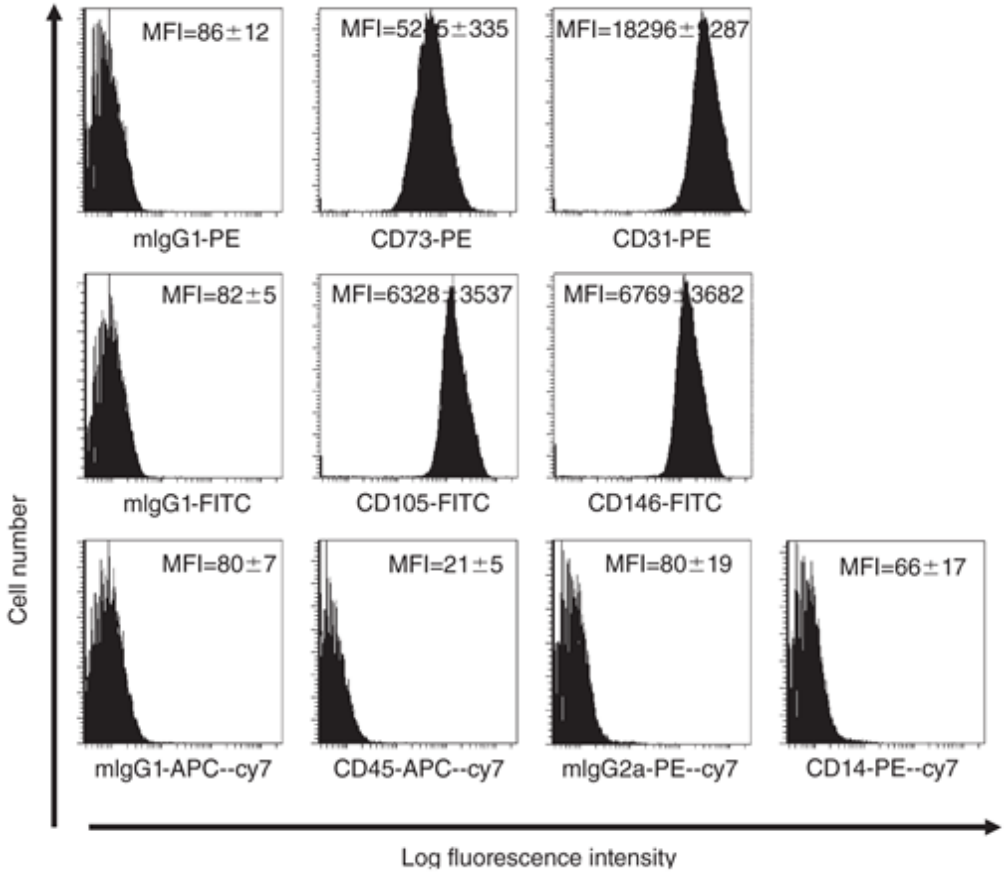

Figure 2.1b – FACS for pHUVECs: Representative flow cytometric phenotyping of HUVECs at P3. These cells were CD31+, CD73+, CD105+ and CD146+ but CD14- and CD45- consistent with an endothelial cell phenotype. MFI = Median fluorescence intensity is the mid-point of the population and is shown along with +/- standard deviation (SD) for n=3

2.2.2 Bone marrow mesenchymal stem/stromal cells (BMMSCs)/human dermal fibroblasts (hDFs)

BMSCs and hDFs were bought from Lonza Biologics at passage 1 and were cultured in complete mesenchymal stem cell growth medium (MSC-GM) (made from mesenchymal stem cell growth medium (MSC-GM) (Lonza Biologics) supplemented with MSC-GM Single Quots (consisting of 0.5ml gentamicin sulphate, amphotericin-B (GA-1000), 50ml mesenchymal cell growth supplement and 10ml L-Glutamine, all from Lonza Biologics). They were passaged as per section 2.2.8 and frozen in aliquots at passage 3 to 5, and used at a given passage as described in specific experiments (*vide infra*).

These cells had a spindle-shaped morphology at passage 3 typical of MSCs (Figure 2.2a) and a classical BMMSC phenotypic FACS profile (Figure 2.2b).

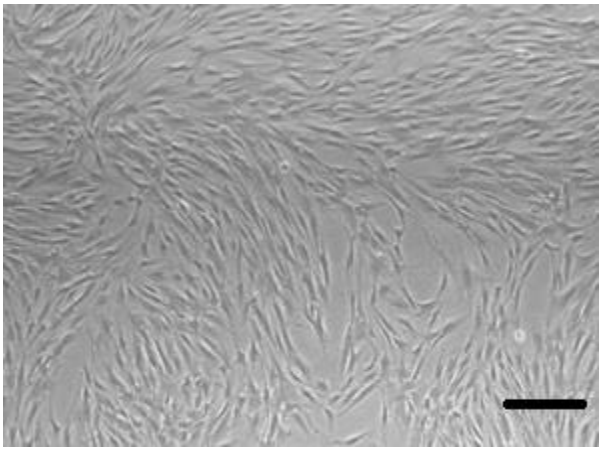

Figure 2.2a – BMMSC morphology: x10 magnification brightfield image of BMMSCs at passage 3 (scale bar 200µm). Note the characteristic fibroblast-like spindle shaped morphology.

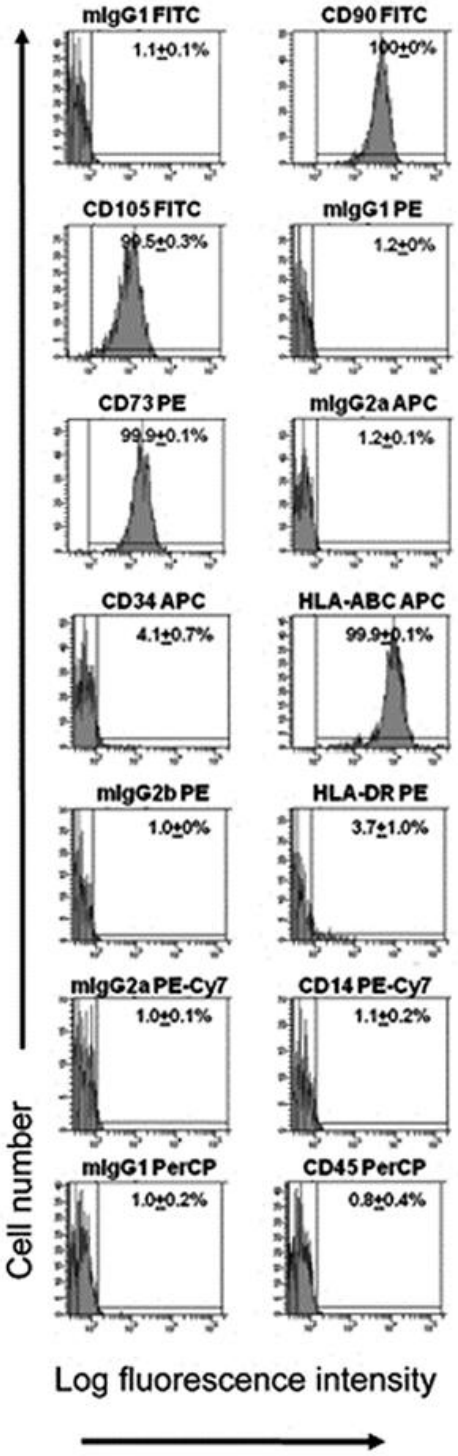

Fig 2.2b - FACS for BMMSCs: Representative flow cytometric phenotyping of BMMSCs at P3. These cells were CD90+, CD73+, CD105+ but CD14-, CD45- and CD34- consistent with an MSC phenotype. Percentage of cells within positive gate are shown in each FACS plot along with MFI and SD (n=3).

2.2.3 Mononuclear cells from umbilical cord blood (MNCs)

Human umbilical cord blood (CB) was collected from the umbilical vein of the placenta from normal term births, with written informed consent and ethical approval from the Oxford John Radcliffe Research Ethical Committee (107853/343015/1/231). CB units were either processed immediately or stored at 4°C overnight and then processed. Any cells used were done so as anonymised linked donations under an HTA licence. The process of isolating MNCs from CB was performed in a laminar flow hood under aseptic conditions. CB units were diluted with CB dilution medium at a ratio of 1:1 if the white blood cell (WBC) count was $<7x10^6$ cells/ml and 1:2 if the count was $>7x10^6$ cells/ml. The medium was made by mixing 500mls Hanks' Balanced Salt Solution (HBSS) without calcium and without magnesium (PAA Laboratories, GmbH) with 1.5g trisodium citrate (VWR International Ltd.) and 2.5g BSA (Sigma Aldrich Ltd.) which was then 0.2µM filter-sterilised. This was stored at 4°C and used within 3 months. 25-30ml diluted CB was carefully layered onto the frit in Accuspin tubes (Sigma Aldrich Ltd.) containing 15ml LSM 177 (PAA Laboratories) pre-spun in the centrifuge at 1000g for 5 minutes at acceleration 9 and brake 9 in a Hettich Rotina 46R centrifuge (DJB Labcare) (all centrifugation took place in this centrifuge unless otherwise specified). MNCs were separated by centrifugation at 1000g for 10 minutes at acceleration 9 and brake 1. Platelet rich plasma was removed from above the MNC buffy coats and then the MNC layers were collected and combined (2 to 4 buffy coats/ 50ml Falcon tube) and CB dilution medium added to make a total volume per Falcon tube of 50ml. These were then centrifuged at 400g at acceleration 9 and brake 9 for 10 minutes at 4°C. After removing supernatant the cell pellets were re-suspended in 10ml dilution medium mixing up to 3 pellets per 50ml Falcon tube. Tubes were then topped up to 50mls with dilution medium and centrifuged for 10 minutes, 200g at acceleration 9 and brake 9 at 4°C. Pellets were pooled and re-suspended in 5mls EGM-2 (Lonza Biologics) with 10% (v/v) FCS (PAA Laboratories, GmbH) then topped up to 50mls with EGM-2 (Lonza Biologics) with 10% (v/v) FCS (PAA Laboratories) and centrifuged for 5 mins at 200g, acceleration 9 and brake 9 at 22°C. Cells were re-suspended in 10mls EGM-2 and a 200µl sample was used to count cells using a Sysmex Haematology Analyser (Sysmex Corporation). Cells were then either frozen as MNCs at a concentration of $1x10^8$ cells/ml as described in section 2.2.8 or were plated onto 6-well plates, pre-coated with collagen I (rat tail) (BD Biosciences), at a

concentration of $2x10^7$ cells/well in EGM-2 (Lonza Biologics) with 10% (v/v) FCS (PAA Laboratories, GmbH). All plates used for experimentation (6 well collagen I-coated, 12 well, 24 well and 96 well) in the course of all experiments were tissue culture grade.

2.2.4 Endothelial cells from umbilical cord blood (CBECs)

Twenty four hours after plating CB MNCs in EGM-2 with 10% FCS (2.2.3), the wells in the 6-well collagen I-coated plates (Lonza Biologics) were washed twice with 1ml of HBSS (PAA Laboratories) and then 4ml fresh medium was added to each well (EGM-2 with 10% (v/v) FCS). After 48 hours, a further full 4ml medium change was undertaken and this continued every 2-3 days until characteristic ECFC colonies (with a cobblestone morphology) were noted. These can be seen in Fig 2.3. These were then cloned using small or large cloning rings (Sigma Aldrich Ltd.). Cloning rings were carefully applied around pre-marked (using a fine-tip permanent marker pen on the underside of the plate) colonies, securing in place by first dipping the rings into sterile Vaseline® (Unilever UK) using ethanol-cleansed forceps. Two 100µl Dulbecco's phosphate buffered saline (PBS) (Lonza Biologics) washes were carefully carried out and then 70-100µl (depending on the size of the cloning ring) of 1x Trypsin-EDTA (PAA Laboratories) was added to cells within the cloning rings and left for 30 seconds or until cells were seen to be lifting off from under the microscope (Nikon Eclipse TE300 brightfield microscope (Nikon UK Ltd). Colonies (1-2 large or 2-3 small) were then placed into new wells of a collagen I-coated 6 well plate (BD Biosciences) along with 4ml EGM-2 with 10% (v/v) FCS medium. Cells were fed with 4ml medium on alternate days until 80% confluent and were then passaged into collagen-coated T25 flasks. When these were 80% confluent, cells were passaged 2-3 times until there were sufficient cells to produce sufficient cells for subsequent experimentation. In order to coat the T25 flasks with collagen, 245µl 4.08µM rat-tail collagen I (BD Biosciences) was added to 19.755ml 0.02N Acetic acid and 3ml of this added to each T25 flask to be coated. After 2 hours incubation at 37°C, 5% CO_2 (Nuaire incubator), plates were washed twice with sterile D-PBS (Lonza Biologics). Flasks not being used immediately could be stored containing D-PBS at 4°C for up to 1 week.

The typical endothelial morphology of CB ECFCs is shown in Figure 2.3 and their phenotype by flow cytometry in Figures 2.4 and 2.5 and Table 2.1. These CB ECFC

derived cells were CD31+, CD73+, CD144+, CD146+ and CD105+ but negative for CD14, CD45, CD90 and CD133. Table 2.2 shows the day that the first ECFC colony was noted and the number of ECFC colonies grown from each cord blood sample as well as outcomes from cloned colonies from these cord blood samples.

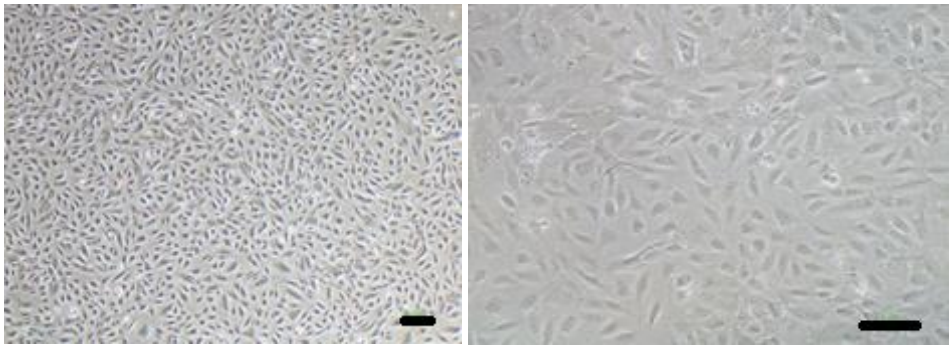

Figure 2.3 – Morphology of CB ECFCs: a) x 4 magnification and b) x 10 magnification (scale bar 200μm) of P3 CBECFCs taken with a brightfield microscope. Note the characteristic cobblestone morphology.

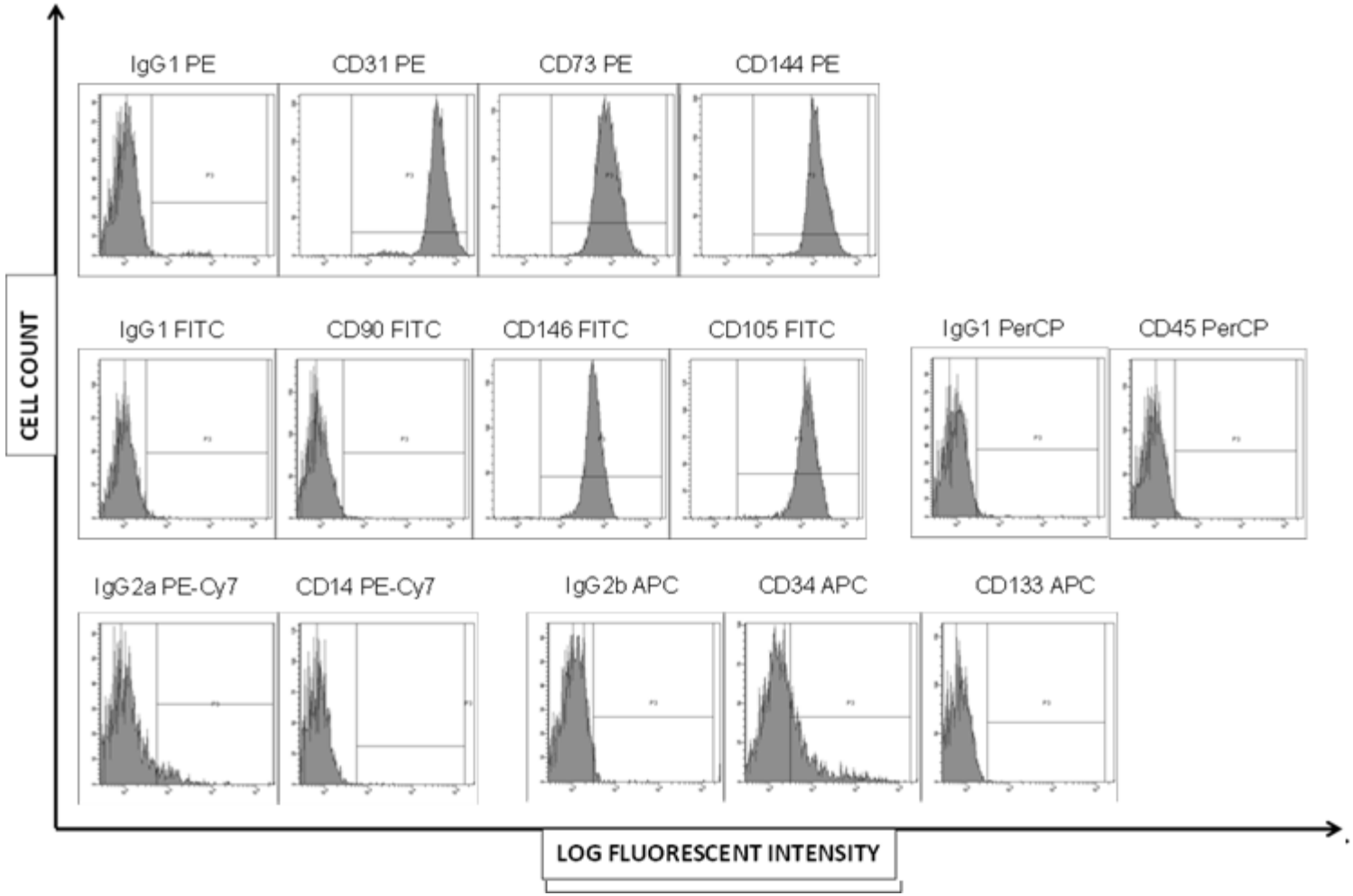

Figure 2.4 – CB ECFC FACS: Representative flow cytometric phenotyping of CBECFCs at P2. These cells were CD31+, CD73+, CD144+, CD146+ and CD105+, CD90-, CD45-, CD14- and CD133- consistent with an endothelial cell phenotype. Table 2.1 shows median fluorescence intensity and number of positive cells.

Stain	Average MFI	SD MFI	Average % cells Positive	SD % cells positive
IgG1 PE	98.0	6.2	2.3	0.4
CD31 PE	37094.0	4894.2	99.9	0.2
CD73 PE	7951.3	866.0	99.9	0.2
CD144 PE	6760.7	4390.5	99.7	0.1
IgG1 FITC	95.0	6.1	1.3	0.7
CD90 FITC	89.3	9.3	1.1	0.4
CD146 FITC	7128.7	1358.6	99.8	0.4
CD105 FITC	14595.3	1785.9	99.8	0.2
IgG2a PE-Cy7	69.7	6.8	3.8	2.5
CD14 PE-Cy7	56.0	24.3	0.8	0.5
IgG1 PerCP	76.0	0.0	1.4	0.0
CD45 PerCP	82.3	8.5	4.5	3.2
IgG2b APC	89.0	0.0	2.0	0.0
CD34 APC	186.7	42.8	42.4	33.3
CD133 APC	78.0	24.6	1.2	0.9

Table 2.1 – CB ECFC FACS: Flow cytometry data for P3 CBECFCs (average n=3). Results are consistent with the FACS histograms seen in Figure 3.8. MFI = median fluorescence intensity

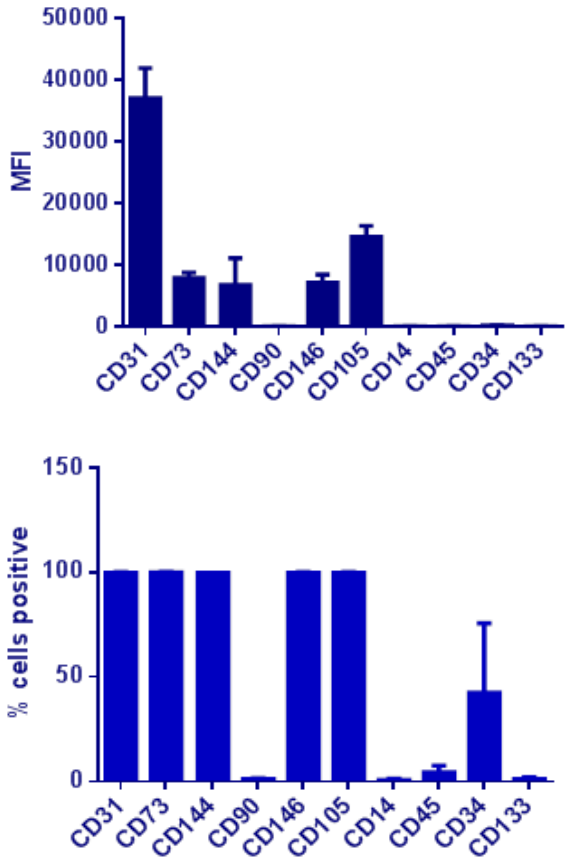

Figure 2.5 – CBECFC flow cytometry data: MFI and percentage of cells positive (n=3)

Table 2.2 – CB ECFC colonies*

Cord Blood number	Date of 1st ECFC colony	No. of colonies by d14	Date of colony cloning (no. cloned)	Outcome
1	d10	3	d13 (3 large)	MSC subpopulation grown
2	d10	16	d10 (7 medium)	Mixed population phenotype
3 and 4 (pooled)	d7	15	d12 (8 medium)	ECFCs phenotyped and frozen
5	d14	2	d14 (1 large, 1 small)	ECFCs phenotyped and frozen
6	d12	4	d12 (1 large, 3 small)	ECFCs phenotyped and frozen
7	d8	8	d10 (3 small, 5 contaminated)	MSCs and ECFCs frozen

*ECFC colony growth following plating of Ficoll buffy coat MNCs from different CB batches.

CBECFCs were isolated from 3 batches of CB and banked for subsequent use at p2-4.

2.2.5 Peripheral blood endothelial cells (PBECs)

Peripheral blood mononuclear cells (PBMCs) were obtained from anonymised human leucocyte cones supplied by the United Kingdom Blood Transfusion Service (donations were anonymised and within the remit of the consent taken at the time of donation). Cones were provided within 4 hours of donation and an aperture was created at either end to allow access to cells under sterile conditions. The cones were back-flushed with air using a 20ml syringe into a 50ml Falcon tube (BD Biosciences) and then with D-PBS (Lonza Biologics) to ensure all cells were transferred from the cone to the Falcon tube which was topped up with D-PBS (Lonza Biologics). The cells then underwent the same density centrifugation as CB (section 2.2.3) to separate the MNC fraction. The PB MNCs were seeded at the same concentration ($2x10^7$ cells/well) as the CB MNCs, in 4ml EGM-2 with 10% (v/v) FCS in collagen I-coated 6-well plates (BD Biosciences). Excess PBMCs were frozen at concentrations of 0.5-$1x10^7$ in liquid nitrogen (section 2.2.8). Feeding and cloning of PBEC colonies was done in the same manner as for the isolation of CBECs (2.2.4).

Peripheral blood leucocyte cones were obtained from NHS Blood & Transplant and cells were plated and cultured in EGM-2 media with 10% (v/v) FCS until ECFC colonies were visualised. These were then cloned and plated on collagen I-coated tissue culture plastic dishes until a bank of ECFCs had been created (Chapter 2.2.5). The cells were characterised by morphology (Fig 2.6) and FACS analysis (Fig 2.7 and 2.8 and table 2.3) to confirm that they were ECFCs. Table 2.4 shows the date that the first PB ECFC colony was noted and the number of ECFC colonies grown from each cord PB sample as well as outcomes from cloned colonies from these cord blood samples.

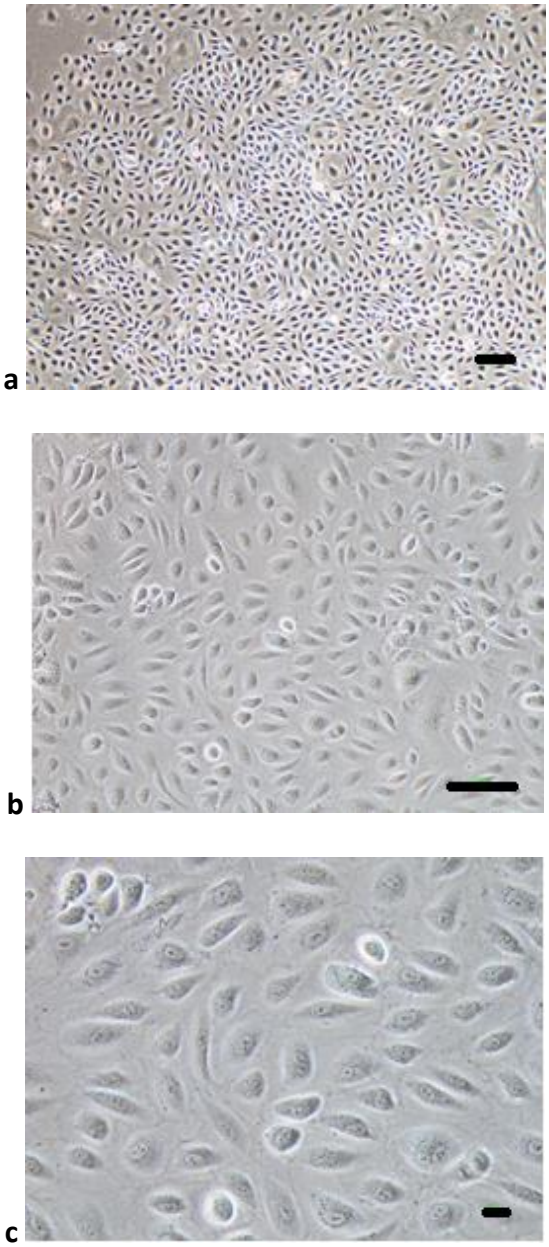

Figure 2.6 – PB ECFC morphology: a) x 4 magnification (scale bar 200μm) b) x 10 magnification (scale bar 200μm) and c) x20 (scale bar 20μm) magnification images of P3 PBECFCs taken with a brightfield microscope. Note the characteristic cobblestone morphology.

The PBECFCs had a typical endothelial morphology (132). For flow cytometic analysis, cells were CD31+, CD73+, CD144+, CD146+ and 105+ as for CBECFCs. A proportion of cells were CD34+ as expected from other studies (83). Negativity for CD45 and CD90 confirmed that they were neither haemopoietic nor mesenchymal cells.

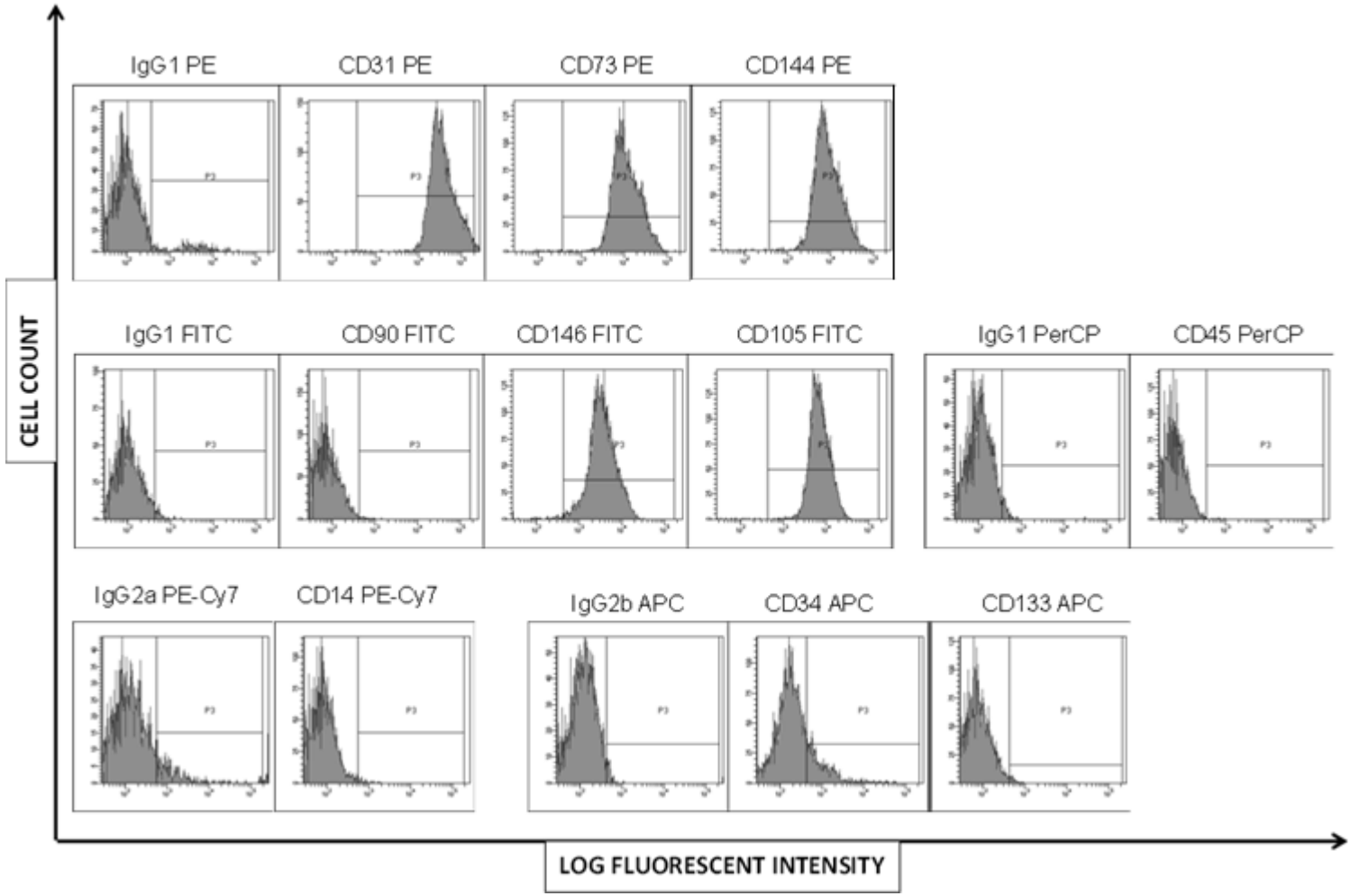

Figure 2.7 – PB ECFC FACS: Representative flow cytometric phenotype PBECFCs at P2. These cells were CD31+, CD73+, CD144+, CD146+ and CD105+ but CD90-, CD45-, CD14- and CD133- consistent with an endothelial cell phenotype. Table 2.3 shows the median fluorescence intensity and number of positive cells.

Stain	Average MFI	SD MFI	Average % cells positive	SD % cells positive
IgG1 PE	95.0	8.2	7.3	6.9
CD31 PE	23297.7	9585.6	99.1	0.4
CD73 PE	5981.7	3700.2	99.3	0.5
CD144 PE	5730.3	1917.8	99.3	0.6
IgG1 FITC	101.0	35.1	7.6	10.6
CD90 FITC	100.0	67.7	9.3	15.3
CD146 FITC	5597.0	1960.3	98.3	1.8
CD105 FITC	7236.7	5519.4	98.5	2.1
IgG2a PE-Cy7	77.3	37.2	6.3	3.5
CD14 PE-Cy7	48.7	18.5	1.5	1.9
IgG1 PerCP	95.0	9.5	2.5	0.2
CD45 PerCP	35.0	15.7	0.1	0.1
IgG2b APC	98.7	7.0	1.6	0.6
CD34 APC	476.7	496.8	34.4	26.8
CD133 APC	73.7	16.9	1.3	1.0

Table 2.3 – PB ECFC FACS: Flow cytometry data for P2 PBECFCs (average n=3). Results are consistent with the FACS histograms seen in Figure 3.8.

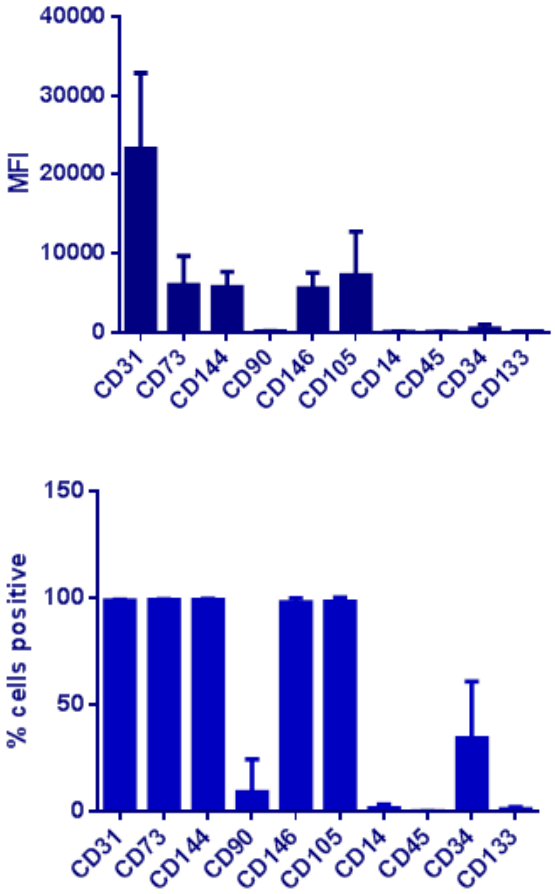

Figure 2.8 – PB ECFC flow cytometry data: MFI and percentage cells positive (n=3)

Table 2.4 – PB ECFC colonies

PB number	Day of 1st ECFC colony	No. of colonies	Day of colony cloning (no. cloned)	Outcome
1	20	1	n/a	Too small to clone
2	13	18 (2 large)	19	Stock created
3	n/a	n/a	n/a	No colonies
4	n/a	n/a	n/a	No colonies
5	8	13	14	Stock created
6	12	4	15	Stock created

ECFC colony growth following plating of Ficoll buffy coat MNCs from different PB batches.

PB ECFCs were isolated from 3 batches of PB and these were banked at p3 for subsequent use.

2.2.6 Adipose derived mesenchymal stem cells (Ad MSCs)

Redundant human adipose tissue was harvested from Deep Inferior Epigastric Perforator (DIEP) flaps that were being used in breast reconstruction surgery, with ethical approval from NRES Committee South Central - Oxford C (12/SC/0567) and full written patient consent.

Skin was mechanically removed from adipose tissue with sharp dissection. The adipose tissue was then placed into HBSS without Ca^{++}/Mg^{++} (Lonza Biologics) as soon as the free tissue transfer (DIEP flap) had been made avascular by disconnection from the donor site blood supply. The adipose tissue was then immediately transported at room temperature (RT) to the research laboratory for processing which was carried out within 1 hour of harvest using the following protocol:

Approximately 200mg of perivascular fat was finely minced using a scalpel and was split between two 50ml Falcon tubes containing a freshly made D-PBS (Lonza Biologics)/Fungizone solution (30μL in 20ml) (Gibco). Adipose tissue was then transferred to Falcon tubes with D-PBS (Lonza Biologics) and 1% v/v penicillin/streptomycin (PAA laboratories) and washed by shaking extensively (ten times) prior to adding to fresh Falcon tubes containing collagenase A (1mg/ml) (Roche), and into a 37°C water bath for 45 minutes shaking gently at 15 minute intervals. The resultant digested adipose tissue was then passed through a 0.22μm filter (Techno plastic products).

The filtrate was topped up with complete EGM-2 (Lonza Biologics) and then centrifuged at 500g and acceleration 9, brake 9, for 10mins at RT. The overlying medium/lipid layer was carefully removed and the cell pellets re-suspended in 1ml complete EGM-2 for counting with a haemocytometer (this cell pellet is known as the stromal vascular fraction or SVF). Approximately $2x10^7$ cells were isolated from every 50mg of adipose tissue (calculated using a haemocytometer – see Chapter 2.2.8) and this amount was plated per well of a collagen I-coated 6 well plate (BD Biosciences). Four ml complete EGM-2 was added to wells and they were placed into a Nuaire incubator at 37°C in 5% CO_2 in air. At 24 hours wells were washed twice with 1ml D-PBS (Lonza Biologics) to remove non-adherent cells (mainly red blood cells) and 4ml

fresh EGM-2 medium was added to each well. Cells were passaged (2.2.8) when 80-90% confluent (approximately 3 days) and transferred directly to uncoated T25 flasks (BD Biosciences). Subsequent passages were carried out in a similar manner, splitting cells at a 1:3 ratio at each step and cells fed were every 2-3 days with fresh medium.

The cells were characterised by a fibroblastoid-like morphology (Fig 2.9) and FACS analysis (Fig 2.10 and 2.11 and table 2.5) to confirm that they were indeed AdMSCs.

Three different batches of Adipose tissue were processed and all produced MSC-like cells morphologically and cells with the correct phenotypic markers following FACS analysis.

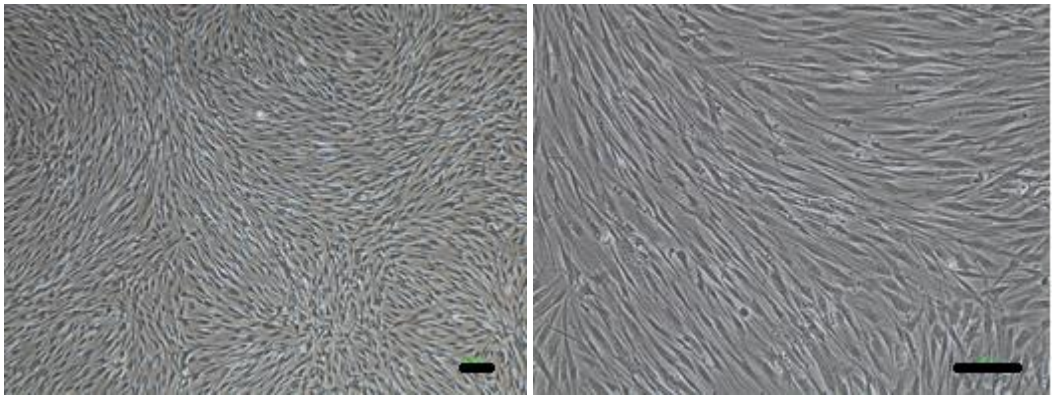

Fig 2.9 – AdMSC morphology: Brightfield microscope images of p1 AdMSCs taken at x4 (left) and x10 (right) magnification (scale bar 200µm). Note the characteristic fibroblast-like spindle shaped morphology.

Phenotypically, AdMSCs at p3 were CD73+, CD105+ and CD90+ and negative for CD31, CD14, CD133 and CD45. Interestingly a proportion of cells were CD34+ as previously reported (131). This differs from BMMSCs which are generally regarded as CD34- (131).

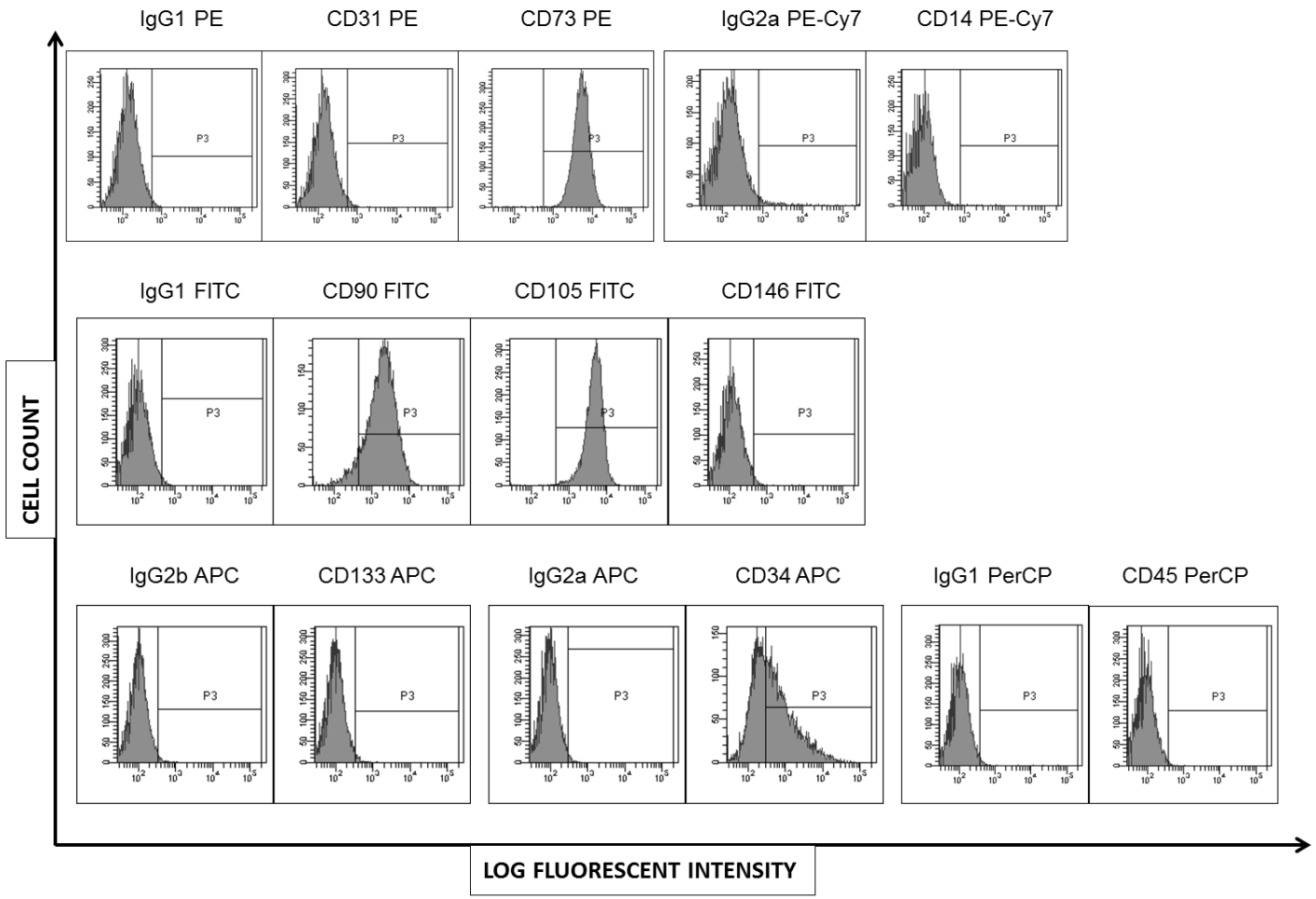

Figure 2.10 – Ad MSC FACS: Representative flow cytometric phenotype AdMSCs at P3. These cells were CD73+, CD90+ and CD105+ but CD31-, CD45-, CD14- CD146- and CD133- consistent with a mesenchymal cell phenotype. Table 2.5 shows the median fluorescence intensity and number of positive cells.

Stain	Average MFI	SD MFI	Average % cells	SD % cells
IgG1 PE	117.7	20.1	1	0.1
CD31 PE	118.3	22.5	1.5	0.4
CD73 PE	11772.3	10070.4	99.7	0.4
IgG2a PE-Cy7	69.7	41.7	2.2	0.3
CD14 PE-Cy7	37.0	27.6	0.1	0.1
IgG1 FITC	98.3	11.6	1	0.2
CD90 FITC	4590.0	5396.2	93.8	5.7
CD146 FITC	109.0	22.6	1.8	1.7
CD105 FITC	1968.3	2403.8	80.3	23.7
IgG1 PerCP	74.7	24.5	1	0.2
CD45 PerCP	60.7	20.2	0.3	0.2
IgG2b APC	62	5.7	1	0.1
CD34 APC	149.7	180.3	21.4	30.8
CD133 APC	56.7	12.7	0.8	0.7

Table 2.5 – AdMSC FACS: Flow cytometry data for P3 AdMSCs (average n=3). Results are consistent with the FACS histograms seen in Figure 3.16.

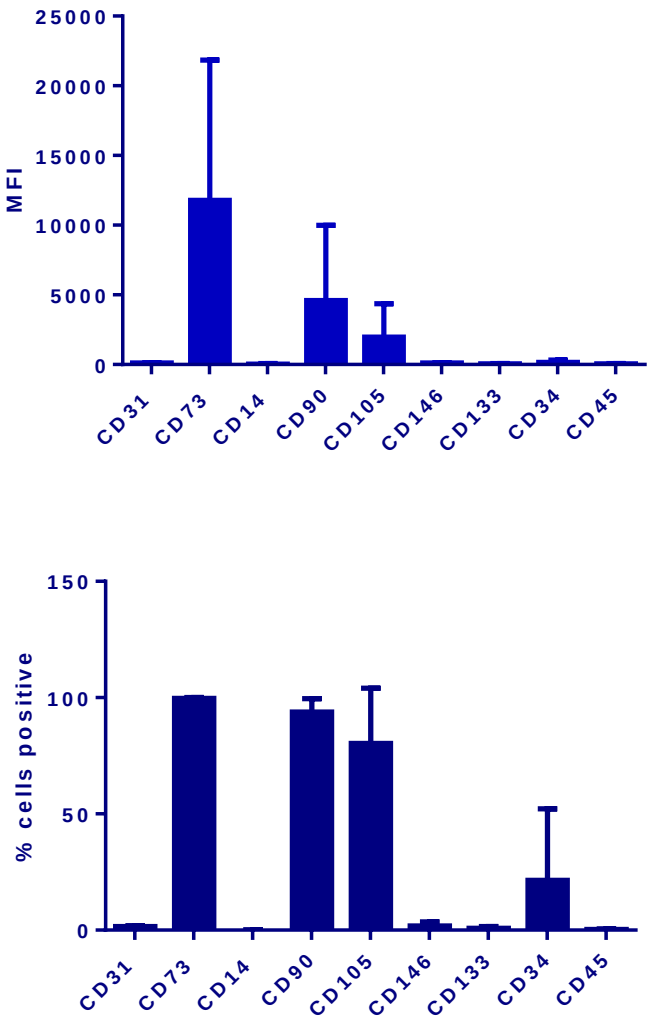

Figure 2.11 – AdMSC flow cytometry data: MFI and percentage cells positive (n=3)

2.2.7 Differentiation of AdMSCs

2.2.7.1 Adipogenesis culture protocol

Three different batches of AdMSCs (P5) were seeded in 1ml of complete MSC-GM (Lonza Biologics) into 6 separate wells (3 for differentiation and 3 for controls) of a 24 well plate ($1.5x10^4$ cells per well) (BD Biosciences). Cells were fed with fresh MSC-GM every 2-3 days until confluent (d6). At 100% confluence, AdMSCs were fed with supplemented adipogenic induction medium (Lonza Biologics) and cultured for 3 days (37°C, 5% CO_2), followed by 2-3 days in supplemented adipogenesis maintenance medium. Non-induced control AdMSCs were fed only with supplemented adipogenic maintenance medium on the same schedule. Adipogenic maintenance medium contained hMSC induction

medium (Lonza Biologics) together with the SingleQuots™ h-insulin (recombinant), L-glutamine, MCGS and GA-1000, whereas adipogenic induction medium contained hMSC adipogenic induction medium (Lonza Biologics) together with these 4 SingleQuots™ and also dexamethasone, indomethacin and IBMX (3-isobuty-l-methyl-xanthine). After 2 weeks, wells were stained with Oil red O (Sigma-Aldrich Ltd.) as follows. Wells were washed with 300µl of D-PBS (Lonza Biologics) and fixed with 300µl of paraformaldehyde (PFA) (2.9.1) for 15 minutes at RT. Oil red O stain (Sigma-Aldrich Ltd.) stock solution was prepared by weighing 300mg of Oil red O powder and combining this with 100ml of 99% (v/v) isopropanol (Sigma Aldrich Ltd. Ltd.). Three parts of this were then mixed with 2 parts of deionized water and having left this for 10 minutes at room temperature (stable for maximum of 2 hours), the Oil red O was then filtered (Whatman No.1 (Sigma Aldrich Ltd. Ltd.)). PFA was removed from wells and 300µl distilled water used to rinse wells. Sixty percent isopropanol (v/v) in water was then used to cover the bottom of each well for 5 minutes and once this had been completed and the isopropanol had been removed, 250µl Oil red O was added to each well and this was left for 5 minutes at room temperature. Wells were rinsed with tap water until the water ran clean. The samples were examined using a Nikon Eclipse TE300 microscope and images taken at x4 magnification with a Hamamatsu ORCA-ER camera (2.12).

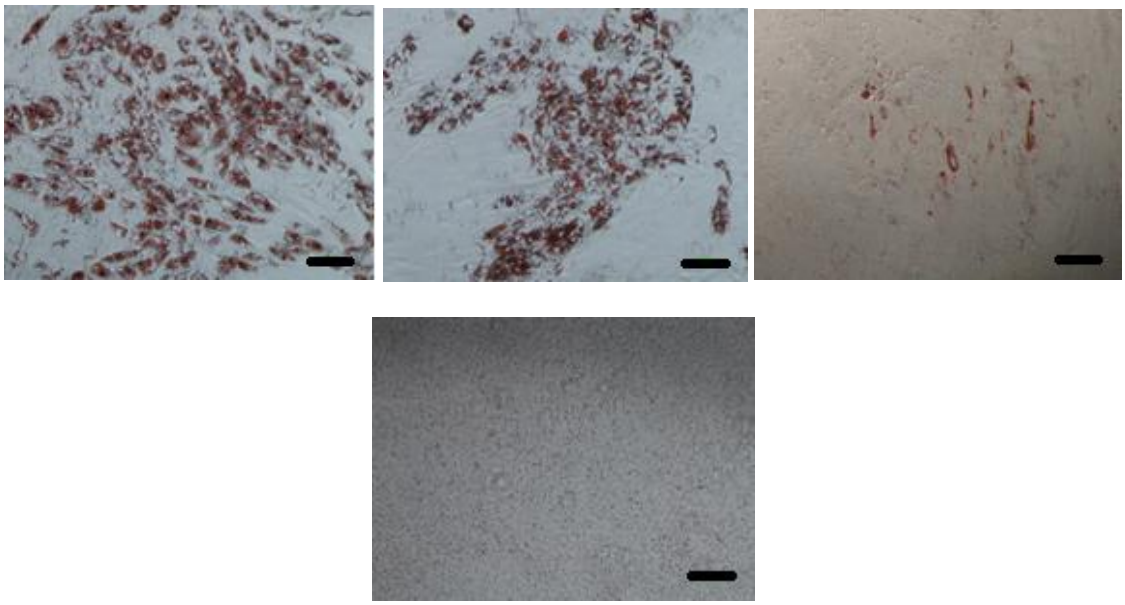

Figure 2.12 – Adipogenic differention of AdMSCs: Oil red O staining of Adipose tissue produced by adipocytes from differentiated AdMSCs – photos taken at x4 magnification (scale bar 200µm) for all 3 different batches (top) and control (bottom).

2.2.7.2 Chondrogenesis culture protocol

AdMSCs ($1.5x10^6$ P5 for 3 different batches) were suspended in incomplete chondrogenic medium (Lonza Biologics) and centrifuged at 150g for 5 minutes, acceleration 9 and brake 9 at RT. Chondrogenic medium was made up with differentiation basal medium (Lonza Biologics) together with the following SingleQuots™ also from Lonza Biologics – dexamethasone, ascorbate, ITS + supplement, GA-1000, sodium pyruvate, prolene and L-glutamine. Cells were re-suspended in 2ml incomplete chondrogenic medium and this split into two separate 15ml Falcon tubes (BD Biosciences) prior to centrifuging again for 5mins at 150g (acceleration 9, brake 9, room temperature) and then discarding the supernatant. One of these cell pellets was then resuspended in 1.5mls complete chondrogenic medium (differentiation group) and the other in incomplete chondrogenic medium (both from Lonza Biologics). Complete chondrogenic medium was made by adding 5µl of 20µg/ml TGF-β3 (Lonza Biologics) to 10mls incomplete chondrogenic induction medium. One half ml was then aliquoted into separate polypropylene Falcon tubes ($2.5x10^5$ cells) and these centrifuged for 5mins at 150g. Supernatant was not aspirated at this stage but caps were loosened a half a turn to enable gas exchange and medium was replaced with fresh complete (differentiation group) or incomplete (control group) chondrogenic medium (Lonza Biologics) every 2-3 days, flicking the pellet after each medium change to ensure pellets were floating. After 14 days, pellets were placed into small bespoke kitchen foil boats and covered with optimal cutting temperature (OCT) compound (Fisher Scientific) and these were rapidly frozen in liquid nitrogen before being stored at -80°C until ready for sectioning. Ten µm sections were cut using a cryotome and fixed on microscope slides before they were stained as follows. 1% (v/v) Alcian blue (Sigma Aldrich Ltd. Ltd.) solution was made up in 0.1N HCL and this was pipetted over the sections and left in situ for 30 minutes. The slides were then rinsed with 0.1N HCL and then distilled water before visualising specimens under the light microscope (Nikon Eclipse TE300 microscope) and recording images at x4 magnification (Fig 2.13). Blue staining indicated synthesis of proteoglycans by chondrocytes.

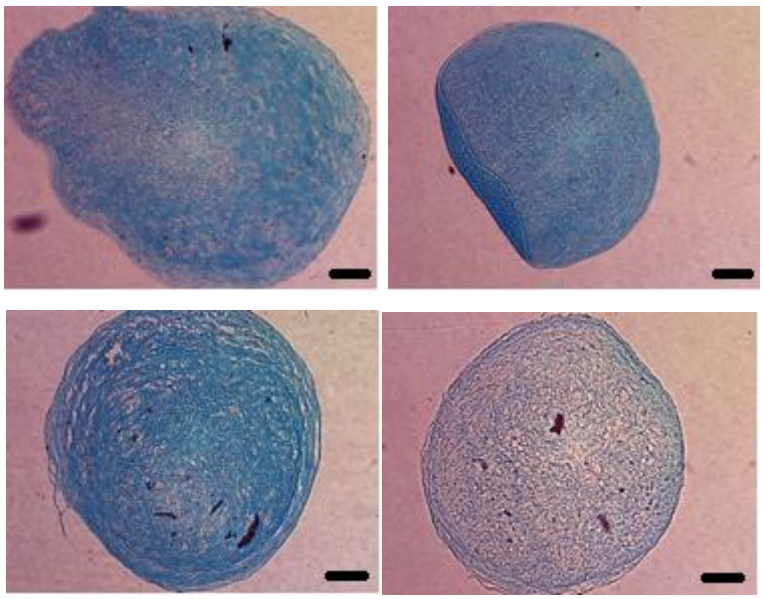

Figure 2.13 – Chondrogenic differention of AdMSCs: Alcian blue staining of collagen produced by chondrocytes from differentiated AdMSCs – photos taken at x4 magnification (scale bar 200µm) for all 3 different batches (top) and control (bottom).

2.2.7.3 Osteogenesis culture protocol

Six wells of a 24-well plate (Lonza Biologics) were each seeded with $6X10^3$ P5 AdMSCs that had been suspended in 0.5ml MSCGM (Lonza Biologics) (for 3 separate batches of AdMSCs i.e. 18 wells in total). After 24 hours incubation at 37°C in 5% CO_2 in air, medium for the 9 'differentiation' wells was replaced with osteogenesis induction medium (Lonza Biologics) and this was repeated every 3-4 days for 2 weeks. Osteogenesis induction medium was made by adding the following SingleQuots™ to hMSC differentiation basal medium – osteogenic (Lonza Biologics): dexamethasone, L-glutamine, ascorbate, penicillin/streptomycin, MCGS, β-glycerophosphate. Control wells had medium replaced with MSC-GM on the same days as differentiation well medium changes. After 2 weeks, wells were stained with Alizarin red S (Sigma Aldrich Ltd.). To do this, wells were washed gently with D-PBS (PAA Laboratories) and then 200µl Alizarin red S was added. This was left *in situ* for 45 minutes after which wells were washed repeatedly with distilled water until the water ran clear. Photos were taken with a light microscope (Nikon Eclipse TE300 microscope) at x4 magnification (Fig 2.14), red staining indicating calcium production from osteoblasts.

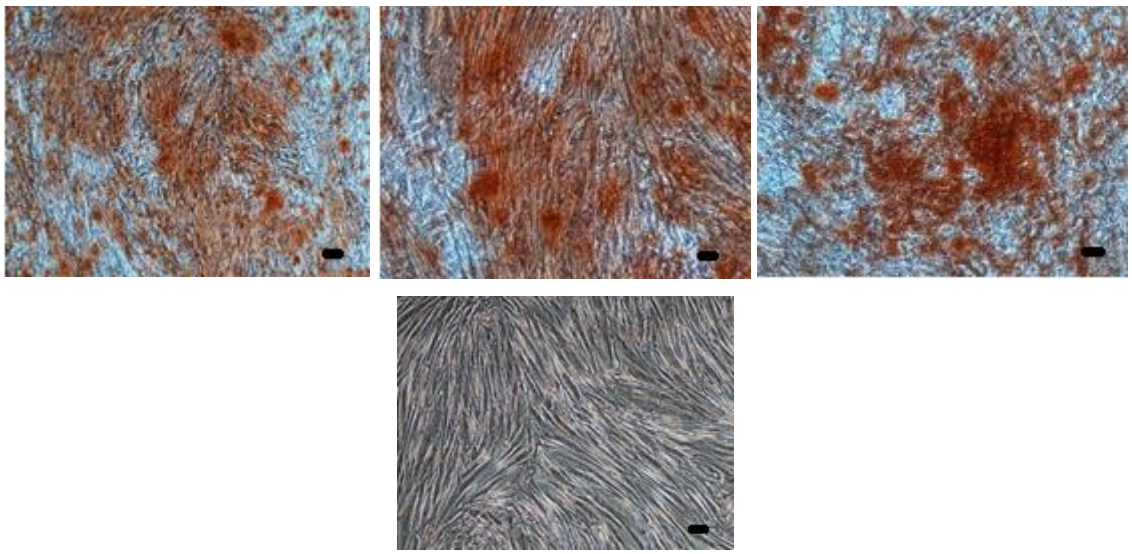

Fig 2.14 – Osteogenic differention of AdMSCs: Alazarin Red staining of calcium produced by osteoblasts from differentiated AdMSCs – photos taken at x4 magnification (scale bar 200µm) for all 3 different batches (top) and control (bottom).

2.2.8 Cell passage, counting and freezing procedures

Where cells were passaged, this refers to the detachment of adherent cells from tissue culture grade flasks or plates (BD Biosciences). For this procedure, cell medium was removed and cells washed twice with enough D-PBS (PAA Laboratories) to cover the cells (ranging from 1ml in a 6 well plate to 10mls in a T150 flask) prior to incubation with 2-5mls 1x trypsin-EDTA or 1x accutase (PAA Laboratories) at 37°C in a Nuaire DH autoflow incubator (Nuaire) in 5% CO_2 in air, until loss of cell adherence on gentle tapping of the flask or culture plate (normally 2-5 minutes). As soon as cells detached the enzyme solution was neutralised with the medium specific to that cell line (section 2.2), cells collected in a Falcon tube (BD Biosciences) and centrifuged at 1200rpm, acceleration 9, deceleration 9 for 5 minutes at 22°C. The cells were then re-suspended in an appropriate volume for counting (approximately $1x10^6$ cells/ml) in their standard culture medium and a 15µl cell suspension sample mixed with 15µl Trypan blue stain (Invitrogen Ltd. Ltd.) and viable cells counted by using a haemocytometer (Neubauer) using a Nikon Eclipse TE300 brightfield microscope (Nikon UK Ltd.). Cells within the outer 4 chambers were counted and an average calculated by dividing this number by 4. To calculate total cell number, the following calculation was used:

Total number of cells = Average cell number per quadrant x 2 (dilution factor) x 10^4 (convert cells/µl to cells/ml) x number of mls of media used to re-suspend cell pellet

The required cell number for experimentation or re-passage was plated appropriately and the remainder were centrifuged at 1200 rpm for 5 minutes, acceleration 9, brake 9, RT. The resultant cell pellet was re-suspended in 90% (v/v) FCS (PAA Laboratories) with 10% (v/v) DMSO (Sigma Aldrich Ltd.) at a concentration of $5x10^5$-$1x10^6$ cells/ml. One ml of this suspension was then transferred to separate cryovials (Sigma Aldrich Ltd.), these placed into a Nalgene® Mr Frosty (Sigma Aldrich Ltd.) and then placed into a -80°C freezer for a minimum of 24 hours prior to storage in liquid nitrogen.

2.3 Fluorescence-activated cell sorter (FACS) analysis

To make the buffer for FACS analysis, 500mls D-PBS (Lonza Biologics) was mixed with 5g bovine serum albumin (BSA) (Sigma-Aldrich Ltd.) and 5mls 2mM EDTA (Sigma-Aldrich Ltd.) and filter-sterilised. This was then stored at 4°C until required and used within 3 months. This was termed magnetic-activated cell sorting (MACS) buffer. Cells for FACS analysis were suspended in MACS buffer in a 15ml Falcon tube so that for every FACS tube $1x10^5$ cells were suspended in 80µl MACS buffer with 20µl FcR block (Miltenyi Biotec) (100µl total). A 15ml Falcon tube was used since several FACS tubes were normally required, producing a total volume of approximately 2mls. This was incubated on ice for 20 minutes to block non-specific antibody sites. One hundred µl of this cell suspension was then added to the stated antibody or isotype control (see below) and vortexed briefly. After 30 minutes incubation in darkness, on ice, cells were washed in 1ml MACS buffer by centrifugation at 1500rpm for 5 minutes, at 4°C in a Heraeus Megafuge 1.0S centrifuge (DJB Labcare). The supernatant was carefully pipetted off and the cell pellet re-suspended in 500µl ice-cold MACS buffer.

Table 2.6: The following quantities of (1x concentration unless stated) isotype controls and antibodies were used for FACS analysis of the various cell types:

BD Biosciences:	**Miltenyi Biotec:**	**R&D Systems:**
IgG1-PE (*Clone MOPC-21*) 20µl	CD45 PerCP (*345809*) 20µl	CD144-PE (*16B1*) 5µl
1gG1-FITC (*MOPC-21*) 20µl	IgG2a-APC (*S43.10*) 10µl	CD105-FITC (*166707*) 10µl
1gG2a-PE-Cy7 (*G155478*) 5µl	CD34-APC (*AC136*) 10µl	
CD31-PE (*WM59*) 20µl	CD133-PE (*293C3*) 11µl	**Millipore:**
CD14-PE-Cy7 (*M5E2*) 5µl	IgG2b-APC (*130092217*) 10µl	CD146-FITC (*P1H12*) 5.5µl (1:20 dilution in MACS buffer)
CD73-PE (*AD2*) 10µl	CD133-APC (*13009054*) 11µl	
CD90-FITC (*5E10*) 2µl		
IgG1-PerCP (*550672*) 20µl		

Cell suspensions were vortexed briefly and then isotype controls were analysed on a BD LSR II flow cytometer (BD Biosciences) using the BD FACSDiva 6 software program (BD Biosciences) in order to set voltages for these tubes aiming for a log fluorescent intensity peak value of 10^2 for each isotype control. Prior to this, the flow cytometer was set-up using cytometer setup and tracking (CST) beads (BD Biosciences). Once voltages had been set, all FACS tubes were analysed for 10,000 events firstly adding DAPI (0.1µg/ml) (Invitrogen Ltd.) viability stain and briefly vortexing the tube. The cell surface cluster of designation markers chosen for demonstrating each cell phenotype and their main antigen expression are shown in table 2.7.

CD31 is recognised to be a haemopoietic and endothelial cell specific surface marker (72,83). CD10 has been used as an MSC marker (133) but is also found on B cells (134) and within epithelioid haemangioendothelioma (a vascular neoplasm) (135) and metastatic renal cell carcinoma (136). CD90 is a more specific cell surface marker for MSCs from BM and adipose tissue (87,105) although it is found on haemopoietic stem cells (137) and has been described as an activation marker on some endothelial cells (138). CD45 is a haemopoietic cell surface marker (83,139,140).

Table 2.7: Cluster of designation markers, their main antigen expression and the isolated cells where they were present.

Marker	Main Antigen Expression	HUVECs	CBECFCs	PBECFCs	BMMSCs	AdMSCs
CD14	Monocytes	-	-	-	-	-
CD31	Endothelial cells, platelets, monocytes, granulocytes, B cells, haematopoietic stem cells	++	++	++		-
CD34	Haematopoietic stem and progenitor cells, endothelial cells, subsets of mesenchymal stem cells		+	+	-	+
CD45	Leucocytes	-	-	-	-	-
CD73	T and B cells, follicular dendritic cells, epithelial cells, endothelial cells and mesenchymal stem cells	++	++	++	++	++
CD90	Stromal cells, mesenchymal Stem Cells, haematopoietic stem cells		-	-	++	++
CD105	Endothelial cells, stromal cells, mesenchymal Stem Cells	++	++	++	++	++
CD133	Haematopoietic stem and progenitor cells, other stem cells eg. Neural, Retinal cells		-	-		-
CD144	Endothelial cells		++	++		
CD146	Blood vessel endothelial cells and some melanoma cell lines, NK cells and neutrophils	++	++	++		-

* ++ strong expression of cell surface marker; + mild expression; - no expression

CB and PB-derived ECFCs have been shown to express CD31, CD141, CD105, CD146 and CD144 but do not express CD45 and CD14 with some expressing CD34 (72). Here, 3 separate batches of CBECFCs and PBECFCs were isolated and not only possessed a classical cobblestone morphology but also expressed CD31, CD73, CD166, CD144, CD146 and 105 with a proportion also showing positivity for CD34 (2.2.4 and 2.2.5). All batches

were negative for CD45 and CD90 confirming that they were neither haematopoietic nor mesenchymal cells.

International Society for Cellular Therapy criteria states that MSCs must be plastic-adherent in standard culture conditions and express CD105, CD73 and CD90. They should also lack CD45, CD14, CD19, HLA-DR and CD34 and differentiate into osteoblasts, adipocytes and (143) chondroblasts *in vitro* (144). In addition to isolating, culturing and expanding 3 batches of MSCs from human adipose tissue, their morphological, phenotypic and differentiation profiles have been confirmed. AdMSCs at p3 were CD73+, CD105+ and CD90+ and negative for CD31, CD14, CD133 and CD45. Given that the aim was to isolate cells with a stromal phenotype that could support ECs *in vitro* it was felt that negativity for CD45 was sufficient to rule out a leucocyte phenotype in the isolated MSCs and that it wasn't necessary to also check for CD19 and HLA-DR negativity (also found on leucocytes). In fact, a proportion of cells were CD34+ (ICST criteria states this shouldn't be the case although CD34+ cells within an AdMSC population has recently been reported [142]). This differs from BMMSCS which are generally regarded as CD34-, which was the case for the BMMSCs obtained from Lonza biologics (142). All batches of AdMSCs that were isolated showed differentiation capacity into adipogenic, osteogenic and chondrogenic tissue.

MSCs are heterogeneous, containing multi-lineage stem and partly differentiated progenitor cells, and are easily expandable *ex vivo*. Together with myeloid cells, they have been demonstrated to enhance the *de novo* formation of stable vasculature by ECFCs in surrogate models of vasculogenesis. In addition to BMMSCs having the ability to regulate new blood vessel formation, stability and function, similar effects have been demonstrated with MSC-like cells from human adipose tissue, the limbal niche, the foetal circulation, amniotic fluid, the vascular wall and umbilical cord blood (143). Having obtained and characterised ECFCs from peripheral blood (PBECFCs) and MSCs from adipose tissue (AdMSCs) it would be of interest to determine the tubule forming capacity of these cells together in comparison to more commonly co-cultured ECs and MSCs from HUVECs and BM respectively (145). This is investigated in detail in Chapter 3.

2.4 µ-chemotaxis 3D assay

Pooled HUVECs were grown to passage 4 or 5 using the protocol described in section 2.2.1. CB (2.2.4) and PB (2.2.5) ECFCs were isolated and expanded then also used between passage 4 and 5 for assessing chemotaxis. The day before conducting the µ-chemotaxis assay, 5mls EBM-2 (Lonza Biologics) with 10% (v/v) FCS (PAA Laboratories) and 5mls EBM-2 with 10% (v/v) FCS were placed into 2 separate Falcon tubes (BD Biosciences) and put into a Nuaire DH autoflow incubator (Nuaire) in 5% CO_2 at 37°C overnight to equilibrate (cap unscrewed slightly to enable gas exchange and reduce bubble formation). A µ-chemotaxis 3-D plate (1 plate per 3 experiments) and plugs (Ibidi GmbH) were also placed into the incubator overnight to equilibrate (these were not removed from their packaging as per manufacturing guidelines).

Depending on cells analysed, HUVECs, CBECFCs or PB ECFCs from an 80% confluent T150 flask (BD Biosciences) were harvested using trypsin-EDTA as in section 2.2.8 and centrifuged in EBM-2 (Lonza Biologics). The cells were then counted after being re-suspended in 5mls EBM-2 and $3x10^5$ cells were placed into each eppendorf that was to be used for a specific gel concentration. Eppendorfs were centrifuged at 2000 rpm for 5 mins in a Heraeus Biofuge pico (DJB Labcare), supernatant removed and residual amount of supernatant/cell suspension checked using a 20µl pipette set at 10µl. To make bovine collagen I gel (Invitrogen Ltd.), collagen I/fibronectin (FN) gel or fibrin gel the components from Tables 2.8, 2.9 and 2.10 were added, adding the collagen I or thrombin last, prior to pipetting gels into viewing chambers of the µ-chemotaxis slides.

Table 2.8: Components for 1mg/ml and 3mg/ml collagen I gels

Component	Collagen I gel	
	1mg/ml	3mg/ml
10x MEM-α medium (Invitrogen Ltd.)	10µl	10µl
0.5% (v/v) NaOH(1M)	0.5µl	1.5µl
5% (v/v) $NaHCO_3$ (7.5%)	5µl	5µl
Remaining cell volume	~10µl	~10µl
distilled deionised H_2O (dependent upon remaining cell vol.)	(~54.5µl)	(~13.5µl)
Collagen I bovine gel (5mg/ml) (Invitrogen Ltd.) (last)	20µl	60µl
TOTAL VOL * Contains $3x10^5$ cells	100µl*	100µl*

Table 2.9: Components for different concentration fibrin gels.

Component	Fibrin gel				
Final concentration	1.25mg/ml	2.5mg/ml	5mg/ml	7.5mg/ml	10mg/ml
Fibrinogen Type I (Sigma)	-	50µl[1]	100µl[1]	125µl[1]	15mg
D-PBS (PAA Laboratories)	-	100µl	100µl	25µl	1ml
Amount of fibrinogen/D-PBS solution	25µl[2] (5mg/ml)	50µl (5mg/ml)	67µl (7.5mg/ml)	60µl (12.5mg/ml)	67µl
10x α-MEM medium (Invitrogen Ltd.)	10µl	10µl	10µl	10µl	10µl
0.5% (v/v) NaOH IN (1M)	0.5µl	1.25µl	2.5µl	3.75µl	0µl
5% (v/v) $NaHCO_3$ (7.5%)	5µl	5µl	5µl	5µl	5µl
Thrombin (Sigma Aldrich Ltd.) (50U/ml; 0.5ml aliquots)	0.3µl	1.25µl	3.35µl	4.5µl	8µl
Distilled deionised H_2O	47.2µl	23.5µl	0.15µl	6.75µl	0µl
Remaining cell volume	12µl	9µl	12µl	10µl	10µl
TOTAL VOL =	100µl*	100µl*	100µl*	100µl*	100µl*

* Contains $3x10^5$ cells; 1. From 15mg/ml stock solution; 2. From 5mg/ml stock solution. Note that in order to make the 10mg/ml gel 15mg fibrinogen was added to 1ml D-PBS and 67µl of this solution was used. This solution was then used to make the 2.5, 5 and 7.5mg/ml gels whereas the 1.25mg/ml gel was made using the 5mg/ml stock solution.

Table 2.10: Collagen I/FN gel

Component	CB/PB ECFCs			
	1	**4**	**5**	**6**
Collagen I conc	**1mg/ml**	**1mg/ml**	**1mg/ml**	**1mg/ml**
FN conc		**50µg/ml**	**100µg/ml**	**150µg/ml**
10x α-MEM	10µl	10µl	10µl	10µl
NaOH IN	0.5µl	0.5µl	0.5µl	0.5µl
$NaHCO_3$	5µl	5µl	5µl	5µl
Remaining cell volume	10µl	10µl	10µl	10µl
H_2O (dependent upon remaining cell vol)	(54.5µl)	49.5µl	44.5µl	39.5µl
Fibronectin# (1mg/ml)	0µl	5µl	10µl	15µl
Collagen I (add last)	20µl	20µl	20µl	20µl
TOTAL VOL=	100µl*	100µl*	100µl*	100µl*

* Contains $3x10^5$ cells; #Fibronectin from human plasma lyophilized powder (Sigma) 100µg/ml

The equilibrated plate was removed from the incubator and plugs were placed into the four main reservoir ports. Collagen I (Invitrogen Ltd.), fibrinogen (Sigma Aldrich Ltd. Ltd.), thrombin (Sigma Aldrich Ltd. Ltd.) and fibronectin (Sigma Aldrich Ltd. Ltd.) were then placed on ice along with eppendorfs containing the remaining components of the gel solution (Tables 2.2 and 2.3). The appropriate amount of Collagen I/Thrombin solution was then added (20µl for 1mg/ml collagen I gel) and mixed. Using a 100µl pipette, the complete gel solution was added to the cell suspension (10µl) and gently mixed. Using pipettes with a specially modified tip (Grenier Bio-One), 6µl gel was carefully injected over the top central channel port (see Figure 2.15). With the thumb still depressing the top of the pipette, the pipette tip was inserted into the lower central channel port to create tight seal then slowly released until gel filled the viewing chamber. If either side was under-filled, a small amount of gel was added as required, and if any bubbles were seen then the pipette containing some gel mixture was placed into the bubble(s) and slowly aspirated. Of note the 3mg/ml collagen I gel and 7.5 and 10mg/ml fibrin gels were extremely viscous and therefore difficult to bring through viewing chamber using negative pressure. All plugs were removed, the lid applied to the plate and then this was placed inside a petri dish containing wet tissue paper to ensure no evaporation prior to placing it into a humidified incubator at 37°C (5% CO_2) for 1 hour for the gel to set. Once the gel had set, 70µl of chemoattractant (10% (v/v) FCS in EBM-2) or control medium (0.5% (v/v) FCS in EBM-2) was slowly injected into the reservoir ports (Figure 2.15). Plugs were then carefully inserted into all ports and the slides were placed into a 37°C heat chamber surrounding a time-lapse microscope. Using a Nikon Eclipse TE300 microscope, a Prior proscan II controlled motorised stage (Nikon UK Ltd.) and a Hamamatsu ORCA-ER camera and Simple PCI automated image capture camera device software (Hamamatsu Photonics UK Ltd), photos at x4 magnification were taken every 5 minutes for 24 hours generating time-lapse sequences. Analysis was carried out using Image J with *manual tracking* and *chemotaxis tool* plugins (see Chapter 4).

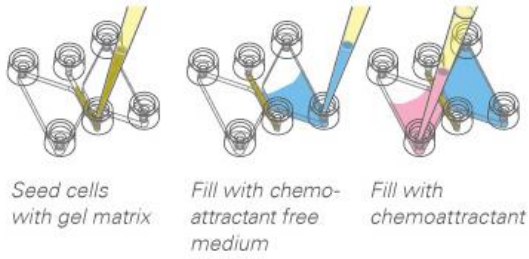

Figure 2.15 – µ-Chemotaxis slide: Left image illustrates the filling of the central channel with 7µl gel and the next 2 images, filling of reservoirs with 70µl chemoattractant/control medium (image courtesy of Ibidi).

2.5 Lentiviral transduction of cells

2.5.1 Human embryonic kidney (HEK) 293FT cells

HEK 293FT growth medium was made by mixing 500mls Dulbecco's Modified Eagle Medium (D-MEM) (high glucose) (Lonza Biologics) with 50mls FCS (PAA Laboratories), 5ml L-glutamine (note D-MEM already contained L-glutamine), 5ml MEM-α Non-Essential Amino Acids (NEAA) medium (Gibco) and 5ml sodium pyruvate (Gibco).

HEK293FT cells were purchased from Invitrogen Ltd. Ltd. and were plated at P2 at a concentration of approximately $5x10^5$ cells in a T150 flask. Forty mls HEK293FT medium was then added. At 48hrs the flask was 80% confluent (Fig 2.16) and was trypsinised using with trypsin-EDTA as in section 2.2.8, to make a bank of P3 HEK293FT cells. These were subsequently used for titering eGFP-labelled lentiviral (LV) particles (see section 2.4.2).

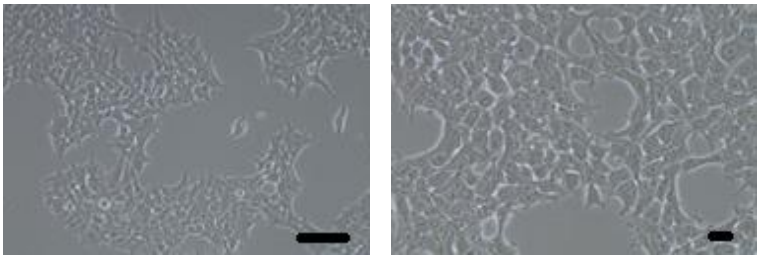

Figure 2.16 – Morphology of p2 HEK293FT cells: x10 (left) (scale bar 200µm) and x20 (right) (scale bar 20µm) magnification images under phase contrast microscopy.

2.5.2 Titration of lentiviral vector stocks

Two T150 flasks (BD Biosciences) of P2 HEK293T cells were passaged and then plated at a concentration of $1x10^5$ cells/well in 1ml HEK293T medium in all wells of a 12-well plate

(BD biosciences). The following day eGFP labelled lentiviral particles were examined for their transduction efficacy. To do this 1ml of viral particles was thawed from -80°C in a normoxic incubator at 37°C and diluted as follows in several 15ml Falcon tubes (BD Biosciences): 40µl neat vector was added to 3.96mls HEK293T medium (dilution factor of 10^{-3}). Then 400µl of this was added to 3.6mls medium and so on for each serial dilution (see Fig 2.17). 1ml diluted vector was added to each well (in triplicate) with concentrations of 10^{-3}, 10^{-4}, 10^{-5} and 10^{-6} (dilution factor). Throughout viral titration, great care was taken in terms of using double gloves and disinfecting all plastic-ware and medium for at least 20 minutes in Virkon. After 72 hours, the number of cells/colonies in each well that had been transduced in triplicate for at least 2 dilutions were counted using a Nikon Eclipse TE2000U microscope (Nikon UK Ltd.) and a Hamamatsu ORCA-ER camera (Hamamatsu Photonics UK Ltd) and the viral titre was estimated using the following equation:

Titre = number of cells/colonies transduced = Transducing Units (T/U.)/ml dilution factor

Example: 150, 133, 181 colonies at $x10^{-5}$ and 20, 10 11 colonies at 10^{-6}

Titre= 154.6 /10^{-5} = 1.54 x10^{7} T.U./ml Titre= 13 / 10^{-6} = 1.3 x10^{7} T.U./ml

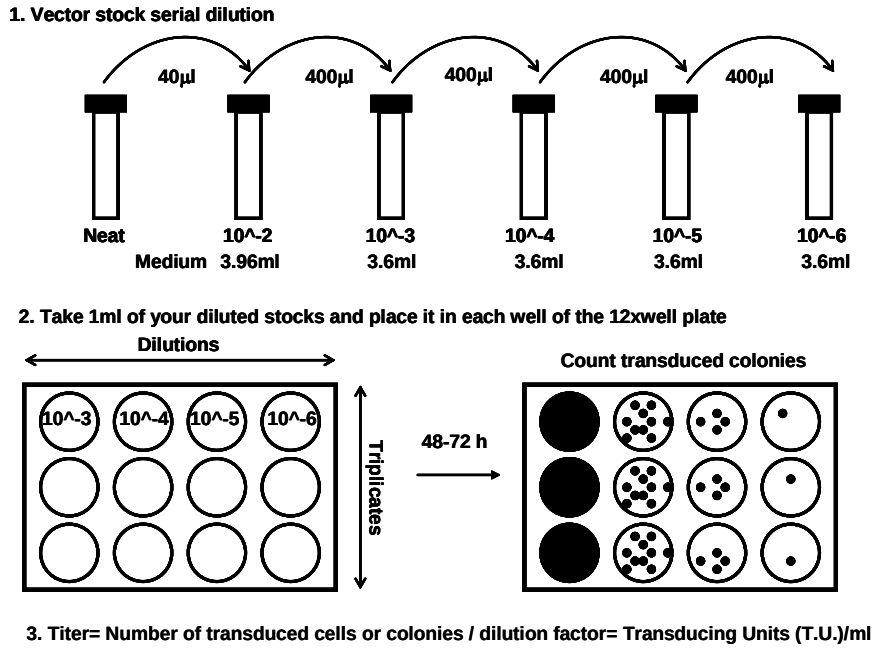

Figure 2.17: Method for carrying out serial dilutions of LV particle vectors

Table 2.11 – eGFP lentiviral vector titre results:

Dilution factor	10^{-3}	10^{-4}	10^{-5}	10^{-6}
eGFP+ cells well 1	++	++	107	12
eGFP+ cells well 2	++	++	109	7
eGFP+ cells well 3	++	++	93	8
Average			**103**	**9**

With a dilution factor of 10^{-3} and 10^{-4} there were too many eGFP positive cells to count accurately but using the higher dilution factors a titre of approximately $1x10^7$ particles/ml was calculated using the algorithm in Fig 2.17.

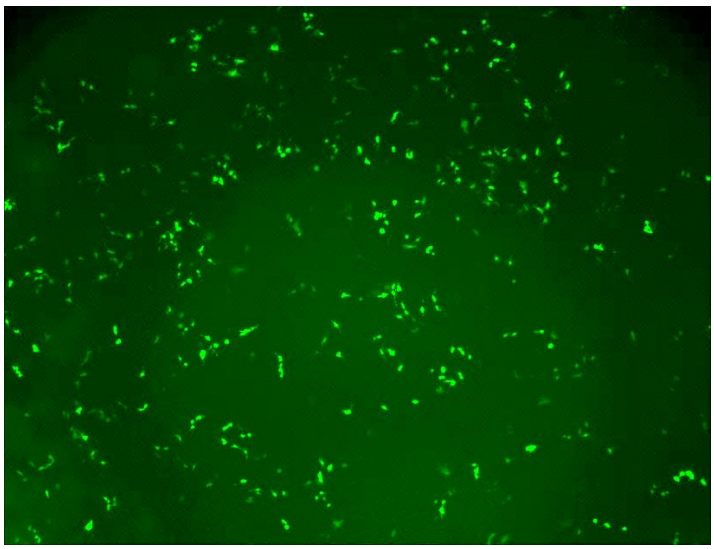

Figure 2.18 – eGFP transduction of HEK293T cells: x4 magnification fluorescence microscopy image taken 72 hours after transfection of HEK293T cells with the eGFP LV vector (10^{-4} dilution)

2.5.3 eGFP Lentiviral transduction

In order to calculate the number of lentiviral transducing units to be added in order to transduce cells the following equation was used:

[MOI (multiplicity of infection) x CN (number of cells in well)] / VT (stock viral titre)

(The desired MOI is TU/cell; the VT units are TU/µl)

For example, for an MOI of 3 (which was used to transduce endothelial progenitor cells [HUVECs/CBECFCs/PBECFCs]), a cell density of 20,000 cells per well and using a VT of $1x10^7$ the number of particles to add would be: $(3x20000)/1x10^4 = 6$ i.e. 6µl of viral stock (titre $1x10^7$ TU/ml) is required per well for an MOI of 3.

Once appropriate amounts of LV particles had been added to flasks containing cells, these were placed into the incubator. Medium containing viral particles was replaced with fresh medium after 2-3 days and once 80% confluent, cells were either frozen in LN or used for experimentation. An MOI of 3 for EC's (HUVECs, CBECFCs and PBECFCs) resulting in 100% (+/-0) cells being transduced.

2.6 Compressed collagen gels

2.6.1 Optimisation of compressed collagen gels

The various concentrations of HUVEC/BMMSC co-cultures (4:1 ratio) were grown to passage 4 or 5, counted with a haemocytometer and transferred to 1.5ml eppendorfs. These were then centrifuged at 2000 rpm for 5 minutes (acceleration 9, brake 9, RT), in a Heraeus Biofuge pico (DJB Labcare). Supernatant was aspirated and the cell pellets were re-suspended in the gel mixture, and then mixed with the correct volume of collagen until homogenous (Table 2.12).

Table 2.12: Constituents required for Collagen I gel for a 56µl volume per well of 96-well plate.

Preparation bovine collagen gel	[Stock]	[Final]	**amount (µL)**
Total Volume of gel			56.00
Final concentration of collagen desired (mg/ml)			2.00
Collagen I (bovine) (Invitrogen Ltd.)	5mg/ml	2mg/ml	22.40
[10x] M-199 (Sigma Aldrich Ltd.)	10x	-	5.60
NaOH (VWR)	1M	-	0.56
[1x] M-199 (Sigma Aldrich Ltd.)	1x	-	25.80
Sodium bicarbonate (Invitrogen Ltd.)	-	-	1.64
rhSCF (R & D systems)	100µg/ml	0.2µg/ml	0.11
rhSDF1α(R & D systems)	100µg/ml	0.2µg/ml	0.11
rhIL-3(R & D systems)	100µg/ml	0.2µg/ml	0.11

For compressed collagen gels, 112µl/240µl volumes were used therefore the volumes listed need to be multiplied 2/4.3x to reach these volumes.

Plated gels were incubated at 37°C for 15 minutes. All absorption wicks apart from those corresponding to the gels to be compressed were removed, and then the compression

lid was placed onto the plated gels and incubated at 37°C for a further 15 minutes. After removing the compression lid, 100µL of top-up growth media (Tables 2.13 and 2.14) was added to all of the gels. Top-up growth media was then aspirated and replaced every 48hrs until day 7 at which point gels were fixed with 4% (v/v) PFA (Chapter 2.8).

Table 2.13: Reagents for making 1ml top-up media for M-199 gel.

Top up growth media	[Stock]	[Final]	**mL**
1x M199 (mL)	1	1	1
Reduced serum II (mL)*	250x	1x	0.004
rhFGF-2 (ng) (R & D systems)	330µg/mL	40ng/mL	0.00012
Ascorbic acid (µg)	20mg/mL	50µg/mL	0.0025
Total Volume of media			1

Table 2.14: How to make reduced serum II*.

Reagent	**Amount**
rh-Insulin (Sigma Aldrich Ltd)	25mg
DMEM (Lonza Biologics Ltd)	500mL
[1M] HCl (Sigma Aldrich Ltd)	1L
Oleic Acid (Sigma Aldrich Ltd)	1g
Holo-transferrin (Sigma Aldrich Ltd)	100mg
Sodium Selenite (Sigma Aldrich Ltd)	10g
BSA (FA free) (Sigma Aldrich Ltd)	10g

*In order to prepare 20ml reduced-serum II supplement (RSII) per the *Stratman et al*. (130) protocol the reagents from Table 2.8 were mixed in the following concentrations:

2.5g bovine serum albumin (essentially fatty acid free and globulin free, min. 99%) (Sigma Aldrich Ltd.) and 17ml distilled water were added to a small beaker with a stir bar and gently mixed until all bovine serum albumin was dissolved. One hundred mg of sodium selenite (Sigma Aldrich Ltd.) was added to 4 ml distilled water in a 15ml falcon tube (BD Bioscience) to make 25mg/ml stock. Twenty five mg of recombinant human insulin (Na^+, Zn^{2+} free) (Sigma Aldrich Ltd.), 1.25ml DMEM (Invitrogen Ltd.), and 60µl 1M HCl was added to a 15ml tube for a total volume of 1.31ml (the solution should turn to a bright clear yellow colour). The 1.31ml insulin solution, 1µl of the 25mg/ml sodium selenite stock, and 25mg human holo-transferrin (Sigma Aldrich Ltd.) was added to the

beaker containing dissolved bovine serum albumin for a total volume of 18.3ml. This was mixed well until all had dissolved. Five mg/ml oleic acid stock solution was prepared by adding 100mg sodium oleate (Sigma Aldrich Ltd.) to 20ml 100% (v/v) EtOH. 4.28ml of the 5mg/ml oleic acid stock solution is required in total. To a 24ml glass vial, 1ml of the oleic acid solution was added and dried under a stream of nitrogen. This was repeated until the entire 4.28mls of oleic acid has dried down. To the glass vial containing the 24.1mg dried oleic acid, 10ml of the bovine serum albumin mixture solution was added and mixed well until the oleic acid had dissolved. The remaining 8.3ml of the bovine serum albumin mixture solution was then also added and mixed well prior to adding 1.7ml distilled water for a final volume of 20ml. Using a syringe and a 0.2µm syringe filter the RSII solution was sterile filtered into a 50ml tube. One ml aliquots were then stored at -20°C. Thawed RSII is maintained at 4°C and can be kept at this temperature for several months for use.

In other optimisation experiments for RAFT 3D, gels containing the above cell quantities were compressed 48 hours after fabrication or were left empty and compressed before re-suspending cells in top-up media and seeding them on top of the compressed gels (see Chapter 4).

2.6.2 Compressed collagen I gels with ECs

In view of limited success attempting to co-culture ECs and MSCs in or on compressed gels (2.6.1), gels were instead compressed with only $6x10^3$, 1.2^4 or $2.4x10^4$ HUVECs (passage 4) basing these concentrations on previous published work using this proprietary equipment (RAFT 3D, TAP biosystems). The RAFT 3D protocol was carried out using only reagents from the equipment pack supplied (Table 2.15). The appropriate volumes of 10x MEM and neutralising agent were used to re-suspend cell pellets before adding collagen I and then plating out 240µl of the above HUVEC concentrations in separate wells of a 96-well plate for compression at day 0 and day 3, in triplicate for both of these time-points and further duplicated so that cell viability could be checked at days 1 and 7 post compression. Reagents were calculated based on the protocols on the RAFT 3D website (TAP biosystems). Whilst awaiting compression in day 3 compressed gels, 100µl DMEM (Lonza Biologics) + 10% (v/v) FCS (PAA laboratories) +

penicillin/streptomycin (PAA Laboratories) was added to wells (top-up medium). 50µl was removed and replaced with 60µl fresh top-up medium every 48 hours.

Table 2.15: RAFT 3D (TAP Biosystems) protocol for fabrication of compressed gels.

Reagent	Volume (ml)
10x MEM	2.8
2mg/ml collagen I	22.4
Neutralising solution	1.624
Cell stock solution	1.2
Total volume per well	0.24

Listed are the volumes required (ml) for sufficient solution for all wells of a 96-well plate. Cell stock solution is the media used to re-suspend the cells.

2.6.3 Compressed collagen I gels with hDFs, BMMSCs or AdMSCs

Separate compressed collagen I gels were fabricated containing 3 different stromal cell lines (hDFs, BMMSCs and AdMSCs) at passage 4, using RAFT 3D reagents and protocols all with a cell concentration of $6x10^3$ cells. As per the RAFT 3D protocol, cells were counted and re-suspended in gel mix (Table 2.15) then plated in a 96-well plate and placed into the incubator for 15 minutes. They were then compressed for 15 minutes using the RAFT 3D compression device before adding 100µl DMEM (Lonza Biologics) + 10% (v/v) FCS (PAA Laboratories) + penicillin/streptomycin (PAA Laboratories) to all wells. After 24 hours half the wells underwent a live/dead stain (2.6.4). The top-up media for remaining wells was changed every 48 hours for the day 7 live/dead stain.

2.6.4 LIVE/DEAD® stain protocol

Culture medium was aspirated and replaced with 100µL D-PBS (Lonza Biologics) then placed onto a rocker with the speed set on medium, for 10 minutes. 'Dead controls' were prepared by adding 25µL of 5% w/v saponin (Sigma Aldrich Ltd.) to the gels 30 minutes before aspirating culture medium, and used to check for Calcein AM background noise. Acellular gels were used as background noise controls for both EthD-1 and Calcein AM. The LIVE/DEAD® stain (Invitrogen Ltd.) was prepared by adding 20µL

of the supplied 2mM EthD-1 stock solution to 10 mL D-PBS (Lonza Biologics), then adding 1µL of the supplied 4mM Calcein AM stock solution, resulting in final concentrations of 0.4µM and 4µM for Calcein AM and EthD-1 respectively. The D-PBS (Lonza Biologics) was then replaced with 100µL of the LIVE/DEAD® stain and incubated for an hour. The gels were then imaged either after 24hrs or after 7 days using a Nikon Eclipse TE300 microscope and a Hamamatsu ORCA-ER camera (Hamamatsu Photonics UK Ltd) and the average number of live and dead cells were calculated from 3 separate images over 3 wells. Percentage viability was calculated using the following equation:

$$\%viability_{d=1\ or\ d=7} = \frac{Number\ of\ live\ cells}{Number\ of\ live + dead\ cells - average(bckgd_{EthD1}1\ \&\ 2)}$$

2.7 Uncompressed collagen I gels

HUVECs, CBECFCs and PBECFCs were labelled with eGFP (2.5) and all cells (these ECs as well as BMMSCs and AdMSCs) were used at P4 or P5. Several different constructs containing variable amounts of ECs and MSCs were fabricated in order to ascertain optimal cell concentrations and gel constituents and specific details for each construct can be found together with results for uncompressed gels, in Chapter 4. The basic constituents for fabricating the uncompressed collagen I gel are described below.

In order to make the collagen I gel, the protocol published by *Stratman et al.* which included the cytokines stem cell factor (R & D systems), interleukin-3 (R & D systems) and stromal-derived-factor-1α (R & D systems), was used (Table 2.12) (124). Once collagen had been added to the other components for the gels and mixed well, this was immediately used to re-suspend cells for experiments where cells were seeded within gels or were plated (all plated were uncoated standard tissue culture plastic) without cells for experiments where cells were seeded onto already polymerised gels. The cells were trypsinised (2.2.8) and counted and appropriate cell numbers were then centrifuged at 1200 rpm for 5 minutes, acceleration 9 and brake 9, RT. The 96-well plate was then placed into a Nuaire DH autoflow incubator (Nuaire) at 37°C in 5% CO_2 in air for 30 minutes for gels to set. All work with the gel and re-suspending of cells prior to placement in the incubator was carried out on ice to prevent premature polymerisation of the gel. 100µl top-up medium (Table 2.13) was then added directly to wells containing gels with cells or was used to re-suspend cell pellets for the other wells. After 48 hours,

50µl top-up medium was removed from each well and 60µl top-up medium was added (10µl extra to take account of evaporation). This half medium change was repeated after a further 48 hours and then 72 hours after this. At day 7, gels were fixed with PFA (2.9) and fluorescent photos were taken using a Nikon Eclipse TE300 microscope and a Hamamatsu ORCA-ER camera (Hamamatsu Photonics UK Ltd).

In the first optimisation experiment, EGM-2 medium (Lonza Biologics) was compared to M-199 (Sigma Aldrich Ltd.), the main constituent for the *Stratman et al.* protocol (124). EGM-2 with 10% (v/v) FCS (PAA Laboratories) was used in place of 10x M-199 and EBM-2 in place of 1x M-199 (Table 2.6). Since EGM-2 already contains numerous cytokines including hFGF-B, VEGF, R^3-IGF-1 and hEGF, no other cytokines were added to the reagents for this gel. Once gels had set, 100µl EGM-2 with (cells on gel) or without cells (cells within gel), was added onto the gels as a 'top-up medium'. Medium changes and fixing of gels were carried out as per the M-199 gels but EGM-2 with 2% (v/v) FCS was used rather than 'top-up medium'.

When CB/PBECFCs were co-cultured with MSCs it was noted that gels contracted away from the edges of the wells in the 96-well plates. In order to address this, 2 separate experiments were conducted whereby either the quantity of MSCs was reduced (therefore hopefully reducing the amount of extracellular matrix [ECM] production) or the collagen I concentration was reduced (from 2 to 1.5 mg/ml). In addition, a double volume gel whereby every reagent quantity was doubled (cells and gel constituents) was also used to see whether vessel formation was supported throughout a thicker gel scaffold.

Constituents for the first 2 variables (low MSC concentration; double volume gel) contained identical reagents to those for previous collagen I gels (doubled for the double volume gel) (Table 2.12). The low collagen I concentration gel had less collagen I per well with the total volume made up to 56µl using increased volume 1x M-199 (Table 2.16).

Table 2.16: low collagen I concentration gel (1.5mg/ml).

	[Stock]	[Final]	**amount (µL)**
Total Volume of gel			56.00
Final concentration of collagen I desired (mg/ml)			1.50
Collagen I (bovine)	5mg/ml	2mg/ml	16.80
[10x] M-199 (Sigma Aldrich Ltd.)	10x	-	5.60
NaOH	1M	-	0.42
[1x] M-199 (Sigma Aldrich Ltd.)	1x	-	31.54
NaHCO3	-	-	1.64
SCF	100µg/ml	0.2µg/ml	0.11
SDF1α	100µg/ml	0.2µg/ml	0.11
IL-3	100µg/ml	0.2µg/ml	0.11

Having determined an optimal cell concentration for PB and CBECFCs when co-cultured with BMMSCs and AdMSCs (2mg/ml collagen I gel; $2x10^5$ ECs with $3x10^4$ MSCs) this setup was used in order to compare co-cultures of the various cells that had been isolated and expanded. Table 2.12 shows the constituents for one well of a 96-well plate. Every possible combination of $2x10^5$ ECs (3 batches of HUVECs, CBECFCs or PBECFCs) with $3x10^4$ MSCs (3 batches of BMMSCs or AdMSCs) were cultured within 56µl of this gel.

Fibronectin (FN) (Sigma Aldrich Ltd.)-containing gels were also fabricated in order to ascertain the influence of this protein on tubule forming capacity. In order to fabricate gels containing FN, sufficient FN was added to gel mixture prior to adding collagen I in order for the final FN concentration to be 100µg/ml whilst still maintaining a final collagen I concentration of 2mg/ml (an equal amount of 1x M199 was removed from the mix to keep gel volume the same).

In order to quantify tubule formation for the different gel constructs, confocal images were taken using a standard confocal microscope and processed using Imaris software (version 7.6.4; Bitplane) with a filament tracer plugin. Threshold (loops) was selected and using the 'slice' setting, the approximate width of tubules was measured and input into the algorithm for the software. In the next window, segmentation settings were corrected so that all tubules were shaded but surrounding gel was removed. A ratio of

branch length to trunk radius of 3.0 was used in every gel and finally all tubules with a length of less than 8µm were removed prior to processing final calculations. Numerous parameters were calculated including number of tubules, tubule length (average and total), tubule diameter (average), tubule volume (average and total) and number of branch points (average and total).

2.7.1 Upscaling to a 24 well plate

In order to assess the role of pre-vascularising gels one method would be to place such constructs into an *in vivo* animal model. One way in which to do this would be to grow a larger gel construct for example in a 1.6cm diameter well of a 24-well plate and then place this into a murine full thickness wound.

For a 96 well plate the requirement is $2x10^5$ ECs and $3x10^4$ MSCs per well therefore in order to upscale cell numbers, one requires $1.2x10^6$ ECs and $1.8x10^5$ MSCs per well for a 24 well plate (Table 2.17).

Table 2.17 Volumes required for upscaling to a 24 well plate from a 96 well plate. (1.91/0.32 = 6) → 336µl gel)

Vessel type	Diam(mm)	Growth area(cm^2)	Total well vol (µl)	Working vol (µl)
96 well	6.35	0.32	360	56
24 well	15.62	1.91	1900	336

Table 2.18: Planned topographical layout of constituents for a 24 well plate of up-scaled gels

	HUV +BM	HUV +BM	PB+ BM	PB+ BM	
	HUV +Ad	HUV +Ad	PB+ Ad	PB+ Ad	

P4/5 ECs and MSCs were trypsinised, counted and centrifuged together ready for re-suspension in gel mix prior to plating and the gel mixes were made as per table 2.12 but with a multiplication factor of 6 for the 24-well plate format.

In the same way as with 96-well plate gels, gels were fabricated on ice (plate and pipette tips in freezer prior to use and on ice during fabrication process). Cells were then re-suspended in the gel mix without collagen I then collagen I was added and mixed. 336µl was then pipetted into separate wells of the 24-well plate as per Table 2.18. Plates were placed into a Nuaire DH autoflow incubator (Nuaire) in 5% CO_2 in air at 37°C for 60 minutes until gels had set and then top-up media (Table 2.13) was added (600µl for each well of the 24-well plates). Medium was changed at 48 hours and then again 48 hours later and gels were fixed in 4% PFA and photos taken at day 7 as per previous uncompressed gels (2.8).

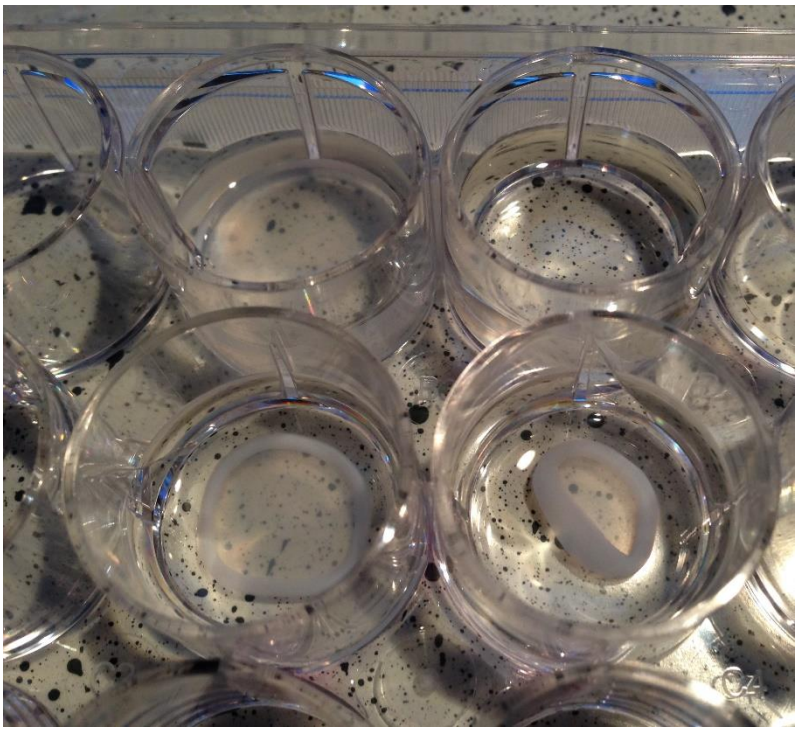

Figure 2.19 – 24-well plate containing collagen I gel: At day 7, pre-vascularised collagen I gels were fixed with 4% (w/v) PFA. This caused the gels to come away from wells but they could be easily flattened again under cover slips for quantitative confocal microscopy. In addition one can see from the images that the gels were substantial, durable and easy to handle despite being uncompressed.

2.8 Fixing of gels

In order to fix the gels, medium was removed from wells and gels were gently washed with 100µl PBS per well. This was aspirated and replaced with 100µl 4% (v/v) Paraformaldehyde (PFA) (2.9.1) per well which was left in situ for 15 minutes. This was aspirated and 2 further 100µl PBS washes performed. Gels were then covered with 200µl PBS and some Parafilm® before being placed into a fridge.

2.8.1 Making 4% paraformaldehyde (PFA)

Sixty mls of hot distilled water was placed into a glass beaker and heated to 60°C on a hot plate in a fume cupboard. Whilst wearing a mask, 4g PFA (Sigma Aldrich Ltd. Ltd.) and a flea were added and the solution mixed. NaOH (1M) was then added drop-wise until the solution became clear (approximately 6 drops). 10mls 10x D-PBS (Lonza Biologics) was then added followed by 4g Sucrose (Sigma Aldrich Ltd.) which helps to preserve cell morphology. This solution was then made up to 100mls with MilliQ H_2O and pH checked aiming for pH 7.2-7.4 (can adjust with HCl). This was filter-sterilised and stored at -20°C until required.

2.9 *In vivo*: uncompressed PBECFC/AdMSC gel in a humanised mouse model

Following confirmation of tubule formation in up-scaled uncompressed gels containing AdMSCs co-cultured with PBECFCs (Chapter 2.8.7 and Chapter 4), 3 of these gels were made in a 24-well plate. After culture for 1 week (with top-up media changes every 48 hours (Table 2.7)), tubule-like structures had formed within the gels and they were ready for implantation into immunodeficient (BALB/c) mice. 24 hours prior implantation, empty 240µl gels without cells were fabricated as controls (Table 2.12).

Gels containing tubule like structures and control gels were cut in half using a scalpel and implanted subcutaneously but above the panniculus carnosus on the dorsum of mice with half a control gel on one side and half a pre-vascularised gel on the other. This was carried out under anaesthesia and was performed by Dr Fadi Issa with full Home Office approval. Gels were secured to underlying panniculus and muscle with 6/0 Prolene (Ethicon, UK) sutures and wounds were then closed with 5/0 vicryl rapide sutures (both Ethicon). This was done to prevent inadvertent migration of the gel that would interfere with subsequent retrieval.

After 14 days, 6 gels from 3 mice (control and pre-vascularised) were explanted along with overlying skin, under full anaesthesia, and were immediately placed into D-PBS with mice being sacrificed immediately following gel harvest. Approximately 15 minutes prior to harvest of the gels, mice were injected through their tail vein with 100µl biotinylated

Lectin from *Lycopersicon esculentum* (tomato) (Sigma Aldrich Ltd.) which had been made up to a concentration of 1mg/ml with D-PBS (Lonza Biologics).

Once all gels had been harvested, D-PBS (Lonza Biologics) was replaced with 4% (w/v) PFA (2.9). After 1 hour in PFA, gels were twice washed gently D-PBS and then placed into bespoke kitchen foil 'boats' and covered with O.C.T. compound (Tissue-Tek). They were rapidly frozen in liquid nitrogen and then stored at -20°C until ready for sectioning. Ten µm sections gels with overlying dermis were then obtained using a cryostat and placed onto microscope slides and stored at -20°C until ready for staining. They were first stained as follows:

A PAP pen (Sigma Aldrich Ltd.) was used to draw around specimens and these were then immediately covered with approximately 100µl D-PBS (Lonza biologics) to prevent dessication. Meanwhile, a 0.5% BSA (v/v) in D-PBS was made into which anti-mouse FcR block (eBioscience) was added at a concentration of 2µl per 100µl to make the final stain buffer (SB). D-PBS overlying the specimens was removed and replaced with 100µl SB which was left for 20 minutes at RT. SB was then removed and replaced with either Streptavidin e450 (eBioscience) (1µl/100µl SB) to stain for lectin from *Lycopersicon esculentum* (tomato), anti-mouse CD31-PE (Biolegend) (5µl/100µl SB) to stain for mouse CD31, or PE Rat IgG2a control antibody (Biolegend) (5µl/100µl SB) for the CD31 PE control. The slides were left in a humidified chamber for 30 minutes at RT, covered with kitchen foil. They were then washed in SB and a drop of Vectashield mounting media for fluorescence (Vector) added prior to covering with a cover slip. Nail varnish was then used to seal the cover slip and slides were refrigerated at 4°C until ready for imaging. Immunostaining using this technique did not enable visualisation of the vasculature within the scaffolds so a CD31 biotinylated stain was carried out instead as per section 2.6 (umbilical cord immunostaining).

2.10 Statistics

For compressed gel cell viability, one-way ANOVA was performed to determine significance between % viability calculations of cell types used, followed by post hoc analysis using the Tukey's honest significance difference (HSD) test to test for significant difference between the various cell types (SPSS V22.0.0). Paired t-tests were performed

to test for significance between % viability calculations at day 1 and day 7 for each cell line.

For endothelial cell migration experiments using μ-chemotaxis 3D and the comparison between different uncompressed gel constructs, one-way ANOVA was performed with post hoc analysis with Tukey's HSD test and Bonferroni and paired t-tests were carried out for subgroup analysis (SPSS V22.0.0).

To compare the number of tubules seen at 14 days in *in vivo* experiments, paired Students t-test was used.

CHAPTER 3

FABRICATION OF A PREVASCULARISED SCAFFOLD

The main aim of this project was to improve existing proprietary dermal scaffolds which are currently in use for the treatment of full thickness wounds (see Chapter 1). One way in which this could be achieved would be to pre-vascularise scaffolds using autologous, adult-derived stem and progenitor cells.

This Chapter therefore examines the migratory properties of 3 different types of endothelial progenitor cells (HUVECs, CBECFCs and PBECFCs) within fibrin and collagen gels. Having determined the optimal gel for ECFC migration, this is then used to co-culture ECFCs with MSCs in compressed and then uncompressed collagen I gels in order to attempt to create 3D pre-vascularised scaffolds.

3.1 Migration of endothelial cells: µ-Chemotaxis 3D

Directed cell migration (chemotaxis) towards a stimulus is a well-defined function of many mammalian and non-mammalian cells. It is essential for wound healing and for the development of bioengineered scaffolds for therapeutic use.

The gold standard for determining efficient homing and migration of stem/progenitor cells within a wound bed and their subsequent revascularisation of the damaged tissue is to effectively repair wounds in the human or a suitable animal model such as an immunodeficient mouse. However, this is time consuming, costly and the Home Office encourages as much *in vitro* analysis as possible prior to using *in vivo* surrogate models. An initial *ex vivo* migration assay reduces animal studies and allows the refinement of conditions for pre-transplant manipulation of cells so that their migratory abilities can be assessed and optimised prior to transplant of matrix components with cells.

Ibidi GmbH (Munich, Germany) has developed a number of µ-slide chemotaxis assays. One is 2-D, where adherent cells are seeded into a chamber with or without a supporting matrix, and another is 3-D, where non-adherent cells or loosely adherent cells are encapsulated within a gel. The cells are then allowed to migrate towards a chemoattractant (Figure 3.1).

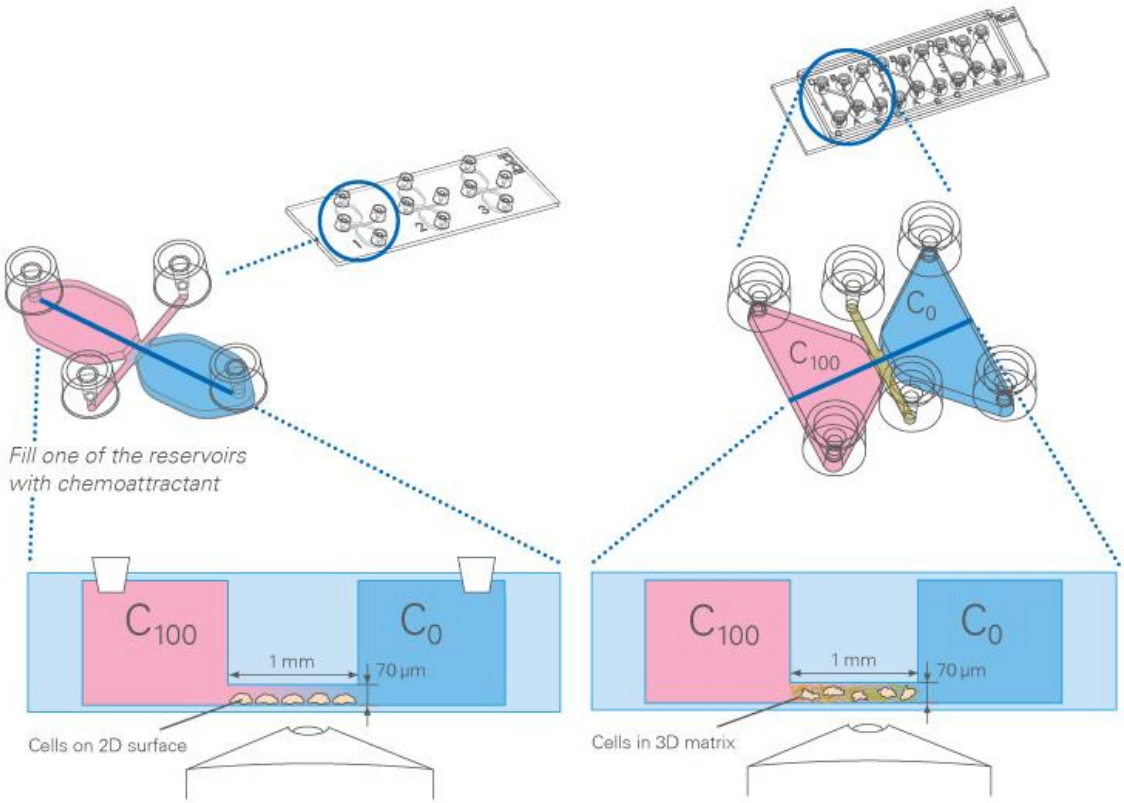

Figure 3.1 – 2-D and 3-D µ-slide chemotaxis: Cells are seeded within a central chamber either in medium (2-D) or a gel scaffold (3-D). Control or chemoattractant medium is then placed into reservoirs either side of the central chamber to stimulate cell migration (image shown with permission of Ibidi GmbH)

Using the 3-D µ-slide chemotaxis chambers from Ibidi GmbH, a reproducible *in vitro* chemotaxis assay can be carried out allowing the tracking of individual HUVECs or ECFCs through a collagen I, fibrin or other matrix by timelapse microscopy. Using Image J plug-ins to provide quantitative, visual and statistical analysis, a large volume of information on both cell chemotaxis and chemokinesis can be obtained. The migratory parameters generated include cell velocity, accumulated distance (total cell path travelled), Euclidean distance (straight distance between cell start and end point), displacement of the centre of mass (average end position of tracked cells), forward migration index (the ratio between the net distance travelled on the relevant axis and the accumulated distance) and directionality (the ratio between Euclidean and accumulated distance) (Figure 3.2). Rayleigh statistics provide an indicator of significantly in-homogeneously distributed populations where $p<0.05$. This assay has the advantage that it is possible to observe not only the chemotactic and chemokinetic effects of a stimulus on cell migration, but also the strength of chemotactic response and cell morphology, viability

and cell-cell interactions during the migratory process through a defined 3D extracellular matrix.

The 2D assay has already been used to demonstrate that HUVECs migrate to a 10% (v/v) FCS positive stimulus showing strong chemotaxis (146) ($p \leq 0.005$) (Figure 3.3).

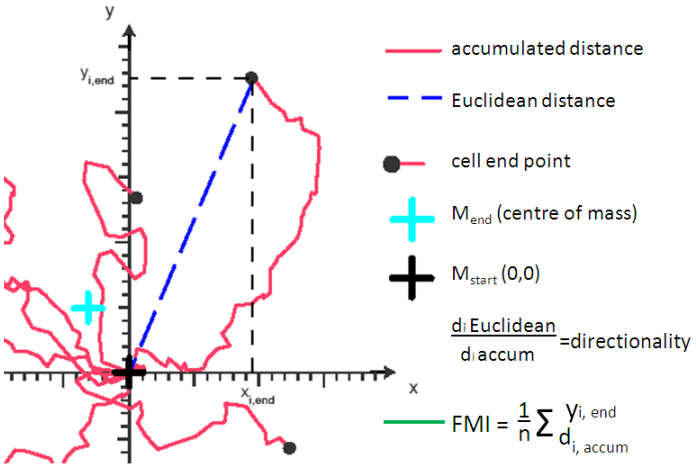

Figure 3.2 – parameters calculated using Image J 'chemotaxis tool' plugin: this figure shows the different parameters that can be calculated by Image J using the raw data provided by the timelapse videos of cell migration within the 3-D µ-slide chemotaxis chambers (image shown with permission of Ibidi GmbH).

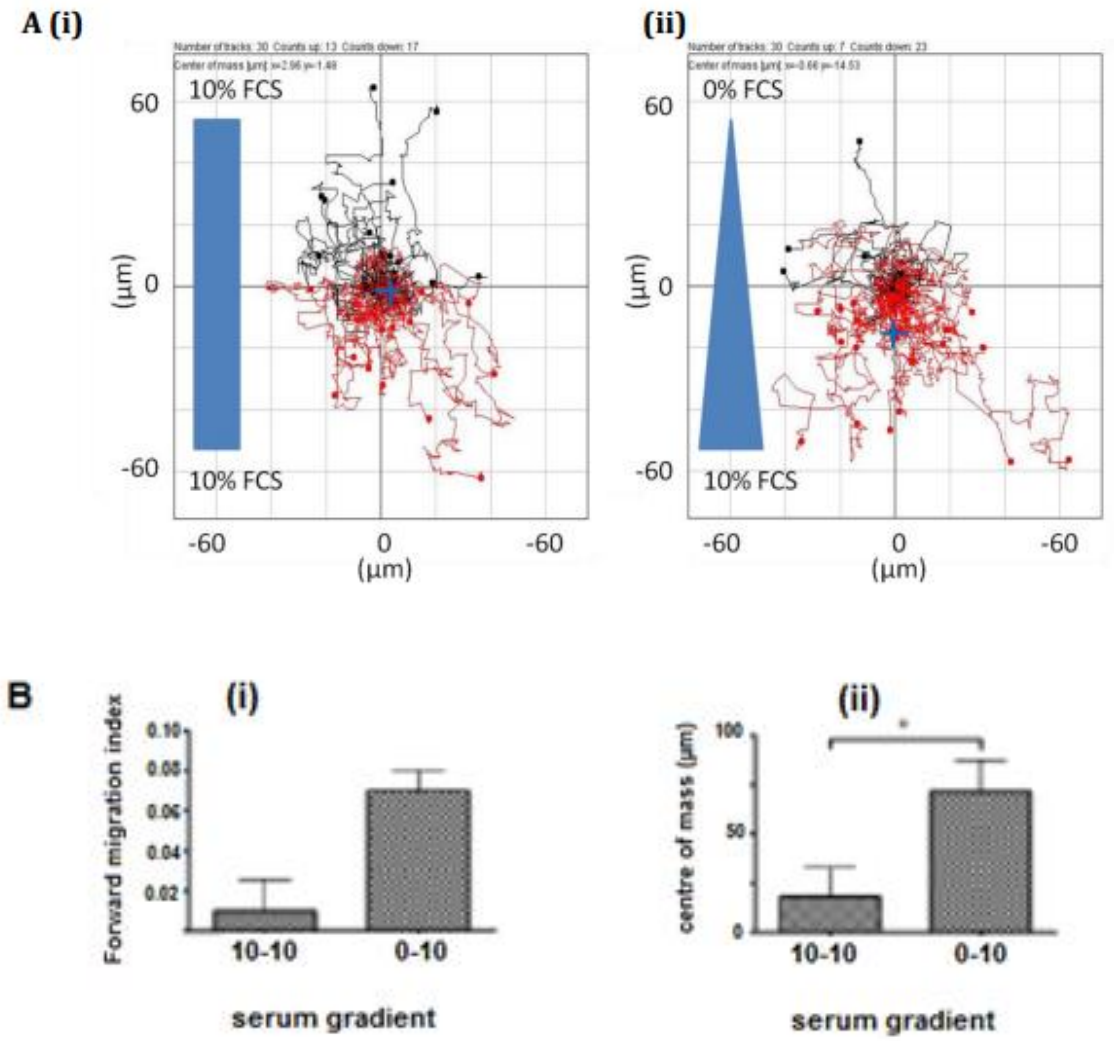

Figure 3.3: Establishing migration using 2D µ-chemotaxis slides with HUVECs. In control conditions, minimal forward migration or shift in centre of mass was seen (Figure 3.3Ai, Bi and Bii). However, when a 0-10% (v/v) positive stimulus was established a significant displacement of centre of mass in the direction of the positive stimulus was seen (p=0.0178) (Mann-Whitney test; n≥3) (Aii and Bii). Red dots represent cells migrating towards the positive stimulus, black, away from the positive stimulus.

In view of the migration of HUVECs towards a 10% (v/v) FCS positive stimulus in this 2D paradigm, the same methodology was used for our 3D µ-chemotaxis assays. Since the majority of scaffolds in the literature are composed of either collagen I (100,104,108) or fibrin (63), these were used to optimise gel concentration.

3.1.1 Aims and objectives for the µ-chemotaxis 3D assay

Previous research (146) has determined an optimal time course of 24 hours for µ-chemotaxis 3D and an optimal chemotactic positive stimulus of 10% (v/v) FCS (146).

These were therefore used to determine the optimal scaffold constituents with the main aims of experiments were therefore to:

1. Use the µ chemotaxis 3D assay to define the optimal matrix composition (fibrin or collagen with or without fibronectin) for EC migration.
2. Compare the migration of different endothelial progenitors (HUVECs, CB ECFCs, PB ECFCs) within the same gel matrix.

In order to ascertain the optimum gel for use when co-culturing ECs with MSCs to attempt to grow tubule-like structures (TLS) in vitro, a number of different fibrin and collagen I concentrations were inserted into the viewing chamber of the µ-chemotaxis slide along with $3x10^5$ HUVECs. Once the optimum gel had been ascertained by these experiments, 3 different batches of HUVECs, CB ECFCs and PB ECFCs were placed into the viewing chamber of slides with 1mg/ml collagen I gel plus or minus fibronectin and their migration over 24 hours examined (see Chapter 2.4 for methodology for chemotaxis gel optimisation).

Throughout this thesis the term 'TLS' is used to describe the interconnecting networks formed when eGFP-labelled ECs align within collagen scaffolds. The gel scaffolds in which ECs were seeded were small (96-well plates) meaning that 'TLSs' don't have clearly identifiable lumina. Nevertheless, the terms tubule or TLS are regularly used interchangeably within published works (73, 142) to describe similar structures and therefore are used within this thesis.

3.1.2 Results: µ-chemotaxis assay

Figure 3.4 shows one viewing chamber of the µ-chemotaxis 3D slide when viewed under the Nikon Eclipse TE300 microscope after the 24 hour timelapse sequence. After 30 randomly chosen cells were tracked using timelapse microscopy, their migratory properties were then scrutinized using Image J (manual tracking plugin). Figure 3.5 shows the migration plots for HUVECs within a bovine collagen I 1mg/ml gel and human fibrin 1.25mg/ml and 2.5mg/ml gels. They demonstrate how collagen I 1mg/ml and fibrin 1.25mg/ml show improved migration in comparison to more concentrated gels in terms of higher displacement of centre of mass, higher accumulated distance and faster velocity (see Table 3.1). Although these parameters were similar whether collagen I

1mg/ml or fibrin 1.25mg/ml gels were used, collagen I 1mg/ml was used for quantified chemotaxis experiments since co-culture of ECFCs and MSCs has been examined more extensively for producing novel dermal substitutes than fibrin. If problems had arisen using collagen I then fibrin would have been examined more closely.

<u>Take home message:</u> 1mg/ml Collagen I gel enables EC migration better than 3mg/ml Collagen I gel

Fig 3.4 - µ chemotaxis assay: Collagen I 1mg/ml at 0 hours (top) and 24 hours (bottom). Note that in addition to migrating within collagen I gel, HUVECs formed TLS-like structures (black arrows) at 24 hours

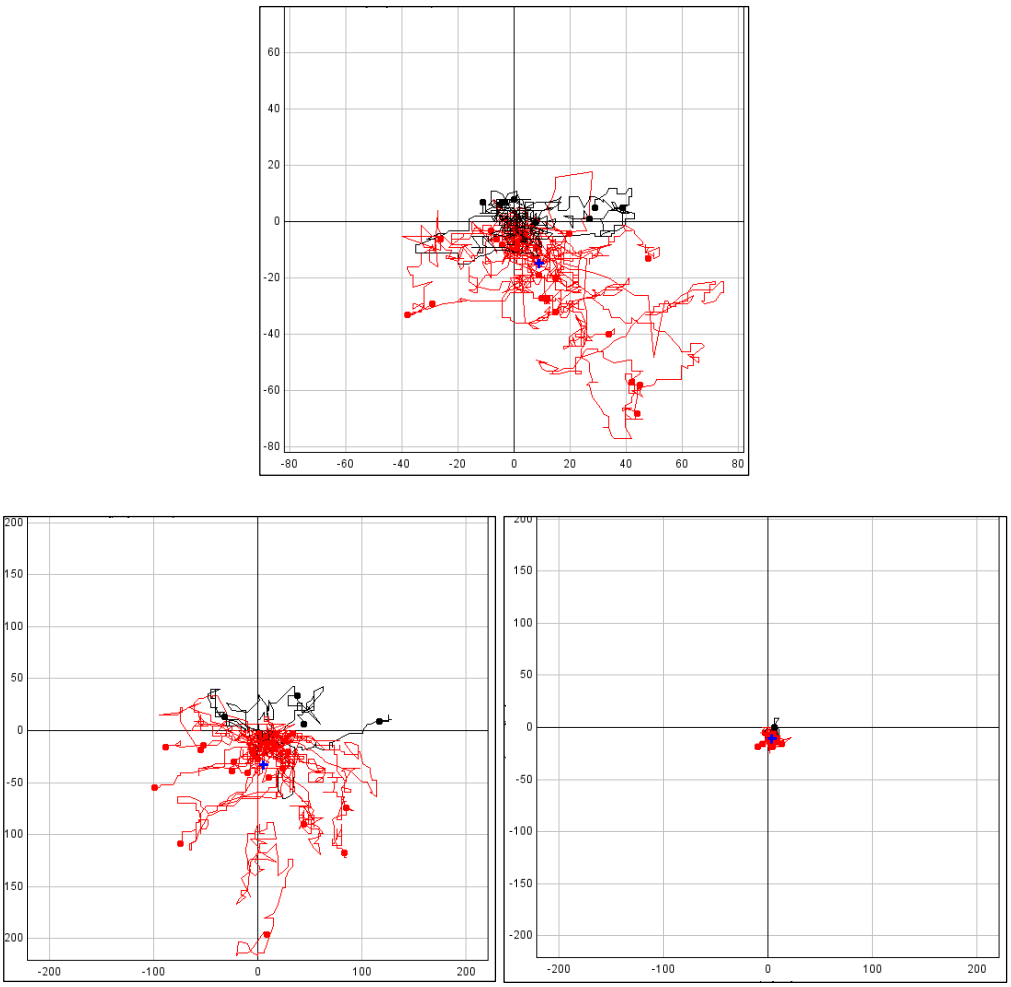

Fig 3.5 – Migration plots for 30 HUVECs in collagen/fibrin gels: Plots showing the migration of 30 tracked pHUVECs over 24 hours with timelapse microscopy within collagen I 1mg/ml (top), fibrin 1.25mg/ml (bottom left) and fibrin 2.5mg/ml (bottom right) with 0.5% (v/v) FCS at top and 10% (v/v) FCS at bottom (plots for 5, 7.5 and 10mg/ml fibrin gels and 3mg/ml collagen I gel not shown but resembled fibrin 2.5mg/ml fibrin gel). Red dots represent cells migrating towards the positive stimulus, black, away from the positive stimulus. X and Y axes are distance travelled in µm.

Table 3.1 – migration results for HUVECs in different optimisation gels:

	Collagen 1mg/ml 10% (v/v) FCS bottom	Fibrin 1.25mg/ml 10% (v/v) FCS bottom	Fibrin 2.5mg/ml 10% (v/v) FCS bottom	Fibrin 5mg/ml 10% (v/v) FCS bottom	Fibrin 7.5mg/ml 10% (v/v) FCS bottom	Fibrin 10mg/ml 10% (v/v) FCS bottom
x Forward migration index	0.0	0.01	0.18	-0.01	0.06	0.09
y Forward migration index	-0.1	-0.07	-0.41	0.05	-0.03	-0.21
Center of mass						
x [μm]	20.4	5.51	4.34	0	1.5	1.46
y [μm]	-32.6	-32.0	-10.2	1.0	0.5	-4.7
Accumulated distance [μm]	416.7 SD:162.1	412.89 SD: 222.7	35.07 SD: 27.7	10.3 SD: 19.29	23.55 SD: 32.47	14.6 SD:31.7
Euclidean distance [μm]	60.98 SD:48.84	58.2 SD: 47.13	11.99 SD: 3.99	3.09 SD: 4.27	9.73 SD: 14.94	5.8 SD:7.3
Mean Velocity [μm/min]	0.28 SD:0.11	0.27 SD: 0.15	0.02 SD: 0.02	0.01 SD: 0.01	0.02 SD: 0.02	0.01 SD:0.02
RALEIGH TEST	0.009	$1.08x10^{-4}$	$1.56x10^{-10}$	0.8126207	0.3398043	0.0023784

Statistics for migration of pHUVECs through 1mg/ml Collagen I gel and 1.25mg/ml, 2.5mg/ml, 5mg/ml, 7.5mg/ml and 10mg/ml Fibrin gels over 24 hours. Negative values for y[μm] centre of mass represent displacement of the centre of mass towards the 10% (v/v) FCS positive stimulus.

3.1.2.2 Migration of endothelial cells (HUVECs/CBECFCs/PBECFCs) through collagen I 1mg/ml gel plus or minus fibronectin

Collagen I gels at a concentration of 1mg/ml were examined with or without adding 100μg/ml FN. The migration of 3 different batches of HUVECs, CBECFCs and PBECFCs was examined. Due to variability between the different batches, very few comparisons between the different cell types within a collagen I gel with or without FN achieved statistical significance for mean accumulated cell distance, mean Euclidean distance or mean velocity (Figure 3.6 A, B and C). Rayleigh statistics provide an indicator of significantly in-homogeneously distributed populations where $p<0.05$ and this information, together with the results for individual batches of ECs can be found in tables 3.2, 3.3 and 3.4. It can be noted that Raleigh statistics were significant for samples with a 10% (v/v) FCS positive stimulus but not in control gels where 0.5% (v/v) FCS was in both reservoirs either side of the collagen I gel.

One-way ANOVA showed significant differences between groups for FMI Y ($p=0.014$) and change in centre of mass Y ($p=0.001$) but not when comparing the 12 different EC/gel combinations for mean accumulated distance ($p=0.215$), mean Euclidean distance ($p=0.131$) or mean velocity ($p=0.720$). Standard t-tests were carried out to look for statistical significance between the different EC subtypes (PBECFCs, HUVECs and CBECFCs) within the different gels (collagen with or without FN). There was an increase

in FMI and change in centre of mass towards a 10% (v/v) FCS positive stimulus (FMI Y, change in centre of mass Y) whether FN was added to the collagen gel or not (Figure 3.6 D and E). This was statistically significant for all EC cells ($p<0.01$** or $p<0.05$* - see Figure 3.6) in most gels. The only constructs where there was not statistical significance were change in centre of mass Y for PBECFCs in collagen I gel with FN ($p=0.11$) and FMI Y for HUVECs in collagen I gel with FN ($p=0.171$) and CBECFCs in collagen I gel without FN ($p=0.40$).

Due to the clear influence that a 10% (v/v) FCS positive stimulus had on the EC cells (Fig 3.6 D and E) a number of statistically significant results were noted for FMI Y and change in centre of mass Y but very few results for mean accumulated distance, mean Euclidean distance or mean velocity were significant since the differences for these parameters were small for the different EC cells. Nevertheless, certain observations from these results could be noted (Figure 3.6 A to C). First of all there was a clear trend for constructs containing FN to have higher values for mean accumulated distance, mean Euclidean distance and mean velocity then otherwise identical gels (EC and collagen I). This trend was statistically significant for PBECFCs for mean accumulated distance [(221.6µm in FN containing gel versus 182.1µm in standard collagen I gel ($p=0.039$)] and mean velocity [0.15µm/s in FN containing gel versus 0.13µm/s in standard collagen I gel ($p=0.039$)] when there was no 10% (v/v) FCS positive stimulus. There was also a statistically significant increase in Euclidean distance travelled for CBECFCs when there was no 10% (v/v) FCS positive stimulus [33.4µm versus 22.6µm ($p=0.038$)] and for HUVECs when there was a 10% FCS (v/v) positive stimulus [47.7µm versus 37.6µm ($p=0.041$)]. There was a trend for increased accumulated distance, Euclidean distance and velocity for PBECFCs compared to CBECFCs and HUVECs (Figure 3.6 A to C) but this was never statistically significant.

Table 3.2a – PBECFC migration through 1mg/ml collagen gel

	PBECFCs Collagen I 1mg/ml +FN 10% (v/v) FCS positive stimulus			PBECFCs Collagen I 1mg/ml +FN 0.5% (v/v) FCS top and bottom of chamber (control)			PBECFCs Collagen I 1mg/ml 10% (v/v) FCS positive stimulus			PBECFCs Collagen I 1mg/ml 0.5% (v/v) FCS top and bottom of chamber (control)		
X Forward migration index	-0.02	-0.03	0.04	-0.05	0.03	0.12	-0.07	0	0.01	0.03	-0.1	0.02
Y Forward migration index	-0.14	-0.16	-0.11	0	0	0.06	-0.15	-0.13	-0.06	0.03	-0.01	0.01
Centre of mass												
X [μm]	-3.18	-5.62	5.63	-11.85	4.72	21.9	-13.2	-0.07	-11.75	4.35	-12.88	6.32
Y [μm]	-33.67	-101.32	-32.48	-1.72	-1.96	16.5	-30.52	-24.6	-33.72	3.75	-0.85	1.35
Accumulated distance [μm]	236.92	560.43	285.51	204.37	233.88	226.41	213.25	192.69	531.14	186.29	177.84	182.23
Euclidean distance [μm]	49.58	170.65	50.57	40.31	32.3	50.03	46.63	38.29	124.38	29.83	24.89	26.43
Mean Velocity [μm/min]	0.16	0.39	0.2	0.14	0.16	0.16	0.15	0.13	0.37	0.13	0.12	0.13
RALEIGH TEST	$3.1x10^{-6}$	0.001	$1.7x10^{-7}$	0.11	0.59	0.05	$1.7x10^{-7}$	$1.3x10^{-6}$	$1.8x10^{-6}$	0.66	0.06	0.43

Statistics for migration of PBECFCs through 1mg/ml Collagen I gel with or without FN over 24 hours. Negative values for y indicate migration towards 10% (v/v) FCS.

Table 3.2b – HUVEC migration through 1mg/ml collagen gel

	HUVECs Collagen I 1mg/ml +FN 10% (v/v) FCS positive stimulus			**HUVECs Collagen I 1mg/ml +FN 0.5% (v/v) FCS top and bottom of chamber (control)**			**HUVECs Collagen I 1mg/ml 10% (v/v) FCS positive stimulus**			**HUVECs Collagen I 1mg/ml 0.5% (v/v) FCS top and bottom of chamber (control)**		
x Forward migration index	0.03	-0.02	0.03	-0.01	0.03	-0.02	-0.04	-0.03	0.06	0.05	0.05	-0.05
y Forward migration index	-0.07	-0.19	-0.07	0.04	0	0.03	-0.10	-0.08	-0.1	-0.02	-0.01	-0.01
Centre of mass												
x [μm]	9.82	-7.05	9.82	-5	7.29	-6	-8.93	-5.66	13.58	18.68	7.28	-10.23
y [μm]	-21.9	-33.75	-21.9	9.67	-1.32	7.67	-13.72	-19.90	-21.23	-5.70	-0.98	-1.81
Accumulated distance [μm]	287.74	194.27	287.74	248.63	206.53	238.63	172.81	223.43	228.81	216.66	163.57	191.47
Euclidean distance [μm]	46.45	50.18	46.45	31.89	28.29	30.89	42.33	33.52	36.93	51.23	24.28	28.82
Mean Velocity [μm/min]	0.2	0.13	0.2	0.17	0.14	0.16	0.31	0.15	0.16	0.38	0.11	0.13
RALEIGH TEST	$5.6x10^{-4}$	0.006	$4.2x10^{-6}$	0.26	0.39	0.17	0.00	0.004	$7.4x10^{-5}$	0.20	0.12	0.12

Statistics for migration of HUVECs through 1mg/ml Collagen I gel with or without FN over 24 hours. Negative values for y indicate migration towards 10% (v/v) FCS.

Table 3.3c – CBECFC migration through 1mg/ml collagen gel

	CBECFCs Collagen I 1mg/ml +FN 10% (v/v) FCS positive stimulus			**CBECFCs Collagen I 1mg/ml +FN 0.5% (v/v) FCS top and bottom of chamber (control)**			**CBECFCs Collagen I 1mg/ml 10% (v/v) FCS positive stimulus**			**CBECFCs Collagen I 1mg/ml 0.5% (v/v) FCS top and bottom of chamber (control)**		
x Forward migration index	-0.03	0.03	-0.05	0.01	0	-0.03	0.04	-0.03	-0.06	-0.06	-0.02	-0.04
y Forward migration index	-0.1	-0.05	-0.11	0	0	0.02	-0.05	-0.08	-0.12	0.03	-0.04	-0.01
Centre of mass												
x [μm]	-10.95	6.59	-12.37	4.35	-0.82	-5.32	5.79	9.52	-9.08	-12.34	-4.72	5.63
y [μm]	-32.55	-23.97	-29.97	-2.55	0.98	3.3	-15.39	-18.45	-22.5	4.27	-7.77	0.15
Accumulated distance [μm]	315.99	391.84	284.68	219.87	327.64	250.7	355.20	240.73	186.68	190.76	186.41	188.65
Euclidean distance [μm]	49.93	69.17	44.59	35.19	33.68	31.26	60.59	33.21	35.91	25.88	4.55	17.45
Mean Velocity [μm/min]	0.22	0.27	0.2	0.15	0.23	0.17	0.25	0.17	0.13	0.13	0.13	0.15
RALEIGH TEST	$4.9x10^{-6}$	0.01	$3.1x10^{-7}$	0.49	0.62	0.30	$1.2x10^{-5}$	$2.3x10^{-4}$	$5.1x10^{-6}$	0.005	0.11	0.24

Statistics for migration of CBECFCs through 1mg/ml Collagen I gel with or without FN over 24 hours. Negative values for y indicate migration towards 10% (v/v) FCS.

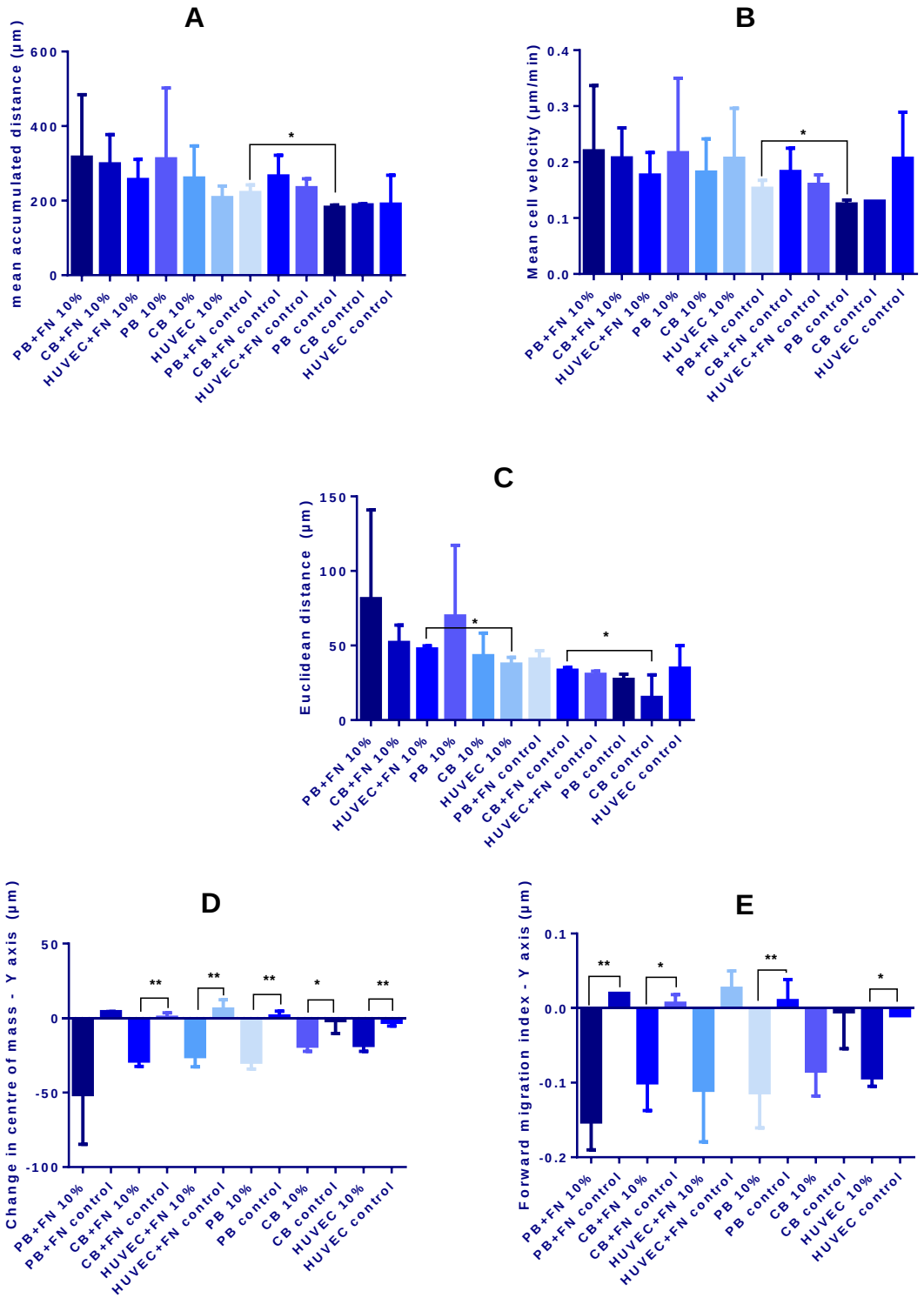

Figure 3.6 – Mean accumulated distance travelled [A], mean cell velocity [B], mean Euclidean distance [C], change in centre of mass (Y) [D] and forward migration index (Y) [E] for 30 ECs in collagen I 1mg/ml with or without FN: Mean accumulated distance, cell velocity and Euclidean distance were higher for FN containing gels than non-FN containing gels though this was only statistically significant for constructs labelled with * = $p<0.05$ or **= $p<0.01$ (unpaired students t-test). PBECFCs migrated further and faster than CBECFCs or HUVECs in most cases although this was never statistically significant. Change in centre of mass (Y) and FMI (Y) were significantly greater when there was a 10% (v/v) FCS positive stimulus for most cases (D and E * or ** for significance) ['10%' = a 10% (v/v) FCS positive stimulus; 'control' = no FCS positive stimulus].

3.1.3 µ-chemotaxis findings

In optimisation experiments using HUVECs, it was demonstrated that:

Fibrin gels and collagen I gels of a concentration of 3mg/ml and above were not conducive to EC migration.

Therefore, a 1mg/ml collagen I gel was used to quantify chemotaxis and chemokinesis parameters for 3 separate batches of HUVECs, CBECFCs and PBECFCs. The main observation was that:

PBECFCs, HUVECs and CBECFCs migrated towards a 10% (v/v) FCS positive stimulus with a statistical significance [one-way ANOVA forward migration index Y (p=0.014); change in centre of mass Y (p=0.001)] showing that the µ-slide chemotaxis 3D (Ibidi, GmbH) is a suitable surrogate for determining efficient directed homing and migration of stem/progenitor cells. In attempting to compare the 3 different EC cells for accumulated cell distance, Euclidean distance and average velocity, there were:

Trends for higher values when 100µg/ml FN was added to gels and also for PBECFCs to travel further and faster than CBECFCs or HUVECs although these results were not statistically significant.

This concentration of FN was chosen as it had been used to improve TLS formation in a previous study at a similar concentration (100). It is important to recognise that although many parameters were higher for PBECFCs than CBECFCs or HUVECs that this may have been because these cell lines seemed to line up into TLS-like structures more readily than PBECFCs in the chemotaxis chambers. Hence the distance travelled and average velocity would fall compared to PBECFCs. For this reason just because PBECFCs seemed to travel further and faster, this did not necessarily mean that they would form better TLSs and it was important to await results of 3D co-cultures before making such conclusions. There is a great deal of scope for the µ-slide chemotaxis 3D assay and what it can be used to ascertain. For example, various other chemo-attractants instead of 10% (v/v) FCS could be used within the reservoirs either side of the central gel channel to see if migration is further improved or other additives to the gel chamber could be considered which may be more conducive to migration of ECs. However, in order to take the project forward the above results provided sufficient

information as a starting point. Based on the chemotaxis outcomes it was reasonable to test only gels of less than 2mg/ml collagen I concentration.

In terms of attempting to fabricate a collagen I scaffold containing a pre-vascularised network of vessels, there are 2 potential paradigms that may be of use clinically – the first is a compressed collagen I gel, onto or into which the progenitor cells required for network formation are seeded, whilst the second is an uncompressed gel containing the required cells, which on development of a vascular network becomes mechanically strong enough to be handled in a clinical setting.

3.2 Compressed collagen gels

3.2.1 Rationale and aims for use of compressed collagen gels

Several authors have attempted to compress gels with the goal of producing a scaffold that was easier to handle for clinical purposes however these have invariably been done with fibroblasts alone (112,147–149). Clinically this would not be a suitable scaffold for skin regeneration as a scaffold containing only fibroblasts would lead to production of ECM and ultimately scar tissue formation unless host ECs invaded the construct to re-establish a new microcirculation at an early stage. One reason why full thickness skin grafts produce a more acceptable cosmetic outcome is the presence of a dermal plexus of blood vessels that helps in the remodelling process of the healing wound. Therefore, the optimum compressed collagen gel should have an EC element within it in addition to primary stromal cells. As MSCs have anti-fibrotic activities and can promote new blood vessel formation (143), the studies concentrated on ECs with AdMSCs.

RAFT 3D (TAP Biosystems) is a proprietary device that can be used to compress collagen gels within a 24, 48 or 96-well plate format in easily replicated fashion (Figure 3.7). It compresses gels to approximately 50 times their normal concentration resulting in a scaffold that is more durable and easier to handle. The aims regarding compressed gels were:

1. Attempt to compress a collagen I gel containing ECs or MSCs or a combination of these primary cell types, using RAFT 3D, and to check for viability following the compression process.

2. Attempt to grow TLSs within these compressed scaffolds.

or

3. Grow vascular networks within an uncompressed gel and compress this, then checking for persistence of these vessels.

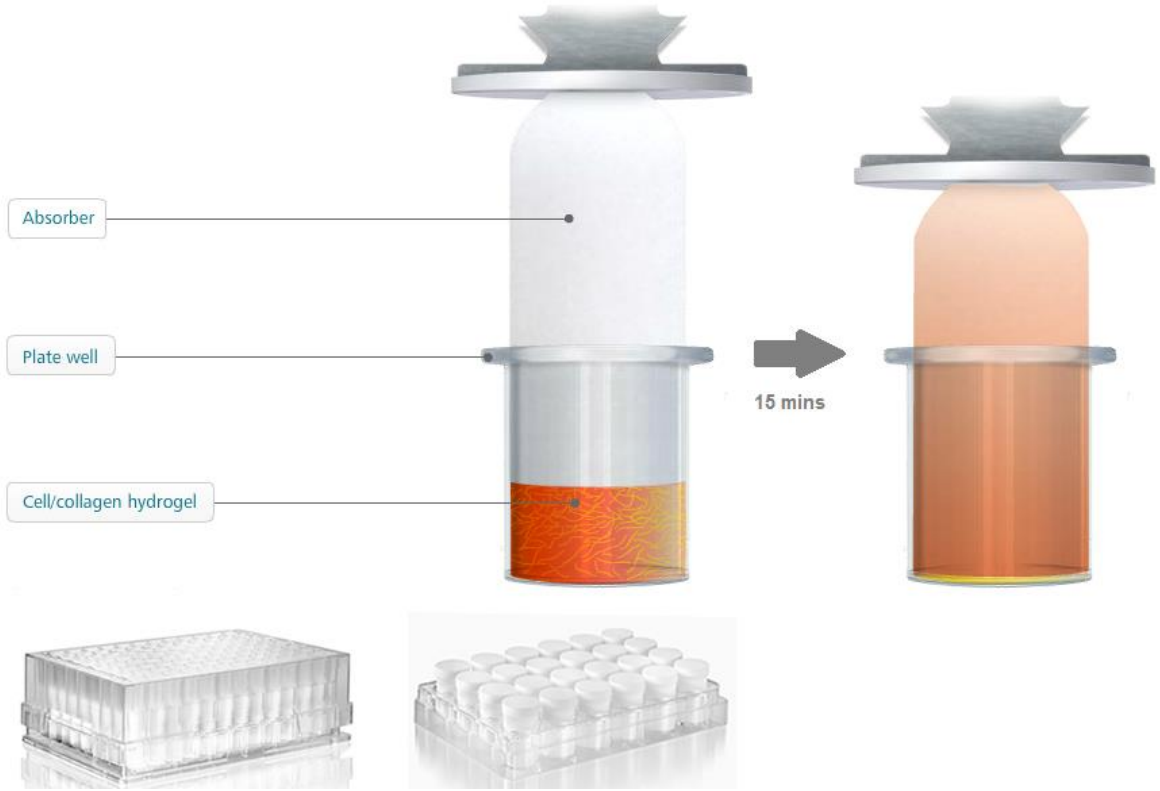

Figure 3.7 – RAFT 3D setup: 96-well and 24-well plates are shown underneath a close-up of the compression device. Note that the wick not only compresses the gel but also absorbs fluid at the same time concentrating the gel approximately 50x (TAP Biosystems).

The RAFT 3D protocol (TAP Biosystems) states that in order to produce a compressed collagen gel containing a fibroblast monoculture one should use 240µl for a 96-well plate. However, previous uncompressed gels containing EC and MSC co-cultures have been fabricated with smaller volume gels (130). Therefore prior to examining compressed gels, uncompressed gels containing varying quantities of HUVECs and BMMSCs were plated within gel volumes of 112µl and 240µl to see whether TLSs would form in thicker gels.

Previous compressed gels in the literature have used concentrations of fibroblasts of between $1x10^5$/ml (147,149) and $2x10^5$/ml (112) within collagen at a concentration of between 1.65 (112,149) and 4.3mg/ml (147). Using $1x10^5$ cells/ml as an example cell concentration within gels and a 240µl volume per well (RAFT protocol) (TAP Biosystems) would mean using $2.4x10^4$ cells in total. In uncompressed gel co-cultures within collagen and fibrin gels a ratio of approximately 4:1 (EC:MSC) is most commonly used (this would equate to $1.92x10^4$ ECs and $4.8x10^3$ MSCs) (63,83,124). Based on these previous examples, the following concentrations of HUVECs and BMMSCs were used in the first optimisation experiment: $4x10^5$ ECs and $8x10^4$ MSCs; $2x10^5$ ECs and $4x10^4$ MSCs; $1x10^5$ ECs and $2x10^4$ MSCs; $5x10^4$ ECs and $1x10^4$ MSCs; $2.5x10^4$ ECs and $5x10^3$ MSCs; $1.25x10^4$ ECs and $2.5x10^3$ MSCs. Higher concentrations, with the same 4:1 ratio were also examined within gels that were compressed at 48 hours rather than immediately: $8x10^5$ ECs and $1.6x10^5$ MSCs; $4x10^5$ ECs and $8x10^4$ MSCs; $2x10^5$ ECs and $4x10^4$ MSCs; $1x10^5$ ECs and $2x10^4$ MSCs.

3.2.2 Prevascularising uncompressed gels prior to compression

No TLS formation was observed by day 4 in 240µL gels (Fig 3.8); this was thought to be due to the gel being too thick resulting in a lack of oxygenation to the cells. Early TLS formation could be observed by day 3 in the 112µL gels, supporting this hypothesis. By day 6 there were extensive microvascular networks throughout the 112µL gels containing $4x10^5$ HUVECs and $8x10^4$ BM-MSCs (Figure 3.10), less so at lower numbers of cells ($2x10^5$ HUVECs and $4x10^4$ BM-MSCs). The former was therefore chosen as an optimum for uncompressed gels.

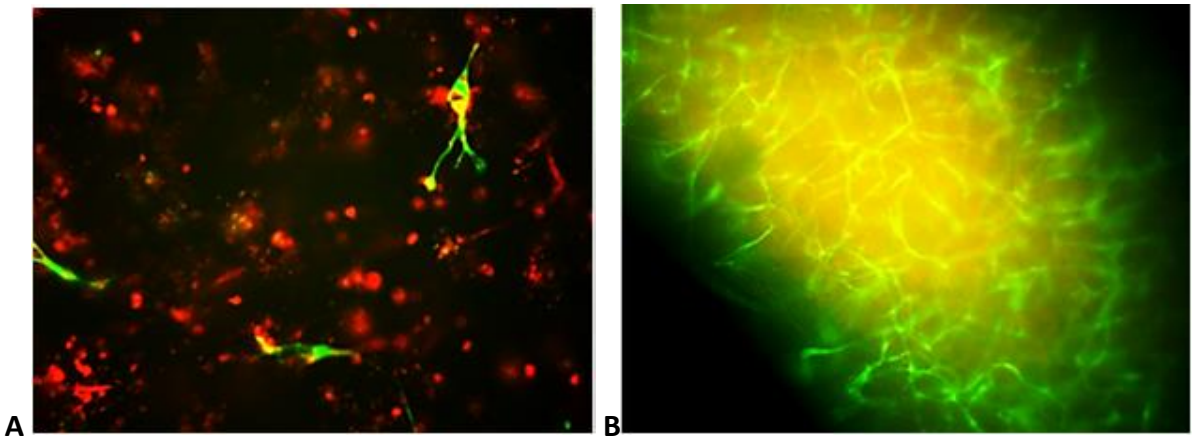

Figure 3.8 – HUVEC/BMMSC co-culture in uncompressed collagen gel: In the x10 magnification image of a 240µL uncompressed gel containing $8x10^5$ HUVECs and $1.6x10^5$ BMMSCs at d4 (A), there were only sporadic TLSs seen. In the x10 magnification image of an 112µL uncompressed gel containing $4x10^5$ HUVECs and $8x10^4$ BMMSCs at d4 there were extensive TLS networks seen (B). MSCs are labelled with cell tracker red and HUVECs with eGFP.

3.2.3 Results for compressed gels

Collagen I gels of 112µL, containing numbers of HUVECs and BMMSCs ranging from the uncompressed optimum quantity ($4x10^5$ HUVECs and $8x10^4$ BMMSCs) to 1/16 of this were compressed at day 0, 2 and 3 using RAFT 3D (see Chapter 2). Only lower numbers of cells along with the optimal concentration (Figure 3.8) were included as the compression would increase the concentration of the cells within the scaffold. No microvascular networks could be seen after compression of gels (Figure 3.9a); shortening the compression time to 5 minutes did not have any effect (Figure 3.9b).

Acellular 240µL collagen I gels were prepared, compressed at d0 and then had cells seeded onto the surface. Lower quantities of cells than $4x10^5$ HUVECs and $8x10^4$ BMMSCs were used as the requirement for a 2D cell monolayer would be far less than for a 3D scaffold. Some TLS formation was seen (Figure 3.10) however this was much less extensive than the uncompressed 112µL gels and was mainly confined to the periphery of the gel.

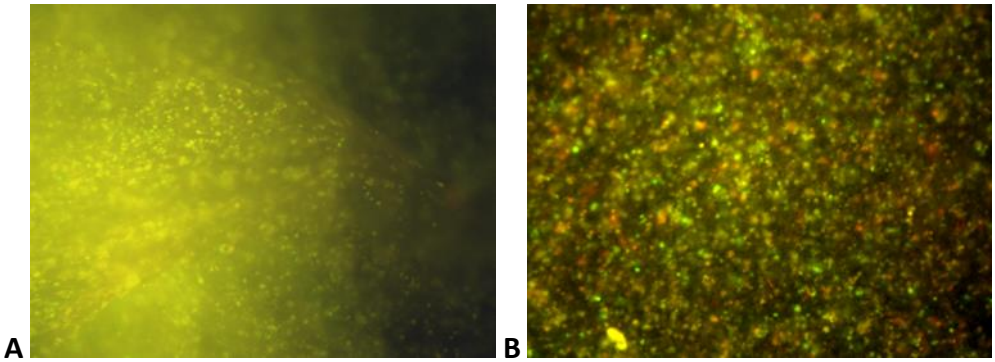

Figure 3.9 – HUVEC/BMMSC co-cultured in compressed collagen gel: a) d6, x10 magnification. 112µL gel compressed at d3 for 15mins, $4x10^5$ HUVECs, $8x10^4$ BMMSCs; b) d4, x10 magnification. 240µL gel compressed d2 for 5mins, $2x10^5$ HUVECS, $4x10^4$ BMMSCs. No microvascular networks were seen. MSCs are labelled with cell tracker red and HUVECs with eGFP.

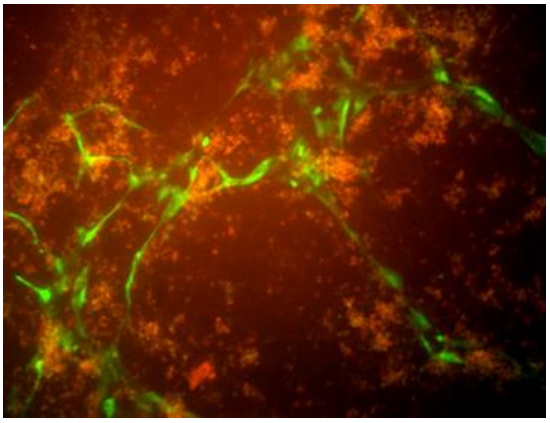

Figure 3.10 – HUVEC/BMMSC co-cultured on top of compressed collagen gel: d6, x10 magnification, 240µL acellular gel compressed d0 for 15mins, $1x10^5$ HUVECs, $2x10^4$ BMMSCs seeded on gel surface. Sporadic TLSs were noted in this case. MSCs are labelled with cell tracker red and HUVECs with eGFP.

In view of no TLSs forming within compressed gels and previously formed TLSs disappearing after the compression process, individual cell types rather than EC/MSC co-cultures were examined. The first primary cell type examined, in view of their necessity for vasculogenesis, was HUVEC. The same concentration of cells and quantities of reagents were used as for the RAFT 3D protocol (TAP Biosystems) (Chapter 2.7). As demonstrated in Figure 3.11 and Figure 3.15, there was 100% non-viability of these cells following compression using RAFT 3D.

TAP Biosystems demonstrated the proof of principle for RAFT 3D using human dermal fibroblast (hDFs). Therefore, in view of no HUVEC survival within the collagen I gel (Figure 3.11 and Figure 3.15) following the RAFT 3D compression process, a compressed gel containing either AdMSCs, BMMSCs or hDFs was tested. Sixty three percent of AdMSCs and 66% hDFs

survived at day 7 post-compression respectively whilst only 9% of BMMSCs did so (Figures 3.12, 3.13, 3.14 and 3.15).

The statistical analysis of the LIVE/DEAD® viability assay for HUVECs, hDFs, AdMSCs and BMMSCs is shown in Figure 3.16. Mean numbers of cells were calculated by counting the number of live cells (green) in 3 randomly chosen areas of compressed gels at x10 magnification and dividing this by the total number of cells (red and green) within these sections. No background noise was detected in acellular or dead controls.

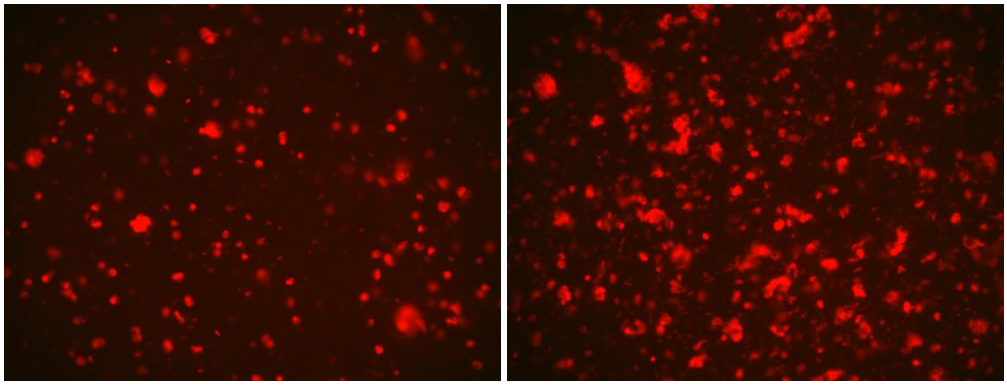

Fig 3.11 – Live/dead stain for HUVECs in compressed collagen gel: x10 magnification images of $1.2x10^4$ (left) and $2.4x10^4$ (right) HUVECs within compressed 2mg/ml collagen I hydrogel 48 hours after compression. Live cells appear green and dead cells red.

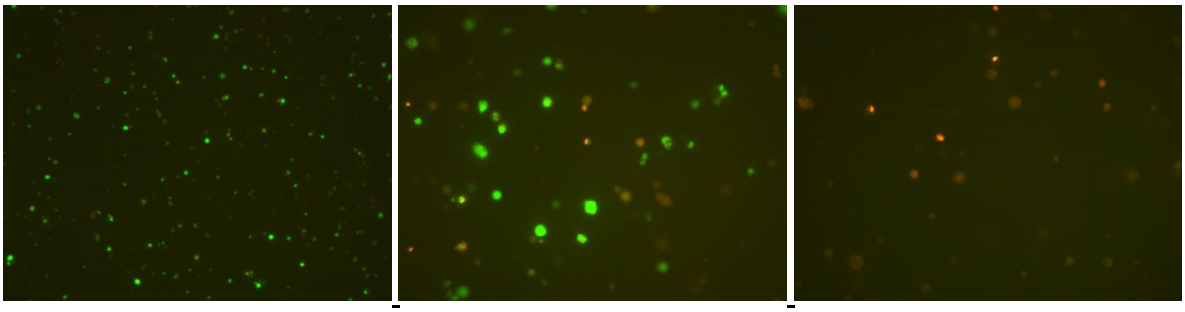

Fig 3.12 – Live/dead stain for AdMSCs in compressed collagen I gel: AdMSCs within a 2mg/ml collagen I hydrogel 48 hours after compression using RAFT 3D. x4 magnification (left); x10 magnification (middle); x10 magnification of dead control (right). Live cells appear green and dead cells red.

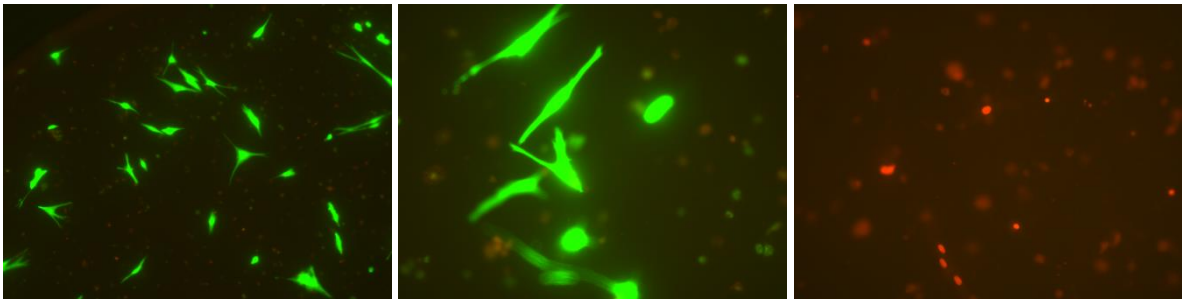

Fig 3.13 – Live/dead stain for hDFs in compressed collagen I gel: hDFs within a 2mg/ml collagen I gel 48 hours after compression using RAFT 3D. x4 magnification (left); x10 magnification (middle); x10 magnification of dead control (right). Live cells appear green and dead cells red.

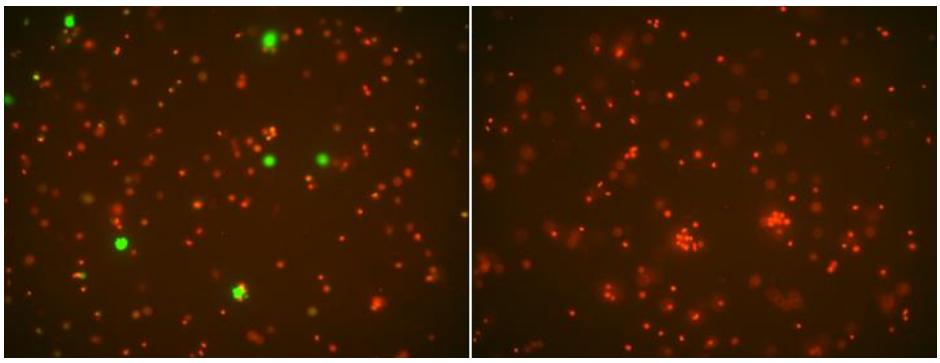

Fig 3.14 – Live/dead stain for hDFs in compressed collagen gel: BMMSCs within a collagen I 2mg/ml gel 48 hours after compression using RAFT 3D. x10 magnification (left); x10 magnification of dead control (right). Live cells appear green and dead cells red.

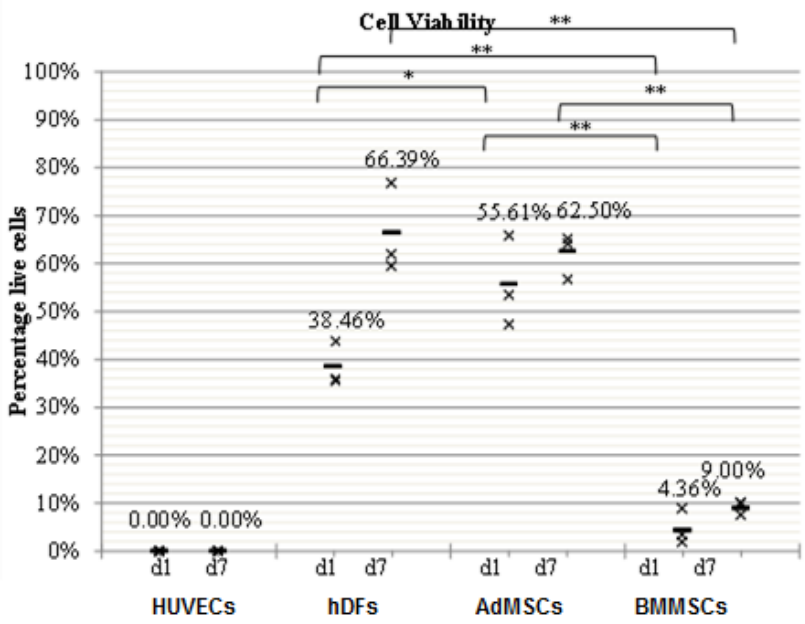

Figure 3.15 – HUVEC/hDF/ATMSC/BMMSC viability following compression: % viability of cells within compressed 2mg/ml collagen I gels. d1 and d7 refer to days after compression. x indicates % viability for single gel, – indicates mean % viability (also given numerically). One way ANOVA with Tukey's *post hoc* analysis on hDFs and MSCs. *p<0.05, **p<0.01

3.2.4 Compressed gels – summary

The aims for compressed gels were to compress a collagen I gel containing ECs and MSCs that had already formed TLSs or would subsequently do so with the expectation that a compressed collagen gel would resist contraction and be easier to handle in a clinical setting. Microvascular networks formed well in uncompressed collagen I gels and penetrated throughout the entire gel provided that the thickness of the gel did not limit passive diffusion of oxygen to the embedded cells. However, no microvascular networks could be seen after compression of collagen I gels containing both HUVECs and MSCs and only very few TLSs were noted when cells were seeded onto already compressed scaffolds. Gels showing good formation of a microvascular network before compression had a distinct lack of any TLSs when imaged afterwards, demonstrating that compression had a significant detrimental effect on existing TLSs as well as on prospective vessel network formation. This was shown to be because HUVECs do not survive the compression process used here, although good viability could be seen in gels containing hDFs and AdMSCs both 24 hours and 1 week after compression. Importantly, % viability of AdMSCs was significantly better ($p<0.01$) than BMMSCs at both day 1 and day 7 post compression. AdMSCs can be harvested with great ease and far less morbidity than BMMSCs. Compression is still a useful technique for improving the strength of the gel without the need for chemical cross linking agents and preventing contraction of the gel due to the cells, however a less forceful compression may be required in order to achieve these properties whilst ensuring survival of endothelial cells.

An alternative method would be to compress collagen I gels containing MSCs and then seed endothelial cells onto the surface of the compressed gel with the expectation that they would form vascular networks that may penetrate the scaffold. This approach has proved successful for the generation of stratified epidermal cell layers on the surface of compressed gels containing fibroblasts (148,149); however preliminary experiments with both cell types seeded onto the surface of a compressed collagen gel formed mainly superficial microvascular networks that were less extensive than in uncompressed gels. Further studies would therefore compare microvascular networks in uncompressed gels with those in compressed gels containing MSCs with HUVECs seeded on top.

In view of these findings, two potential options were available in order to create a scaffold containing a viable microvascular network. The first would be to modify (most likely reduce) the compression process but this would risk negating the main reasons for carrying out the process in the first place – to improve handling of the scaffold and reduce secondary contraction. The second option would be to simply seed the ECs and MSCs within an uncompressed gel and examine whether the process of TLS formation would stabilise the gel sufficiently to make this suitable for a potential clinical application.

Main conclusions:

- **No microvascular networks were seen after compression of collagen I gels containing HUVECs and MSCs.**
- **Only very few TLSs were noted when cells were seeded onto already compressed scaffolds.**
- **Gels showing good formation of a microvascular network before compression had no TLSs afterwards.**
- **HUVECs when seeded in isolation within collagen I gels do not survive the compression process but AdMSCs have high post-compression viability, both 24 hours and 1 week after compression.**

3.3 Uncompressed collagen gels

3.3.1 Aims for use of uncompressed collagen I gels

Aims for uncompressed collagen gels were as follows:

1. To co-culture HUVECs with BMMSCs at a variety of concentrations on top of and within collagen I gels optimising the production of a pre-vascularised collagen gel matrix.

2. To co-culture human PBECFCs and AdMSCs within these optimised collagen I gels to create a pre-vascularised collagen I gel that would be suitable in a clinical paradigm.

In order to form the basis for optimising gels, the angiogenesis protocol of Koh et al. was used as it had been shown to enable TLS formation in collagen gels through the co-culture of ECs with pericytes (5). In addition the cytokines stem cell factor (SCF), Stromal-cell derived factor

1α (SDF-1α) and Interleukin-3 (IL-3) were also added as per the amendments of Stratman et al. (6) to further improve TLS formation. The main difference between this protocol and the one used in my own uncompressed gels was that a 2mg/ml collagen I gel was used rather than the 2.5 or 3.75mg/ml that Koh et al. used, basing this lower concentration on the migration assays where ECs failed to migrate through a 3mg/ml collagen gel but successfully migrated through a 1mg/ml gel.

3.3.2 Results for uncompressed gels – Pilot experiments using HUVECs and BMMSCs

As a pilot experiment to ascertain the optimal seeding density for ECs and MSCs co-cultured within a collagen I gel and to compare this to placing these cells onto the surface of a collagen gel, various concentrations of HUVECs (Lonza Biologics) and BMMSCs (Lonza Biologics) were placed together within or on top of a bovine collagen I gel (2mg/ml) (Invitrogen) with either M-199 (Sigma Aldrich) or EGM-2 (Lonza Biologics) providing the medium component to the gel. In this experiment the following concentrations of HUVECs and BMMSCs were co-cultured within or on top of an EGM-2 or M-199 based collagen I gel (Chapter 2, section 2.8): $4x10^4$ ECs and $1x10^1$ MSCs; $1x10^5$ ECs and $2.5x10^4$ MSCs; $2x10^5$ ECs and $5x10^4$ MSCs. When HUVECs and BMMSCs were seeded within a 2mg/ml collagen gel containing either M-199 (Sigma Aldrich) or EGM-2 (Lonza Biologics) TLS-like structures were noted within both as early as 48 hours however they were not seen when identical concentrations of cells were seeded onto the gels, cells instead growing to near confluence on these gels. TLS-like structures were fully formed by day 7 (Figure 3.16), they were more uniform and extensive with M-199 than EGM-2 and they remained stable until day 14.

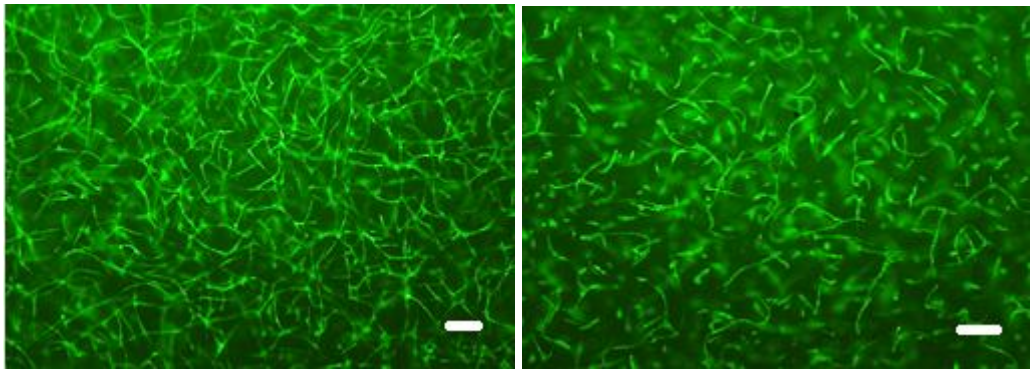

Fig 3.16 Uncompressed collagen I gel pilot experiment (comparison of medium): x4 magnification images of HUVECs;BMMSCs ($2x10^5$;$5x10^4$) within 2mg/ml collagen I gel [M-199 (left); EGM-2 (right)] (see Chapter 2.2.1 for constituents of EGM-2)(scale bar = 200μm).

In the first pilot experiment (Fig 3.16) it was shown that TLSs formed most readily within but not on the surface of the M-199 based 2mg/ml collagen I gel with an optimum concentration of $2x10^5$ HUVECs with $5x10^4$ MSCs. Therefore, this concentration of cells was again used for the next step, this time substituting CBECFCs or PBECFCs for HUVECs (Fig 3.17). Given that there was very little TLS formation when cells were placed onto gels, this experiment was not conducted for CB or PBECFCs. The 2 concentrations used were $2x10^5$ ECs with $5x10^4$ BMMSCs (optimal concentration from pilot experiment 1) and $3x10^5$ ECs with $7.5x10^4$ BMMSCs. Fifty µl medium was removed from wells and replaced with 60µl top-up medium at 24 hours (Table 2.6). This was repeated at 96 hours and photos were taken at d7 after fixing specimens with PFA (Chapter 2.9). Photos were taken using a Nikon Eclipse TE300 microscope and a Hamamatsu ORCA-ER camera (Hamamatsu Photonics UK Ltd).

CB ECFC:BMMSC and PBECFC:BMMSC containing gels contracted away from wells but reducing the concentration of MSCs to $3x10^4$ stopped this from occurring whilst TLSs still formed readily.

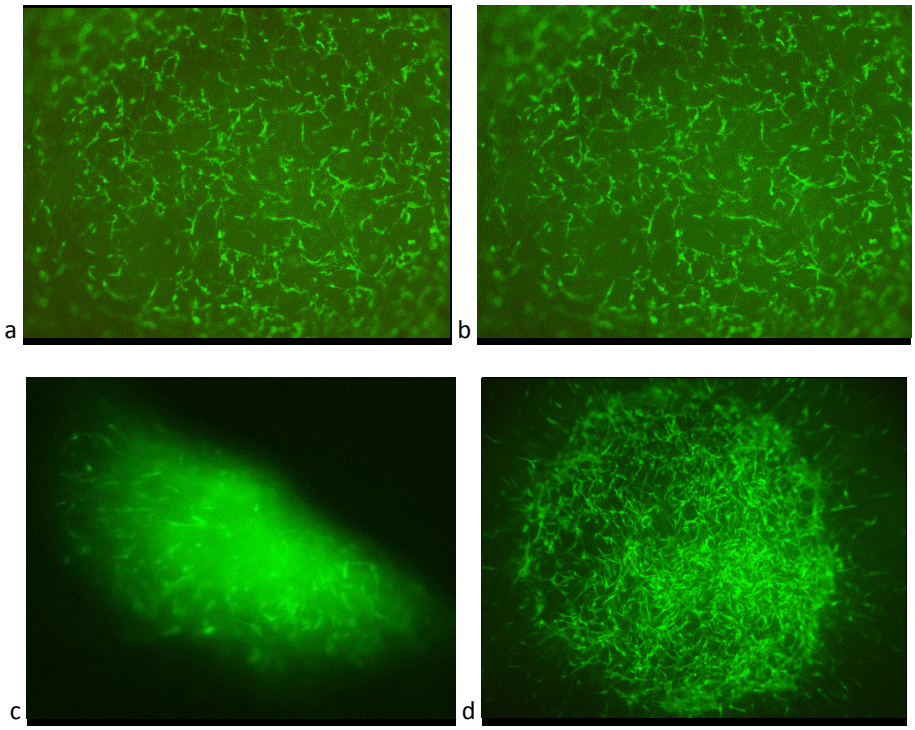

Fig 3.17 – Uncompressed collagen I gel pilot experiment 2 (ECFCs and MSCs): Day 4. a) $2x10^5$ HUVECs:$3x10^4$ AdMSCs; b) $2x10^5$ HUVECs:$3x10^4$ BMMSCs; c) $2x10^5$ PBECFCs:$3x10^4$ AdMSCs; b) $2x10^5$ PBECFCs:$3x10^4$ BMMSCs in 2mg/ml collagen I gel (x4 magnification). TLS appeared to form with all 4 combinations of cells but due to contraction and folding of the PBECFC/AdMSC containing gel the TLSs are less well circumscribed in this image (c).

Once cell numbers and components for the collagen I gel had been piloted by carrying out the experiments in 3.3.2 (EC $2x10^5$ cells: MSC $3x10^4$ cells; M199 medium; SCF, SDF-1α and IL-3 added to gel), the following experiments were carried out with this setup, so that quantitative data regarding the TLS forming capacity of different cells could be ascertained via:

1. Co-culturing a batch of AdMSCs with 3 batches of PBECFCs, CBECFCs and HUVECs.
2. Co-culturing a batch of BMMSCs with 3 batches of PBECFCs, CBECFCs and HUVECs.
3. Co-culturing a single batch of PBECFCs/CBECFCs/HUVECs with 3 batches of AdMSCs.
4. Co-culturing a single batch of PBECFCs/CBECFCs/HUVECs with 3 batches of BMMSCs.

By conducting the above experiments, it would be possible to not only confirm or refute the TLS-forming capacity of the different batches of isolated cell types (PBECFCs, CBECFCs, AdMSCs) but also to identify the 'best batch' of each cell type as every co-culture combination would be examined.

3.3.3 Will TLSs form with 3 different batches of PB ECFCs/CB ECFCs/HUVECs?

Three separate batches of the 3 EC subtypes were co-cultured with a single batch of either BMMSCs or AdMSCs to confirm the tubule-forming capacity of the ECs. Figure 3.18 shows x10 magnification fluorescence microscope images of the gold standard gel ($2x10^5$ HUVECs and $3x10^4$ BMMSCs) from pilot experiments above. Figures 3.19 to 3.21 show the results from co-culturing 3 different batches of PBECFCs, CBECFCs and HUVECs with a single batch of BMMSCs or AdMSCs.

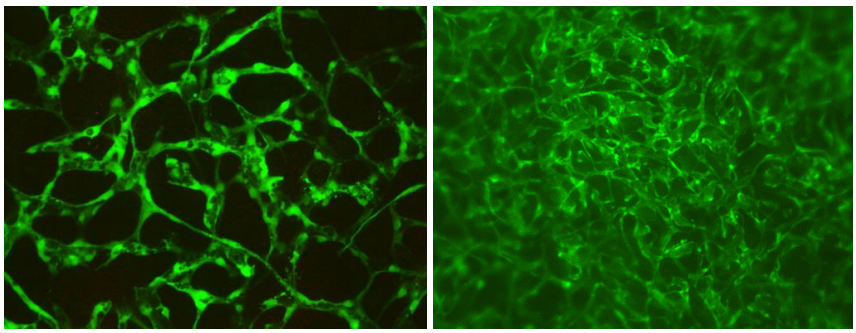

Fig 3.18 – Comparing AdMSCs to BMMSCs with HUVECs: Representative day 7 images taken at x10 magnification after co-culturing $2x10^5$ HUVECs: $3x10^4$ AdMSCs (left) or $2x10^5$ HUVECs: $3x10^4$ BM MSCs (right) in 2mg/ml collagen I gel.

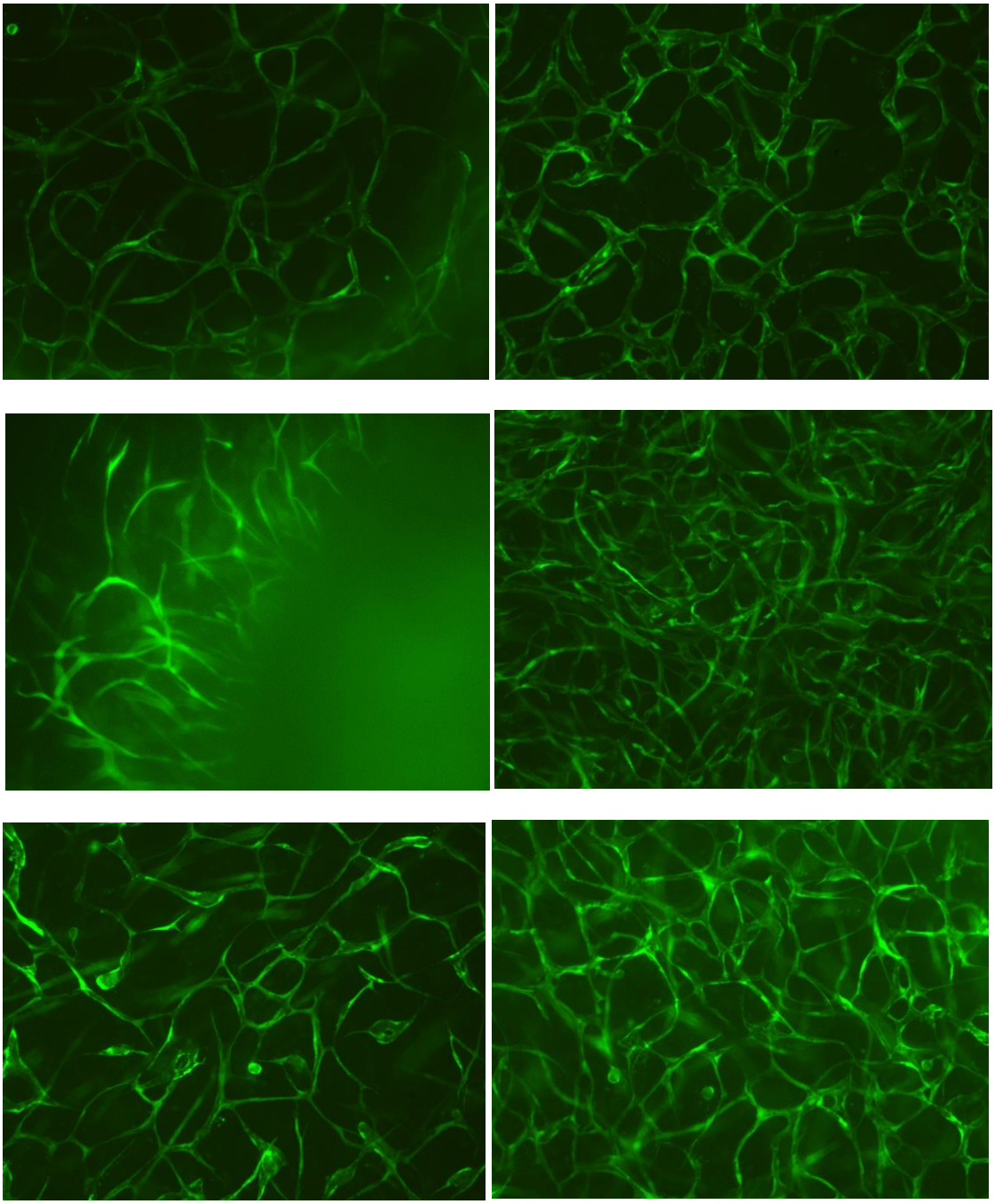

Fig 3.19 – Comparing 3 different batches of PBECFCs with AdMSCs/BMMSCs: Representative day 7 images taken at x10 magnification after co-culturing $2x10^5$ PBECFC:$3x10^4$ AdMSCs (left); $2x10^5$ PBECFCs:$3x10^4$ BM MSCs (right) in 2mg/ml collagen I gel for 3 batches of PBECFCs (PB2 top; PB5 middle; PB8 bottom).

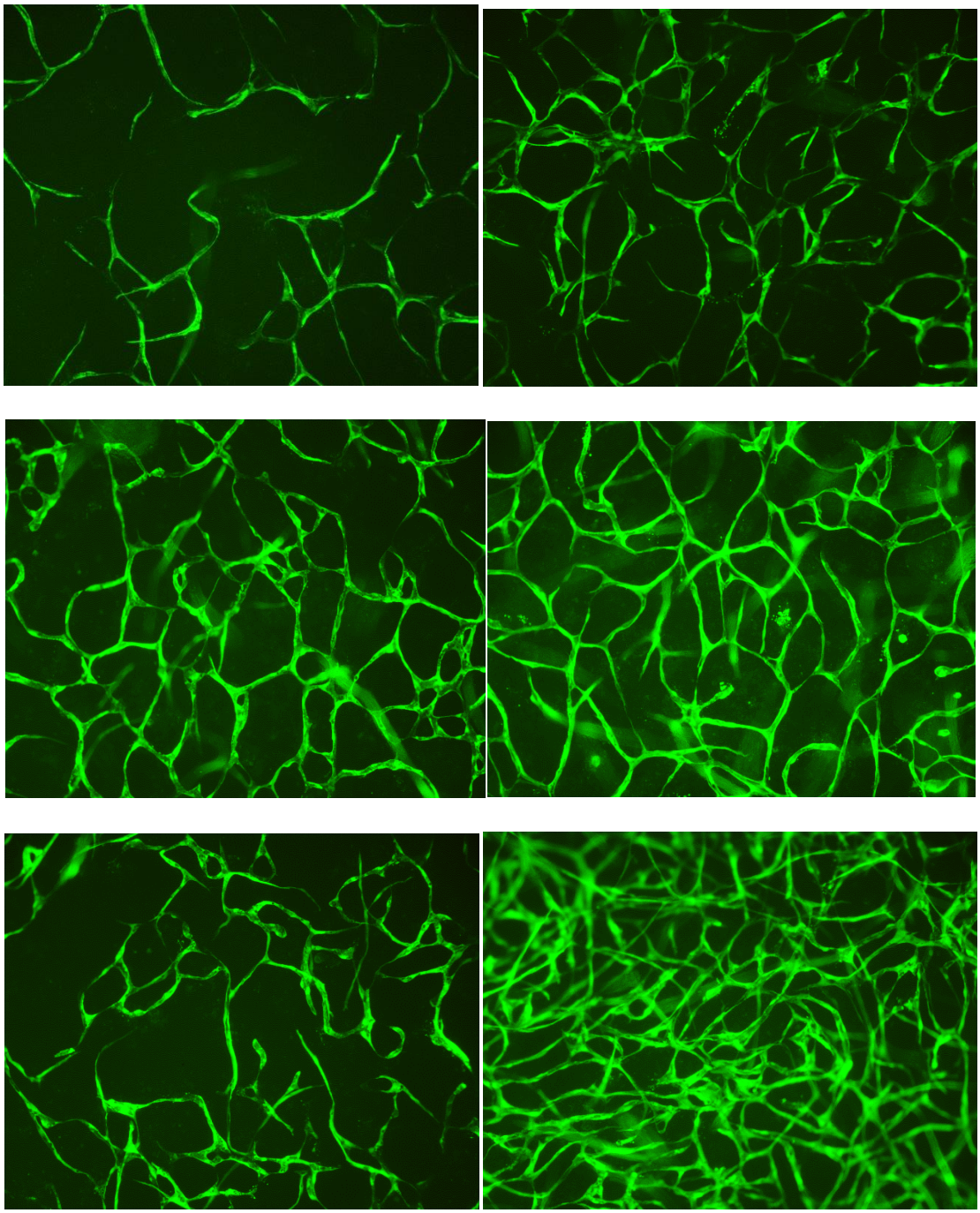

Fig 3.20 – Comparing 3 different batches of CBECFCs with AdMSCs/BMMSCs: Representative day 7 images taken at x10 magnification after co-culturing $2x10^5$ CBECFC:$3x10^4$ AdMSCs (left); $2x10^5$ CBECFCs:$3x10^4$ BM MSCs (right) in 2mg/ml collagen I gel for 3 batches of CBECFCs (CB1 top; CB2 middle; CB3 bottom).

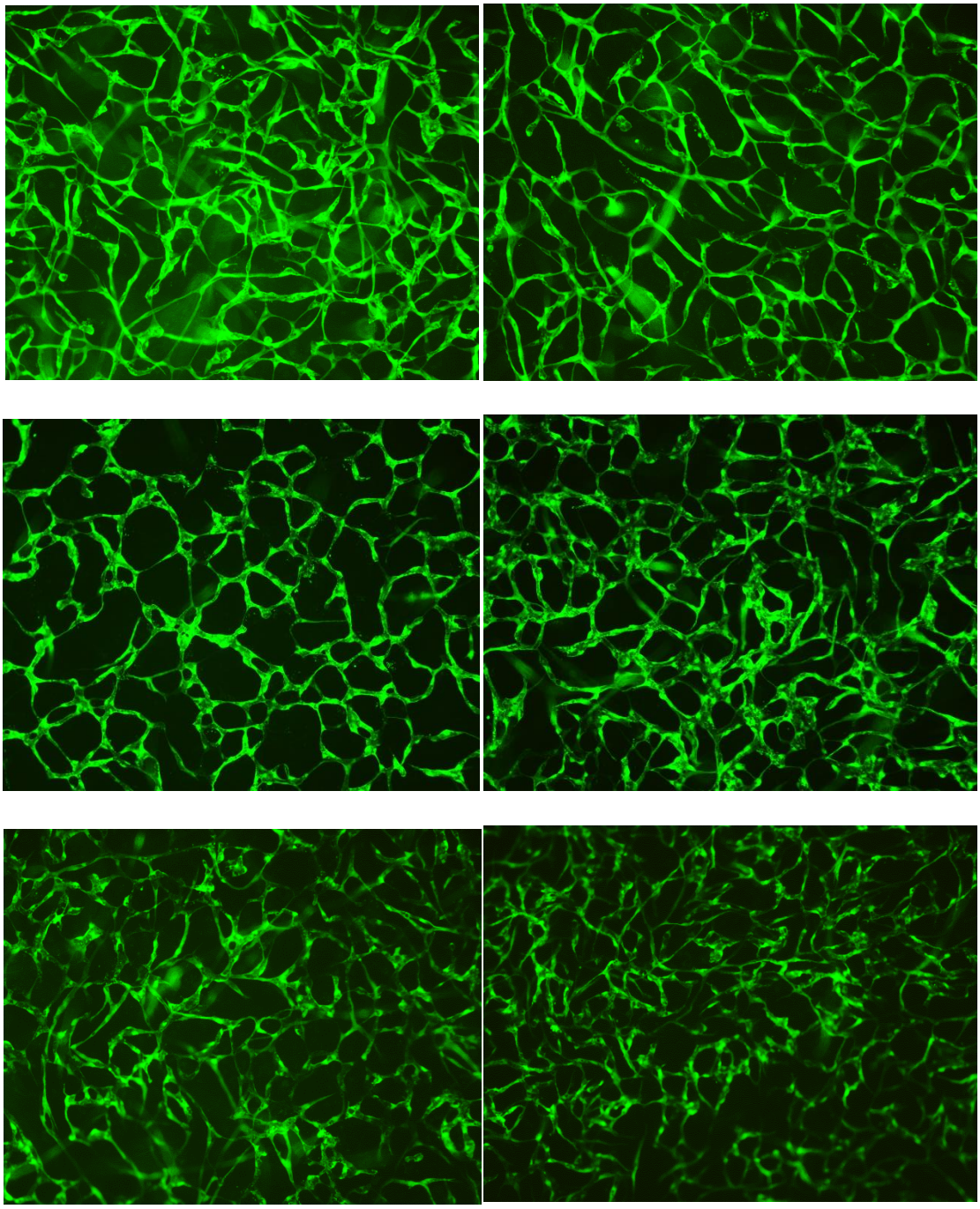

Fig 3.21 – Comparing 3 different batches of HUVECs with AdMSCs/BMMSCs: Representative day 7 images taken at x10 magnification after co-culturing $2x10^5$ HUVECs:$3x10^4$ AdMSCs (left); $2x10^5$ HUVECs:$3x10^4$ BM MSCs (right) in 2mg/ml collagen I gel for 3 batches of HUVECs (HUVECs1 top; HUVECs2 middle; HUVECs3 bottom).

Figures 3.19 to 3.21 show the representative images of TLS-forming capacity of 3 different batches of PBECFCs, CBECFCs and HUVECs when they have been co-cultured with either AdMSCs or BMMSCs. However, these images only show this ability qualitatively. In order to quantify outcomes it was necessary to take confocal images of the gels and use Imaris 3D

(Bitplane) (Chapter 2, section 2.8) to ascertain the number of TLSs, total TLS length, total TLS area, total TLS volume, number of branch points, average TLS diameter and width of gel containing TLSs. Note that for this last parameter, this measurement was the depth of gel containing TLSs (penetration), not the total gel thickness which ranged from 200-300µm. Figure 3.22 shows the results for each separate batch of ECs providing evidence as to the best combination of cells for each parameter. Figure 3.23 then takes an average from the 3 different batches for each individual cell so that PBECFCs can be compared to HUVECs and CBECFCs for their TLS forming capacity when co-cultured with the 2 different stromal cells (Ad and BMMSCs). In addition, CBECFCs and HUVECs were also examined in gels containing fibronectin (FN). Of particular note from Figure 3.22, PB5ECFCs formed more TLSs and sub-TLSs than the other PBECFC batches and levels were similar whether AdMSCs or BMMSCs were used. TLS length, volume and number of branch points were also highest for this batch of PBECFCs although average diameter was slightly higher for PB2 ECFCs. It can clearly be seen from Figure 3.22 that there was large a variation in parameters between the 3 batches of PBECFCs, CBECFCs and HUVECs when co-cultured with AdMSCs or BMMSCs. However, the graphs do confirm the fact that all batches formed quantifiable TLSs as seen in Figures 3.19 to 3.21.

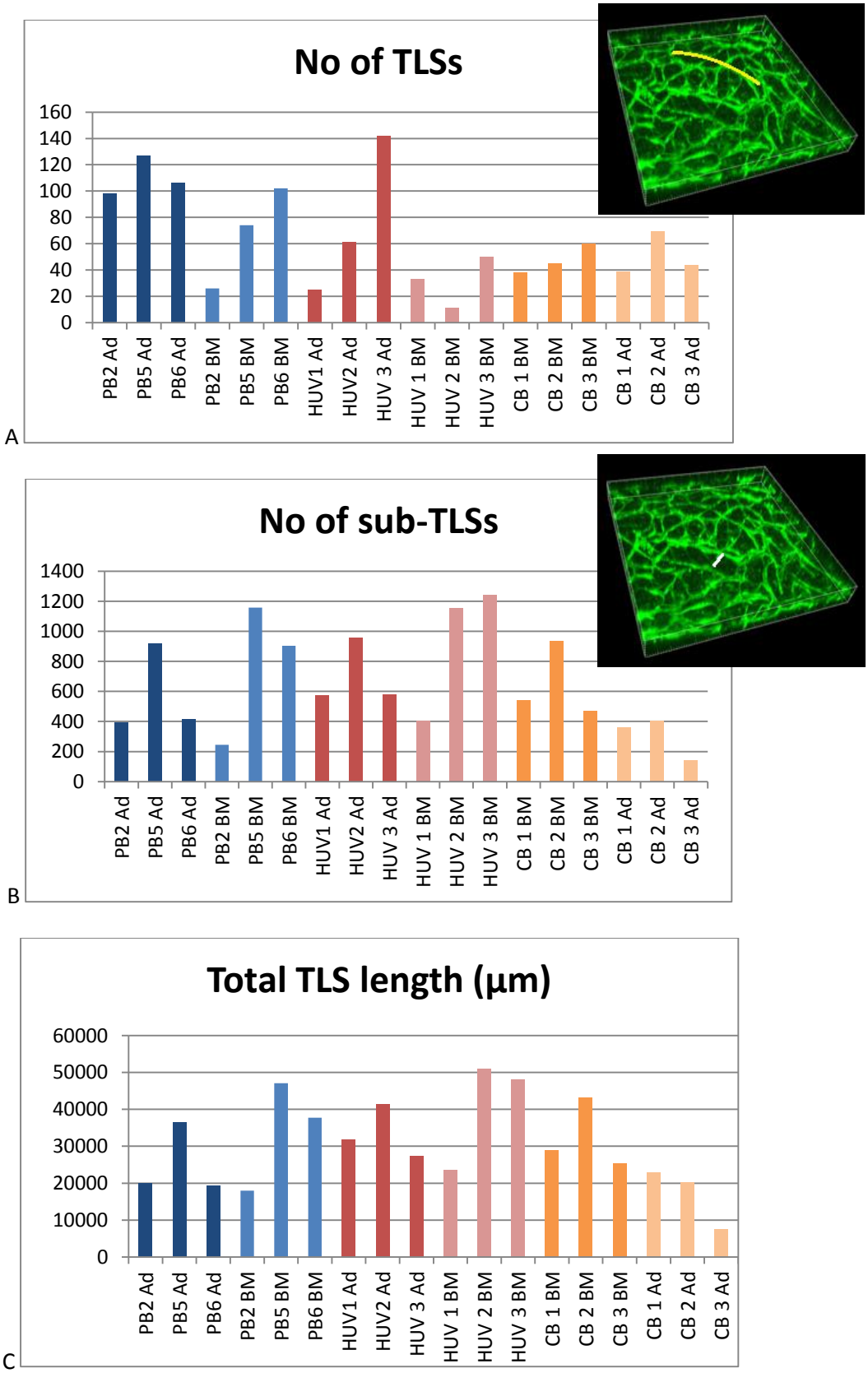

Fig 3.22 – Individual gel construct results following Imaris 3D processing: Number of TLSs (A), number of sub-TLSs (B) and total TLS length (C). From PBECFC batches, PB5 had the most sub-TLSs and total TLS length whether cultured with AdMSCs or BMMSCs. Sub-TLSs were those tubules connecting to other tubules but with a of less than 3µm.

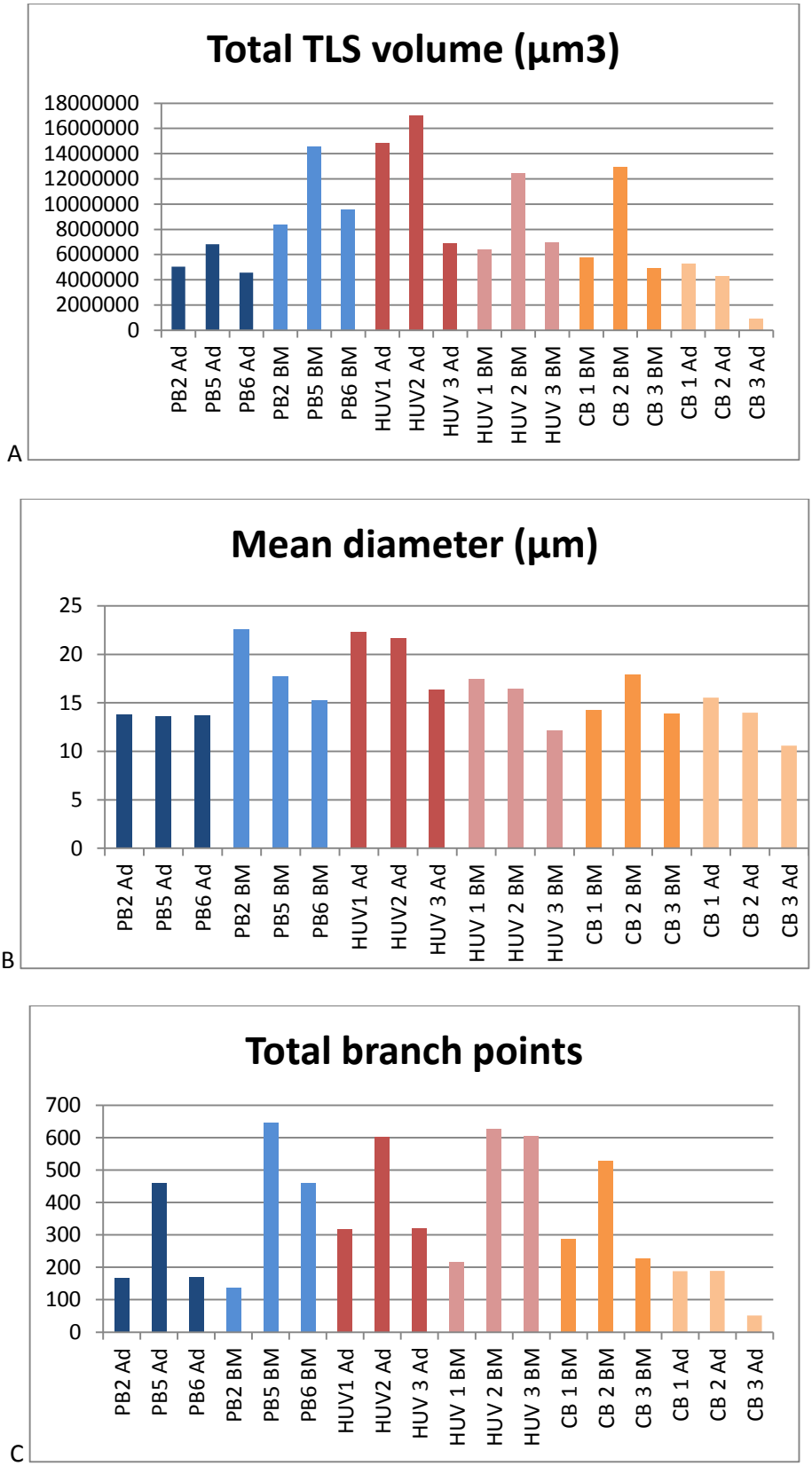

Fig 3.23 – Individual gel construct results following Imaris 3D processing: Total TLS volume (A), mean diameter (B) and number of branch points (C). From PBECFC batches, PB5 had highest value for all parameters when cultured with AdMSCs and TLS volume and number of branch points with BMMSCs.

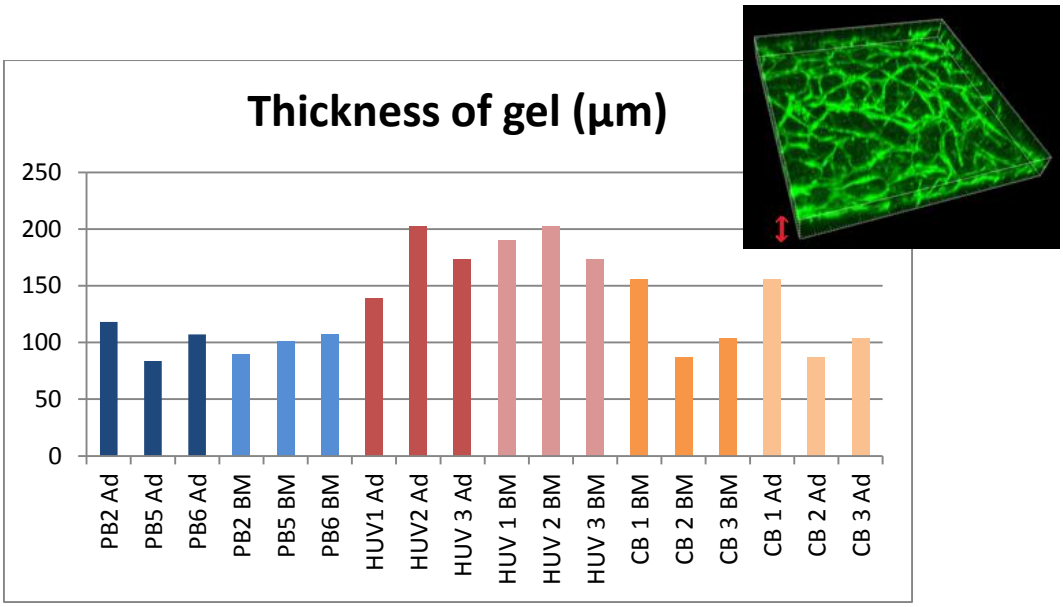

Fig 3.24 – Individual gel construct results following Imaris 3D processing – thickness of gel: The average thickness of gels was approximately 300µm but the penetrance of tubules within gels was less than this value. This graph demonstrates the thickness of gel that was penetrated by TLSs for the different co-cultures of ECs and MSCs.

Fig 3.25 (next 2 pages) – Average Imaris 3D results from 3 separate batches of PBECFCs/CBECFCs/HUVECs when co-cultured with AdMSCs or BMMSCs: The mean for the parameters from Figures 3.2-3.4, from 3 different batches of PBECFCs, CBECFCs or HUVECs (the latter 2 with or without FN) when co-cultured with AdMSCs or BMMSCs.

* = $P<0.05$ (unpaired Students t-test, n=3)

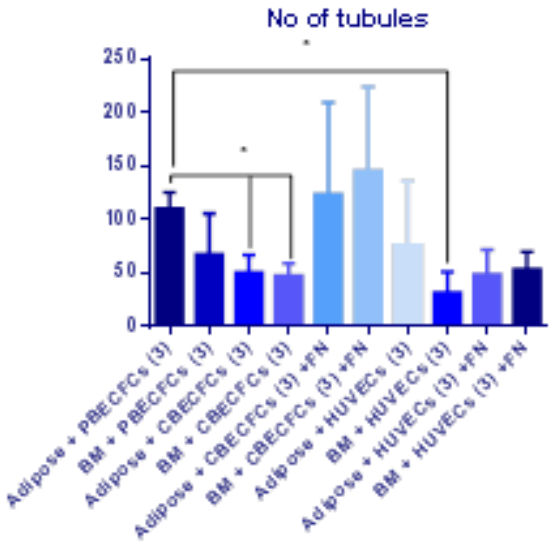
No of tubules
250
200
150
100
50
0
*
*
Adipose + PBECFCs (3)
BM + PBECFCs (3)
Adipose + CBECFCs (3)
BM + CBECFCs (3)
Adipose + CBECFCs (3) +FN
BM + CBECFCs (3) +FN
Adipose + HUVECs (3)
BM + HUVECs (3)
Adipose + HUVECs (3) +FN
BM + HUVECs (3) +FN

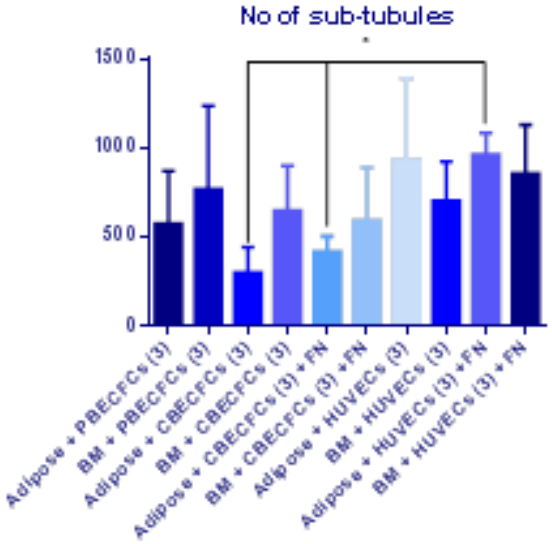
No of sub-tubules
1500
1000
500
0
*
Adipose + PBECFCs (3)
BM + PBECFCs (3)
Adipose + CBECFCs (3)
BM + CBECFCs (3)
Adipose + CBECFCs (3) +FN
BM + CBECFCs (3) +FN
Adipose + HUVECs (3)
BM + HUVECs (3)
Adipose + HUVECs (3) +FN
BM + HUVECs (3) +FN

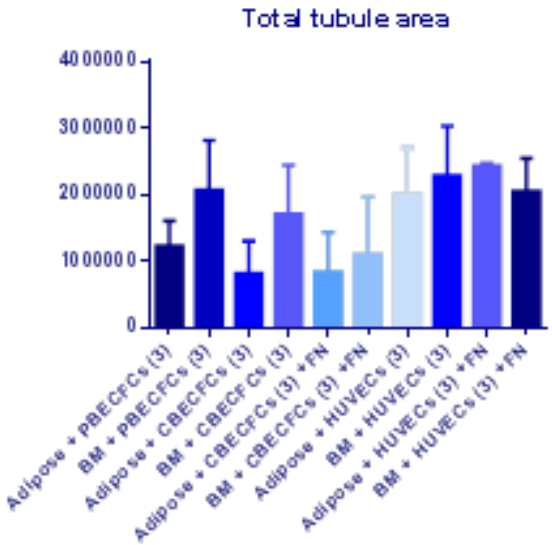
Total tubule area
4000000
3000000
2000000
1000000
0
Adipose + PBECFCs (3)
BM + PBECFCs (3)
Adipose + CBECFCs (3)
BM + CBECFCs (3)
Adipose + CBECFCs (3) +FN
BM + CBECFCs (3) +FN
Adipose + HUVECs (3)
BM + HUVECs (3)
Adipose + HUVECs (3) +FN
BM + HUVECs (3) +FN

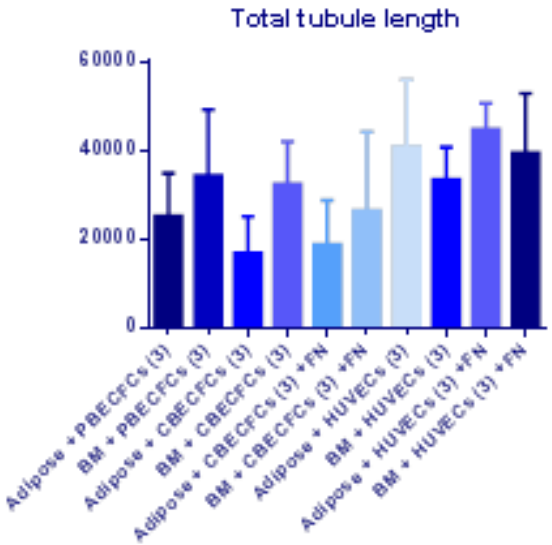
Total tubule length
60000
40000
20000
0
Adipose + PBECFCs (3)
BM + PBECFCs (3)
Adipose + CBECFCs (3)
BM + CBECFCs (3)
Adipose + CBECFCs (3) +FN
BM + CBECFCs (3) +FN
Adipose + HUVECs (3)
BM + HUVECs (3)
Adipose + HUVECs (3) +FN
BM + HUVECs (3) +FN

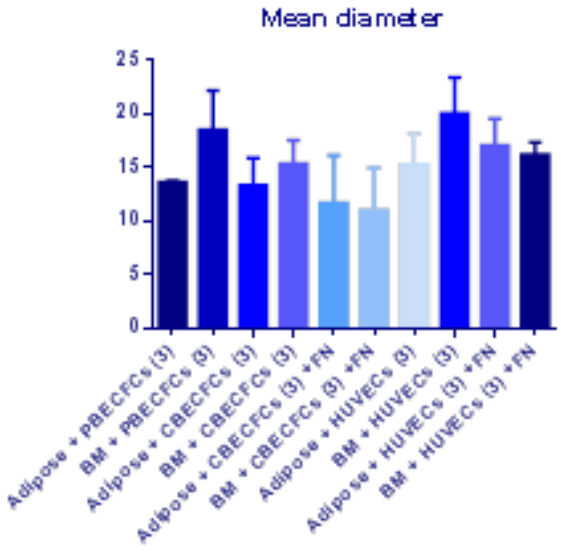
Mean diameter
25
20
15
10
5
0
Adipose + PBECFCs (3)
BM + PBECFCs (3)
Adipose + CBECFCs (3)
BM + CBECFCs (3)
Adipose + CBECFCs (3) +FN
BM + CBECFCs (3) +FN
Adipose + HUVECs (3)
BM + HUVECs (3)
Adipose + HUVECs (3) +FN
BM + HUVECs (3) +FN

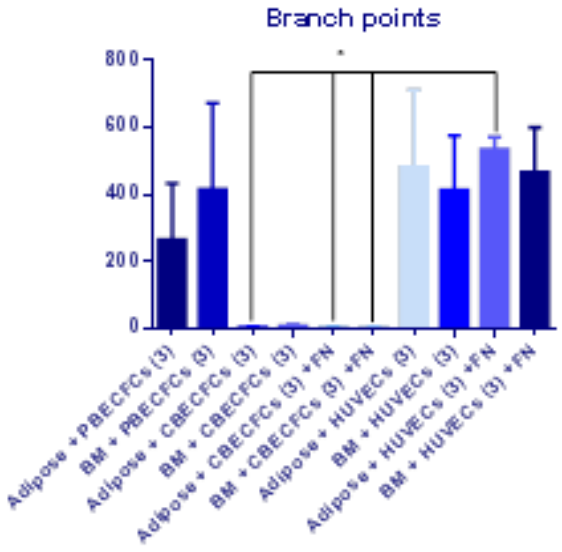
Branch points
800
600
400
200
0
*
Adipose + PBECFCs (3)
BM + PBECFCs (3)
Adipose + CBECFCs (3)
BM + CBECFCs (3)
Adipose + CBECFCs (3) +FN
BM + CBECFCs (3) +FN
Adipose + HUVECs (3)
BM + HUVECs (3)
Adipose + HUVECs (3) +FN
BM + HUVECs (3) +FN

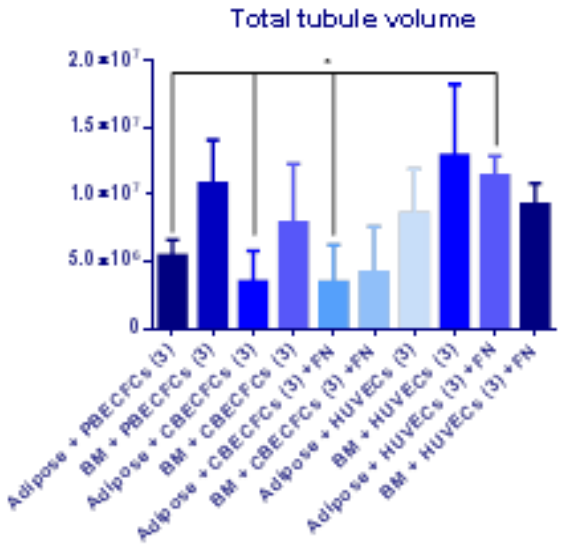
Total tubule volume
2.0×10⁷
1.5×10⁷
1.0×10⁷
5.0×10⁶
0
*
Adipose + PBECFCs (3)
BM + PBECFCs (3)
Adipose + CBECFCs (3)
BM + CBECFCs (3)
Adipose + CBECFCs (3) +FN
BM + CBECFCs (3) +FN
Adipose + HUVECs (3)
BM + HUVECs (3)
Adipose + HUVECs (3) +FN
BM + HUVECs (3) +FN

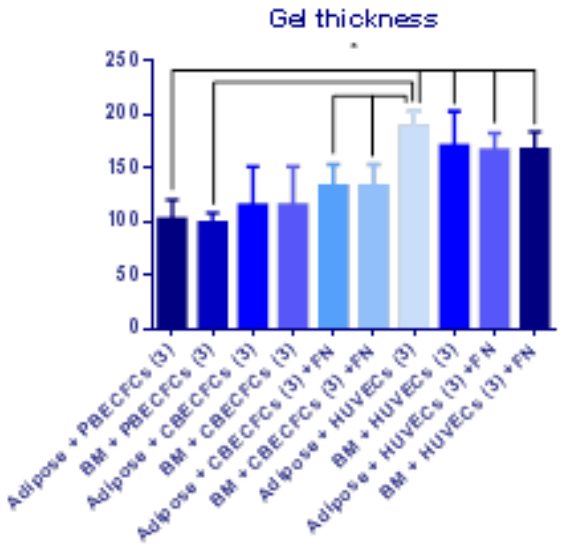
Gel thickness
250
200
150
100
50
0
*
Adipose + PBECFCs (3)
BM + PBECFCs (3)
Adipose + CBECFCs (3)
BM + CBECFCs (3)
Adipose + CBECFCs (3) +FN
BM + CBECFCs (3) +FN
Adipose + HUVECs (3)
BM + HUVECs (3)
Adipose + HUVECs (3) +FN
BM + HUVECs (3) +FN

Fig 3.25 shows that there were very few parameters where there was a statistically significant difference between the EC subtypes whether they were co-cultured with AdMSCs or BMMSCs. When HUVECs were co-cultured with AdMSCs within a 2mg/ml collagen I gel containing FN the total TLS volume was significantly higher than AdMSCs with CBECFCs (with [p=0.019] or without FN [p=0.026]) and also higher than when PBECFCs were cultured with AdMSCs (p=0.046). In addition, collagen I 2mg/ml gels were penetrated further with HUVEC and BM or AdMSC-containing constructs (with or without FN), than CB or PB ECFC-containing constructs. This was particularly the case when comparing the HUVEC (n=3) construct containing AdMSCs and added FN to the construct containing PBECFCs (n=3) together with either BM (p=0.003) or Ad derived MSCs (p=0.002).

3.3.4 Will TLSs form with 3 different batches of AdMSCs/BMMSCs?

Figures 3.26 to 3.28 show the results from co-culturing 3 different batches of BMMSCs or AdMSCs with a single batch of PBECFCs (3.26), CBECFCs (3.27) or HUVECs (3.28). Imaris 3D (Bitplane) was again used to quantify TLSs within the different constructs after confocal images had been taken. Figures 3.29-3.31 show the results for each separate batch of ECs providing evidence as to the best combination of cells for each parameter. Figure 3.32 then takes an average from the 3 different batches for each individual cell type so that AdMSCs can be compared to BMMSCs for their TLS forming capacity when co-cultured with each of the 3 different endothelial cells.

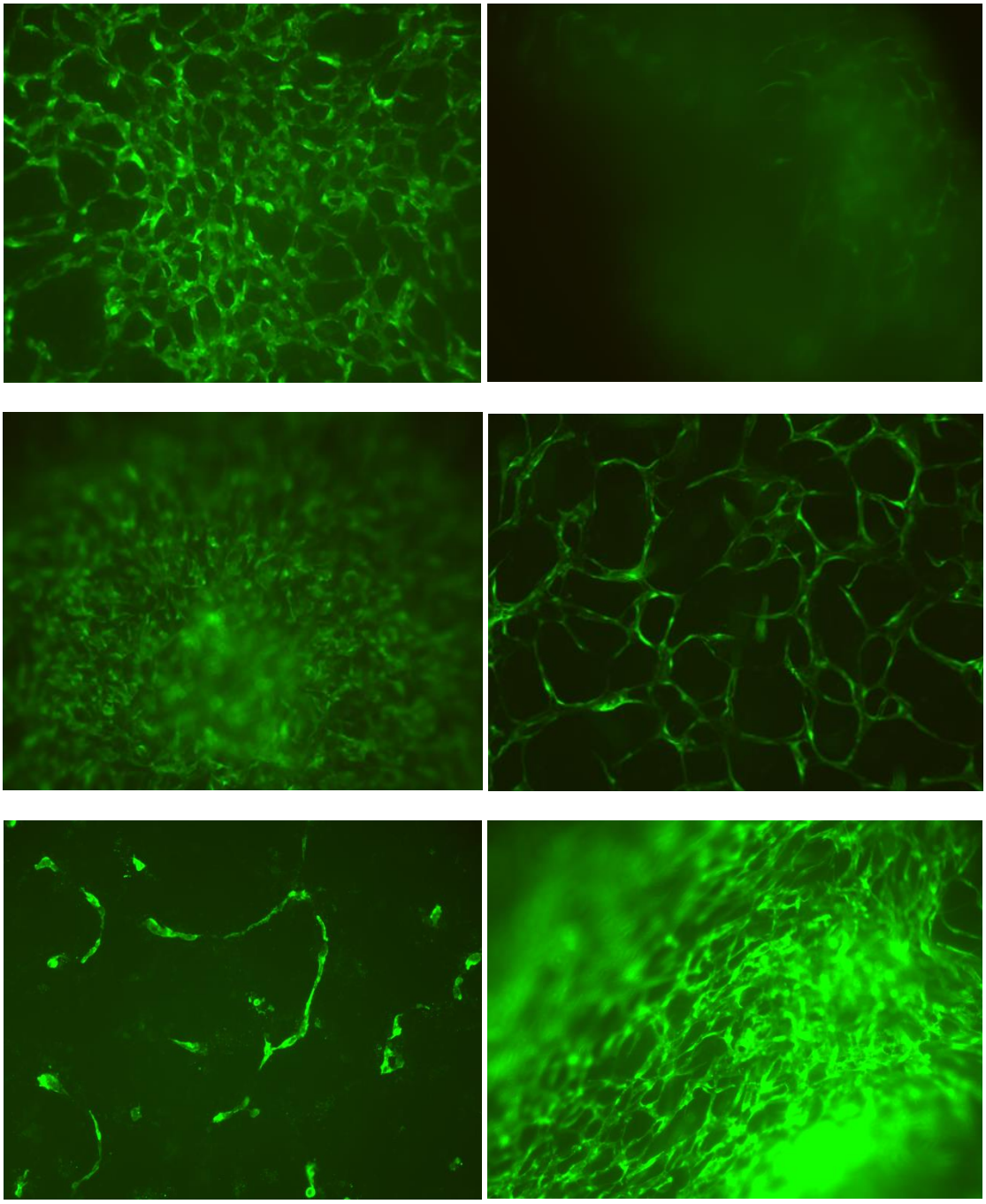

Fig 3.26 – Comparing 3 different batches of AdMSCs/BMMSCs with PBECFCs: Day 7 images taken at x10 magnification of $2x10^5$ PBECFC:$3x10^4$ AdMSCs (L); $2x10^5$ PBECFCs:$3x10^4$ BM MSCs (R) in 2mg/ml collagen I gel for 3 batches of AdMSCs and BMMSCs (Ad1/BM1 top; Ad2/BM2 middle; Ad5/BM3 bottom).

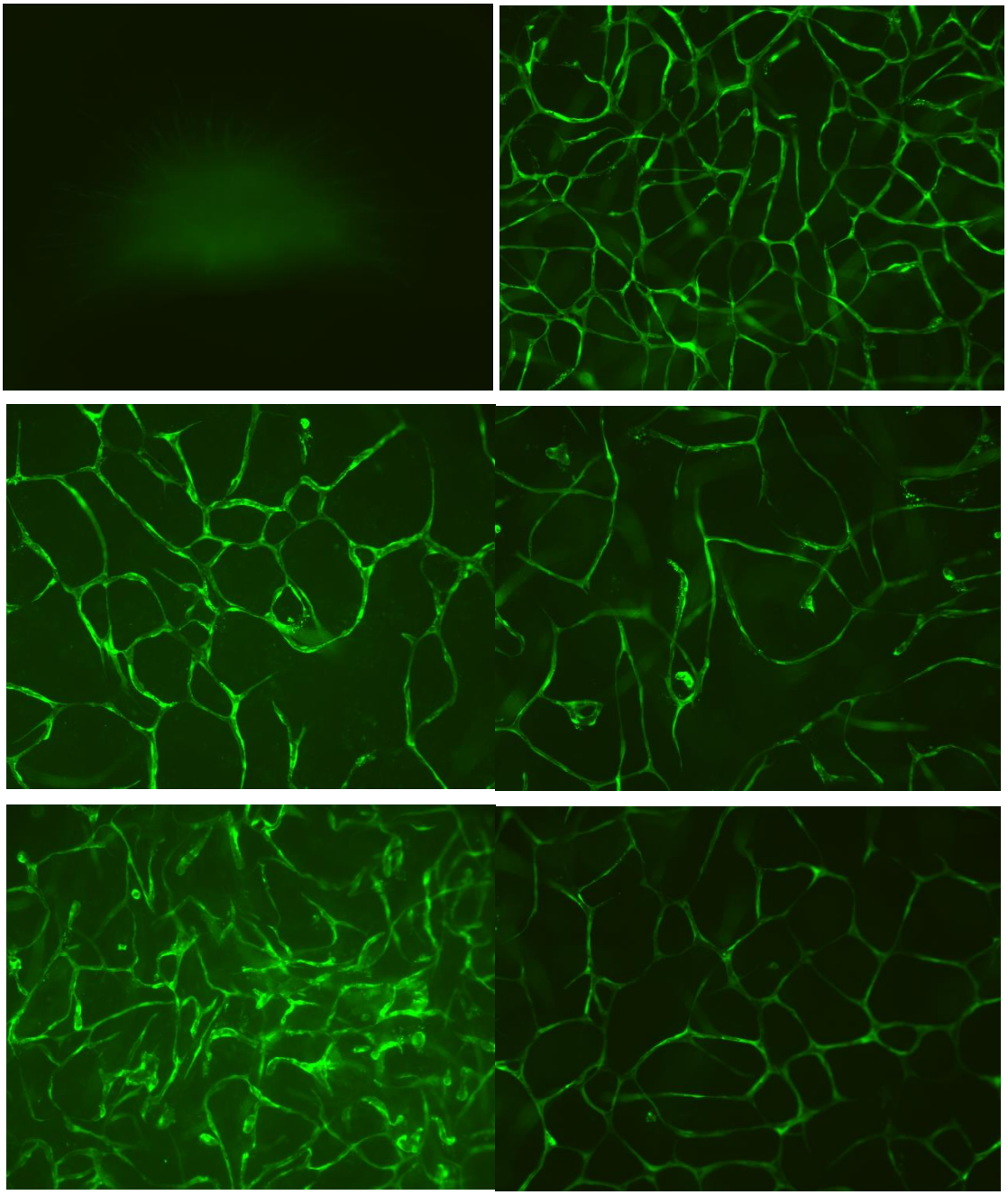

Fig 3.27 – Comparing 3 different batches of AdMSCs/BMMSCs with CBECFCs: Day 7 images taken at x10 magnification of $2x10^5$ CBECFC:$3x10^4$ AdMSCs (L); $2x10^5$ CBECFCs:$3x10^4$ BM MSCs (R) in 2mg/ml collagen I gel for 3 batches of AdMSCs and BMMSCs (Ad1/BM1 top; Ad2/BM2 middle; Ad5/BM3 bottom).

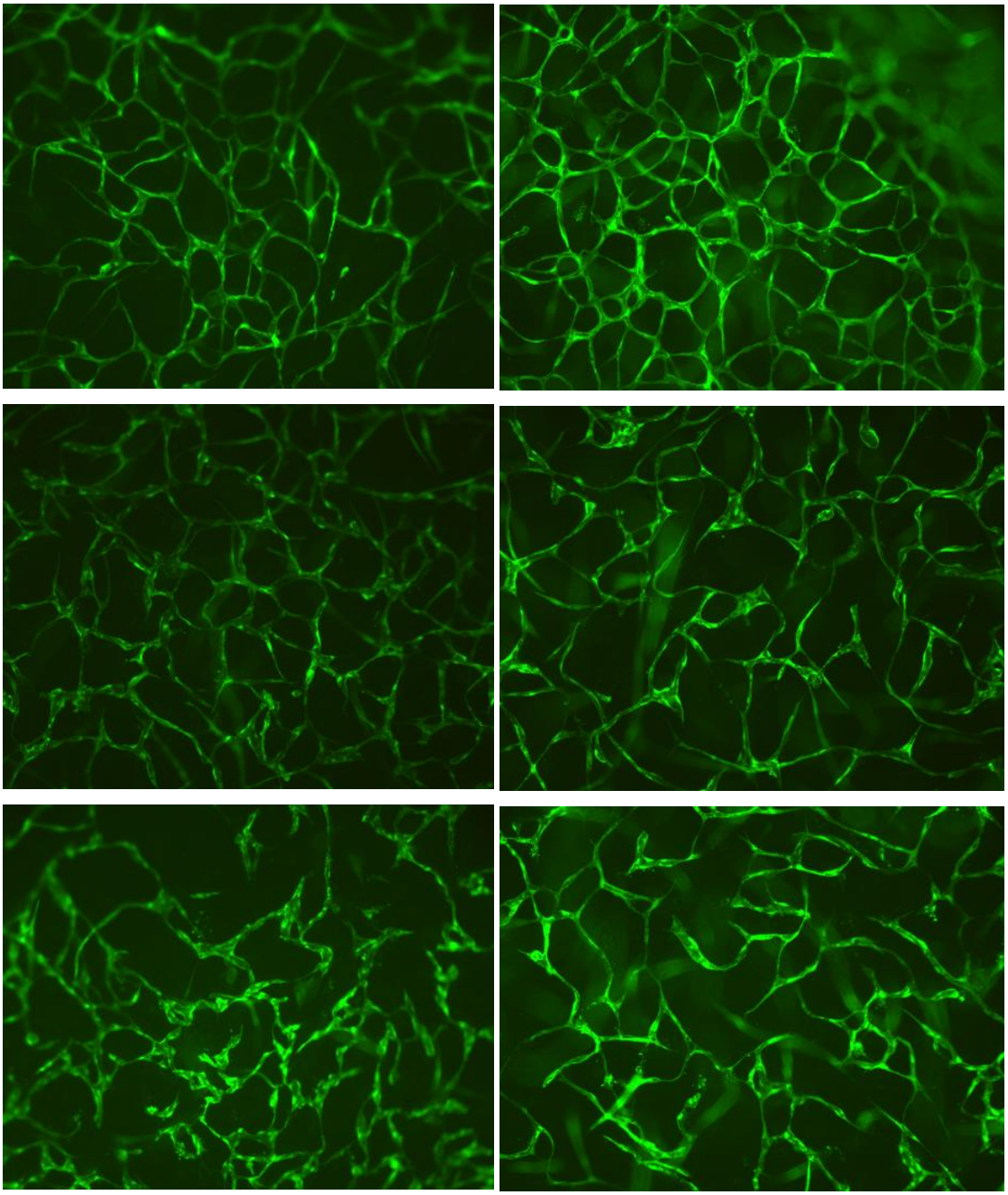

Fig 3.28 – Comparing 3 different batches of AdMSCs/BMMSCs with HUVECs: Day 7 images taken at x10 magnification of $2x10^5$ HUVECs:$3x10^4$ AdMSCs (L); $2x10^5$ HUVECs:$3x10^4$ BM MSCs (R) in 2mg/ml collagen I gel for 3 batches of AdMSCs and BMMSCs (Ad1/BM1 top; Ad2/BM2 middle; Ad5/BM3 bottom).

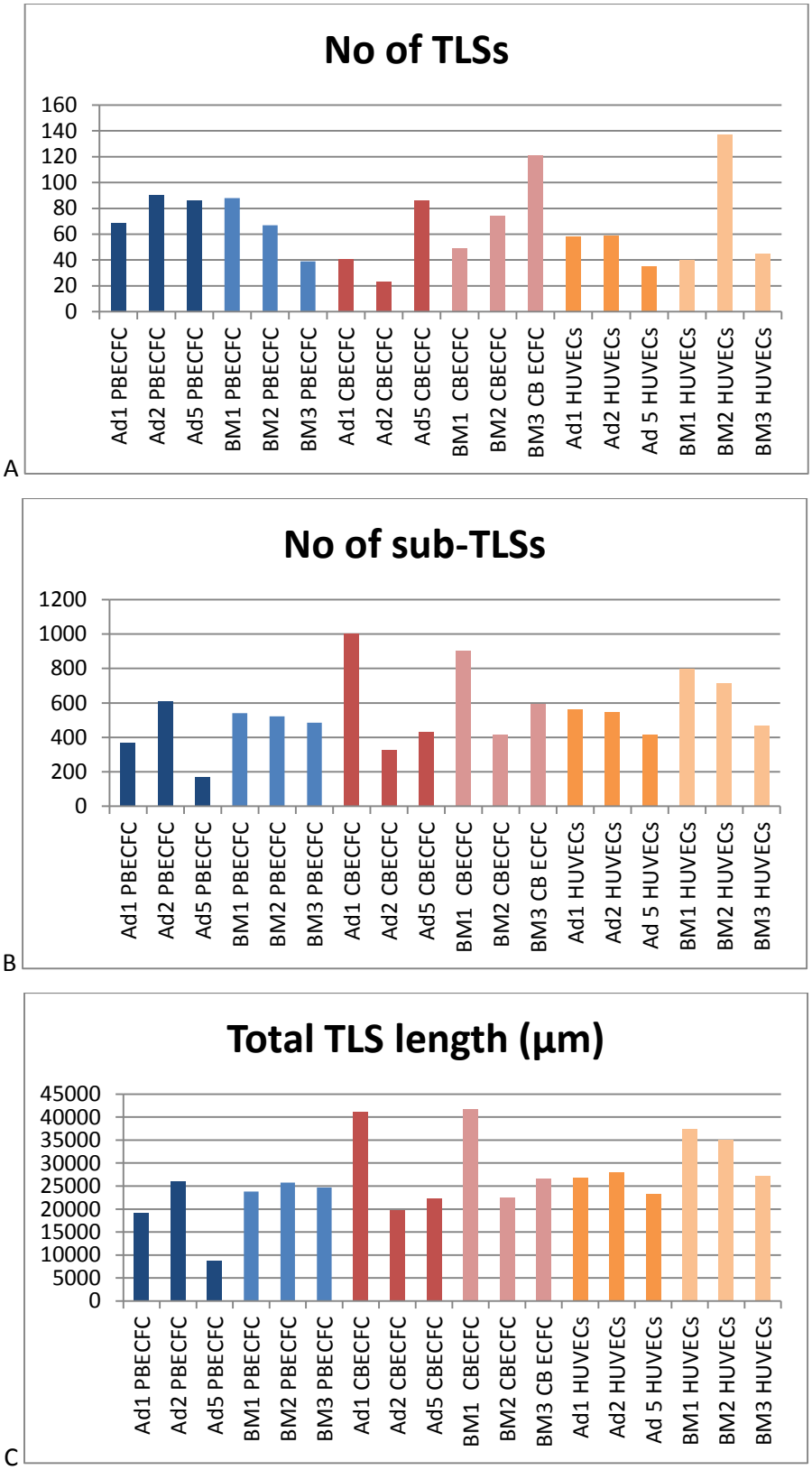

Fig 3.29 – Individual gel construct results following Imaris 3D processing: Number of TLSs (A), number of sub-TLSs (B) and total TLS length (C). Ad2 (the second AdMSC batch) produced networks with the most TLSs, sub-TLSs and total TLS length when co-cultured with PBECFCs.

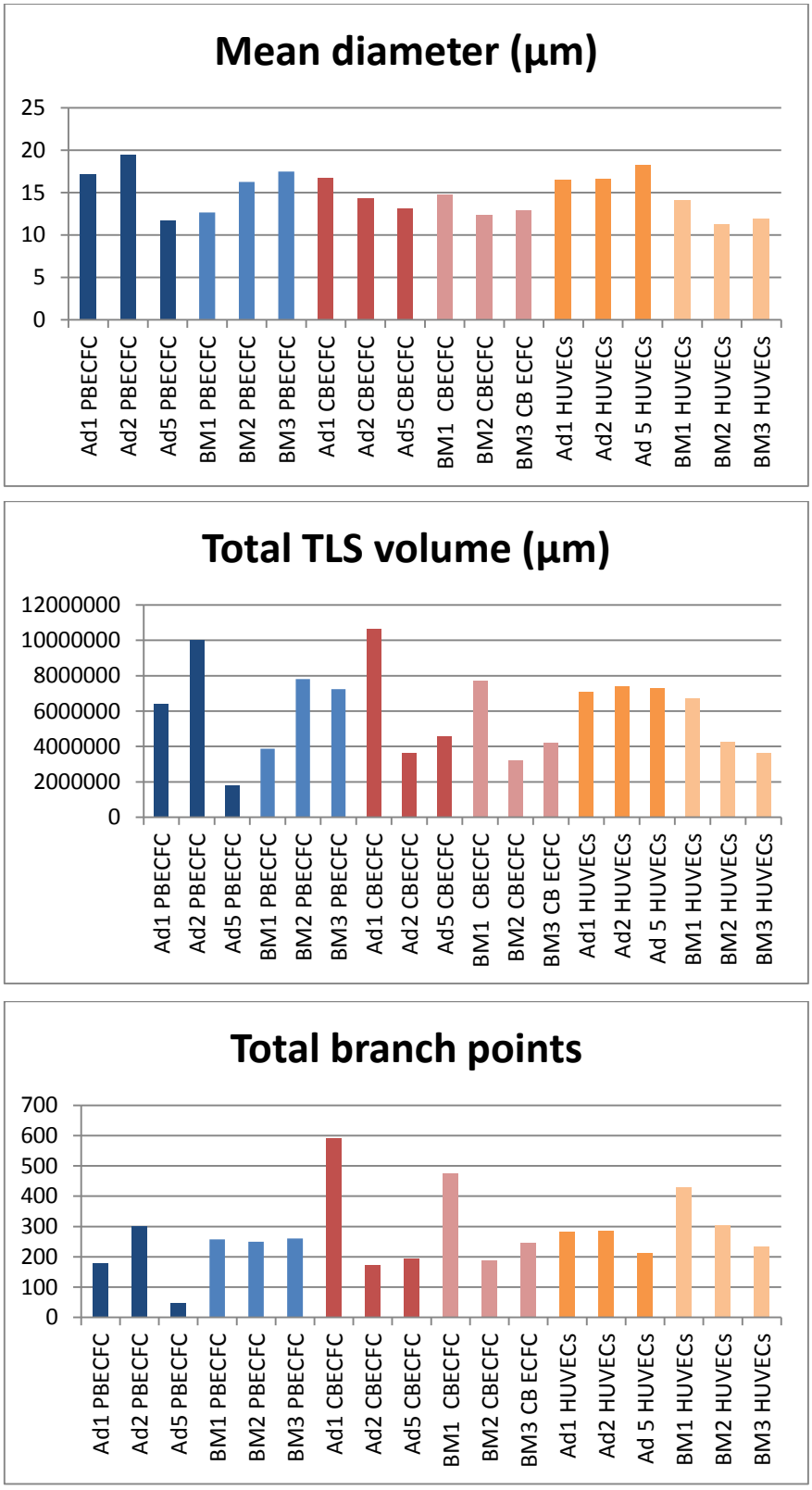

Fig 3.30 – Individual gel construct results following Imaris 3D processing: Total TLS volume (A), mean diameter (B) and number of branch points (C). Ad2 produced networks with the highest mean diameter, total TLS volume and number of branch points when co-cultured with PBECFCs.

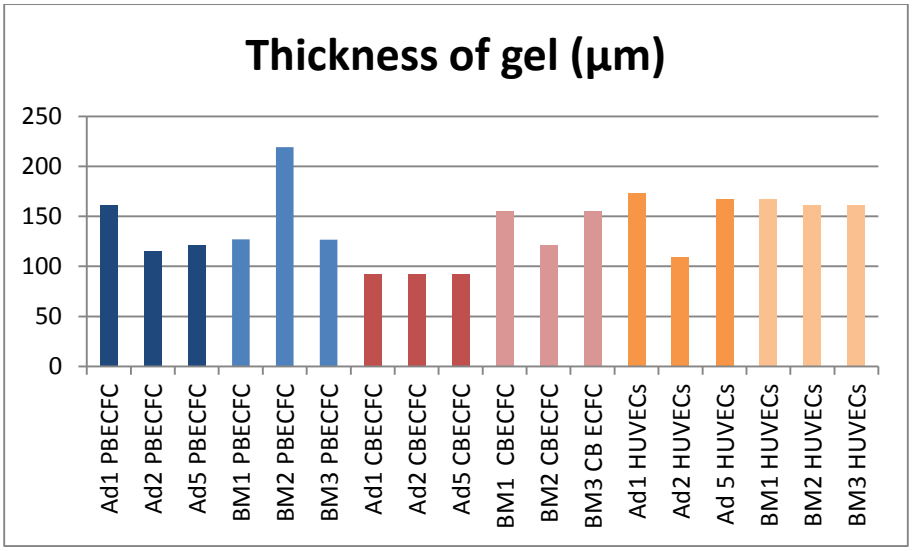

Fig 3.31 – Individual gel construct results following Imaris 3D processing – thickness of gel: The average thickness of gels was approximately 300µm. This graph demonstrates the thickness of gel that was penetrated by TLSs for the different co-cultures of ECs and MSCs.

Fig 3.32 (next 2 pages) – Average Imaris 3D results from 3 batches of AdMSCs or BMMSCs when co-cultured with ECs: The mean for the parameters from Figures 3.29-3.31, from PBECFCs, CBECFCs or HUVECs when co-cultured with 3 different batches of AdMSCs or BMMSCs.

* = $P<0.05$ (unpaired Students t-test, n=3)

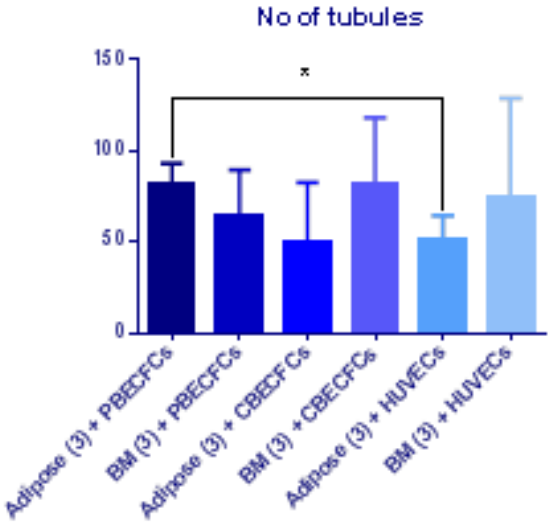
No of tubules
150
100
50
0
*
Adipose (3) + PBECFCs
BM (3) + PBECFCs
Adipose (3) + CBECFCs
BM (3) + CBECFCs
Adipose (3) + HUVECs
BM (3) + HUVECs

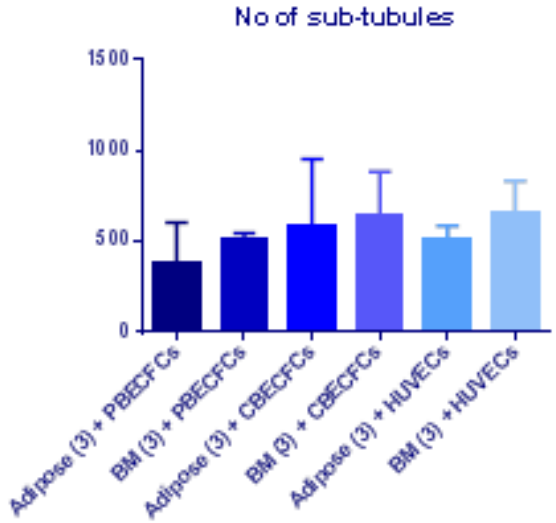
No of sub-tubules
1500
1000
500
0
Adipose (3) + PBECFCs
BM (3) + PBECFCs
Adipose (3) + CBECFCs
BM (3) + CBECFCs
Adipose (3) + HUVECs
BM (3) + HUVECs

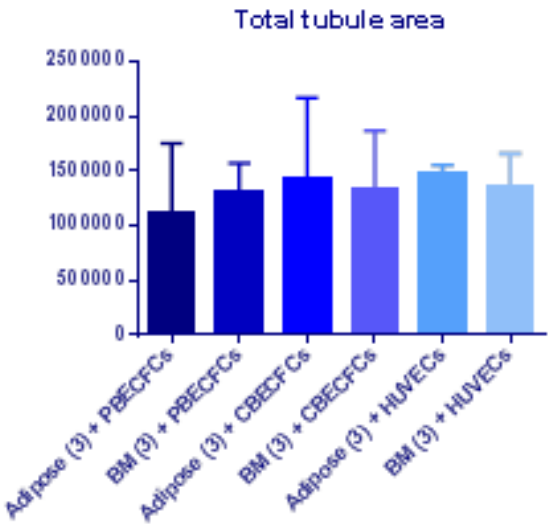
Total tubule area
250000
200000
150000
100000
50000
0
Adipose (3) + PBECFCs
BM (3) + PBECFCs
Adipose (3) + CBECFCs
BM (3) + CBECFCs
Adipose (3) + HUVECs
BM (3) + HUVECs

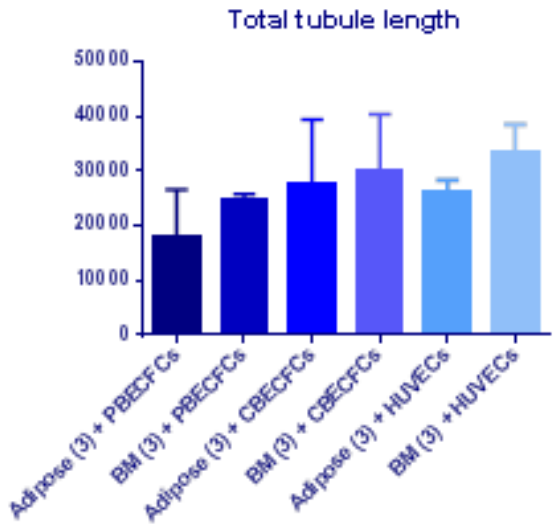
Total tubule length
50000
40000
30000
20000
10000
0
Adipose (3) + PBECFCs
BM (3) + PBECFCs
Adipose (3) + CBECFCs
BM (3) + CBECFCs
Adipose (3) + HUVECs
BM (3) + HUVECs

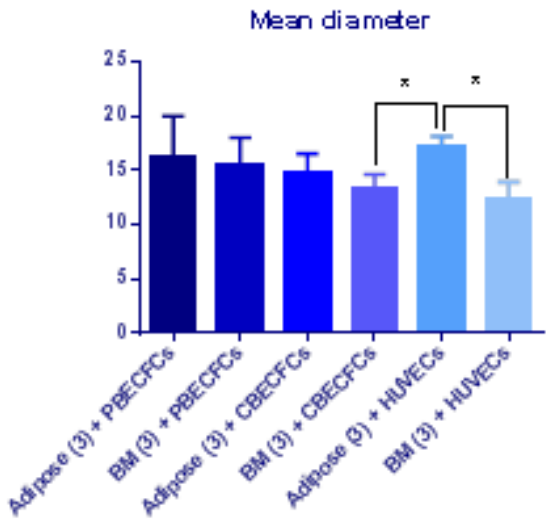
Mean diameter
25
20
15
10
5
0
*
*
Adipose (3) + PBECFCs
BM (3) + PBECFCs
Adipose (3) + CBECFCs
BM (3) + CBECFCs
Adipose (3) + HUVECs
BM (3) + HUVECs

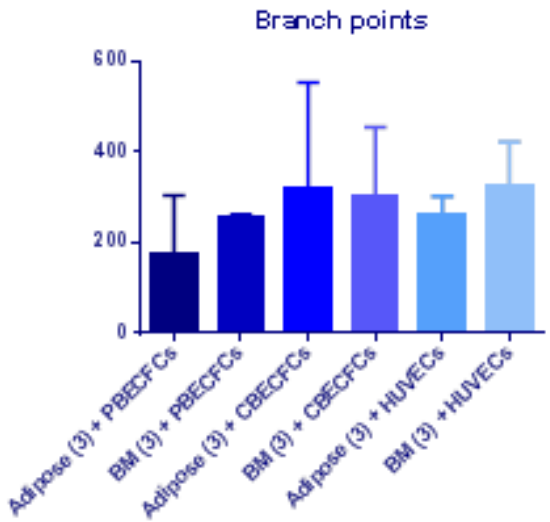
Branch points
600
400
200
0
Adipose (3) + PBECFCs
BM (3) + PBECFCs
Adipose (3) + CBECFCs
BM (3) + CBECFCs
Adipose (3) + HUVECs
BM (3) + HUVECs

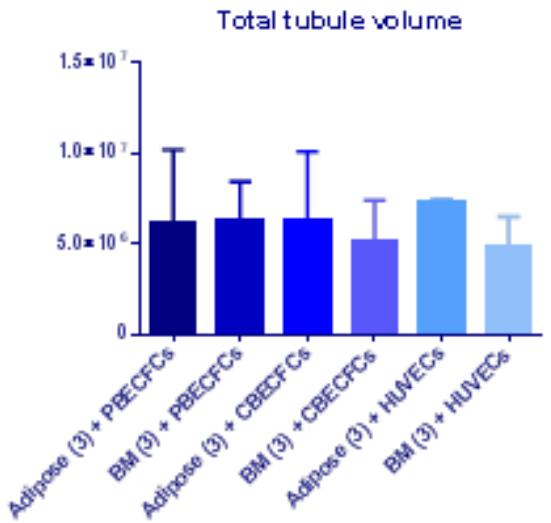
Total tubule volume
1.5×10 7
1.0×10 7
5.0×10 6
0
Adipose (3) + PBECFCs
BM (3) + PBECFCs
Adipose (3) + CBECFCs
BM (3) + CBECFCs
Adipose (3) + HUVECs
BM (3) + HUVECs

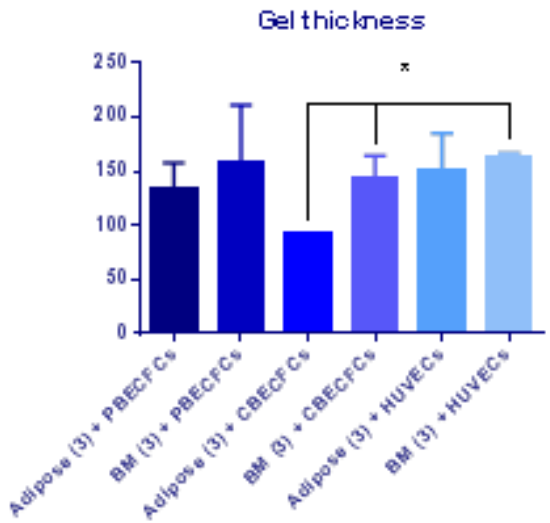
Gel thickness
250
200
150
100
50
0
*
Adipose (3) + PBECFCs
BM (3) + PBECFCs
Adipose (3) + CBECFCs
BM (3) + CBECFCs
Adipose (3) + HUVECs
BM (3) + HUVECs

In figure 3.32, it is clear that as was the case when co-culturing 3 different batches of the different EC subtypes (HUVECs, CBECFCs and PBECFCs) with a single AdMSC or BMMSC batch (Figure 3.25) that when taking averages from 3 separate batches of AdMSCs and BMMSCs that these also form similar TLSs within collagen I gels *in vitro* whether HUVECs, CBECFCs or PBECFCs are used in the co-culture. When PBECFCs were combined with AdMSCs (n=3) they formed more TLSs than any other EC(HUVECs;CBECFCs)/MSC co-culture (this was significantly more than when HUVECs were combined with AdMSCs [p=0.04]). This point is encouraging with respect to attaining the ultimate goal of a pre-vascularised scaffold fabricated using adult derived stem/progenitor cells. However, this number only took into account main TLS trunks and not TLSs coming off at branch points which often form the vast majority of total TLSs. Indeed, sub-TLSs, total TLS area and total TLS volume are probably more relevant parameters to measure in order to determine the optimal pre-vascularised gel. Looking at the results for these 3 parameters, there were no statistically significant differences between the different co-cultures of ECs and AdMSCs or BMMSCs. For all three EC types there were more sub-TLSs when BMMSCs were used in the co-culture than when AdMSCs were used but this result did not reach statistical significance. The total TLS area and total TLS volume were slightly higher when BMMSCs were used in combination with PBECFCs than with AdMSCs but AdMSCs produced higher values for total TLS area and volume than BMMSCs when co-cultured with CBECFCs or HUVECs (none of these results were statistically significant). In terms of penetration of networks within collagen I gels ('gel thickness'), HUVECs co-cultured with AdMSCs and with BMMSCs spread the deepest within gels although this was only significant for HUVECs/BMMSCs compared to CBECFCs/AdMSCs (p=0.001). This confirmed the results seen when 3 batches of HUVECs were all cultured with a single batch of AdMSCs or BMMSCs. In these experiments TLSs again perfused to a greater depth than when CBECFCs or PBECFCs were used (Figure 3.25).

3.4 Discussion

One of the important properties that needed to be considered as part of the gel fabrication process was how readily endothelial cells would migrate within the proposed scaffold as this would be key to neo-vascularisation. In this thesis the μ-chemotaxis 3D device created by Ibidi was used to examine endothelial cell migration within fibrin or collagen. Previously the

Boyden chamber or a similar trans-well type device (150) has been used to examine chemotaxis but these have limitations in the number of parameters that can be measured. µ-chemotaxis 3D has the benefit that it allows for a distinction between chemotactic responses (displacement of centre of mass and the forward migration index of the cells), and chemokinetic responses such as total cell path travelled in any direction (accumulated distance) and cell velocity in a 3-dimensional matrix (146). Another benefit of this simple device is that it is possible to use reagents sparingly but still to make several conclusions regarding the relative pros and cons for different gel constructs. Fibrin gels and collagen I gels of a concentration of 3mg/ml and above were not conducive to EC migration. In addition using a 1mg/ml collagen I gel it was shown that PBECFCs, HUVECs and CBECFCs migrated towards a 10% (v/v) FCS positive stimulus with a statistical significance [one-way ANOVA forward migration index Y ($p=0.014$); change in centre of mass Y ($p=0.001$)] showing that the µ-slide chemotaxis 3D (Ibidi, GmbH) is a suitable surrogate for determining efficient homing and migration of stem/progenitor cells. There is scope with the µ-slide chemotaxis 3D to use various other chemo-attractants instead of 10% (v/v) FCS within the reservoirs either side of the central gel channel to see if migration is further improved. For example, it would be possible to compare the chemoattractive properties of AdMSC supernatant to BMMSC supernatant to see whether endothelial progenitors were influenced by one more than the other. In addition, other additives to the gel chamber could be considered which may be improve EC migration. Fibronectin was trialled in this thesis and was added to the basic constituents of the collagen I 1mg/ml gel. Although not statistically significant, there were trends for higher accumulated cell distance, Euclidean distance and average velocity when 100µg/ml FN was added to gels and also for PBECFCs to travel further and faster than CBECFCs or HUVECs. Endothelial cell migration is a motile process directionally regulated by chemotactic (migration towards soluble chemoattractants), haptotactic (towards immobilised ligands), and mechanotactic (driven by mechanical forces) stimuli that also involves degradation of the extracellular matrix to enable progression of the migrating cells. Typically, chemotaxis of endothelial cells is driven by growth factors such as VEGF and basic fibroblast growth factor (bFGF), whereas haptotaxis occurs due to endothelial cell migration activation in response to integrins binding to ECM component. Other chemotactic promoters include angiopoietins, FGF-2, hepatocyte growth factor, platelet-derived growth factor, epidermal growth factor, transforming growth factor-β, interleukins, tumor necrosis factor-α

, platelet-activating factor, ephrins and soluble adhesion molecules (151). Any one or a combination of these could be added to the reservoir of the µ-slide chemotaxis 3D assay to easily determine the relative influence on cell migration for the different EC subtypes and to see whether they would significantly increase cell migration and thus the likely rate of TLS formation. Although the µ-slide chemotaxis 3D carries much scope for comparing numerous variables involved in cell chemotaxis and chemokinesis (146), there are drawbacks. Although there was a statistically significant difference for migration towards a 10% v/v FCS positive stimulus, for other comparisons between the EC subtypes there was a lack of statistical significance. This occurred most likely as a result of the steep learning curve associated with setting up the assays which meant that although experiments were carried out in triplicate, there was a high amount of variability between each assay. Although it is clearly advantageous in terms of preserving expensive reagents, to use only 6µl of collagen mix for each assay, it means that tiny changes in technique when setting up the assay or microscopic bubbles within chambers can lead to big changes in outcomes. In even the most experienced hands several replicates would need to be carried out in order to get statistically significant results.

Native skin has collagen as its main constituent and therefore it is unsurprising that most proprietary scaffolds are collagen-based. Cell-seeded collagen scaffolds could therefore potentially be utilised for skin tissue engineering. However, gels tend to contract significantly after being mixed with cells and in addition, collagen in low concentrations (as optimised in the µ-slide chemotaxis 3D assay) is mechanically weak. Previous studies have compared compressed and uncompressed gels for gel contraction rate, morphology, viability of seeded cells and mechanical properties (129,147). The results showed that the compression could significantly reduce the contraction of the collagen gel and improve its mechanical property. In addition, seeded dermal fibroblasts survived well in the compressed gel and epidermal cells seeded on top developed into a stratified epidermal layer (148). In this thesis, a compressed collagen gel scaffold was fabricated through the expulsion of liquid from reconstituted gels by plastic compression. However, despite basing compressed collagen I scaffolds on optimised chemotaxis gels and existing literature, vessels that formed within gels were no longer seen once the gels had been compressed. In addition, in compressed collagen I gels containing MSC or EC monocultures, HUVECs had a 100% mortality following compression

and the majority of BMMSCs also died after gels were compressed. Encouragingly however, more than 60% of hDFs or AdMSCs survived the plastic compression process. Since *in vivo* and *in vitro* 'living dermal equivalents' have been created from fibroblast-based dermal matrices seeded with epithelial cells (85,112), there is a potential niche for producing a skin substitute that is based on a collagen sheet containing viable AdMSCs.

Yet the main aim for this research was to produce a pre-vascularised scaffold using adult derived stem and progenitor cells so a compressed scaffold where endothelial cells did not survive would not serve this purpose. Therefore a variety of EC and MSC combinations were seeded within an uncompressed 2mg/ml collagen I gel the constituents of which were based on existing scaffolds (130) and results from the μ-slide chemotaxis 3D assay.

Various methods exist for the quantification of TLSs in 2D (152). In this Chapter 3D images of collagen I gels were acquired using confocal microscopy and Imaris software (Bitplane) was then used to render these 2D stacks, quantifying the rendered images using the Imaris filament tracer plugin. Although this has mainly previously used for the quantification of neurons (153), there is evidence in the literature of its value in quantifying blood vessel parameters when looking at vascular remodelling in the retina (154). By quantifying the TLSs that formed within collagen I 2mg/ml gels containing different ECs (HUVECs, CBECFCs or PBECFCs), co-cultured with either BMMSCs or AdMSCs, it was possible to confirm that all of the potential combinations of these stem and progenitor cells formed TLSs *in vitro*. Although averages from 3 different batches of the different cells were used to confirm this conclusion, looking at each gel separately is was possible to determine the best batch for forming TLSs, both qualitatively and quantitatively, an important point to consider when it came to planning up-scaled gels for *in vivo* experimentation (Chapter 4).

CHAPTER 4

UPSCALING OF PRE-VASCULARISED COLLAGEN I GELS AND THEIR IN VIVO APPLICATION

4.1 Introduction

In Chapter 3, EC migration within a variety of collagen I and fibrin gel concentrations was explored. Having determined the optimal conditions for EC migration, the vascularisation of a compressed bovine collagen I 2mg/ml gel with stem and progenitor cells was examined but the compression process led to the loss of already formed tubules and was not amenable to neo-angiogenesis. As a result, several different uncompressed 2mg/ml collagen I gels were fabricated to try to optimise tubule formation. This ultimately led to the production of a 56µl gel in a 96 well plate format that contained the cytokines SDF-1α, SCF and IL-3 together with $2x10^5$ ECs and $3x10^4$ MSCs. In this construct, tubules formed regardless of which combination of ECs (HUVECs, CBECFCs or PBECFCs) and MSCs (BMMSCs or AdMSCs) was used. Although every combination of ECs and MSCs produced tubules in 96 well plates, PB5 and Ad2 produced networks with the highest number of tubules and subtubules as well as the highest total tubule area and total tubule volume. Therefore these batches of ECFCs and AdMSCs were used for scaling up of gels.

Aims for upscaling collagen I gels and in vivo work

The aims for this Chapter were as follows:

1. Scale up the optimised co-culture of PBECFCs and AdMSCs from a 96-well to a 24-well format. In this way collagen I gels with a 1.6cm diameter would be produced that would be suitable to implant into a murine *in vivo* model. In addition this would confirm that increasing the gel size did not compromise tubule formation and this could pave the way for the production of much larger pre-vascularised sheets that could be used clinically.
2. Place pre-vascularised scaled up collagen I gels into a murine *in vivo* model along with empty collagen I gels to compare how these integrated with the host vasculature.

4.2 Results

4.2.1 Scaling up pre-vascularised collagen I gels

PBECFCs or HUVECs were co-cultured together with AdMSCs or BMMSCs within the optimised 2mg/ml collagen I gel (Chapter 3) with all components scaled up from a 96 to a 24 well plate format and tubules formed within the 4 different constructs (Fig 4.1). Following confirmation that these would still form tubules, the scaled up gels could now be implanted into a murine *in vivo* model.

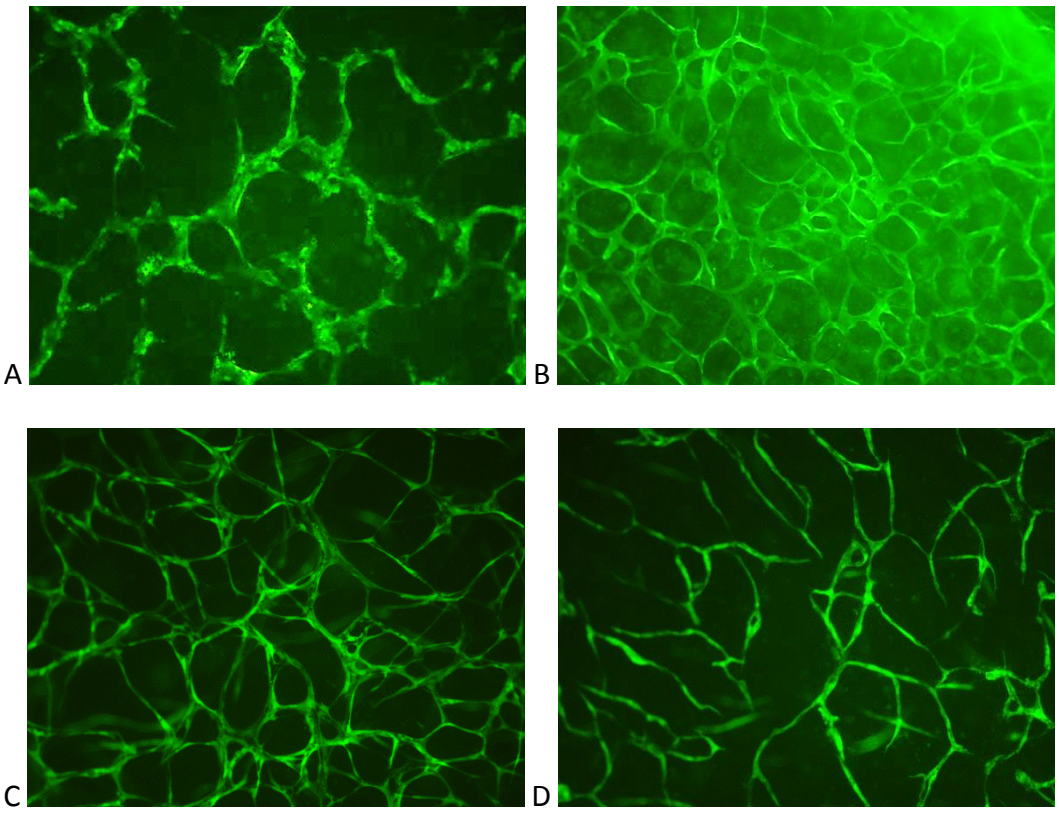

Figure 4.1 – scaled up pre-vascularised collagen I gel: x10 magnification images of tubules within a 2mg/ml collagen gel containing a co-culture of A) PBECFCs and AdMSCs; B) PBECFCs and BMMSCs; C) HUVECs and AdMSCs; D) HUVECs and BMMSCs ($1.2x10^6$ ECs and $1.8x10^5$ MSCs in each construct).

4.2.2 Implantation of gels in immunodeficient murine model

The optimum batch of PBECFCs and AdMSCs for tubule formation from Chapter 3 was co-cultured within the scaled up 2mg/ml collagen I gel in triplicate. Simultaneously, 3 sets of an empty gel containing no cells but otherwise identical constituents were also fabricated. These

gels were bisected and a pre-vascularised section was placed subcutaneously onto one side of a mouse dorsum whilst on the contralateral side, the equivalent non-vascularised control was placed in an identical manner. A total of three mice had the identical placement of hemi-segments of pre-vascularised and control gel on either side of the dorsum. After 14 days, mice were injected with 100µl biotinylated lectin from *Lycopersicon esculentum* (Sigma Aldrich) then mice were sacrificed. Gels together with overlying dermis were excised and fixed using 4% PFA (Chapter 2.9) and were then sectioned and stained for mouse CD31 and for lectin, the former to show mouse vasculature within gels and the latter to show perfusion of constructs since lectin binds to endothelial cells. Therefore once injected into mouse tail vein, the presence of lectin within constructs would confirm their perfusion (see Chapter 2). Figure 4.2 shows the underside of excised murine skin and gels from day 14 mice with pre-vascularised gels appearing macroscopically to be more highly perfused than controls.

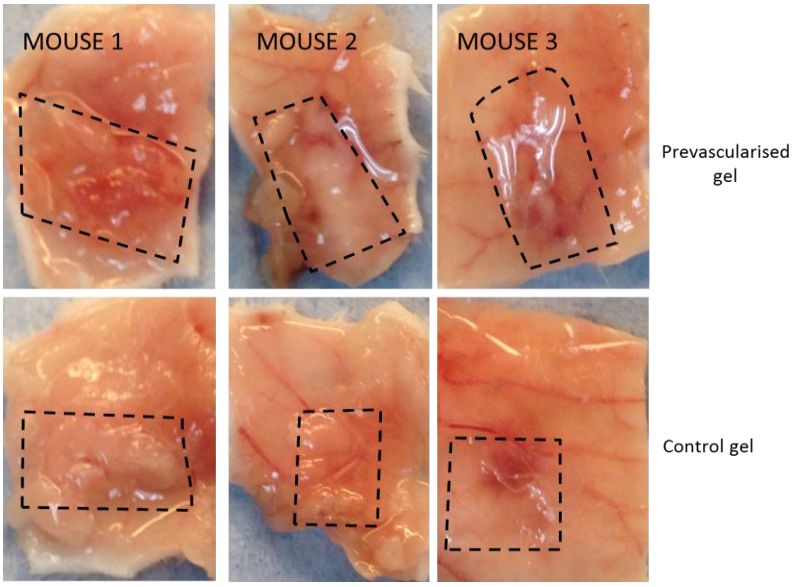

Figure 4.2 – Pre-vascularised versus control gel day 14: Images of the underside of excised mouse dermis showing the macroscopic difference between pre-vascularised gels and control gels at day 14. Approximate outlines of gels are indicated by dotted lines. Overall the pre-vascularied mice appear to have increased perfusion compared to control gels both in the gels themselves and in the immediate vicinity.

It was not possible to visualise the Streptavidin e450 (eBioscience) stain for lectin from *Lycopersicon esculentum* (tomato) or the anti-mouse CD31-PE stain to check for murine vessels (Chapter 2.10) using a fluorescence microscope. Concentrations used had been optimised previously within the Stem Cell research group by Dr Sarah Hale for the staining of

mouse femur sections however the concentrations of reagents and incubation periods did not work for these mouse skin sections (10µm). To try to optimise the protocol for mouse skin would have necessitated examining numerous different concentrations and incubation periods and given that there were time-constraints to complete the *in vivo* work for this project the decision was made to instead use a human CD31 biotinylated stain as per Chapter 2.6. This also did not clearly demonstrate tubules which were therefore likely mouse derived. However, counterstaining with haematoxylin and eosin (H&E) demonstrated the presence of red blood cells (RBCs) and these were used to calculate the number of vessels within x10 magnification image of prevascularised gels and controls. The average from 3 mice was recorded and compared for statistical significance between the control gel and pre-vascularised one (Table 4.1). Figures 4.3 to 4.6 show the increased number of perfused vessels seen within the architecture of pre-vascularised gels compared to controls.

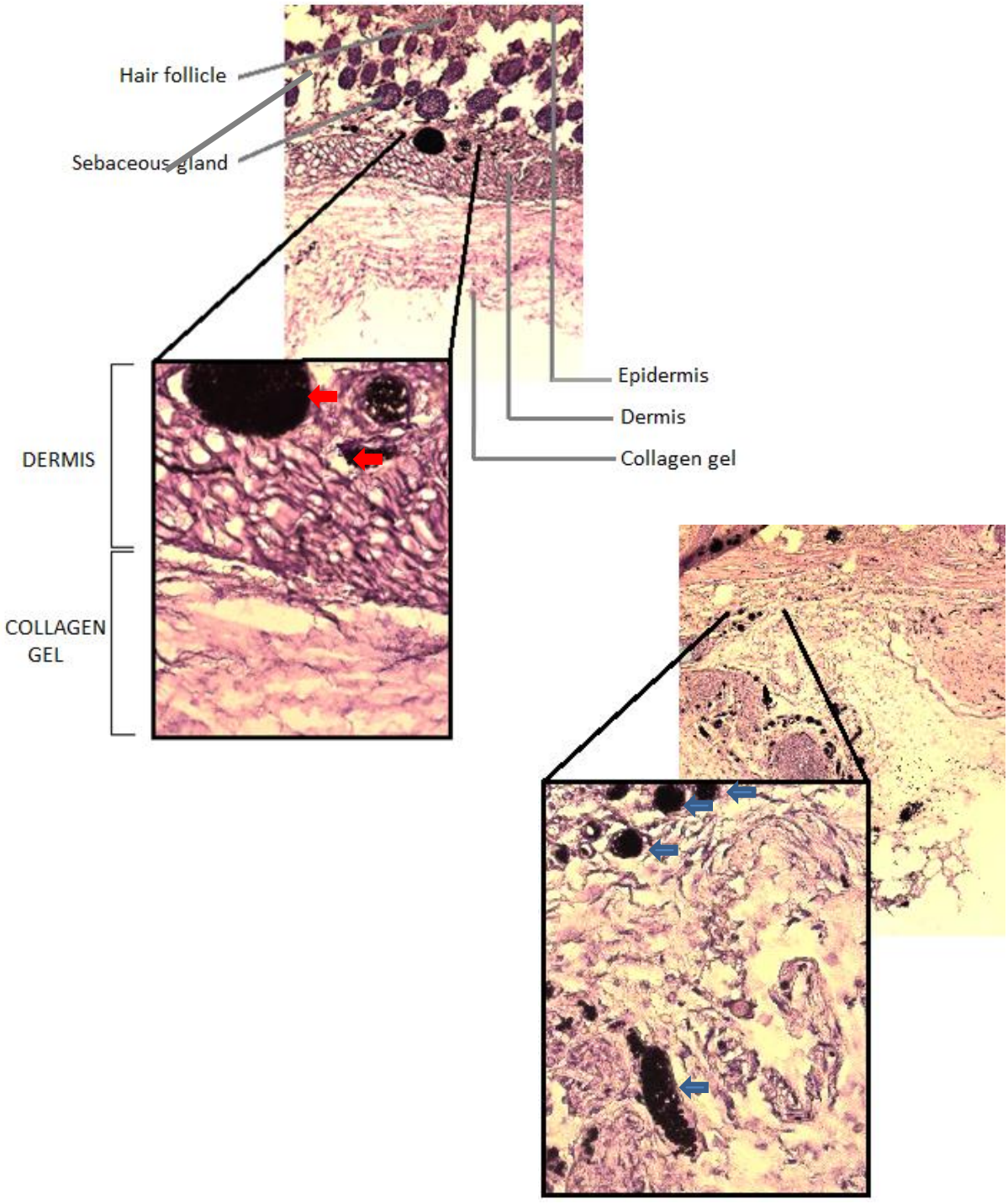

Figure 4.3 –Haematoxylin and Eosin (H&E) staining of sections of mouse 1 dermis with underlying gel construct at day 14: x10 and x40 images of 10µm sections of mouse dermis with underlying collagen I gel. The upper image shows the control gel and although vessels are seen within the dermis (red arrows), there are no vessels seen within the gel itself at day 14. The lower image shows the pre-vascularised gel and there are several vessels seen within the gel at day 14 (blue arrows). As the images show, there was no staining for human CD31, but H&E counterstaining enabled visualisation of tubules by staining RBCs.

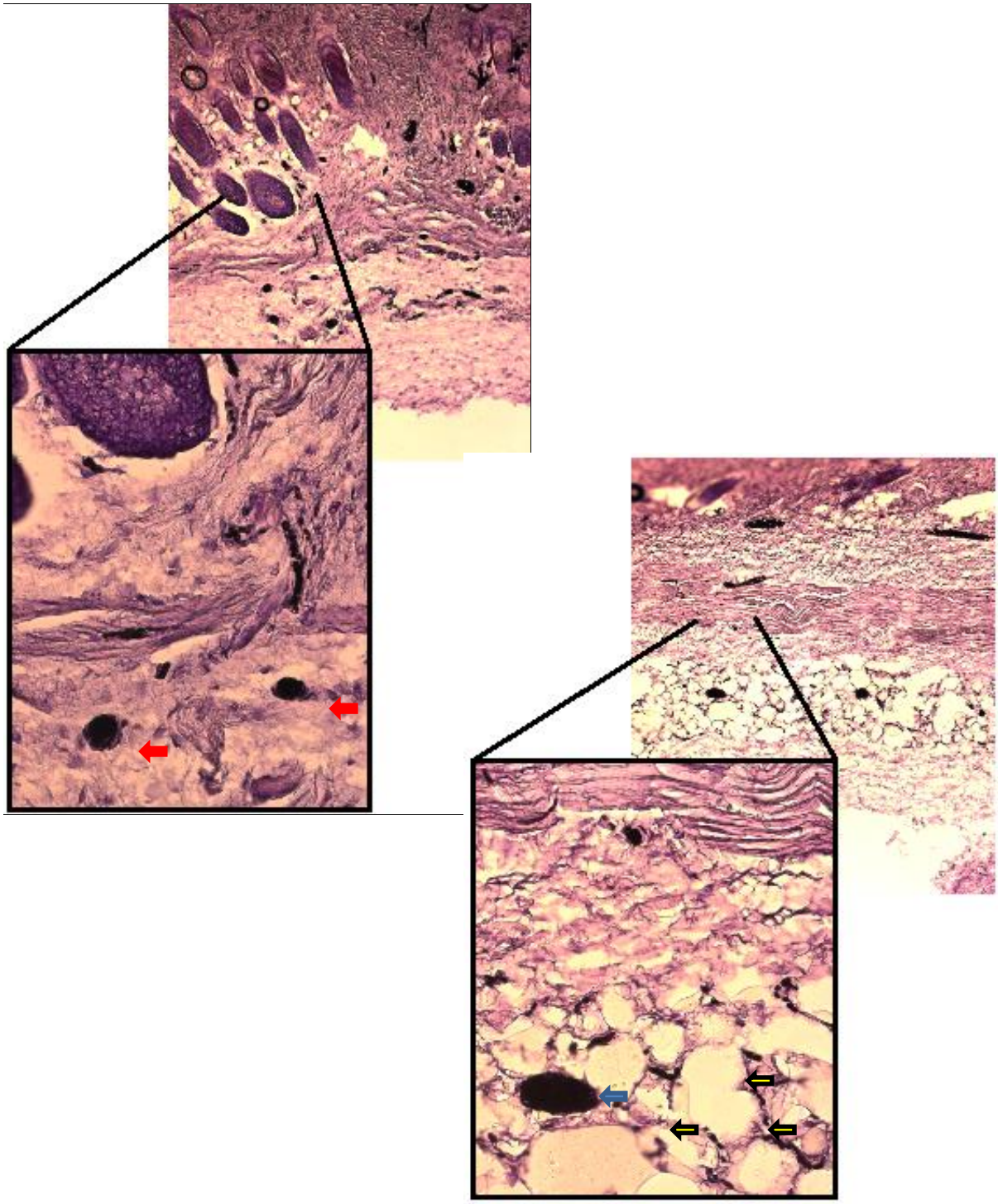

Figure 4.4 – Haematoxylin and Eosin (H&E) staining of sections of mouse 2 dermis with underlying gel construct at day 14: x10 and x40 images of 10µm sections of mouse dermis with underlying collagen I gel. The upper image shows the control gel with several perfused vessels seen within the dermis and only few vessels within the gel itself (red arrows). The lower image shows the pre-vascularised gel and in addition to a large perfused vessel seen here (blue arrow), there are also several interconnecting smaller tubules (yellow arrows) that are all perfused as evidenced by the presence of RBCs within their lumen (best seen on x40 image).

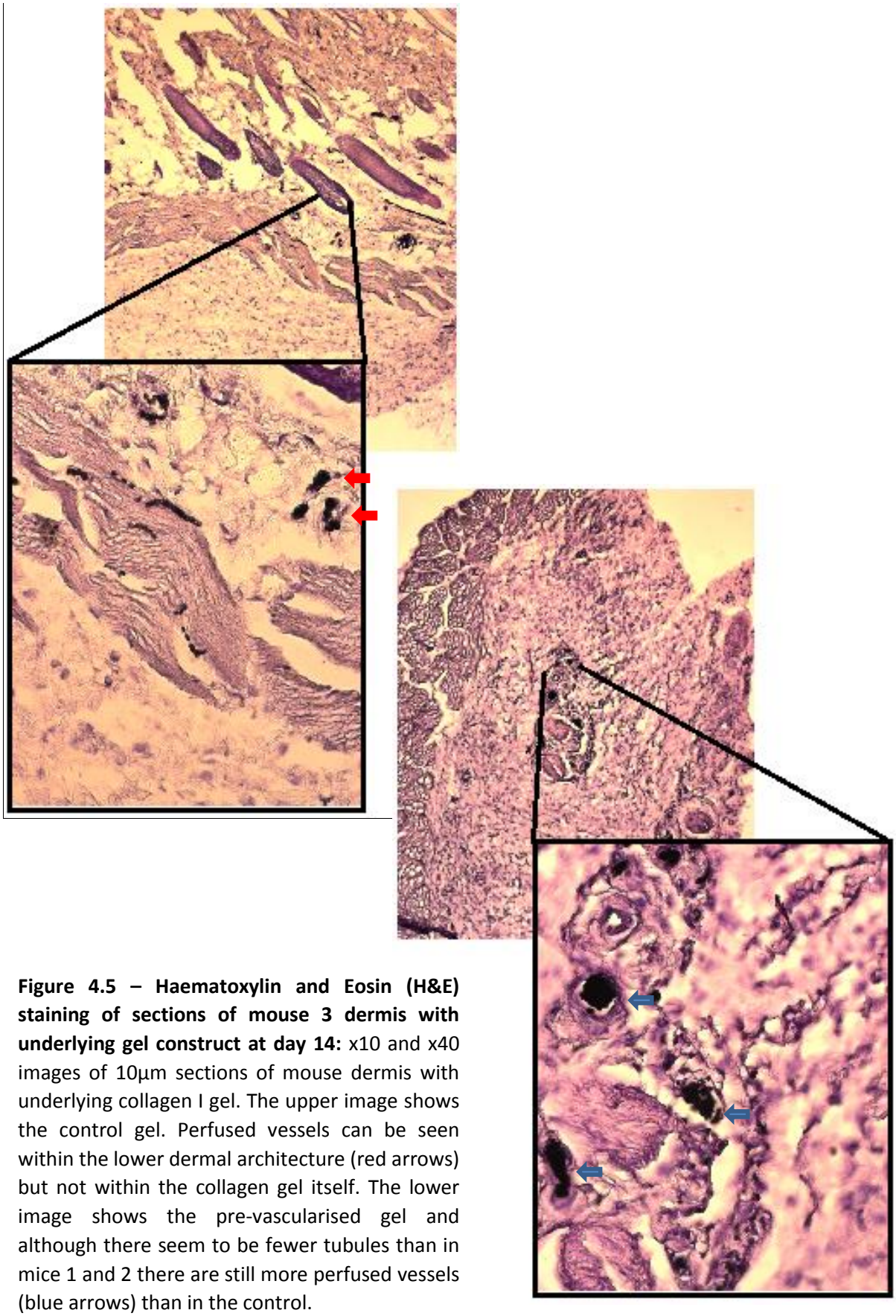

Figure 4.5 – Haematoxylin and Eosin (H&E) staining of sections of mouse 3 dermis with underlying gel construct at day 14: x10 and x40 images of 10µm sections of mouse dermis with underlying collagen I gel. The upper image shows the control gel. Perfused vessels can be seen within the lower dermal architecture (red arrows) but not within the collagen gel itself. The lower image shows the pre-vascularised gel and although there seem to be fewer tubules than in mice 1 and 2 there are still more perfused vessels (blue arrows) than in the control.

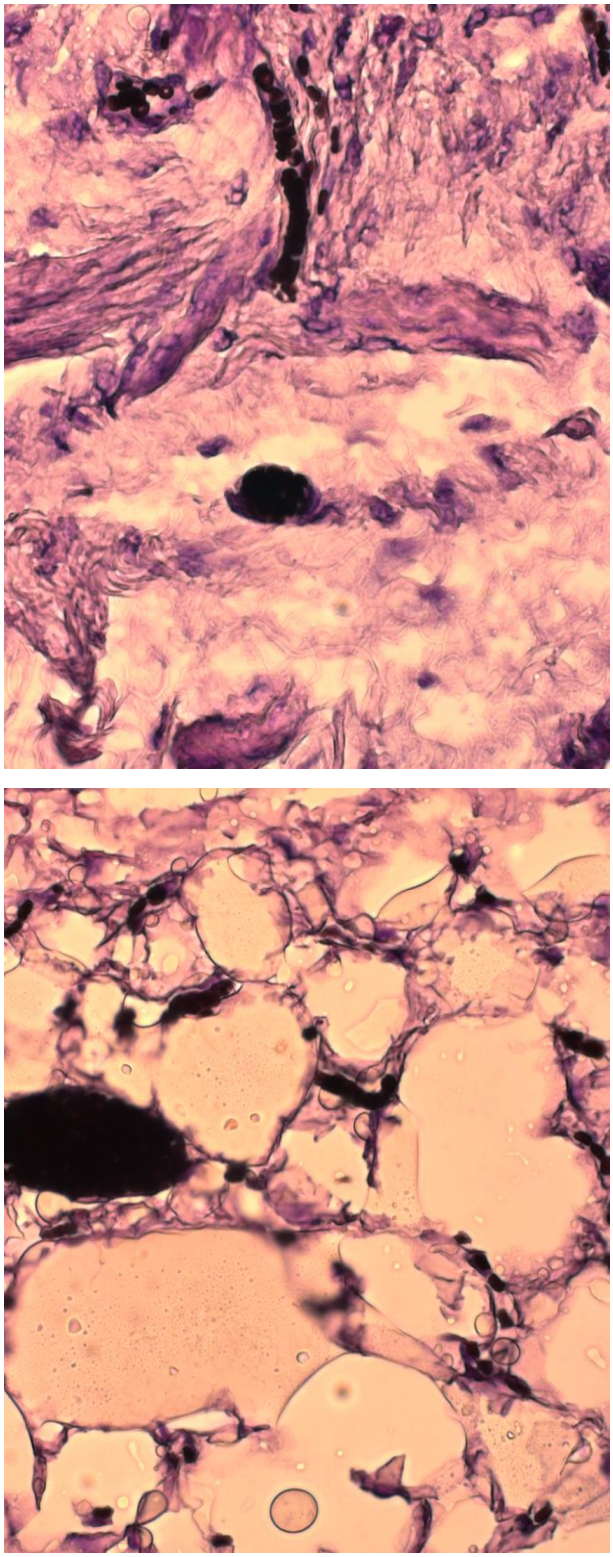

Figure 4.6 – Haematoxylin and Eosin (H&E) staining of sections of mouse 2 dermis with underlying gel construct at day 14: x60 images of 10µm sections of mouse dermis with underlying collagen I gel that show RBCs more clearly than x10 and x40 images. The top image shows the control gel and the bottom image shows the pre-vascularised gel.

Table 4.1: Number of RBC containing vessels seen per x10 magnification field

	Mouse 1	Mouse 2	Mouse 3	Average	SD
Vessels control	0	8	2	3.3	4.2
Vessels prevasc.	27	26	10	21	9.5

Table 4.1 shows the number of RBC containing vessels for the 3 different mice seen in pre-vascularised and control gels, as well as the average and standard deviation

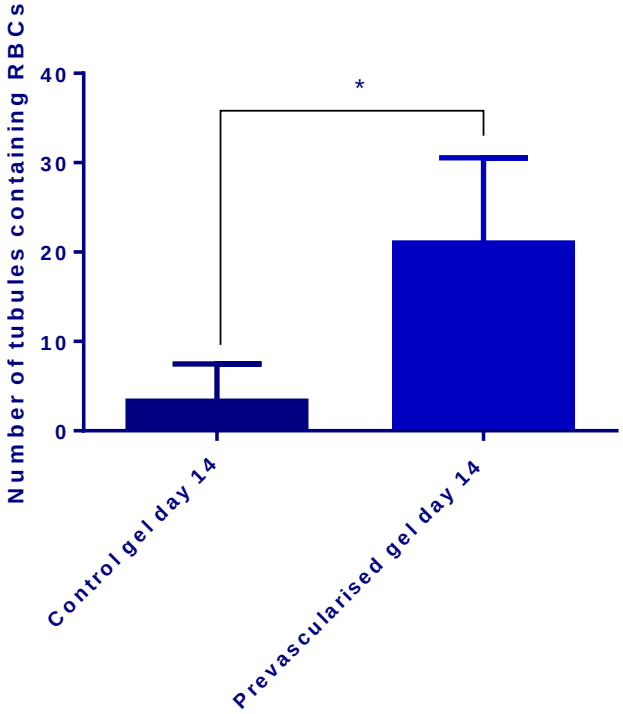

Figure 4.7 – Graph showing the number of tubules containing RBCs within control and prevascularised gels: x10 images were examined and the number of tubules containing RBCs was counted (n=3). There were significantly more tubules in prevascularised gels (*p=0.04)

Table 4.1 shows that there were almost 7 times as many RBC containing vessels seen within pre-vascularised gels than control gels at day 14 (p=0.04 paired t-test). In order to calculate the number of vessels for table 4.1, only vessels of a diameter greater than 1 RBC-width were included to negate RBCs that leaked from vessels during sectioning. Figure 4.4 (x40 magnification image) shows several RBC-containing tubules with a diameter of only 1 RBC-width in the pre-vascularised gel but these were not included within the analysis. Had they

been included the difference between control and pre-vascularised gels would have been even greater.

4.3 Discussion

There were two broad aims for this Chapter. The first was to scale up the optimised co-culture of PBECFCs and AdMSCs from a 96-well to a 24-well format whilst maintaining the formation of tubule-like structures. The second was to implant this gel into a murine *in vivo* model with the hypothesis being that a pre-vascularised gel would integrate with the host more readily than an empty collagen I gel.

When reagents were scaled up for a 24 well plate, tubules formed within the collagen I gel with every combination of ECs (PBECFCs/HUVECs) with MSCs (BM/Ad) (Figure 4.1). Pre-vascularised gels made using only adult-derived stem and progenitor cells (PBECFCs and AdMSCs), when placed into subcutaneous pockets in mice were compared to a collagen I gel without cells but otherwise identical. The primary end-point for assessing integration of these 2 constructs with the murine tissue was to examine for the presence of perfused vessels within the construct(s) and to determine whether these vessels were formed from murine or human endothelial cells.

The main issues with the *in vivo* experiments performed in this Chapter were accurately quantifying tubule formation and attempting to determine whether these tubules were human ECFC or murine EC derived. Counting the number of perfused vessels within a x10 magnification field (using the presence of RBCs within lumina as a surrogate for this) was a satisfactory method for estimating the level of wound-host integration and most authors advocate this technique for quantification of capillary like structures (62,83,102,105). However, in addition to this, other staining methods are also often performed to further delineate whether tubules are host or donor-derived and the role of MSCs in their stabilisation. For example human-CD31 fluorescence staining has been used for the former and eGFP labelling of MSCs for the latter (105). In addition, intravital fluorescence microscopy (155) has been used for *in vivo* microscopic observation of microcirculation and this would be a useful adjunct to determine at which stage implanted gels connect with the host vasculature.

In order to further investigate the potential of PBECFCs and AdMSCs within a collagen I scaffold it would be preferable to titrate human and murine CD-31 fluorescence stains and reagent incubation periods until scaffold tubules are identified as either murine or human EC derived, or both. In addition, staining of MSCs would help to demonstrate the role of AdMSCs in the development of the neo-vasculature. Finally, given the ultimate goal of producing a clinically relevant dermal (and epidermal) scaffold, it is important to also compare the number tubules seen when a pre-vascularised collagen I scaffold is placed onto a murine wound to the number when a collagen I gel is implanted immediately after seeding with PBECFCs and AdMSCs. Since both of PBECFCs and AdMSCs have a well-defined phenotype (72,143,144), it may be possible to isolate them directly from a patient through flow activated cell sorting (FACS) and to then create a scaffold that rapidly integrates with the host without necessitating a period of *ex vivo* pre-vascularisation. Whether this would be a feasible alternative could only be ascertained by examining scaffolds containing stem cells immediately after their harvest, prior to them forming tubules and should this also lead to improved host-scaffold integration as was the case with the pre-vascularised gels in this Chapter, then it would provide a much faster, and therefore more suitable scaffold for tissue engineering. Had time allowed, the key experiment to carry out would have been to compare one of the 'pre-vascularised' gels to a gel containing PBECFCs and AdMSCs that hadn't yet formed TLSs. If wound integration (using RBC containing tubules as a surrogate for this) occurred to the same extent with such a gel, this could prove extremely useful in creating a scaffold that could be used at least 1 week earlier in a clinical scenario.

CHAPTER 5

Discussion and future perspectives

5.1 Introduction

Vascularisation is a vital stage in wound healing and is crucial to the integration of skin substitutes with a wound bed (34). This MD thesis has examined how stem and progenitor cells can be isolated from adult blood and adipose tissue, expanded and co-cultured within an optimised collagen I scaffold to form a pre-vascularised dermal substitute. This pre-vascularisation increased the rate of host-scaffold integration in comparison to an acellular control in an *in vivo* murine model emphasising a potential improvement on existing proprietary dermal substitutes.

5.2 Scarring

It is important to note that although a vascularised dermal replacement may increase the rate of host-scaffold integration, this may not necessarily lead to an improved cosmetic and/or functional wound healing outcome. Overproduction of granulation tissue – that is, the new connective tissue and tiny blood vessels that form on the surface of a healing wound – can lead to hypertrophic scars (156). Therefore, dermal scaffolds containing blood vessels may also contain more primed active fibroblasts and lead to excessive microvascular regeneration, including lateral branching, which subsequently degenerates, in part, promoting nodule formation and remodelling (156). Nevertheless, research has demonstrated that increased hypertrophic scarring occurs in wounds taking longer than 3 weeks to heal (6). Therefore there is also a strong argument that a pre-vascularised scaffold which would enable immediate split skin grafting rather than a 2 stage procedure using an existing proprietary acellular scaffold such as Integra® or Matriderm® would produce a better functional and cosmetic outcome. It is unlikely that the fine networks of blood vessels within a prevascularised scaffold would contribute to the kind of increased scarring associated with an over-granulating wound. Further, with the arrival of bioengineered autologous epithelial sprays and sheets in recent years, a pre-vascularised dermis could be further enhanced to create a living skin equivalent also containing an epithelial layer that could be applied in a single stage to heal a full-thickness defect without necessitating a new donor site.

5.3 Stem/progenitor cells and vasculogenesis

In order to produce a pre-vascularised scaffold it is necessary to use a population of endothelial cells and to co-culture these with stromal cells/pericytes. The former are required to form new vessels whilst the latter stabilise them (62,133). Numerous authors have demonstrated that endothelial cells derived from neonatal human dermis (HDMECs) or umbilical vein (HUVECs) will form a microvasculature within scaffolds *in vitro* (73,83,157,158). However, both HUVECs and HDMECs originate from non-adult tissues and therefore would not be suitable for clinical use due to the immunogenicity they would illicit from the host. They express proteins relevant for alloimmunity, including MHC molecules, costimulators, adhesion molecules, cytokines, chemokines and have the ability to initiate allogeneic CD4+ and CD8+ memory T cell responses *in vitro* and *in vivo* (159). This is an issue that also needs to be considered for CBECFCs. Although the expansion capacity for CBECFCs is almost limitless and their harvest carries no morbidity for patients, these cells have the same immunogenic issues as HUVECs and HDMECs. For this reason, the ideal endothelial cell for use in developing a pre-vascularised dermal scaffold should be easily isolated from the same patient for which its use is intended – an adult-derived endothelial progenitor cell. In this thesis, ECFCs were isolated from the peripheral blood of NHS donors. A 500ml blood donation underwent leukopheresis to make it suitable for transfusion, and the resultant leukocyte cone which would have otherwise been discarded was processed to isolate the ECFCs using a similar technique to that previously established for CBECFC isolation from a MNC fraction (73,77) (Chapter 2.5). These cells were then expanded *in vitro* and co-cultured with AdMSCs within a collagen scaffold to produce a pre-vascularised scaffold using only adult-derived progenitor/stem cells. Although endothelial and mesenchymal cells in this thesis were derived from different donors, this was merely done to limit the impact on patients from whom the adipose tissue was sourced. Given that ECFCs could be sourced for experimentation from peripheral blood leucocyte cones that would have been otherwise discarded, it was not felt justifiable to consent the breast reconstruction patients for taking blood from them in addition to the adipose tissue that would otherwise have been discarded. Since *in vivo* experiments were conducted on immunodeficient mice there was no contraindication to using PBECFCs from one patient and AdMSCs from another. A criticism to using this methodology is that a 500ml blood donation was required to isolate the MNC

fraction (leucocyte cone). Attempting to replicate this technique in a clinical scenario would lead to a physiological and ethical dilemma. For example, if a patient with a large body surface area burn attended accident and emergency, although harvesting adipose tissue for retrieving AdMSCs would not cause major morbidity, taking 500mls of blood could put more strain on an already physiologically compromised patient. However, there are 2 ways around this caveat for using adult-derived PBECFCs. The first involves taking the MNCs from 500mls of peripheral blood then re-transfusing the blood back into the patient thus negating the physiological insult. The second, more straightforward option, would be to take a much smaller amount of peripheral blood and to isolate and expand the ECFCs from here, as described by Hofmann *et al.* (95). This technique was not used in this thesis as time limitations meant that already established techniques within the laboratory would give the best chance of obtaining the desired PBECFCs. However, having shown a proof of principle using PBECFCs and AdMSCs from a leucocyte cone and discarded adipose tissue respectively, the literature shows us that it would be feasible to isolate the PBECFCs from a 5ml blood sample ($1.5x10^8$ ECFCs could be isolated within 25 days) (95) and the AdMSCs from a small amount of debrided fat/lipoaspirate and that these could then be rapidly expanded and co-cultured to make a large pre-vascularised dermal scaffold in less than 30 days.

One of the most important conclusions that resulted from this research was that ECFCs derived from adult patients had a similar vasculogenic potential to HUVECs and CBECFCs, a vital determinant in the context of tissue engineering. There was no statistical difference in the number of sub-tubules, total tubule length and total tubule volume when PBECFCs were co-cultured with BMMSCs or AdMSCs than when CBECFCs or HUVECs were used. Furthermore, there were more main tubule trunks when PBECFCs were co-cultured with AdMSCs than when HUVECs were used ($p=0.04$) further emphasising that the adult-derived ECFCs had a good vasculogenic potential.

In this thesis, leucocyte cones from blood donors were anonymised and demographic information was not provided making it difficult to postulate the relationship between different donors and whether ECFCs were likely to be obtained. ECFC colonies were obtained from 3 out of 6 batches that were processed (on average at day 11 [n=3]). This lack of consistency probably represented a learning curve for isolation of the ECFCs rather than a predictable 50% overall success rate. Indeed, authors using the MNC centrifugation technique

described in this thesis have had no difficulty obtaining ECFCs from much smaller volumes of peripheral blood (5-100mls) (72,82,95). In addition, it has previously been shown that endothelial progenitors are mobilised into the systemic circulation of burned patients (160) adding weight to the expectation that these cells of interest could be isolated from such patients, expanded and then used to help produce a pre-vascularised collagen scaffold.

5.4 From bench to bedside

The current treatment for large full thickness skin loss is largely focussed on autograft and/or allograft in addition to the ever-increasing use of synthetic skin substitutes such as Biobrane®, Matriderm® or Integra®. Biobrane® has been shown to be particularly useful in superficial partial-thickness burns leading to reduced pain, hospital stay and wound healing time (161) and although it has been associated with permanent scarring in partial-thickness scald wounds (162). Integra® has been used widely for deep partial-thickness and full-thickness burn wounds. It has been shown to be superior to autograft and allograft in terms of wound healing time but has also been shown to lead to higher rates of wound infection and lower graft take (163). Matriderm® has the same indications as Integra® and similar engraftment rates and can accommodate an immediate SSG with no diminished graft take but this perceived advantage over Integra® no longer holds true since a thinner single-stage Integra® is now available that performs as well as Matriderm® in animal studies (54). Some clinical trials have shown no difference in scar elasticity between Matriderm® and SSG alone (164) but others have shown increased skin quality and hand range of motion when Matriderm® is used (165) together with SSG.

Although existing synthetic skin substitutes clearly have a role in the management of acute and chronic, superficial and deep wounds, further improvements are still being sought. A pre-vascularised scaffold could achieve improved cosmesis and graft take and ultimately may enable the creation of a completely autologous tissue engineered skin including an epithelial layer which would negate the need for harvesting a SSG altogether. Existing dermal substitutes have the disadvantage that they are not able to replace the dermal and epidermal layer simultaneously. The outcomes demonstrated in this thesis, in particular the increased number of perfused vessels seen within *in vivo* murine models when pre-vascularised collagen I gels were used compared to empty gels, show that the dermal component of a pre-

vascularised scaffold can be produced *in vitro*, using autologous stem and progenitor cells, and lead to better integration with a living host.

In order to move from 'bench to bedside' with this pre-vascularised dermal scaffold, several questions need to be addressed:

5.4.1 Can a suitable scaffold be produced on a large enough scale to be clinically viable?

Solving the problem of how to rapidly re-vascularise grafts will expedite the wound healing process and therefore limit scar formation. However, although the ability to select ECFCs post-natally from PB and adipose tissue is possible, the process still takes several weeks and the ECFC content is generally considered low. Techniques for isolating ECFCs from adult blood include plating Ficoll buffy coats (82) or directly plating a 5ml sample of blood prior to isolation of MNCs and then washing off non-adherent cells after 24 hours (95). Both techniques are time consuming the former taking 10 weeks to grow $1x10^{10}$ cells, the latter 30 days for $1x10^{8}$ cells. This time constraint combined with the relative scarcity of ECFCs in adult blood – a standard adult sample of 20mls of blood may contain as little as a single ECFC (82) – are their major drawbacks as a potential autologous cell to use for tissue engineering. Even ECFCs isolated from adipose tissue that show classical cobblestone morphology and form capillary-like tubes in Matrigel® take several weeks to expand up to $1x10^{8}$ cells (87).

Even though it may take several weeks to expand sufficient numbers to produce a microvascular network in a dermal substitute, in large burns this time window often exists. After the essential debridement of the burn to reduce this risk of mortality from a systemic inflammatory response, the patient is often temporised physiologically with allograft or temporary skin substitutes until further donor sites become available for grafting.

Nevertheless, ways in which the rate of ECFC expansion could be increased are likely to be vital to their potential clinical application in the form of tissue engineered constructs containing pre-formed microvascular networks. Hollow fibre bioreactors made with the biodegradable material poly(lactide-co-glycolide) (PLGA) have been used to expand osteogenic cell lines at rates at least equivocal to standard tissue culture plastic (166). By optimising the construction of such bioreactors and the flow rate of media from within, an ideal environment for endothelial cell growth can be created. In addition to increasing the rate of expansion, hollow fibre bioreactors also save on media as any waste from cells is

siphoned off and the media can otherwise flow for several days in a circuit without needing to be changed.

In order to investigate the potential for fabricating a bioreactor for endothelial progenitor expansion, HUVECs were plated on standard 96-well plates. Having optimised the cell number required to record a noticeable increase in proliferation using the CellTiter-Fluor™ cell viability assay (Appendix 1), HUVECs, CBECFCs and PBECFCs were then plated onto the 3 different materials (tissue culture plastic; PLGA; polystyrene) and it was noted that PB ECFCs proliferated at least as quickly on our own fabricated polystyrene plates as they did on standard tissue culture plastic (Appendix 2). It would be reasonable from these pilot experiments to hypothesise that a polystyrene based hollow fibre bioreactor would enable rapid PBECFC expansion whilst having the added benefit of reducing costs for reagents. An alternative approach to negate the time pressure for ECFC isolation and expansion could be to seed scaffolds with MSCs and then allow these cells with or without added chemokines to attract ECFCs into the wound. In this way ECFCs from the whole body would be available rather than from a limited amount of blood.

5.4.2 What are the safety barriers to producing such a product?

MSCs have been increasingly used for tissue engineering and immunosuppressive therapy in recent years. The ability to source these cells from adipose tissue has helped to reduce the potential morbidity associated with their harvest from BM. However, *ex vivo* amplification prior to clinical application is still required to obtain sufficient therapeutic doses. The same premise applies to ECFCs, which to date have not been used in clinical subjects. In fact, these cells, as explained in Chapter 1, are even more difficult to isolate and expand. Translation into clinical-grade large-scale expansion necessitates precise definition and standardisation of all procedural parameters and although xenogenic additives such as fetal calf serum are still widely used for cell culture, their use clinically carries many potential risks including prion and viral transmissible diseases. Fortunately, authors have already demonstrated GMP-grade production MSCs (167) and ECFCs (168) to be possible. Furthermore, the latter, that were expanded using human platelet lysates rather than animal sera, showed significantly lower apoptosis rates and increased proliferation. Indeed, extensively expanded ECFCs could settle on scaffold biomaterials and form tubular structures in Matrigel assays (168).

5.4.3 Can this pre-vascularised scaffold be used in humans?

The first clinical trial using culture-expanded MSCs was carried out in 1995 where 15 haem-oncology patients received injections of autologous BMMSCs as part of a safety and feasibility study. In October 2012, there were 218 registered clinical trials using MSCs for a wide range of therapeutic applications. Most of these were in Phase I (safety studies, n = 42), Phase II (proof of concept for efficacy in human patients, n = 57), or combined Phases I and II studies (n = 105). Only a small number were in Phase III (comparing a newer treatment to the standard or best known treatment, n = 8) or combined Phases II and III (n = 6) (169). Nevertheless, the evidence base for MSCs as a therapeutic agent for treating a wide range of conditions in humans is growing rapidly and more importantly they appear to be well tolerated, most trials reporting a lack of any adverse effects (170). Examples of areas where MSC therapy has been trialled include acute myocardial infarction, stroke, liver cirrhosis, amyotrophic lateral sclerosis, graft-versus-host disease (GVHD), solid organ transplant rejection, and autoimmune disorders (169).

Although MSCs derived from BM, umbilical cord blood and adipose tissue have now been studied extensively, ECFC trials in human subjects have not taken off. The main reason for this is that ECFCs are far less well understood than MSCs. The discovery of MSCs can be traced back to the 1960s (171) whereas the concept of an endothelial progenitor cell was not proposed until Asahara *et al.* in 1997 (172) and true endothelial colony forming cells (ECFCs) are still not fully understood in terms of the cell surface markers and behavioural phenotypes that define them when they are isolated from different sources. Furthermore, *ex vivo*-cultured ECFCs can be contaminated by other cell types in peripheral blood such as circulating MSCs, smooth muscle progenitors and inflammatory cells (173). Although endothelial progenitors have not yet been used in human studies, the therapeutic concept of ECFC transplantation has been established by several animal models of hindlimb ischaemia. BMMSCs, PBMNCs, CD34 positive MNCs and CD133 positive cells have all been examined with outcomes suggesting that cell-based therapy could be feasible in patients with critical limb ischaemia.

Appendix 1: Proliferation assay (CellTiter-Fluor™ Cell Viability Assay)

Using the CellTiter Fluor™ cell viability assay it was determined that HUVEC cell concentrations of 1250 and under showed only very minimal increase in GF-AFC fluorescence after 96 hours and no significant difference when varying the number of cells (Fig 5.1). Using GF-AFC fluorescence increase as a surrogate for proliferation would therefore not be possible if using cell concentrations of 1250 or less. However, when plating 2500, 5000 or 10000 HUVECs there was a significant rise in the mean fluorescence after 96 hours particularly for the higher concentrations of cells. These results were consistent whether recorded from above or below the wells using a Victor2 plate reader (PerkinElmer, UK). However, recordings taken from above with the lid off the 96-well plates were much more relatable to those taken from underneath than when the lid was still in situ. This was likely as a result of condensation forming on the underside of the lid whilst in the incubator.

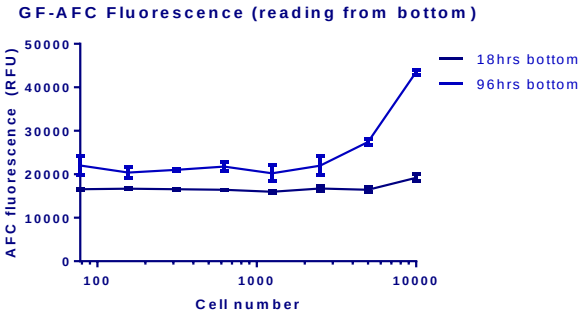

A

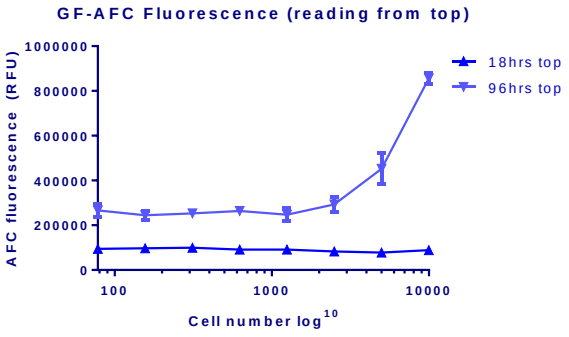

B

Fig 5.1 – pHUVECs: GF-AFC fluorescence recordings at 18 and 96 hours from underneath (a) and above (b) 96-well plates (with lid off for both). Only when using cell concentrations of 1250 and above was a noticeable increase in GF-AFC seen.

The mean fluorescence was also recorded from tissue culture plastic (TCP)-bottomed wells that were empty and those containing media with no cells (Fig 5.2). There was almost no baseline GF-AFC fluorescence from these 2 types of well (empty; containing media only) and the values also did not change after 96 hours from those recorded at 18 hours demonstrating that the TCP plate and media produce a negligible amount of recordable fluorescence when there are no cells present and that this does not change over time.

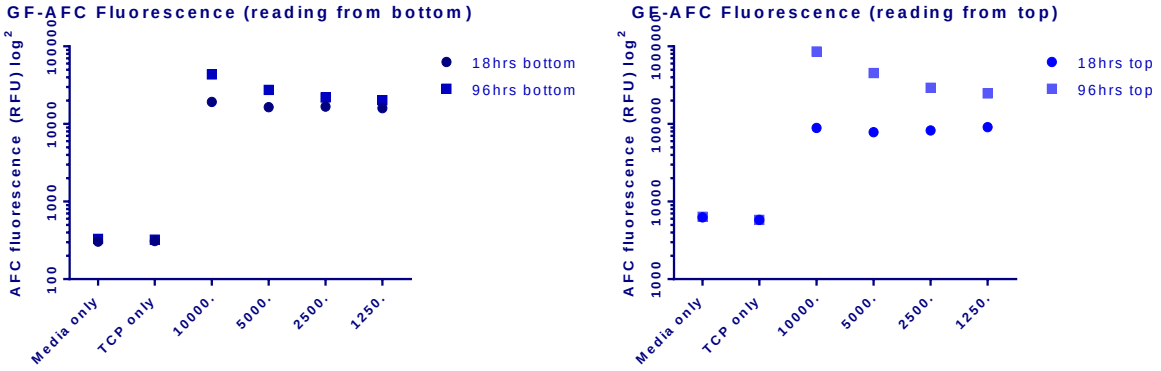

Fig 5.2 – pHUVECs: GF-AFC fluorescence recordings at 96 hours (log^{10}) from wells containing pHUVECs (10000 to 1250 shown), media only or empty TCP wells to show background fluorescence produced by media and empty wells and how this changes over time.

Appendix 2: HUVEC/CB ECFC/PB ECFC proliferation assay in PLGA/polystyrene lined plates

Following the optimisation of the CellTiter Fluor™ cell viability assay, 5 different concentrations of HUVECs, CBECFCs and PBECFCs (1250; 2500; 5000; 10000 and 20000 cells) were plated in triplicate in 96-well plates made from either tissue culture plastic (TCP), PLGA or polystyrene (PS). Recordings of GF-AFC fluorescence were then taken at 18 hours and 96 hours to act as a surrogate for cell proliferation (worked out by subtracting the baseline reading at 18 hours from the 96 hour reading).

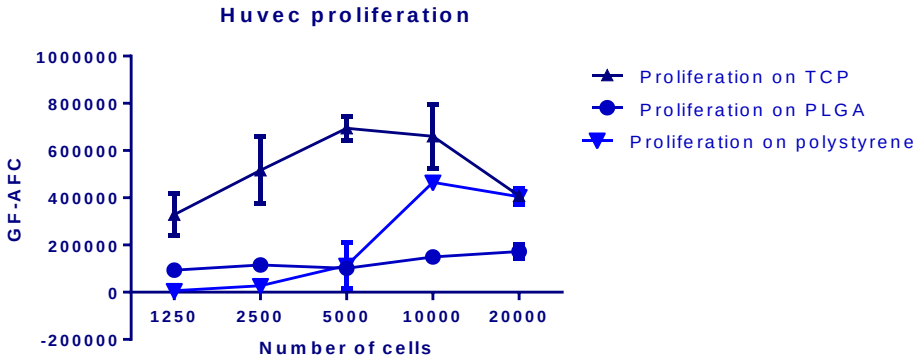

Fig 5.3a – pHUVECs: GF-AFC fluorescence recordings at 18 and 96 hours taken from above TCP, PLGA and PS wells (with lid off). Note that the surrogate for proliferation (increase in GF-AFC between 18hrs and 96hrs) is similar on TCP and PS but is limited on PLGA and is optimal at a concentration of around 10000 cells.

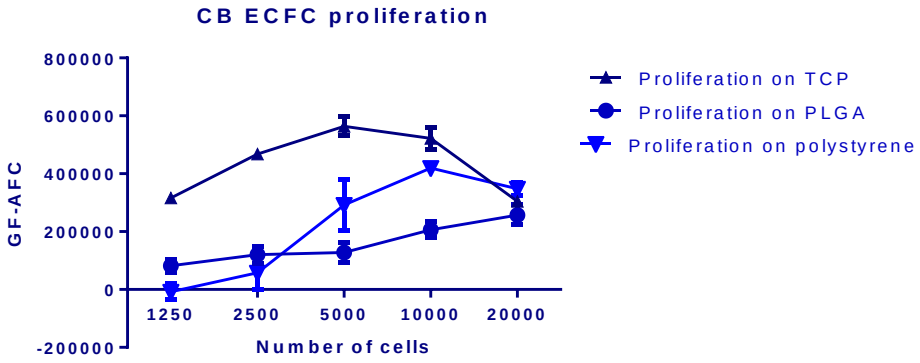

Fig 5.3b – CB ECFCs: GF-AFC fluorescence recordings at 18 and 96 hours from above TCP, PLGA and PS wells (with lid off). As was the case with pHUVECs increase in GF-AFC between 18hrs and 96hrs is similar on TCP and PS and optimal at a concentration of 5000-10000 cells but is limited on PLGA, although it does increase slightly as cell number increases.

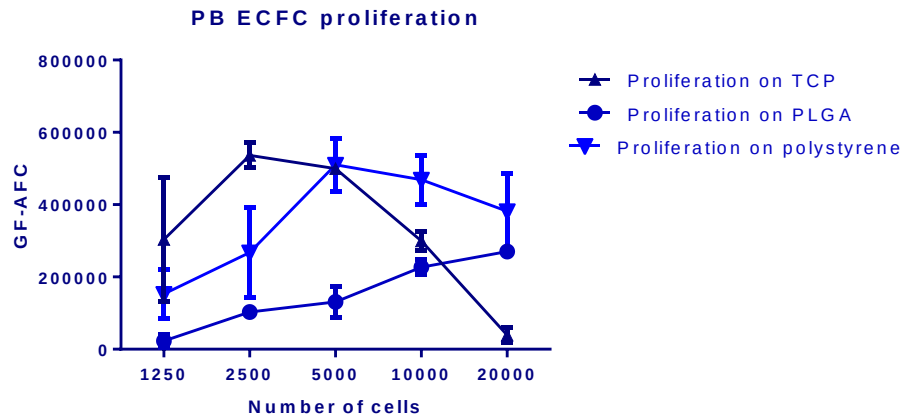

Fig 5.3c – PB ECFCs: GF-AFC fluorescence recordings at 18 and 96 hours from above TCP, PLGA and PS wells (with lid off). The surrogate for proliferation (increase in GF-AFC between 18hrs and 96hrs) is similar on TCP and PS and peaks at around 5000 cells. Increase in GF-AFC expression on PLGA rises with increasing cell number but never reaches as high as the peak expression for TCP or PS.

References

1. Chaucer G. Troilus & Criseyde. 1385(a 1400). Available from: http://ebooks.gutenberg.us/DjVu_Collection/DJEDS/CHAUCER/TROILUS/Download.pdf

2. Brown BC, Moss TP, McGrouther DA, Bayat A. Skin scar preconceptions must be challenged: importance of self-perception in skin scarring. JPRAS 2010; 63(6): 1022-9

3. Harding KG, Morris HL, Patel GK. Science, medicine and the future: healing chronic wounds. BMJ 2002;324(7330):160–3.

4. Hettiaratchy S, Dziewulski P. Introduction. In: ABC of burns. 2005;1-3

5. Ahn CS, Maitz PKM. The true cost of burn. Burns. 2012; 38(7):967-74.

6. Cubison TCS, Pape SA, Parkhouse N. Evidence for the link between healing time and the development of hypertrophic scars (HTS) in paediatric burns due to scald injury. Burns 2006; 32(8):992–9.

7. Auger FA, Lacroix D, Germain L. Skin substitutes and wound healing. Skin Pharm and Physiol 2009;22(2):94–102.

8. Yildirimer L, Thanh NTK, Seifalian AM. Skin regeneration scaffolds: a multimodal bottom-up approach. Trends in biotech 2012;30(12):638–48.

9. Wells C. Skin and wound care manual online. 2012. Available at: http://westernhealth.nl.ca/uploads/PDFs/wound care manual for dianne clements final.pdf

10. Behrens DT, Villone D, Koch M, Brunner G, Sorokin L, Robenek H, et al. The epidermal basement membrane is a composite of separate laminin- or collagen IV-containing networks connected by aggregated perlecan, but not by nidogens. J Biol Chem 2012;287(22):18700–9.

11. Bikle DD. Vitamin D metabolism and function in the skin. Mol Cell Endocrinol 2011;347(1-2):80–9.

12. Janssens a S, Heide R, den Hollander JC, Mulder PGM, Tank B, Oranje a P. Mast cell distribution in normal adult skin. J Clin Pathol 2005;58(3):285–9.

13. Watt FM, Jensen KB. Epidermal stem cell diversity and quiescence. EMBO Mol Med 2009;1(5):260–7.

14. Ema H, Suda T. Two anatomically distinct niches regulate stem cell activity. Blood 2012; 120(11):2174-81.

15. Fuchs E, Chen T. A matter of life and death: self-renewal in stem cells. EMBO reports 2012;1–10.

16. Mascré G, Dekoninck S, Drogat B, Youssef KK, Broheé S, Sotiropoulou P a, et al. Distinct contribution of stem and progenitor cells to epidermal maintenance. Nature 2012;489(7415):257–62.

17. Fuchs E. Scratching the surface of skin development. Nature 2007;445(7130):834–42.

18. Tumbar T, Guasch G, Greco V, Blanpain C, Lowry WE, Rendl M, et al. Defining the epithelial stem cell niche in skin. Science 2004;20(3):359–63.

19. Blanpain C, Lowry WE, Geoghegan A, Polak L, Fuchs E. Self-renewal, multipotency, and the existence of two cell populations within an epithelial stem cell niche. Cell 2004;118(5):635–48.

20. Van Keymeulen A, Blanpain C. Tracing epithelial stem cells during development, homeostasis, and repair. J Cell Biol 2012;197(5):575–84.

21. Plikus M V, Gay DL, Treffeisen E, Wang A, Supapannachart RJ, Cotsarelis G. Epithelial stem cells and implications for wound repair. Semin Cell Dev Biol 2012;23(9):946-53.

22. Lu CP, Polak L, Rocha AS, Pasolli HA, Chen S-C, Sharma N, et al. Identification of stem cell populations in sweat glands and ducts reveals roles in homeostasis and wound repair. Cell 2012;150(1):136–50.

23. Biedermann T, Pontiggia L, Böttcher-Haberzeth S, Tharakan S, Braziulis E, Schiestl C, et al. Human eccrine sweat gland cells can reconstitute a stratified epidermis. J Invest Dermatol 2010; 130(8):1996–2009.

24. Danner S, Kremer M, Petschnik AE, Nagel S, Zhang Z, Hopfner U, et al. The use of human sweat gland-derived stem cells for enhancing vascularization during dermal regeneration. J Invest Dermatol 2012; 132(6):1707–16.

25. Rittié L, Sachs DL, Orringer JS, Voorhees JJ, Fisher GJ. Eccrine sweat glands are major contributors to reepithelialization of human wounds. Am J Pathol 2013; 182(1):163–71.

26. Culliford IV A, Hazan A. Dermatology for plastic surgeons. In: Grabb and Smith's Plastic Surgery. (Ed.6) 2007;105.

27. Paquet-Fifield S, Schlüter H, Li A, Aitken T, Gangatirkar P, Blashki D, et al. A role for pericytes as microenvironmental regulators of human skin tissue regeneration. Journal Clin Investig 2009;119(9):2795–806.

28. Brown JJ, Bayat A. Genetic susceptibility to raised dermal scarring. Brit Jour Dermatol 2009;161(1):8–18.

29. Shevchenko R V, James SL, James SE. A review of tissue-engineered skin bioconstructs available for skin reconstruction. J Royal Soc, Interface 2010;7(43):229–58.

30. Gerlach JC, Johnen C, Ottoman C, Bräutigam K, Plettig J, Belfekroun C, et al. Method for autologous single skin cell isolation for regenerative cell spray transplantation with non-cultured cells. Int J Artif Organs 2011;34(3):271–9.

31. Vloemans a FPM, Hermans MHE, van der Wal MB a, Liebregts J, Middelkoop E. Optimal treatment of partial thickness burns in children: A systematic review. Burns 2014; 40(2):177–90.

32. Highton L, Wallace C, Shah M. Use of Suprathel® for partial thickness burns in children. Burns 2013; 39(1):136–41.

33. Wainwright DJ, Bury SB. Acellular dermal matrix in the management of the burn patient. Aesthet surgery journal 2011;31(7 Suppl):13S–23S.

34. MacNeil S. Progress and opportunities for tissue-engineered skin. Nature 2007;445(7130):874–80.

35. Orlando G, Wood K, De Coppi P, Baptista P, Binder K, Bitar K, et al. Regenerative medicine as applied to general surgery. Ann Surg 2012;255(5):867–80.

36. Velazquez E, Murphy GF. Histopathology of the Skin (Ed.10). 2009;38–50.

37. Rnjak J, Ph D, Wise SG, Mithieux SM, Weiss AS. Severe Burn Injuries and the Role of Elastin in the Design of Dermal Substitutes. Tissue Eng Part B Rev 2011;17(2):81-91.

38. Pham C, Greenwood J, Cleland H, Woodruff P, Maddern G. Bioengineered skin substitutes for the management of burns: a systematic review. Burns 2007;33(8):946–57.

39. Heitland A, Piatkowski A, Noah EM, Pallua N. Update on the use of collagen/glycosaminoglycate skin substitute-six years of experiences with artificial skin in 15 German burn centers. Burns 2004;30(5):471–5.

40. Cervelli V, Lucarini L, Cerretani C, Spallone D, Palla L, Brinci L, et al. The use of MatriDerm® and skin grafting in post-traumatic wounds. International Wound Journal 2010;7(4):400–5.

41. Ryssel H, Gazyakan E, Germann G, Ohlbauer M. The use of MatriDerm in early excision and simultaneous autologous skin grafting in burns--a pilot study. Burns 2008;34(1):93–7.

42. Koenen W, Felcht M, Vockenroth K, Sassmann G, Goerdt S, Faulhaber J. One-stage reconstruction of deep facial defects with a single layer dermal regeneration template. J Eur Acad Dermatol Venereol 2011;25(7):788–93.

43. Gravante G, Delogu D, Giordan N, Morano G, Montone A, Esposito G. The use of Hyalomatrix PA in the treatment of deep partial-thickness burns. J burn care res 2007;28(2):269–74.

44. Travia G, Palmisano PA, Cervelli V, Esposito G, Casciani CU. The use of fibroblast and keratinocyte cultures in burns treatment. Ann Burns Fire Disast 2003;XVI(1)

45. Marston WA, Hanft J, Norwood P, Pollak R. The efficacy and safety of Dermagraft in improving the healing of chronic diabetic foot ulcers: results of a prospective randomized trial. Diabetes Care 2003;26(6):1701–5.

46. Hansbrough JF, Cooper ML, Cohen R, Spielvogel R, Greenleaf G, Bartel RL, et al. Evaluation of a biodegradable matrix containing cultured human fibroblasts as a dermal replacement beneath meshed skin grafts on athymic mice. Surg1992;111(4):438–46.

47. Waymack P, Duff RG, Sabolinski M. The effect of a tissue engineered bilayered living skin analog, over meshed split-thickness autografts on the healing of excised burn wounds. Burns 2000;26(7):609-19.

48. Moustafa M, Bullock AJ, Creagh FM, Heller S, Jeffcoate W, Game F, et al. Randomized, controlled, single-blind study on use of autologous keratinocytes on a transfer dressing to treat nonhealing diabetic ulcers. Regen Med 2007;2(6):887–902.

49. Rössner E, Smith MD, Petschke B, Schmidt K, Vitacolonna M, Syring C, et al. Epiflex(®) a new decellularised human skin tissue transplant: manufacture and properties. Cell Tissue Bank 2011;12(3):209–17.

50. Adamakis I, Tyritzis SI, Stravodimos KG, Migdalis V, Mitropoulos D, Constantinides C a. A novel approach for the surgical management of Peyronie's disease using an acellular, human dermis tissue graft: preliminary results. World J Urol 2011;29(3):399–403.

51. Hogg P, Rooney P, Ingham E, Kearney JN. Development of a decellularised dermis. Cell Tissue Bank 2012;14(3):465-74.

52. Macleod TM, Williams G, Sanders R, Green CJ. Histological evaluation of Permacol as a subcutaneous implant over a 20-week period in the rat model. Br J Plast Surg 2005;58(4):518–32

53. Ryssel H, Radu CA, Germann G, Otte M, Gazyakan E. Single-stage Matriderm® and skin grafting as an alternative reconstruction in high-voltage injuries. Int Wound J 2010;7(5):385–92.

54. Böttcher-Haberzeth S, Biedermann T, Schiestl C, Hartmann-Fritsch F, Schneider J, Reichmann E, et al. Matriderm 1 mm versus Integra Single Layer 1.3 mm for one-step closure of full thickness skin defects : a comparative experimental study in rats. PediatrSurg Int 2012;28(2):171–7.

55. Gravante G, Sorge R, Merone A, Tamisani AM, Di Lonardo A, Scalise A, et al. Hyalomatrix PA in burn care practice: results from a national retrospective survey, 2005 to 2006. Ann Plast Surg 2010;64(1):69–79.

56. Boyer D, Bartelt M, Heieck J. Comparison of E-Z Derm and Jelonet dressings for partial skin thickness burns. Nebr Med J. 1989;68(1):390–4.

57. Zhu N, Warner RM, Simpson C, Glover M, Hernon CA, Kelly J, et al. Treatment of burns and chronic wounds using a new cell transfer dressing for delivery of autologous keratinocytes. Eur J Plast Surg 2005;28(5):319–30.

58. Munster AM. Cultured skin for massive burns. A prospective, controlled trial. Ann Surg 1996;224(3):372–7.

59. Tremblay P-L, Hudon V, Berthod F, Germain L, Auger F a. Inosculation of tissue-engineered capillaries with the host's vasculature in a reconstructed skin transplanted on mice. Am J Transplant 2005;5(5):1002–10.

60. Cheng G, Liao S, Kit Wong H, Lacorre DA, Di Tomaso E, Au P, et al. Engineered blood vessel networks connect to host vasculature via wrapping-and-tapping anastomosis. Blood 2011;118(17):4740–9.

61. Sun G, Zhang X, Shen Y-I, Sebastian R, Dickinson LE, Fox-Talbot K, et al. Dextran hydrogel scaffolds enhance angiogenic responses and promote complete skin regeneration during burn wound healing. Proc Natl Acad Sci USA 2011;108(26):20976–81.

62. Montaño I, Schiestl C, Schneider J, Pontiggia L, Luginbühl J, Biedermann T, et al. Formation of human capillaries in vitro: the engineering of prevascularized matrices. Tissue Eng Part A 2010 Jan;16(1):269–82.

63. Chen X, Aledia AS, Ghajar CM, Griffith CK, Putnam AJ, Hughes CCW, et al. Prevascularization of a fibrin-based tissue construct accelerates the formation of functional anastomosis with host vasculature. Tissue Eng Part A 2009;15(6):1363–71.

64. Watt SM, Athanassopoulos A, Harris AL, Tsaknakis G. Human endothelial stem/progenitor cells, angiogenic factors and vascular repair. J R Soc Interface 2010;(7)S731–S751.

65. Critser PJ, Voytik-Harbin SL, Yoder MC. Isolating and defining cells to engineer human blood vessels. Cell Prolif 2011;44 Suppl 1:15–21.

66. Yoder MC. Endothelial progenitor cell: a blood cell by many other names may serve similar functions. Journ Mol Med 2013;91(3):285–95.

67. Hill JM, Zalos G, Halcox JPJ, Schenke WH, Waclawiw MA, Quyyumi AA, et al. Circulating endothelial progenitor cells, vascular function, and cardiovascular risk. NEJM 2003;348(7):593–600.

68. Mukai N, Akahori T, Komaki M, Li Q, Kanayasu-Toyoda T, Ishii-Watabe A, et al. A comparison of the tube forming potentials of early and late endothelial progenitor cells. Exp Cell Res 2008;314(3):430–40.

69. Yoder MC, Mead LE, Prater D, Krier TR, Mroueh KN, Li F, et al. Redefining endothelial progenitor cells via clonal analysis and hematopoietic stem/progenitor cell principals. Blood 2007;109(5):1801–9.

70. Gulati R, Jevremovic D, Peterson TE, Chatterjee S, Shah V, Vile RG, et al. Diverse origin and function of cells with endothelial phenotype obtained from adult human blood. Circ Res 2003;93(11):1023–5.

71. Ingram DA, Mead LE, Moore DB, Woodard W, Fenoglio A, Yoder MC. Vessel wall-derived endothelial cells rapidly proliferate because they contain a complete hierarchy of endothelial progenitor cells. Blood 2005;105(7):2783–6.

72. Ingram DA, Mead LE, Tanaka H, Meade V, Fenoglio A, Mortell K, et al. Identification of a novel hierarchy of endothelial progenitor cells using human peripheral and umbilical cord blood. Blood 2004;104(9):2752–60.

73. Athanassopoulos A, Tsaknakis G, Newey SE, Harris AL, Kean J, Tyler MP, et al. Microvessel networks in pre-formed in artificial clinical grade dermal substitutes in vitro using cells from haematopoietic tissues. Burns 2012; 38(5):691-701.

74. Coldwell KE, Lee SJ, Kean J, Khoo CP, Tsaknakis G, Smythe J, et al. Effects of obstetric factors and storage temperatures on the yield of endothelial colony forming cells from umbilical cord blood. Angiogenesis 2011;14(3):381–92.

75. Zhou B, Tsaknakis G, Coldwell KE, Khoo CP, Roubelakis MG, Chang C-H, et al. A novel function for the haemopoietic supportive murine bone marrow MS-5 mesenchymal stromal cell line in promoting human vasculogenesis and angiogenesis. Brit J Haem 2012;57(3)(3):299–311.

76. Walker NG, Sc B, Mistry AR, Ph D, Smith LE, Eves PC, et al. A Chemically Defined Carrier for the Delivery of Human Mesenchymal Stem / Stromal Cells to Skin Wounds. Tissue Eng Part C 2012;18(2):143-55

77. Zhang Y, Fisher N, Newey SE, Smythe J, Tatton L, Tsaknakis G, et al. The impact of proliferative potential of umbilical cord-derived endothelial progenitor cells and hypoxia on vascular tubule formation in vitro. Stem Cells Dev 2009;18(2):359–75.

78. Tura O, Skinner EM, Robin Barclay G, Samuel K, Gallagher RC, Brittan M, et al. Late outgrowth endothelial cells resemble mature endothelial cells and are not derived from bone marrow. Stem cells 2013. 31(2):338-48

79. Lin Y, Weisdorf DJ, Solovey a, Hebbel RP. Origins of circulating endothelial cells and endothelial outgrowth from blood. J Clin Invest 2000 Jan;105(1):71–7.

80. Smadja DM, Cornet a, Emmerich J, Aiach M, Gaussem P. Endothelial progenitor cells: characterization, in vitro expansion, and prospects for autologous cell therapy. Cell Biol Toxicol 2007;23(4):223–39.

81. Bompais H, Chagraoui J, Canron X, Crisan M, Liu XH, Anjo A, et al. Human endothelial cells derived from circulating progenitors display specific functional properties compared with mature vessel wall endothelial cells. Blood 2004;103(7):2577–84.

82. Mead LE, Prater D, Yoder MC, Ingram D. Isolation and characterization of endothelial progenitor cells from human blood. Current Protoc Stem Cell Biol 2008; (2):Unit 2C.

83. Melero-Martin JM, Khan Z a, Picard A, Wu X, Paruchuri S, Bischoff J. In vivo vasculogenic potential of human blood-derived endothelial progenitor cells. Blood 2007;109(11):4761–8.

84. Wood JA, Colletti E, Mead LE, Ingram D, Porada CD, Zanjani ED, et al. Distinct contribution of human cord blood-derived endothelial colony forming cells to liver and gut in a fetal sheep model. Hepatol 2012;1–11.

85. Hendrickx B, Verdonck K, Van den Berge S, Dickens S, Eriksson E, Vranckx JJ, et al. Integration of blood outgrowth endothelial cells in dermal fibroblast sheets promotes full thickness wound healing. Stem cells 2010;28(7):1165–77.

86. Hendrickx B, Vranckx JJ, Luttun A. Cell-based vascularization strategies for skin tissue engineering. Tissue Eng Part B 2011;17(1):13–24.

87. Beckstrøm KJ, Brinchmann JE. Human Adipose Tissue as a Source of Cells With Angiogenic Potential. Cell Transplant 2012;21(235):235–50.

88. Sanz L, Santos-Valle P, Alonso-Camino V, Salas C, Serrano A, Vicario JL, et al. Long-term in vivo imaging of human angiogenesis: critical role of bone marrow-derived mesenchymal stem cells for the generation of durable blood vessels. Microvasc Res 2008;75(3):308–14.

89. Karvonen SL, Vaajalahti P, Marenk M, Janas M, Kuokkanen K. Birthmarks in 4346 Finnish newborns. Acta Derm Venereol 1992;72(1):55–7.

90. Gosain AK, Santoro TD, Larson DL, Gingrass RP. Giant congenital nevi: a 20-year experience and an algorithm for their management. Plast Reconstr Surg 2001;108(3):622–36.

91. Kopp J, Magnus Noah E, Rübben A, Merk HF, Pallua N. Radical resection of giant congenital melanocytic nevus and reconstruction with meek-graft covered integra dermal template. Dermatol Surg 2003 Jun;29(6):653–7.

92. Arneja JS, Gosain AK. Giant congenital melanocytic nevi of the trunk and an algorithm for treatment. J Craniofac Surg 2005. p. 886–93.

93. Shelley WC, Leapley AC, Huang L, Critser PJ, Zeng P, Prater D, et al. Changes in the frequency and in vivo vessel-forming ability of rhesus monkey circulating endothelial colony-forming cells across the lifespan (birth to aged). Pediatr Res 2012;71(2):156–61.

94. Roubelakis MG, Tsaknakis G, Pappa KI, Anagnou NP, Watt SM. Spindle shaped human mesenchymal stem/stromal cells from amniotic fluid promote neovascularization. PLoS One. 2013;8(1):547.

95. Hofmann NA, Reinisch A, Strunk D. Isolation and large scale expansion of adult human endothelial colony forming progenitor cells. J Vis Exp. 2009;28(32).

96. Lin R-Z, Moreno-Luna R, Muñoz-Hernandez R, Li D, Jaminet S-CS, Greene AK, et al. Human white adipose tissue vasculature contains endothelial colony-forming cells with robust in vivo vasculogenic potential. Angiogenesis 2013;16(4):735-44.

97. Case J, Mead LE, Bessler WK, Prater D, White HA, Saadatzadeh MR, et al. Human CD34+AC133+VEGFR-2+ cells are not endothelial progenitor cells but distinct, primitive hematopoietic progenitors. Exp Hematol 2007;35(7):1109–18.

98. Timmermans F, Van Hauwermeiren F, De Smedt M, Raedt R, Plasschaert F, De Buyzere ML, et al. Endothelial outgrowth cells are not derived from CD133+ cells or CD45+ hematopoietic precursors. Arterioscler Thrombosis Vasc Biol 2007;27(7):1572–9.

99. Yoder MC. Human endothelial progenitor cells. Cold Spring Harb Perspec Med 2012;2(7).

100. Schechner JS, Nath a K, Zheng L, Kluger MS, Hughes CC, Sierra-Honigmann MR, et al. In vivo formation of complex microvessels lined by human endothelial cells in an immunodeficient mouse. Proc Natl Acad Sci USA 2000 Aug 1;97(16):9191–6.

101. Koike N, Fukumura D, Gralla O, Au P, Schechner JS, Jain RK. Tissue engineering: creation of long-lasting blood vessels. Nature 2004;428(6979):138–9.

102. Wu X, Rabkin-Aikawa E, Guleserian KJ, Perry TE, Masuda Y, Sutherland FWH, et al. Tissue-engineered microvessels on three-dimensional biodegradable scaffolds using human endothelial progenitor cells. Am J Physiol Heart Circ Physiol 2004;287(2):H480–7.

103. Tonello C, Vindigni V, Zavan B, Abatangelo S, Abatangelo G, Brun P, et al. In vitro reconstruction of an endothelialized skin substitute provided with a microcapillary network using biopolymer scaffolds. FASEB J 2005;19(11):1546–8.

104. Stahl A, Wu X, Wenger A, Klagsbrun M, Kurschat P. Endothelial progenitor cell sprouting in spheroid cultures is resistant to inhibition by osteoblasts: a model for bone replacement grafts. FEBS lett 2005;579(24):5338–42.

105. Melero-Martin JM, De Obaldia ME, Kang S-Y, Khan Z a, Yuan L, Oettgen P, et al. Engineering robust and functional vascular networks in vivo with human adult and cord blood-derived progenitor cells. Circ Res 2008;103(2):194–202.

106. des Rieux A, Ucakar B, Mupendwa BPK, Colau D, Feron O, Carmeliet P, et al. 3D systems delivering VEGF to promote angiogenesis for tissue engineering. J Control Release 2011;150(3):272–8.

107. Helary C, Bataille I, Abed A, Illoul C, Anglo A, Louedec L, et al. Concentrated collagen hydrogels as dermal substitutes. Biomat 2010:481–90.

108. Hadjipanayi E, Cheema U, Mudera V, Deng D, Liu W, Brown R a. First implantable device for hypoxia-mediated angiogenic induction. J Control Release 2011;153(3):217–24.

109. Hegen A, Blois A, Tiron CE, Hellesøy M, Micklem DR, Nör JE, et al. Efficient in vivo vascularisation of tissue-engineering scaffolds. J Tissue Eng Regen Med 2011;5(4)e52-62.

110. Yee D, Hanjaya-Putra D, Bose V, Luong E, Gerecht S. Hyaluronic Acid hydrogels support cord-like structures from endothelial colony-forming cells. Tissue Eng Part A 2011;17(9-10):1351–61.

111. Rao RR, Peterson AW, Ceccarelli J, Putnam AJ, Stegemann JP. Matrix composition regulates three-dimensional network formation by endothelial cells and mesenchymal stem cells in collagen/fibrin materials. Angiogenesis 2012;253–64.

112. Ananta M, Ph D, Brown RA, Mudera V. A Rapid Fabricated Living Dermal Equivalent for Skin Tissue Engineering : An In Vivo Evaluation in an Acute Wound Model. Tissue Eng Part A 2012;18:353–61.

113. Stratman AN, Davis GE. Endothelial cell-pericyte interactions stimulate basement membrane matrix assembly: influence on vascular tube remodeling, maturation, and stabilization. Microsc microanal 2012;18(1):68–80.

114. Sacharidou A, Stratman AN, Davis GE. Molecular mechanisms controlling vascular lumen formation in three-dimensional extracellular matrices. Cells Tissues Organs 2012;195(1-2):122–43.

115. Davis GE, Stratman AN, Sacharidou A, Koh W. Chapter Three - Molecular Basis for Endothelial Lumen Formation and Tubulogenesis During Vasculogenesis and Angiogenic Sprouting. Internat Rev Cell Mol Biol 2011. p. 101–65.

116. Stratman AN, Schwindt AE, Malotte KM, Davis GE. Endothelial-derived PDGF-BB and HB-EGF coordinately regulate pericyte recruitment during vasculogenic tube assembly and stabilization. Blood 2010;116(22):4720–30.

117. Sekine H, Shimizu T, Sakaguchi K, Dobashi I, Wada M, Yamato M, et al. In vitro fabrication of functional three-dimensional tissues with perfusable blood vessels. Nature comm 2013;4:1399.

118. Sakaguchi K, Shimizu T, Horaguchi S, Sekine H, Yamato M, Umezu M, et al. In vitro engineering of vascularized tissue surrogates. Sci reports 2013;3:1316.

119. Carletti E, Motta A, Migliaresi C. Scaffolds for tissue engineering and 3D cell culture. Haycock JW, editor. Methods Mol Biol 2011;695(2):17–39.

120. Melchels FPW, Barradas AMC, Van Blitterswijk CA, De Boer J, Feijen J, Grijpma DW. Effects of the architecture of tissue engineering scaffolds on cell seeding and culturing. Acta Biomat 2010;7(9):3432–45.

121. Engelhardt S, Hoch E, Borchers K, Meyer W, Krüger H, Tovar GEM, et al. Fabrication of 2D protein microstructures and 3D polymer-protein hybrid microstructures by two-photon polymerization. Biofabrication 2011;3(2):025003.

122. Pankov R. Fibronectin at a glance. J Cell Sci 2002;115(20):3861–3.

123. Critser PJ, Kreger ST, Voytik-Harbin SL, Yoder MC. Collagen matrix physical properties modulate endothelial colony forming cell-derived vessels in vivo. Microvasc Res 2010;80(1):23–30.

124. Stratman AN, Davis MJ, Davis GE. VEGF and FGF prime vascular tube morphogenesis and sprouting directed by hematopoietic stem cell cytokines. Blood 2011;117(14):3709–19.

125. Pan W, Pham VN, Stratman AN, Castranova D, Kamei M, Kidd KR, et al. CDP-diacylglycerol synthetase-controlled phosphoinositide availability limits VEGFA signaling and vascular morphogenesis. Blood 2012;120(2):489–98.

126. Krueger J, Liu D, Scholz K, Zimmer A, Shi Y, Klein C, et al. Flt1 acts as a negative regulator of tip cell formation and branching morphogenesis in the zebrafish embryo. Devel Camb Eng 2011;138(10):2111–20.

127. Chan YC, Roy S, Khanna S, Sen CK. Downregulation of endothelial microRNA-200b supports cutaneous wound angiogenesis by desilencing GATA binding protein 2 and vascular endothelial growth factor receptor 2. Arterioscl thromb vasc biol 2012;32(6):1372–82.

128. Roy S, Sen CK. miRNA in wound inflammation and angiogenesis. Microcirc 2011;19(3):224–32.

129. Alekseeva T, Hadjipanayi E, Abou Neel E, Brown R. Engineering stable topography in dense bio-mimetic 3D collagen scaffolds. Euro Cell Mater 2012;23:28–40.

130. Koh W, Stratman AN, Sacharidou A, Davis GE. Chapter 5 In Vitro Three Dimensional Collagen Matrix Models of Endothelial Lumen Formation During Vasculogenesis and Angiogenesis. Methods Enzymol 2008;443(08):83–101.

131. Lin C, Ning H, Lin G, Lue TF. Is CD34 truly a negative marker for mesenchymal stromal cells? Cytotherapy 2012;14(10):1159-63.

132. Reinisch A, Hofmann N a, Obenauf AC, Kashofer K, Rohde E, Schallmoser K, et al. Humanized large-scale expanded endothelial colony-forming cells function in vitro and in vivo. Blood 2009;113(26):6716–25.

133. Traktuev DO, Merfeld-Clauss S, Li J, Kolonin M, Arap W, Pasqualini R, et al. A population of multipotent CD34-positive adipose stromal cells share pericyte and mesenchymal surface markers, reside in a periendothelial location, and stabilize endothelial networks. Circ Res 2008;102(1):77–85.

134. Oberlin E, Fleury M, Clay D, Petit-cocault L, Candelier J, Mennesson B, et al. VE-cadherin expression allows identification of a new class of hematopoietic stem cells within human embryonic liver. Blood 2010;116(22):4–6.

135. Weinreb I, Cunningham KS, Perez-Ordoñez B, Hwang DM. CD10 Is expressed in most epithelioid hemangioendotheliomas: a potential diagnostic pitfall. Arch Pathol Lab Med 1965;133(12):1965-8.

136. Jung S-M, Kuo T. Immunoreactivity of CD10 and inhibin alpha in differentiating hemangioblastoma of central nervous system from metastatic clear cell renal cell carcinoma. Mod Pathol 2005;18(6):788–94.

137. McDermott SP, Eppert K, Lechman ER, Doedens M, Dick JE. Comparison of human cord blood engraftment between immunocompromised mouse strains. Blood. 2010;116(2):193–200.

138. Kollert F, Christoph S, Probst C, Budweiser S, Bannert B, Binder M, et al. Soluble CD90 as a potential marker of pulmonary involvement in systemic sclerosis. Arthritis Care Res 2013;65(2):281–7.

139. Carpenter L, Malladi R, Yang C-T, French A, Pilkington KJ, Forsey RW, et al. Human induced pluripotent stem cells are capable of B-cell lymphopoiesis. Blood 2011;117(15):4008–11.

140. Fuchs S, Hermanns MI, Kirkpatrick CJ. Retention of a differentiated endothelial phenotype by outgrowth endothelial cells isolated from human peripheral blood and expanded in long-term cultures. Cell Tissue Res 2006;326(1):79–92.

141. Farias V a, Linares-Fernández JL, Peñalver JL, Payá Colmenero J a, Ferrón GO, Duran EL, et al. Human umbilical cord stromal stem cell express CD10 and exert contractile properties. Placenta 2011;32(1):86–95.

142. Donovan D, Brown N, Bishop E, Lewis C. Comparison of three in vitro human 'angiogenesis' assays with capillaries formed in vivo Angiogenesis 2001;4(2):113-121

143. Watt SM, Gullo F, van der Garde M, Markeson D, Camicia R, Khoo CP, et al. The angiogenic properties of mesenchymal stem/stromal cells and their therapeutic potential. Br Med Bull 2013;108:25–53.

144. Dominici M, Le Blanc K, Mueller I, Slaper-Cortenbach I, Marini F, Krause D, et al. Minimal criteria for defining multipotent mesenchymal stromal cells. The International Society for Cellular Therapy position statement. Cytotherapy 2006;8(4):315–7.

145. Critser PJ, Yoder MC. Endothelial colony-forming cell role in neoangiogenesis and tissue repair. Curr Opin Organ Transplant 2010;15(1):68–72.

146. Pepperell EE, Watt SM. A novel application for a 3-dimensional timelapse assay that distinguishes chemotactic from chemokinetic responses of hematopoietic CD133(+) stem/progenitor cells. Stem Cell Res 2013;11(2):707–20.

147. Hu K, Shi H, Zhu J, Deng D, Zhou G, Zhang W, et al. Compressed collagen gel as the scaffold for skin engineering. Biomed Microdevices 2010;12(4):627–35.

148. Levis HJ, Peh GSL, Toh K-P, Poh R, Shortt AJ, Drake R a L, et al. Plastic compressed collagen as a novel carrier for expanded human corneal endothelial cells for transplantation. PLoS One 2012;7(11):e50993.

149. Levis HJ, Brown R a, Daniels JT. Plastic compressed collagen as a biomimetic substrate for human limbal epithelial cell culture. Biomaterials 2010;31(30):7726–37.

150. Chen H-C. Boyden chamber assay. Methods Mol Biol. 2005;294:15–22.

151. Lamalice L, Le Boeuf F, Huot J. Endothelial cell migration during angiogenesis. Circ Res 2007;100(6):782–94.

152. Khoo CP, Micklem K, Watt SM. A comparison of methods for quantifying angiogenesis in the matrigel assay in vitro. Tissue Eng Part C Methods. 2011;17(9):895–906.

153. Nayak D, Johnson KR, Heydari S, Roth TL, Zinselmeyer BH, McGavern DB. Type I Interferon Programs Innate Myeloid Dynamics and Gene Expression in the Virally Infected Nervous System. PLoS Path 2013;9(5).

154. McKenzie JAG, Fruttiger M, Abraham S, Lange CAK, Stone J, Gandhi P, et al. Apelin is required for non-neovascular remodeling in the retina. Am J Pathol. 2012;180(1):399–409.

155. Laschke MW, Rücker M, Jensen G, Carvalho C, Mülhaupt R, Gellrich N-C, et al. Improvement of vascularization of PLGA scaffolds by inosculation of in situ-preformed functional blood vessels with the host microvasculature. Ann Surg 2008;248(6):939–48.

156. Kischer CW, Pindur J, Krasovitch P, Kischer E. Characteristics of granulation tissue which promote hypertrophic scarring. Scanning Microsc. 1990;4(4):877–887; discussion 887–888.

157. Nör JE, Peters MC, Christensen JB, Sutorik MM, Linn S, Khan MK, et al. Engineering and characterization of functional human microvessels in immunodeficient mice. Lab Invest. 2001;81(4):453–63.

158. Peters MC, Polverini PJ, Mooney DJ. Engineering vascular networks in porous polymer matrices. J Biomed Mater Res. 2002;60(4):668–78.

159. Suárez Y, Shepherd BR, Rao DA, Pober JS. Alloimmunity to Human Endothelial Cells Derived from Cord Blood Progenitors. J Immunol 2012;179(11):7488-96.

160. Fox a, Smythe J, Fisher N, Tyler MPH, McGrouther D a, Watt SM, et al. Mobilization of endothelial progenitor cells into the circulation in burned patients. Br J Surg 2008;95(2):244–51.

161. Mandal A. Paediatric partial-thickness scald burns - Is Biobrane the best treatment available? Int Wound J. 2007;4(1).

162. Ahmadi H, Williams G. Permanent scarring in a partial thickness scald burn dressed with Biobrane. J Plast Reconstr Aesthetic Surg. 2009;62(5):697–8.

163. Heimbach D, Luterman A, Burke J, Cram A, Herndon D, Hunt J, et al. Artificial dermis for major burns. A multi-center randomized clinical trial. Annals of surgery. 1988 p. 313–20.

164. Kolokythas P, Aust MC, Vogt PM, Paulsen F. Dermal subsitute with the collagen-elastin matrix Matriderm in burn injuries: a comprehensive review. Handchir Mikrochir Plast Chir. 2008;40(6):367–71.

165. Ryssel H, Germann G, Kloeters O, Gazyakan E, Radu CA. Dermal substitution with Matriderm in burns on the dorsum of the hand. Burns. 2010;36(8):1248–53.

166. Ellis MJ, Chaudhuri JB. Poly(lactic-co-glycolic acid) hollow fibre membranes for use as a tissue engineering scaffold. Biotechnol Bioeng 2006;96(1):177–87.

167. Fekete N, Rojewski MT, Fürst D, Kreja L, Ignatius A, Dausend J, et al. GMP-compliant isolation and large-scale expansion of bone marrow-derived MSC. PLoS One. 2012;7(8).

168. Denecke B, Horsch LD, Radtke S, Fischer JC, Horn PA, Giebel B. Human endothelial colony-forming cells expanded with an improved protocol are a useful endothelial cell source for scaffold-based tissue engineering. J Tissue Eng Regen Med; Feb 25 2013 (epub ahead of print).

169. Sharma RR, Pollock K, Hubel A, McKenna D. Mesenchymal stem or stromal cells: a review of clinical applications and manufacturing practices. Transfusion 2014;54(5):1418–37.

170. Otto WR, Wright NA. Mesenchymal stem cells: from experiment to clinic. Fibrogenesis and Tissue Repair 2011;4(20).

171. Friedenstein AJ, Petrakova K V, Kurolesova AI, Frolova GP. Heterotopic of bone marrow. Analysis of precursor cells for osteogenic and hematopoietic tissues. Transplantation. 1968;6(2):230–47.

172. Asahara T. Isolation of Putative Progenitor Endothelial Cells for Angiogenesis. Science 1997;275(5302):964–6.

173. Wang C, Huang P, Chen J, Lin S, Lee M. Clinical Application of Endothelial Progenitor Cell : Are We Ready? 2013;479–87.